Catalysis of thiol-disulfide chemistry in the context of plastid *c*-type cytochrome assembly

Dissertation

Presented in Partial Fulfillment of the Requirements for the Degree Doctor of Philosophy in the Graduate School of The Ohio State University

By

Ankita Das

Graduate Program in Molecular Genetics

The Ohio State University

2023

Dissertation Committee

Dr. Patrice P. Hamel, Advisor

Dr. Iris Meier

Dr. Amanda Bird

Dr. Natividad Ruiz

Abstract

The *c*-type cytochromes or cytochromes *c* are heme-containing metalloproteins that act as electron carriers in energy transducing membranes involved in processes such as photosynthesis and respiration. The maturation of cytochromes *c* requires covalent attachment of the heme cofactor to a heme-binding motif (C*XX*CH)in the apocytochrome *c*. In chloroplasts, cytochrome *c* assembly depends on factors known as **CCS** (Cytochrome *c* Synthesis), that are essential for the heme attachment reaction taking place in the thylakoid lumen The covalent attachment of heme requires the heme-linking cysteines of apocytochrome *c* to be maintained in a reduced state (providing free -SH) by the operation of a trans-thylakoid disulfide reducing pathway. CCDA, a polytopic thylakoid membrane oxido-reductase, and CCS5, a thioredoxin-like protein, are two components of a trans-thylakoid disulfide-reducing pathway, which also operates in bacteria This pathway transfers electrons from stroma via signature redox motifs and sequential thiol-disulfide exchanges from CCDA to CCS5 to reduce apocytochrome *c* disulfide bonded CXXCH in the thylakoid lumen. CCS4, first identified in the unicellular alga *Chlamydomonas reinhardtii,* is a thylakoid-bound stroma-facing component of this disulfide-reducing pathway with no residue or motif suggestive of a biochemical activity. A *ccs4* mutant is partially deficient for photosynthesis (due to a defect in cytochrome *c* assembly) and can be rescued by application of exogenous thiols or overexpression of *CCDA*. In this work,

we evidenced that CCDA accumulation is decreased in a *ccs4* mutant but not in a *ccs5* mutant, suggesting a functional interaction between CCS4 and CCDA. Our genetic studies show that CCS4 and CCS5 are partially redundant for the delivery of reducing power for the apocytochrome *c* C*XX*CH reduction. We also show that gain-of-function mutations in the *CCS4* gene that correspond to changes in the stromal domain of the protein can suppress a *ccs5*-null mutant. This suggests that activity of the second pathway can be enhanced in the absence of the first, which is CCS5-dependent. CCS4-like proteins occur in the green lineage, and we show that HCF153, a distant ortholog from *Arabidopsis thaliana*, can substitute for *Chlamydomonas* CCS4. The mechanism of apocytochrome *c* C*XXC*H reduction by CCS4 is unclear but we discuss the possible function of CCS4 in the context of its similarity to COX16, a mitochondrial protein involved in a disulfide reducing pathway. In Chapter 3, we demonstrate that the apocytochrome *c*, the substrate of the heme attachment reaction, is first enzymatically oxidized by LTO1, a VKOR homolog in plastids via a trans-thylakoid oxidizing pathway, and subsequently reduced by the disulfide-reducing pathway. Characterization of a *lto1* mutant shows a photosynthetic growth defect which can be attributed to a specific loss of PSII activity by fluorescence rise and decay kinetics. Holocytochrome *c* assembly is restored in a *ccs4ccs5* double mutant, which is completely blocked, in the presence of the *lto1* mutation. However, there is no rescue of the tight photosynthetic growth defect despite the regain of holocytochrome *c* accumulation in the *ccs4 ccs5 lto1* mutant. Other regain of cytochrome *c* assembly upon LTO1 loss of function is not enough to restore photosynthetic growth in a *ccs4ccs5* double mutant, other targets of LTO1 might be required for photosynthesis in the absence of the reducing

pathway. It is also possible that CCS4 and CCS5 control other aspects of photosynthesis beside the redox control of the heme attachment reaction that does not depend on LTO1 oxidation. Thus, the defect in the heme attachment step is corrected upon inactivation of LTO1 but any additional function that CCS4 and CCS5 might have, is not. We discuss the analogy between cytochrome *c* assembly thylakoids and bacteria, where the accepted model postulates that a reducing pathway exists or is required to counter the oxidation of heme-linking cysteines into a disulfide in the apocytochrome *c* substrate.

Dedication

This dissertation is dedicated to my family in India, and friends in Columbus for their unconditional love and support.

Acknowledgments

I would like to express my deepest gratitude and appreciation to all the individuals who have contributed to the completion of this doctoral thesis. Their guidance, support, nd encouragement were invaluable throughout this journey.

First, I would like to extend my sincere gratitude to my supervisor, Dr. Patrice Paul Hamel, for his expertise and patience. His insightful comments and constructive feedback have been instrumental in shaping this thesis and my overall research experience. His perspectives have enriched the quality of this thesis and I am deeply appreciative of his contributions. I would also like to thank the members of thesis committee, Dr. Iris Meier, Dr. Amanda Bird, and Dr. Natividad Ruiz, for their valuable insights, critical feedback, and for dedicating their time and expertise to review my progress. I am truly grateful for their mentorship and guidance.

I would like to thank previous lab member, Dr. Stéphane Gabilly for laying the foundation of Chapter 2 of this thesis, Dr. Nitya Subramanian for teaching me the basic skills and techniques that were imperative to my research. I would also like to thank our collaborators, Dr. Igor Jouline, Dr. Katia Andrianova for their Bioinformatics work. The contributions of the people mentioned above resulted in the acceptance of our manuscript and I am truly grateful for that.

My sincere appreciation to the undergraduate students of the lab, Kate Kravets and Cami Hebner, whose work of generating the triple mutants has been crucial to Chapter 3 of this thesis. I would also like to thank other members of the lab who made my time in the lab enjoyable.

I am indebted to my friends in Columbus, especially my cohort of Molecular Genetics, for their support, resources, guidance, mentorship, and the much-needed encouragement and motivation. Their unwavering belief in me made me believe in myself and made me grow as a Scientist and a person. They have been a constant source of inspiration, motivation, and intellectual exchange.

My heartfelt thanks go to my family for their love, encouragement, and support throughout this long and challenging journey. Their patience, encouragement, and belief in me have been my greatest motivation and I am forever grateful for their presence in my life.

In conclusion, I am grateful for each and every person who has supported and contributed to this research endeavor, and I thank them for being a part of this significant milestone in my academic journey.

Vita

2015 …… BS-MS Dual Degree,

Indian Institute of Science Education and Research, Bhopal, India

2016 …… Junior Research Fellow,

Indian Institute of Science Education and Research, Mohali, India

2016 – Present …… Graduate Teaching Associate,

Department of Molecular Genetics,

The Ohio State University, USA

Fields of Study

Major Field: Molecular Genetics

Table of Contents

List of Tables

List of Figures

Preamble

The following thesis explores the diverse facets of disulfide bond dynamics, shedding light on the intricate interplay between oxidative and reductive processes. Disulfide bonds, formed by the covalent linkage between two cysteine residues, play a vital role in stabilizing protein structures and modulating protein functions. This thesis seeks to delve into the role of disulfide bond chemistry in the context of plastid *c*-type cytochrome assembly.

Throughout this thesis, different steps that are critical for the assembly of *c*-type cytochromes have been discussed in detail, ranging from the different types of *c*-type cytochromes, their transport across an energy transducing membrane, and their maturation via covalent attachment to a heme prosthetic group. In Chapter 1, disulfide bond formation and reduction have been explored, with an emphasis on the intricacies of thiol-disulfide chemistry required for cytochrome *c* assembly in bacteria, mitochondria, and plastids. Specifically, Sections II, III.C., V, and VI lay the foundation required to understand disulfide reduction and thiol oxidation in the chloroplasts, which are further elaborated upon in Chapters 2 and 3, respectively.

Through comprehensive literature review in Chapter 1, experimentation and critical analysis in Chapters 2 and 3, this thesis endeavors to provide valuable insights into the complex world of thiol-disulfide chemistry.

1. Introduction

I. CYTOCHROMES *C* IN ENERGY TRANSDUCING MEMBRANES

I.A. Energy transducing membranes

All living cells rely on at least one energy-conversion process taking place in a highly spe

specialized membrane (Fig. 1.1).

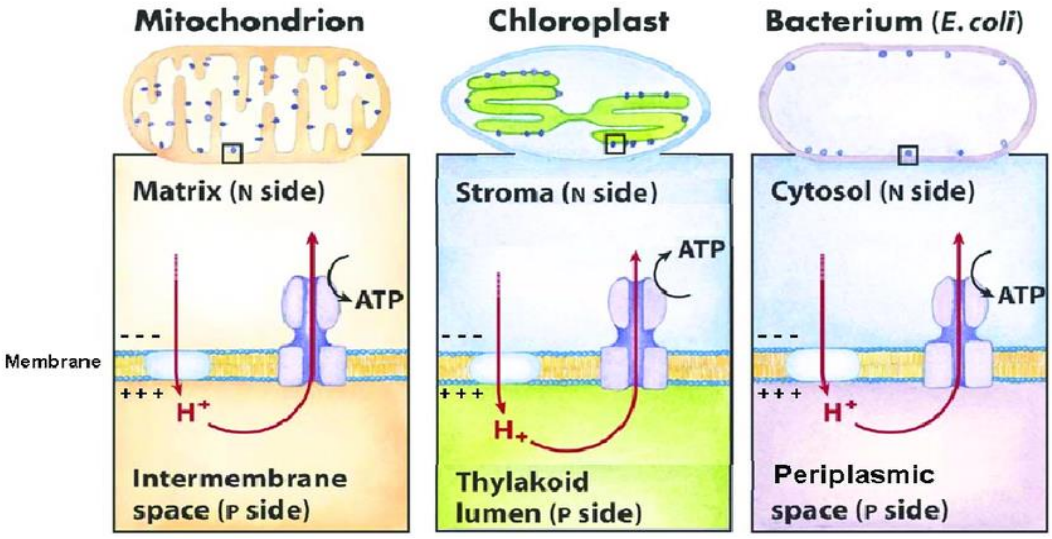

Figure 1.1 Energy-transducing membranes, primary and secondary proton pumps

(Lehninger's Principles of Biochemistry - 5th edition). A primary pump (in blue) couples electron transfer to the formation of a proton gradient. A secondary pump (in purple) then uses this gradient to synthesize ATP. Generally, the terms "*n*-side" or "*p*-side" are used to refer to the cellular spaces delimited by the membrane. The *n*-side or negative side designates the matrix of the mitochondria, the stroma of the chloroplast and the cytosol of bacteria. The *p*-side or positive side refers to the intermembrane space, the lumen and the periplasm. The image is extracted from (Malnoë, 2011).

Archaea and bacteria have one energy-converting membrane, the plasma membrane (Park *et al.*, 2023). In eukaryotes, the energy-converting membrane is the mitochondrial inner membrane while in photosynthetic eukaryotes, energy conversion occurs in the mitochondria as well as the thylakoid membrane inside the chloroplast (Das *et al.*, 2021; Park *et al.*, 2023). Energy-transducing membranes are the sites of a series of oxidoreduction reactions resulting in the generation of ATP, the universal energy currency in living organisms (Fig. 1.1). The electron transfer reactions are coupled with the translocation of protons (or in some rare cases, sodium) across the membrane, generating an electrochemical proton gradient across the membrane. The direction of proton translocation occurs from the bacterial or archaeal cytoplasm, the mitochondrial matrix and chloroplast stroma, which is referred to as the *n*-side (*n* for negative) to the bacterial or archaeal periplasm, the mitochondrial intermembrane space, the thylakoid lumen, which by convention is referred to as the *p*-side (*p* for positive) (Fig.1.1). The electrochemical proton gradient is utilized by F-ATPase, a class of ATP synthase yielding synthesis of ATP from phosphorylation of ADP on the *n*-side of the membrane (Kühlbrandt, 2019; Nirody *et al.*, 2020). The electron-linked phosphorylation of ADP to ATP is called oxidative phosphorylation and takes place in the mitochondria in eukaryotes (Vercellino *et al.*, 2022). In chloroplasts`, the sunlight energy is used for phosphorylation of ADP to ATP, a process referred to as photophosphorylation (Yahia *et al.*, 2019).

I.B. Cytochromes

In most energy-transducing membrane systems, generation of the electrochemical gradient across the membrane relies on the operation of cytochromes, a large family of molecules

that transfer electrons. The term ‘cytochrome’ was first coined by David Keilin in 1925 (Bendall, 2016) to describe a set of intracellular proteins that are heme-binding and undergo oxidation and reduction (Ma *et al.*, 2019). These heme-binding or hemoproteins occur as soluble or membrane-bound molecules and perform vital function as one-electron carriers during energy transducing processes such as respiration and photosynthesis (Bertini *et al.*, 2006; Ma *et al.*, 2019). Heme is a protoporphyrin-iron complex in which the iron atom in the protoporphyrin ring switches between Fe (II) (red.) and Fe (III) (ox.) states via reversible reduction and oxidation reactions (Swenson *et al.*, 2020). Cytochromes are classified into *a*, *b*, *c*, *d* and *o*-types depending on the type of bound heme and the covalent or non-covalent association of the prosthetic group to the apoform of the protein (Alvarez-Paggi *et al.*, 2017; Layer, 2021; Ma *et al.*, 2019; Swenson *et al.*, 2020). With the exception of *c*-type cytochromes, cytochromes *a, b, d* and *o*-types, do not contain a specific heme binding motif but a heme binding pocket that is typically enriched in hydrophobic and non-polar residues and fewer charged residues (Li *et al.*, 2011; Smith *et al.*, 2010). While all types of cytochromes are present in bacteria and archaea, mitochondria and chloroplasts do not contain cytochromes of the *d* and *o*-types (Alvarez-Paggi *et al.*, 2017; Layer, 2021; Ma *et al.*, 2019; Swenson *et al.*, 2020). Heme B or ferroprotoporphyrin IX is the simplest form of heme synthesized and is attached non-covalently in *b*-type cytochromes (Fig. 1.2). Examples of *b*-type cytochromes, are the cytochrome *b* subunit of the cytochrome bc_1 complex in mitochondria (Complex III) and cytochrome *b* of the b_6f complex in the chloroplast, which are di-heme cytochromes (Cline *et al.*, 2016; Nelson *et al.*, 2004; Vercellino *et al.*, 2022). Other examples of *b*-type cytochromes include cytochrome P_{450},

nitric oxide synthase, cytochrome b_5 and cytochrome b_{562}, which do not function in energy-transduction (Arnesano *et al.*, 1999; Crane *et al.*, 1998; Hall *et al.*, 2022; Meng *et al.*, 2022). Heme A, D and O are formed by chemical modification of heme B (Fig. 1.2) (Swenson *et al.*, 2020).

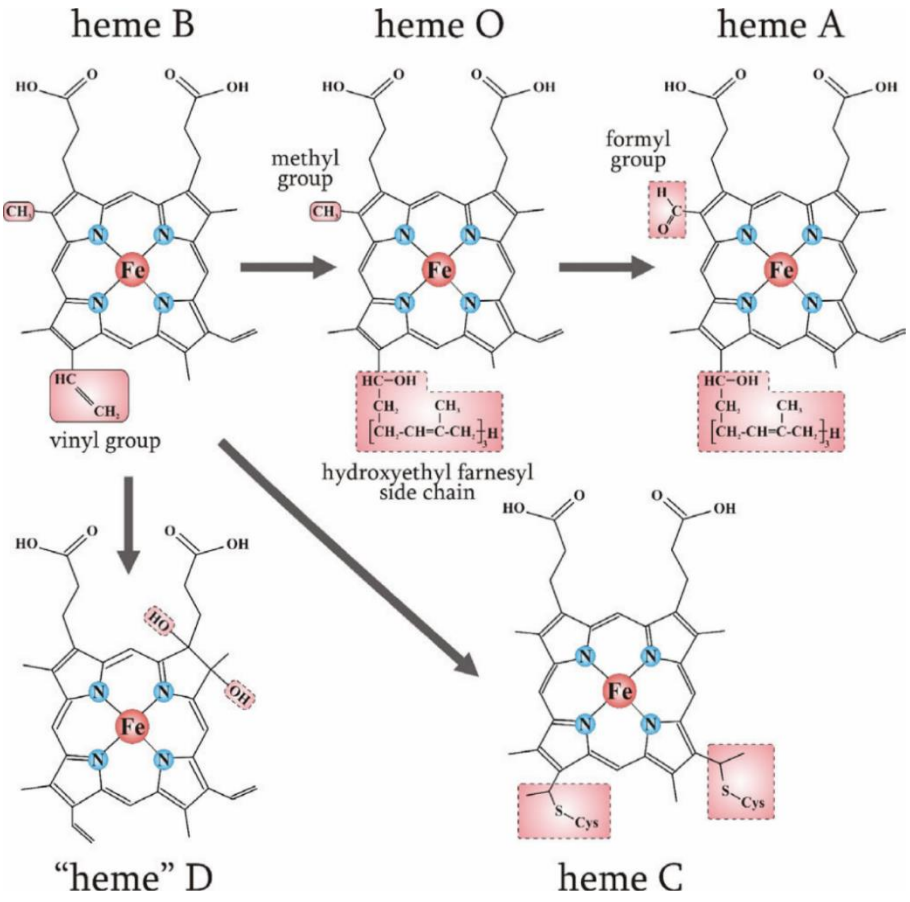

Figure 1.2. Structures of heme B, heme O, heme A, heme D

In heme D, a double bond in a pyrrole ring has been reduced, so it is a chlorin, rather than a real heme), and heme C (structure of heme C is like heme B except that heme C is covalently bound to polypeptide via thioether bridges). The image is extracted from (Belevich, 2007)

Heme A formation is a sequential process that starts from heme B and involves farnelysation of a vinyl side group at C2 position in heme B to form heme O as the first step. Subsequently, heme O is modified to have a formyl group by hydroxylation of a methyl group at C8 position of the porphyrin ring, resulting in the formation of heme A. The best-known example of an *a*-type cytochrome is cytochrome aa_3, a catalytic subunit of cytochrome *c* oxidase which is the Complex IV respiratory enzyme in the mitochondrial electron transport chain (De Vrij *et al.*, 1983; Vercellino *et al.*, 2022). Cytochromes of the *c* type or *c*-type cytochromes are distinct from the other cytochromes because it is the only class of cytochromes where heme B is attached to a heme-binding site (or motif) in the protein via covalent linkage (Alvarez-Paggi *et al.*, 2017; Das *et al.*, 2021). Heme B is defined as heme C when covalently attached to the C*XX*CH motif of apocytochrome *c* via thioether linkage. Most common examples of *c*-type cytochromes are mitochondrial cytochrome c_1 of the respiratory cytochrome bc_1 complex, and plastid cytochrome *f* of the cytochrome b_6f complex, which despite its name is a *c*-type cytochrome (Cline *et al.*, 2016; Nelson *et al.*, 2004; Vercellino *et al.*, 2022). Heme D is similar to heme A in that it carries the hydroxyethylfarnesyl group but not the formyl group (Bowman *et al.*, 2008). Examples of cytochrome *d* include bacterial respiratory cytochrome *bd* complexes (Friedrich *et al.*, 2022), cytochrome cd_1, the nitrite reductase catalyzing the reduction of nitrite to nitric oxide in organisms such as *Thiosphaera pantotropha* and *Pseudomonas aeruginosa* (Ferguson *et al.*, 2000).

I.C. *c*-type cytochromes

The *c*-type cytochromes, also referred to as cytochromes *c*, are a group of 75,000 metalloproteins with one or several covalently attached heme(s) as a prosthetic group (Das *et al.*, 2021; Harvat *et al.*, 2009; Kranz *et al.*, 2009; Moore, 1987). Heme is attached via two cysteines of a conserved heme-binding motif (C_1XXC_2H) contained within the apocytochrome via thioether bonds in which histidine serves as the proximal ligand of the heme iron (Bowman *et al.*, 2008; Das *et al.*, 2021) (Fig. 1.3).

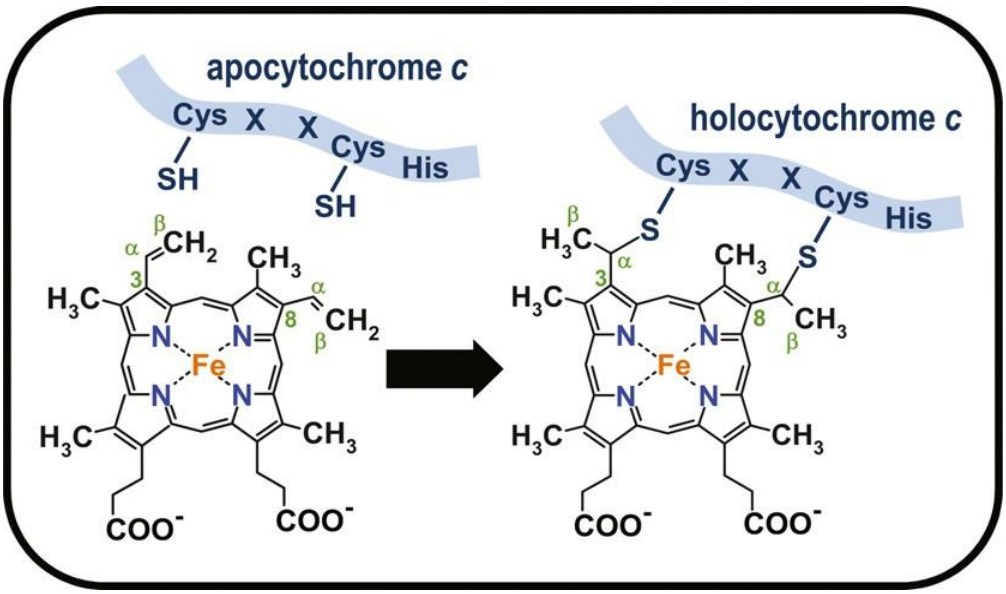

Figure 1.3. Stereospecific heme attachment reaction

HCCS (Holocytochrome *c* synthase) is the enzyme responsible for the stereospecific addition of the cysteinyl thiols from the apocytochrome CXXCH motif (shown in blue) to the α carbons at the vinyl group in positions C3 and C8 of Fe-protoporphyrin IX (heme, shown in black with iron in orange and nitrogen in blue). This reaction occurs on the p-side of the energy-transducing membranes. The numbering of the carbons atoms in the porphyrin rings follows the rules of the International Union of Pure and Applied Chemistry (IUPAC). The image is extracted from (Hamel *et al.*, 2009).

While C_1XXC_2H is the most common heme-binding site, variations do exist in terms of number of intervening residues (X), number of heme-linking cysteines and the identity of the proximal heme ligand. Since heme is an asymmetrical molecule, the α and β carbons of the vinyl side chains can theoretically react with the cysteine thiols to form eight products but the formation of only one product is favored where the α-carbons at position C3 (2-vinyl) and position C8 (4-vinyl) of heme are invariably linked to the thiols of the first and second cysteines respectively in the C_1XXC_2H motif (Fig. 1.3).

This is defined as a 'stereospecific' attachment of heme to apocytochrome *c* (Barker *et al.*, 1999; Das *et al.*, 2021). The residues (X) between the two cysteines are highly variable and all any amino acids (including Gly, Pro and His) except cysteines have been found to serve as 'X' in nature (Bowman *et al.*, 2008). Cytochromes *c* with an engineered C_1CXC_2H or C_1XCC_2H motif can still form the corresponding holoform with a correctly attached heme moiety suggesting that the presence of a cysteine as an intervening residue does not interfere with heme binding (Allen *et al.*, 2009). The iron atom in the heme conducting electron transport is coordinated by the four nitrogen atoms in the heme porphyrin ring and two axial ligands of the apocytochrome polypeptide (Fig. 1.3). The imidazole group of the histidine residue in the conserved C*XX*CH motif always serves as the proximal axial ligand, whereas the distal ligand is usually a methionine residue (Alvarez-Paggi *et al.*, 2017; Bertini *et al.*, 2006). In some rare cases the distal ligand can be tyrosine, asparagine or histidine, such as in SHP (*Sphaeroides* Heme Protein), a *c*-type cytochrome in *Rhodobacter sphaeroides* (Leys *et al.*, 2000) or cytochrome *f* in the b_6f complex (Martinez *et al.*, 1994). Heme attachment sites that vary from the C*XX*CH motif with histidine as the axial ligand

can be found in some cytochromes *c* such as cytochromes *c* and c_1 in the mitochondria of *Euglena, Trypanosoma* and *Leishmania* where heme forms a single thioether bond with a A*XX*CH or a FXXCH motif (Ikegami *et al.*, 1968; Pettigrew *et al.*, 1975; Priest *et al.*, 1992). Another exception is the C*XX*CK motif in the pentaheme nitrite reductase NrfA where heme covalently binds to two cysteines with lysine serving as the proximal axial ligand (Einsle *et al.*, 1999). Cytochromes with multiple hemes usually containing longer heme-binding motifs, for example, $C(X)_4CH$, $C(X)_3CH$ and $C(X)_{15}CH$ motifs are respectively found in the tetraheme cytochrome c_3, dihemes cytochromes *c3* and c_{552}, and the multiheme cytochrome MccA (Bowman *et al.*, 2008; Das *et al.*, 2021). An unusual heme binding motif (C*X*CH) with one instead of two intervening residues is present in several multiheme cytochromes *c* in bacteria and archaea (Ferousi *et al.*, 2019). While *c*-type cytochromes with a C*XX*CH motif are only found on the *p*-side of energy transducing membranes, there is a subclass of cytochromes *c* on the *n*-side of the membrane. Such cytochromes *c* are very rare and the only known examples are cytochrome b_6 of the cytochrome b_6f complex in chloroplasts and cyanobacteria, and cytochrome *b* of the cytochrome *bc* complex in firmicutes (Cline *et al.*, 2016; Das *et al.*, 2021). In these cytochromes, a single heme B binds covalently to a cysteine that is not part of a conserved motif in addition to two other hemes B that are non-covalently bound to the apocytochrome (de Vitry *et al.*, 2004; Kurisu *et al.*, 2003; Stroebel *et al.*, 2003). The heme is attached via a thioether bond and water or a hydroxyl act as the only axial ligand. So, cytochrome b_6 of the cytochrome b_6f complex and cytochrome *b* of the cytochrome *bc* complex in firmicutes are both *b*-type and *c*-type cytochromes.

The *c*-type cytochromes can be further subdivided into different ‘types’ or ‘classes’ according to their structural and redox properties (Ambler, 1991; Bowman *et al.*, 2008). Class I is the largest group and contains small 8-12 kDa soluble *c*-type cytochromes with His/Met axial ligation. Most cytochromes of this class contain one heme group covalently attached to the heme-binding motif at the N terminus and methionine as a distal ligand at the C terminus (e.g., mitochondrial cytochromes *c* and c_1). Hemes attached to cytochromes of this class are usually low spin (S=0 in the ferrous and S=1/2 in the ferric state), Class II contains *c*-type cytochromes with a heme attachment site near the C terminus and a signature four-helix bundle structure (e.g., cytochrome *c* in *Rhodobacter capsulatus*). Class II contains many high-spin heme cytochromes where the heme C is called heme C’ and some low-spin cytochromes with methionine as a distal ligand at the N-terminus. Class III is defined by multiheme cytochromes with a bis-histidine ligation and low reduction potential (e.g., cytochrome c_3 in *Desulfovibrio vulgaris*). Class IV consists of tetraheme cytochromes, with one bis-histidine- and three histidine/methionine-ligated hemes, structurally related the bacterial photosynthetic reaction center and containing additional non-heme prosthetic groups such as flavin, molybdopterin, *etc*. (Bowman *et al.*, 2008; Das *et al.*, 2021; Moore *et al.*, 1990).

II. ASSEMBLY OF *C*-TYPE CYTOCHROMES

Cytochrome *c* assembly is defined as the formation of holocytochrome *c* by the stereospecific covalent attachment of the heme cofactor to the C*XX*CH motif of apocytochrome *c*. The two substrates required for this reaction, apocytochrome *c* and heme,

originate from a different cellular site and need to be transported across at least one biological membrane. The covalent attachment of heme to apocytochrome *c* occurs post-translationally on the *p*-side of all energy transducing membranes. This seemingly simple chemical reaction. i.e. the covalent attachment of heme to apocytochrome *c* requires several critical prerequisite steps to be completed: 1) synthesis and transport of apoprotein and heme across at least one lipid bi-layer (via distinct and independent pathways) to the *p*-side of the membrane, 2) maintenance of heme and heme-linking cysteines of apoprotein in a reduced state by the provision of reducing equivalents, and 3) stereospecific covalent attachment of heme to the apoprotein via thioether linkages (Babbitt *et al.*, 2015; Cline *et al.*, 2016; Das *et al.*, 2021; Kranz *et al.*, 1998; Mavridou *et al.*, 2013; Verissimo *et al.*, 2014). The critical steps of cytochrome *c* biogenesis are described below.

II.A. Apoprotein transport

Apocytochromes are synthesized and translocated in an unfolded state across at least one biological membrane to reach the *p*-side of the energy-transducing membrane. In archaea and bacteria, the apocytochromes are translocated across cytoplasmic membrane. In mitochondria, apoforms of cytochromes *c* are synthesized in the cytoplasm and imported across the mitochondrial outer membrane into the mitochondrial IMS. In the chloroplasts, one apocytochrome *c* is synthesized in the stroma and imported across the thylakoid lumen while the two other cytochrome *c* are synthesized in the cytoplasm and transported across the two membranes of the chloroplast envelope before import into the thylakoid lumen. Except for mitochondrial soluble cytochrome *c*, the transport of *c*-type cytochromes occurs

via general protein translocation machineries. There is a large body of experimental evidence demonstrating that for organellar and bacterial cytochromes, apoprotein translocation and heme transport are independent processes (Cline *et al.*, 2016; Nakamoto *et al.*, 2000). Below is a brief description of the transport pathways for bacterial and organellar *c*-type cytochromes.

II.A.1. Transport of bacterial apocytochromes

In bacteria, apoforms of cytochromes *c* are translocated via the major route of protein transport called the SEC or *Sec*retory pathway (Papanikou *et al.*, 2007; Thöny-Meyer *et al.*, 1997; Tsirigotaki *et al.*, 2017; Tsirigotaki *et al.*, 2017). This pathway is composed of Sec proteins and translocate unfolded proteins with a specific target signal. Apocytochromes are synthesized as precursor polypeptides with a cleavable translocation signal peptide at the N-terminus (Thöny-Meyer *et al.*, 1997). In bacteria, precursor proteins are first recognized and targeted to the Sec complex at the cytoplasmic membrane by the cytoplasmic chaperone protein, SecB. SecB binds to the mature part of the protein by recognizing the exposed hydrophobic surface (Randall *et al.*, 1998) and targets the protein to the Sec translocase complex at the cytoplasmic membrane where the N-terminal signal peptide binds to SecA (Driessen *et al.*, 2001; Fekkes *et al.*, 1998). SecA, a peripheral protein, is the motor subunit of the Sec translocase (composed of the integral SecY, SecE and SecG proteins) and is bound to the complex via a direct interaction with SecY (Karamanou *et al.*, 2008). SecA promotes translocation of preproteins across the translocase pore by ATP hydrolysis by binding to the preprotein in its ATP-bound state,

transporting it across the SecY pore, and releasing it in its ADP-bound state (Economou *et al.*, 1994; Erlandson *et al.*, 2008). Each cycle of ATP hydrolysis is accompanied by transport of 20-30 residues of the preprotein, followed by cleavage of the N-terminal signal sequence (van der Wolk *et al.*, 1997).

Experiments with bacterial cytochromes *c* elucidated for the first time that apoprotein transport to the *p*-side of the membrane and processing was required for apo to holoform conversion (Cline *et al.*, 2016; Nakamoto *et al.*, 2000). Moreover, several lines of experimental evidence established that apoprotein translocation followed by processing was independent of heme transport (Cline *et al.*, 2016; Nakamoto *et al.*, 2000). In one experiment, pulse-chase analysis of cytochrome c_{550} showed that lead peptidase is required for the cleavage of the N-terminal signal peptide in apoforms of cytochromes *c*, but not for the maturation of holocytochrome *c* (Thöny-Meyer *et al.*, 1997). Pulse-chase analysis of intermediates of the soluble *Bradyrhizobium japonicum* cytochrome c_{550}, a 12 kDa *c*-type cytochrome, revealed the presence of cytoplasmic pre-apocytochrome *c* and no processed apoform in the periplasmic fraction in *secA* and *secY* mutants. In *Δccm* mutants that are specifically defective in heme attachment reaction, the processed apocytochrome was detected in the periplasm but no holoform accumulated (Thöny-Meyer *et al.*, 1997). Some cytochromes *c* like cytochrome c_2 of *Rhodobacter sphaeroides* can be translocated into the periplasm in the absence of translocation signal, by virtue of additional elements that are part of the mature protein (Brandner *et al.*, 1994).

II.A.2. Transport of apocytochromes in mitochondria

Transport of the soluble apocytochrome *c* occurs in the absence of a signal peptide unlike cytochrome c_1, which contains two distinct mitochondrial targeting signals (Arnold *et al.*, 1998; Diekert *et al.*, 2001). Initially, apocytochrome *c* was thought to cross the membrane spontaneously using negatively charged phospholipids due to its strong tendency to insert into the lipid bilayer (Jordi *et al.*, 1992). However, reconstitution of the import reaction of the apocytochrome *c* using proteoliposomes harboring purified TOM complex subunits (translocase of the outer mitochondrial membrane) from *Neurospora crassa* and *in organello* analysis of cytochrome *c* import in yeast have shown that the general import pore (GIP) – protein, Tom40 and the central receptor protein, Tom22 (both components of the TOM complex) are required for transport of apocytochrome *c* (Diekert *et al.*, 2001; Wiedemann *et al.*, 2003). Transport of apocytochrome *c* across the outer membrane of mitochondria occurs via a pathway that is distinct from the canonical TOM pathway utilized by other proteinstargeted to the mitochondria, suggesting that TOM complex offers more than one pathway for translocation of preproteins across the outer membrane (Diekert *et al.*, 2001). HCCS, the assembly factor for mitochondrial cytochrome *c* acts as an import receptor and facilitates entry of apocytochrome *c* by forming a complex with it (Dumont *et al.*, 1991) followed by catalysis of the heme attachment reaction. Mitochondrial cytochrome c_1, on the other hand, uses a typical N-terminal pre-sequence and the TOM complex to enter the IMS (Sadler *et al.*, 1984). Translocation is driven by the inner membrane potential which facilitates transport of the N terminal signal across the membrane, where a second 'sorting signal' is recognized by the TIM17/23 complex to arrest the protein at the inner membrane (Neupert, 1997; Pfanner *et al.*, 2001), followed by

cleavage of the sorting signal by inner membrane proteases (Imp1/2) and release of the mature protein in the IMS (Nunnari *et al.*, 1993). In addition, the C-terminus of cytochrome c_1 contains a hydrophobic stretch constituting an internal mitochondrial targeting signal that ensures insertion of the protein in the inner membrane in the correct orientation (Arnold *et al.*, 1998).

II.A.3. Transport of apocytochromes in plastids

The *c*-type cytochromes in the chloroplasts are either nuclear-encoded (cytochrome c_6 and cytochrome c_{6A}) or plastid encoded (cytochrome *f*) and contain an N-terminal import signal to the chloroplast (Ballabani *et al.*, 2023; Gabilly *et al.*, 2017). The nuclear encoded apocytochromes contain a bipartite signal sequence for chloroplast import where the first signal targets the apoforms to the chloroplast envelope membrane import apparatus (Nakamoto *et al.*, 2000; Worrall *et al.*, 2008). This first signal is processed upon translocation via the TOC and TIC translocation complexes to generate an intermediate form (Kim *et al.*, 2023; Richardson *et al.*, 2020). This intermediate form carries a N-terminal sequence acting as a signal for translocation across the thylakoid membrane into the lumen using the Sec machinery. The assumption is that translocation across the thylakoid membrane is Sec-dependent because there is no twin arginine motif identifying the ΔpH pathway, the other import pathway into the lumen in the signal sequences of nuclear-encoded plastid apocytochromes (New *et al.*, 2018; Pei *et al.*, 2022). Cytochrome *f* is synthesized in the stroma with an N-terminal extension required for translocation across the thylakoid membrane. *In vitro* experiments have shown that

precursor of tobacco cytochrome *f* can be imported to isolated pea thylakoids using the Sec pathway (Nohara *et al.*, 1996). All apoforms of plastid cytochromes *c* are processed by the lumen resident protease upon import in the lumen (Nakamoto *et al.*, 2000).

II.B. Heme synthesis and delivery

Heme is a prosthetic group and one of the most abundant representatives of a class of molecules known as tetrapyrrolic macrocycles (Bryant *et al.*, 2020). Tetrapyrroles are composed of four pyrrolic rings that are attached to one another via methine bridges, with the only exception being corrinoids which lacks one bridge carbon between the first and the fourth ring (Heinemann *et al.*, 2008). Heme, and other cyclic tetrapyrroles such as bacteriochlorophylls, chlorophylls, Vitamin B_{12}, siroheme, coenzyme F_{430}, and heme d_1 (Banerjee *et al.*, 2003; Bryant *et al.*, 2020; Friedmann *et al.*, 1990) differ in the oxidation states of the pyrrole rings and have the ability to chelate diverse divalent metal ions such as Fe^{2+} (heme), Mg^{2+} (bacteriochlorophylls and chlorophylls), Ni^{2+} (coenzyme F_{430}) and Co^{2+} (vitamin B_{12}) (Heinemann *et al.*, 2008; Thauer *et al.*, 1994; Vavilin *et al.*, 2002). Heme functions as essential moiety for enzymes and electron carriers involved in electron transport and its synthesis is dependent on several enzymes. The heme B (iron-protoporphyrin IX) contains the iron atom coordinated at the center of a large heterocyclic ring called porphyrin (Fig. 1.3) and is synthesized in bacteria and eukaryotes by a highly conserved tetrapyrrole biosynthesis pathway (Layer, 2021; Swenson *et al.*, 2020). Heme biosynthesis occurs in the cytoplasm in bacteria, whereas in animals and fungi, heme synthesis starts and ends in the mitochondria with a few intermediate reactions occurring

in the cytosol (Layer, 2021; Swenson *et al.*, 2020). In photosynthetic eukaryotes, chlorophyll and heme are the main tetrapyrroles and the entire tetrapyrrole synthesis pathway including heme synthesis occurs in the plastids, with chlorophyll being the other major end product (Willows *et al.*, 2023). Chlorophyll and heme are produced via a common pathway until the formation of the tetrapyrrole intermediate called protoporphyrin IX (Fig. 1.4).

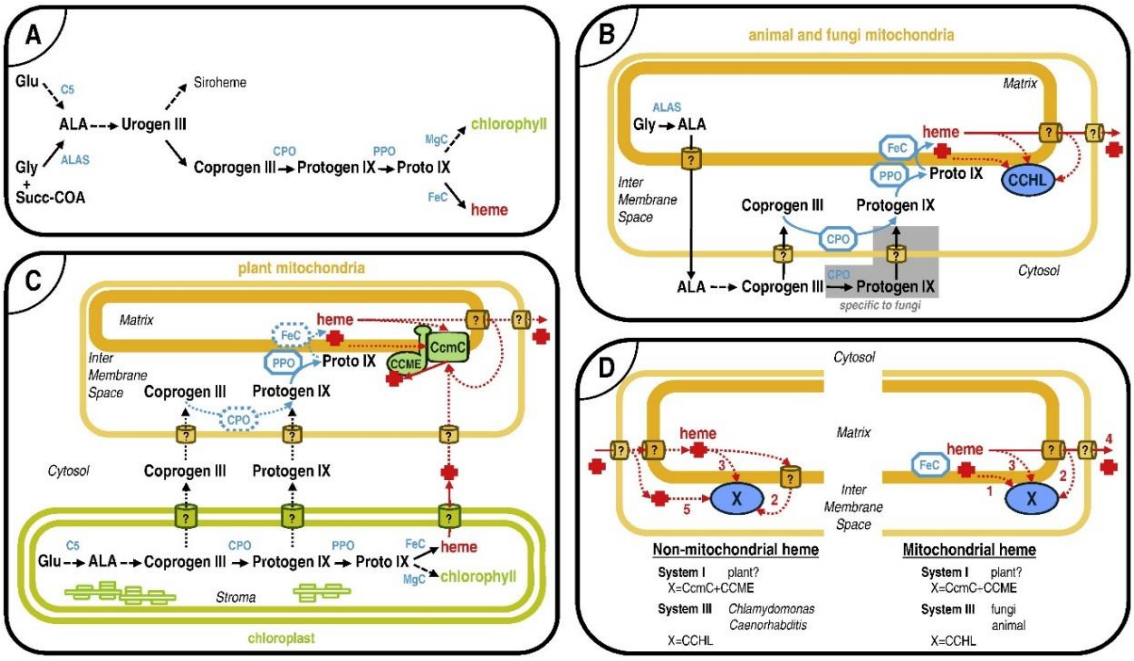

Figure 1.4. Heme synthesis pathway

Heme biosynthesis and trafficking routes in eukaryotes. (A) Shows the part of the tetrapyrrole biosynthetic pathway leading to the synthesis of chlorophyll and heme. C5 stands for the C5 pathway, ALAS for 5-amino-levulinate synthase, CPO for coproporphyrinogen oxidase, PPO for protoporphyrinogen oxidase, MgC for magnesium chelatase and FeC for ferrochelatase. Glu is an abbreviation for glutamate, Gly is for glycine, and Succ-CoA is for succinyl-CoA. Urogen III is an abbreviation for uroporphyrinogen III, Coprogen III for coproporphyrinogen III, Protogen IX for proto-

-porphyrinogen IX and Proto IX for protoporphyrin IX. Siroheme is an iron- containing modified tetrapyrrole similar in structure to both heme and chlorophyll and is synthesized in bacteria and plastids. (B) Shows the localization of the heme synthesis intermediates and enzymes in yeast and animals. (C) Gives the localization of the heme synthesis intermediates and enzymes as well as heme delivery proteins in plant mitochondria. For chloroplasts, the sub-organellar localization of the enzymes is not represented. (D) Proposes alternative routes for the trafficking of heme to its site of assembly with c-type cytochromes in the absence or in presence of FeC in mitochondria. The different routes are proposed for the maturation pathways I and III in different model organisms. The numbers 1 to 5 refer to possible heme delivery routes as described in the text. Broken line arrows represent enzymatic pathways performed in multiple steps, whereas dotted arrows represent hypothetical movements of heme or of heme precursors. Standard arrows represent either single enzymatic steps or accepted heme or heme precursor movements. Cylinders with a question mark symbolize the various transporters, importers or exporters, envisaged for the trafficking of heme or of heme precursors in the respective proposed models. The image is from (Hamel *et al.*, 2009)

Heme biosynthesis starts with the production of 5-aminolevulinic acid (ALA) via two different, and unrelated pathways (Layer, 2021; Swenson *et al.*, 2020). The first pathway, called Shemin pathway, is found in animals and fungal mitochondria, α-proteobacteria, and involves formation of ALA in a single step by condensation of glycine and succinyl-coA by the enzyme 5-aminolevulinic synthase (ALAS). The second pathway, called C5 pathway, is found in most bacteria, archaea, cyanobacteria and in plastids of photosynthetic eukaryotes. The C5 pathway involves a multistep process where ALA is formed from tRNA-bound glutamate. The initial substrate glutamyl-tRNA is reduced by glutamyl-tRNA reductase (GluTR) to form glutamate-1-semialdehyde (GSA) in a NADPH-dependent manner. In the subsequent reaction, GSA is transaminated by pyridoxamine 5'-phosphate (PMP)-dependent glutamate-1-semialdehyde-2,1-aminomutase (GSAM) to form ALA. The subsequent steps of Protoporphyrin IX formation from ALA is common to all organisms and consists of the following steps: 1) formation of the first cyclic tetrapyrrole

intermediate uroporphyrinogen III (UROGEN) by condensation of two ALA molecules, 3) decarboxylation of uroporphyrinogen III to coproporphyrinogen III (COPROGEN), 4) oxidation of coproporphyrinogen III to protoporphyrinogen IX (PROTOGEN) catalyzed by coproporphyrinogen III oxidase (CPO), 5) conversion of protoporphyrinogen IX to protoporphyrin IX (PROTO) by protoporphyrinogen IX oxidase (PPO), and finally 6) insertion of one atom of ferrous iron into protoporphyrin IX by ferrochelatase to form protoheme or heme B**.** In animals and fungi where ALA is synthesized by the Shemin pathway, ALAS is localized in the mitochondrial matrix. After ALA is produced in the matrix, it is released out of the mitochondria into the cytosol where heme synthesis proceeds until the formation of COPROGEN in animals, or PROTOGEN intermediate in fungi. The oxidation of COPROGEN to PROTOGEN occurs in the IMS in animals which is supported by the fact that CPO, the enzymes catalyzing this reaction is also found in the IMS (Elder *et al.*, 1978; Grandchamp *et al.*, 1978). In fungi, on the other hand, CPO resides in the cytosol (Camadro *et al.*, 1986) and catalyzes the oxidation of COPROGEN to PROTOGEN in the cytosol, following which PROTOGEN is transported into the mitochondrial IMS via unknown mechanisms. The conversion of PROTOGEN to Protoporphyrin IX is catalyzed by PPO, which is an IMS-facing enzyme in the inner membrane of mitochondria. The final step of heme synthesis is catalyzed by ferrochelatase (FC, localized in the inner mitochondrial membrane facing the matrix). In photosynthetic eukaryotes, formation of ALA by the C5 pathway and the subsequent steps until the formation of COPROGEN occur exclusively in the plastids. The occurrence of CPO and PPO enzymes in both plastids and mitochondria of land plants suggests that the pathway

downstream of COPROGEN also operates in the mitochondria (Hamel *et al.*, 2009; Pratibha *et al.*, 2017). The unambiguous demonstration that FC also localizes to the mitochondria remains to be provided in land plants (Hamel *et al.*, 2009) but there is increasing evidence supporting FC activity in the mitochondrion (Hey *et al.*, 2016). In the green alga *Chlamydomonas reinhardtii*, a single gene produces two splice variants encoding FC isoforms and re-examination of earlier experimental evidence suggests plastid and mitochondrial localization for each isoform (van Lis *et al.*, 2005) , supporting the view that the mitochondrion in some photosynthetic eukaryotes is also a site for heme synthesis (Willows *et al.*, 2023).

III. DIFFERENT MATURATION SYSTEMS FOR *C*-TYPE CYTOCHROMES

The final step of *c*-type cytochrome maturation is the stereospecific covalent attachment of heme to the conserved C*XX*CH heme binding motif in apocytochrome *c*. This reaction is common to the conversion of all apoforms of *c*-type cytochromes to their respective holoforms, regardless of their occurrence in each energy-transducing system (bacteria, archaea or organelles), or their heme content (monoheme or multiheme). Hence, the identification of different assembly or maturation systems (I, II, III and V) defined by a different set of assembly proteins and unique signature proteins across different species to execute the biogenesis of cytochromes *c* came as a surprise (Babbitt *et al.*, 2015; Gabilly *et al.*, 2017; Kranz *et al.*, 2009; Mavridou *et al.*, 2013; Simon *et al.*, 2011; Travaglini-Allocatelli, 2013; Verissimo *et al.*, 2014) (Fig. 1.5).

Formation of the single heme C (also referee to as heme C*i*) to apoform of cytochromes *c* on the *n*-side occurs via System IV or CCB pathway (**c**ofactor assembly on complex **C** subunit **B**) (Stroebel *et al.*, 2003). Heme C_i is attached to a single cysteine of on the apoprotein and has no amino acid residue providing proximal and distal heme ligands. Heme C_i is found in organisms performing oxygenic photosynthesis including photosynthetic eukaryotes and cyanobacteria and in the bacterial phylum firmicutes (de Vitry, 2011; Kurisu *et al.*, 2003; Stroebel *et al.*, 2003). Since heme C_i is located on the *n*-side of membranes, which is the site of heme synthesis, the CCB pathway is a unique system for cytochrome *c* maturation and does not require a heme transport mechanism unlike for the assembly of cytochromes *c* on the *p*-side.(de Vitry, 2011; Kurisu *et al.*, 2003).

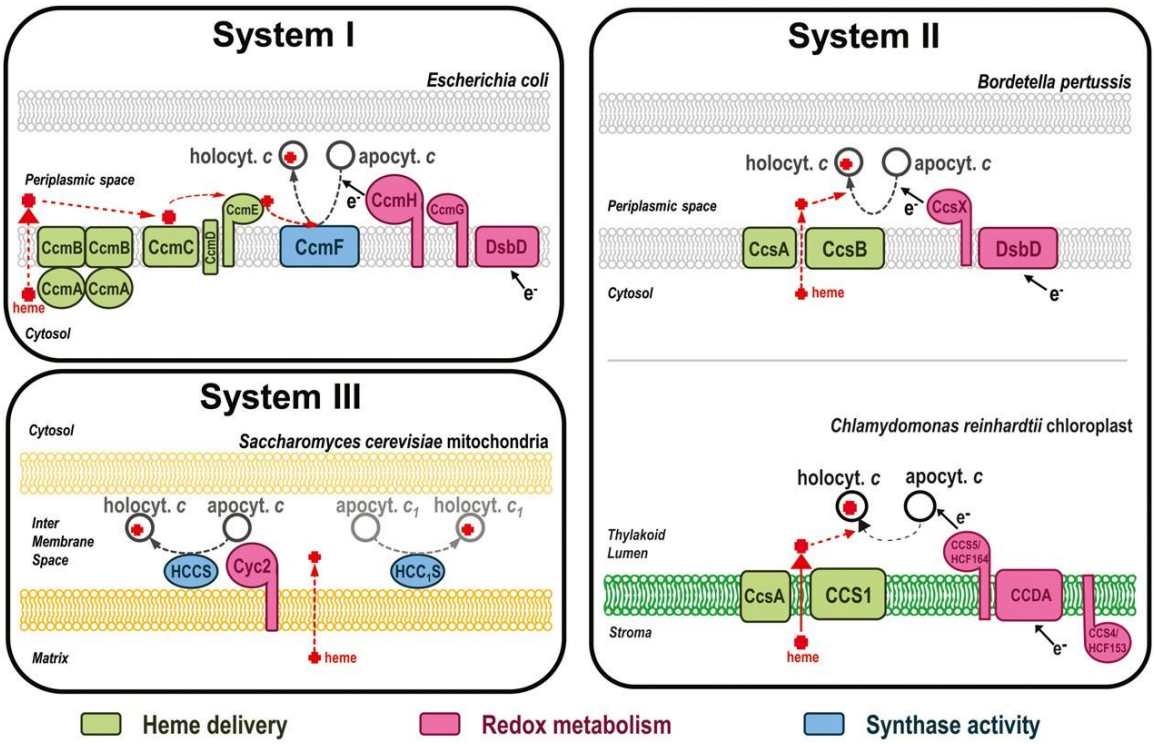

Figure 1.5. Overview of systems I, II and III for cytochromes c assembly

The cytochrome *c* assembly components of bacterial system I (e.g. *E. coli*), bacterial system II (e.g *B. pertussis*), chloroplast system II (e.g. *Chlamydomonas reinhardtii*) and system III (e.g. mitochondria of *S. cerevisiae*) are represented using a color code for assigned function. Green components are involved in heme delivery, the pink components are implicated in redox chemistry (thiol-based chemistry or heme reduction), and the blue components are postulated to carry the holocytochrome *c* synthase function. In grey are the bacterial inner and outer membranes. In orange are the mitochondrial membranes, the outer membrane (light orange) and the inner membrane (dark orange). The thylakoid membrane is shown in green. Some components carry more than one function. For instance, CcmF is a component that carries the heme reduction and the holocytochrome *c* synthase functions. CcsA/ResC and CCS1/CcsB/ResB display the heme delivery and holocytochrome *c* synthase activities. The image is extracted from (Das *et al.*, 2021)

III.A. Different systems of cytochrome *c* maturation

Cytochrome *c* maturation is carried out by a set of eight or nine proteins that belong to **System I or CCM pathway** (**c**ytochrome ***c*** **m**aturation) in α- and γ- proteobacteria, in some β- and a subset of δ- proteobacteria (e.g., *Desulfivibrio desulfuricans*), some gram-positive bacteria (e.g., *Deinococcus*), in all archaea, in the mitochondria of most land plants and some green algae, and several flagellates and ciliates in protozoans (e.g., *Reclinomonas americana*, *Paramecium* spp.). **System II or CCS pathway** (**c**ytochrome ***c*** **s**ynthesis) is comprised of three or four proteins and functions in β- (e.g., *Neisseria and* Bordetella spp.), ε- (e.g., *Helicobacter pylori*) and most representatives of δ- proteobacteria (e.g., *Geobacter metallireducens*), in Gram-positive bacteria (e.g., *Bacillus subtilis*, *Mycobacterium* spp.), cyanobacteria, and in the chloroplasts of all photosynthetic eukaryotes including members of the plant lineage (e.g., land plants, and green and red algae), brown algae, euglenoids, diatoms and heterokonts. There is no evidence of System II functioning outside of bacteria and plastids (Beckett *et al.*, 2000; Das *et al.*, 2021; Le Brun *et al.*, 2000; Travaglini-Allocatelli, 2013).

System III or HCCS pathway (**h**olocytochrome ***c*** **s**ynthase) is confined to the mitochondria of fungi, metazoans, some protozoa (e.g. *Dictyostelium discoideum*), apicomplexan parasites (e.g., *Plasmodium falciparum*), some red and green algae, some land plant species and all animals (Allen, 2011; Babbitt *et al.*, 2015; Das *et al.*, 2021; Giegé *et al.*, 2008; Mavridou *et al.*, 2013; Travaglini-Allocatelli, 2013) **System V or KCCS** (**K**inetoplastid **C**ytochrome **C S**ynthase) pathway is restricted to the mitochondria of Kinetoplastids and Euglenoids which possess mitochondrial *c*-type cytochromes with a F/AXXCH motif, and a heme moiety bound via a single thioether linkage (Allen, 2011; Belbelazi *et al.*, 2021). This system is poorly characterized and KCCS, which appears to be a highly diverged form of HCCS was recently identified in a subtractive phylogenetic approach using the genome information of kinetoplastids (Belbelazi *et al.*, 2021).

Although the different systems share some commonalities, each system can still be recognized by a specific signature factor that interacts with heme during the maturation process : CcmE for system I, CcsB/CCS1 for system II and HCCS for system III The diversity of cytochrome *c* assembly pathways is perplexing but there is an underlying assumption that the assembly components fulfill the biochemical requirements defined for the heme attachment reaction: heme transport to the site of assembly (*p*-side) and handling prior to the attachment reaction, chemical reduction of ferriheme to ferroheme, preparation of the heme linking cysteines by maintaining the thiols in the reduced form and formation of the thioether bond. While System I components have been assigned a biochemical function in the assembly process, there are missing

components for some of the biochemical requirements in Systems II and III (Cline *et al.*, 2016; Das *et al.*, 2021). For example, a mechanism for heme reduction is not apparent in System II and in System III, the components involved in heme transport, heme reduction and the control of the redox state of the heme-linking cysteines are yet to be identified (Cline *et al.*, 2016; Das *et al.*, 2021).

III.B. System I or CCM pathway

Cytochrome *c* maturation by System I or the CCM pathway involves eight to nine components CcmABCDEFGH(I), where CcmBCF are polytopic membrane proteins, CcmEGHI are membrane-anchored proteins with functional domains facing the *p*-side, CcmD is a membrane-anchored protein with a *n*-side exposed domain and CcmA is a soluble protein on the *n*-side. This system is the most studied in α-proteobacteria such as *Rhodobacter*, *Paracoccus,* and *Rhizobium* and *Escherichia coli*, which still remains the model microorganism for bacterial System I (Cline *et al.*, 2016; Das *et al.*, 2021; Kranz *et al.*, 2009; Travaglini-Allocatelli, 2013; Verissimo *et al.*, 2014). For mitochondrial System I, the plant *Arabidopsis thaliana* is the experimental model of choice (Bonnard *et al.*, 2010; Giegé *et al.*, 2008). In *E. coli,* all the Ccm proteins are encoded by a single operon and were thought to co-localize on the bacterial inner membrane forming a 'maturase' supercomplex (Cianciotto *et al.*, 2005; Thöny-Meyer, 1997; Thöny-Meyer *et al.*, 1995). However, in other species, the Ccm components are encoded by two or more genomic loci (*e.g.*, two loci, *ccmABCDG* and *ccmIEFH* in *Bradyrhizobium japonicum* and four loci *ccmADBCDG*, *ccmFH*, *ccmE* and *ccmI* in *Rhodobacter capsulatus*) (Beckman *et al.*, 1992; Deshmukh *et al.*, 2000; Lang *et al.*, 1996; Ramseier *et al.*, 1991). In *Arabidopsis thaliana*,

ccmA, *ccmE*, and *ccmH* are nuclear-encoded (Meyer *et al.*, 2005; Rayapuram *et al.*, 2007; Spielewoy *et al.*, 2001) whereas *ccmBC* and *ccmF* (split into $ccmF_{N1}$, $ccmF_{N2}$ and $ccmF_{C}$) are encoded in the mitochondria (Unseld *et al.*, 1997). Regardless of the genomic distribution in different species, the Ccm components are believed to carry out similar functions that can be divided into different biochemical activities a) delivery and handling of heme by CcmADCDEF, b) heme substrate reduction by CcmF, c) preparation of apocytochrome *c* substrate by reduction of the disulfide between the heme-linking thiols by CcmG and d) thioether bond formation by covalent attachment by CcmF, CcmH and CcmI (Das *et al.*, 2021; Verissimo *et al.*, 2014).

III.B.1. A heme relay system on the p-side

In System I bacteria, heme is synthesized on the *n*-side and the mechanisms of heme transport to the *p*-side remain speculative. In System I mitochondria, the mitochondrial origin of heme is still debated and heme might be imported from the plastid (Hamel *et al.*, 2009). In System I bacteria, heme translocation might be through a protein channel or through the inner and outer leaf of the membrane. (Chambers *et al.*, 2021; Kranz *et al.*, 2009). Synthesis of heme on the *n*-side of the membrane does not seems to a requisite for System I cytochrome *c* maturation since holocytochrome *c* assembly can still proceed in bacterial heme-deficient mutants supplied with exogenous heme (Richard-Fogal *et al.*, 2007). In System I, if the question of heme transport to the *p*-side remains unanswered, the accepted view favors a model in which the heme relay by the Ccm components begins on the *p*-side. Heme interacts with CcmC and is loaded onto a ‘pre-adduct’ complex formed by CcmCDE (Fig. 1.6). After loading, a ‘post-adduct’ complex of CcmCDE is formed

where oxidized heme covalently binds to CcmE (Fig. 1.7). Next, heme containing CcmE is released from CcmC by the activity of CcmAB and is presented to CcmF. CcmF then reduces heme followed by its release from CcmE (Fig. 1.8). Following heme reduction, CcmF, in complex with CcmH, presents heme to apocytochrome *c* for covalent ligation (Fig. 1.9)

III.B.1.a. Formation of 'pre-adduct' complex

The first step of heme relay in System I involves the formation of CcmCDE "pre-adduct" complex (Fig. 6). One key protein in the formation of the pre-adduct complex is CcmC, an integral membrane protein with six transmembrane helices and a short 'WWD' domain and conserved histidines exposed to the *p*-side (Lee *et al.*, 2007). Proteins with 'WWD'

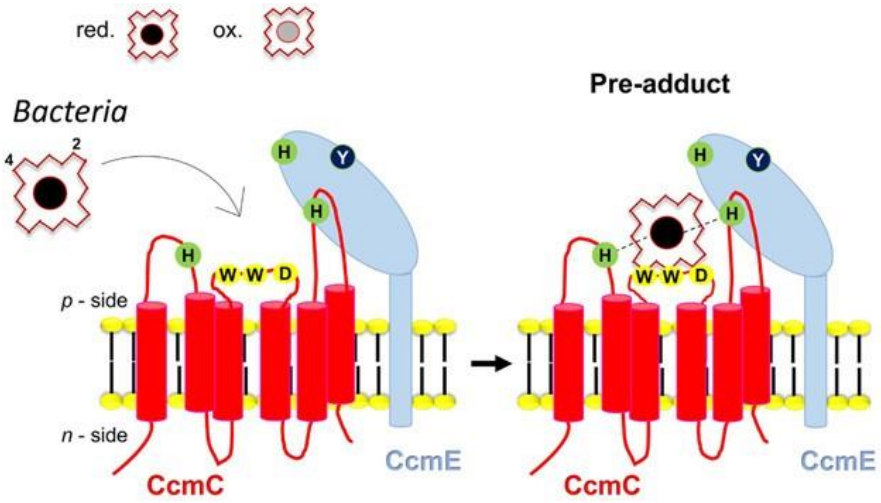

Figure 1.6. Formation of a heme-CcmCDE complex

Reduced heme is loaded onto the "pre-adduct" complex formed by CcmCDE, where heme interacts via "WWD" motif of CcmC.The conserved histidines of CcmC serve asa xial ligands for coordinating the Fe atom of heme and CcmE also provides surfaces of interaction with heme. CcmD is not shown. The image is extracted from (Das *et al.*, 2021).

domain in a conserved 'WGXΦWXWDXRLT' motif (Φ represents an aromatic residue and X represents any residue) belong to 'heme handling protein' or 'HHP' family (Beckman *et al.*, 1992; Goldman *et al.*, 1998; Lee *et al.*, 2007). CcmC belongs to the 'HHP' family and has been shown to interact with heme directly by affinity chromatography on hemin agarose (Ren *et al.*, 2001; Richard-Fogal *et al.*, 2010). Reduced heme is loaded onto this complex via interaction with 'WWD' domain of CcmC and axial ligation by the *p*-side histidines. While the tryptophan-rich motif and the conserved His residues of CcmC are not absolutely required for heme binding, they are, however, required for interaction with CcmE. Chemical cross-linking experiments (Sutherland *et al.*, 2018) and the recent CryoEM structure of CcmC with exogenous heme (Li *et al.*, 2022) support the view that *p*-side histidines and several residues in the WWD motif provide interaction with heme in CcmC. The small CcmD protein consists of one transmembrane domain and interacts with CcmC and is required for the interaction between CcmC and CcmE (Ahuja *et al.*, 2005; Schulz *et al.*, 1999). CcmE is also required for heme binding to CcmC and a buried heme-binding site in CcmE serves as an additional surface of interaction of heme in the CcmCDE complex (Das *et al.*, 2021; Harvat *et al.*, 2009; Kranz *et al.*, 2009).

III.B.1.b. Formation of 'post-adduct' complex

The second step involves the formation of a 'post-adduct' CcmCDE complex (Fig. 1.7) containing ferriheme covalently linked via its vinyl-2 to an histidine in a conserved H*XXX*Y motif in CcmE, while being axially ligated by the CcmC *p*-side histidines (Das *et al.*, 2021; Kranz *et al.*, 2009). Following this, heme containing CcmE is released from

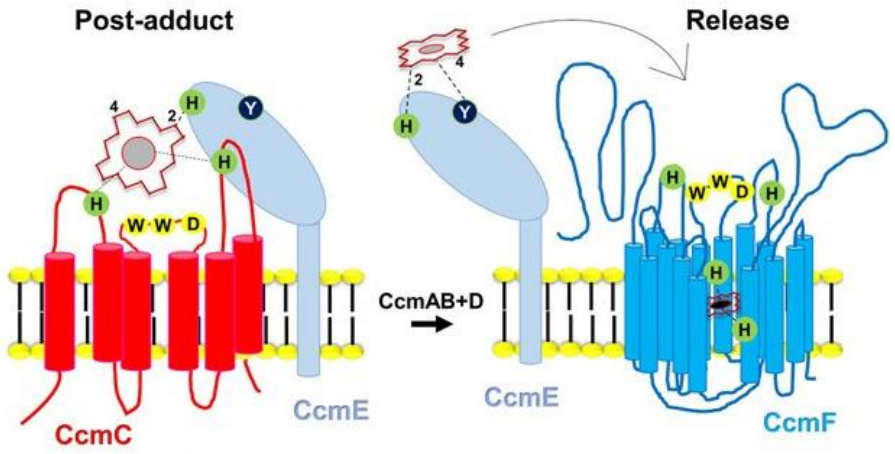

Figure 1.7. Formation of a post-adduct CcmCDE complex and release of heme containing CcmE

A 'post-adduct' complex of CcmCDE is formed where heme is oxidized and covalently linked to a conserved histidine of CcmE via the vinyl-2, while still axially ligated by CcmC histidines. Next, heme containing CcmE is presumed to be released from CcmC by the activity of CcmAB and is also dependent upon CcmD. The image is extracted from (Das *et al.*, 2021).

CcmC by the action of CcmA and CcmB via the ATP*ase* activity which provides the mechanical force for this release (Fig. 1.7) (Das *et al.*, 2021; Travaglini-Allocatelli, 2013). CcmA and CcmB belong to the ABC transporter family (**A**TP **b**inding **c**assette) and were, therefore, initially considered to be responsible for translocation of heme from *n*-side to the *p*-side of the membrane (Travaglini-Allocatelli, 2013). CcmA is a soluble, *n*-side protein and has been shown to possess ATP*ase* hydrolysis activity *in vitro* (Christensen *et al.*, 2007). CcmB is a six transmembrane domain, integral protein and is always encoded adjacent to *ccmA*. Heme containing CcmE is released from CcmC only when CcmA and CcmB are coexpressed (Kranz *et al.*, 2009; Travaglini-Allocatelli, 2013) and the heme on released CcmE is no longer coordinated by CcmC histidines and is axially ligated by the conserved tyrosine residue in the H*XXX*Y motif of CcmE (Das *et al.*, 2021; Kranz *et al.*,

2009) (Fig. 1.7). The release of heme containing CcmE is also dependent on the presence of CcmD (Richard-Fogal *et al.*, 2008). Released heme binding CcmE is then free to interact with CcmF and CcmH, which exist in a "holocytochrome *c* synthase complex (Ren *et al.*, 2002; San Francisco *et al.*, 2014; Sanders *et al.*, 2008).

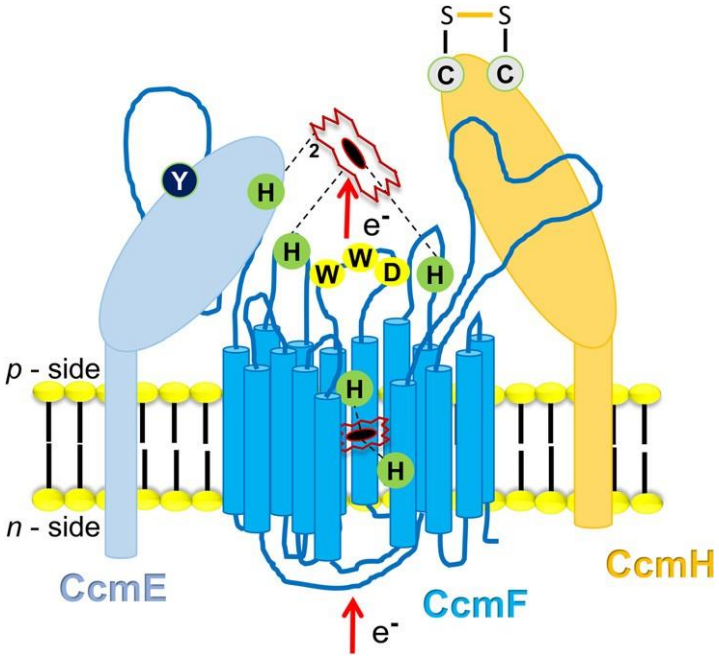

Figure 1.8. CcmF-dependent Heme reduction

CcmF contains a non-covalently bound structural heme B coordinated axially by conserved histidines present in its transmembrane domains. CcmF transfers electrons to the ferriheme bound to CcmE via the B-type heme, resulting in its reduction to ferroheme and presumed release from CcmE. In complex with CcmH, CcmF is postulated to present heme to apocytochrome *c* via "WWD" motif for covalent attachment. Heme is shown coordinated via the CcmF histidines and still covalently attached to CcmE. The disulfide bond in CcmH is shown in yellow, and the electron transfer is shown by red arrows. The image is extracted from (Das *et al.*, 2021).

III.B.2. Heme reduction by CcmF

With 15 transmembrane domains, a conserved heme-interacting 'WWD' domain and histidines on the *p*-side CcmF is a large integral membrane protein of the 'Heme Handling Protein' (HHP) family (Lee *et al.*, 2007; Ren *et al.*, 2002; Travaglini-Allocatelli, 2013) whose 3D structure was recently solved (Brausemann *et al.*, 2021) (Fig. 1.8). Spectroscopic and biochemical analyses of recombinant CcmF revealed the presence of a membrane embedded structural heme B with bis-histidinyl coordination that is also detected in the tertiary structure of the protein (Brausemann *et al.*, 2021; Richard-Fogal *et al.*, 2009).

The structural heme is positioned below a large within-membrane cavity that opens toward the outer leaflet of the lipid bilayer and is partially capped by the *p*-side exposed WWD domain of CcmF (Brausemann *et al.*, 2021). Molecular docking analysis suggests that this internal cavity could act as a binding pocket for the heme substrate, which is presented to CcmF as covalently bound to CcmE. While the current model suggests that heme chaperoned by CcmE reaches CcmF from the soluble milieu on the *p*-side, the presence of this putative heme binding cavity favors an alternative model where the heme substrate is provided for the ligation reaction from within the membrane (Brausemann *et al.*, 2021; Brown *et al.*, 2021). Because heme iron is oxidized in the CcmCDE complex and must undergo reduction to be detached from CcmE, the proposed model is that the structural heme in CcmF is ideally located to serve as redox center to transfer electrons for reduction of the heme substrate in the cavity (Brausemann *et al.*, 2021; Das *et al.*, 2021). Although the source of reducing power *in vivo* is not yet identified, a putative quinol-binding pocket

was identified in CcmF and quinol-dependent reduction of CcmF structural heme was observed *in vitro* (Mavridou *et al.*, 2013; Richard-Fogal *et al.*, 2009). Other natural reductants such as flavin or NADH could also serve as the source of electrons based on the midpoint potential of CcmF structural heme (Richard-Fogal *et al.*, 2009).

III.B.3. Heme ligation by CcmF

After reduction of the heme substrate, CcmF, in complex with CcmH (CcmHI in instances where CcmI is a separate component), catalyzes formation of thioether bond formation via its synthase activity (Das *et al.*, 2021; Kranz *et al.*, 2009) (Fig. 1.9). There is biochemical evidence that CcmF interacts with CcmH and constitutes the minimal System I holocytochrome *c* synthase (Ren *et al.*, 2002; San Francisco *et al.*, 2014; Verissimo *et al.*, 2011). In *Arabidopsis*, CCMF is split into $CCMF_{N1}$, $CCMF_{N2}$ and $CCMF_{C}$. Arabidopsis CCMH, heterologously produced in *E. coli*, immunoprecipitates with bacterial CcmF. In mitochondria, CCMH exists in a high molecular weight complex with all three CCMF proteins (Meyer *et al.*, 2005). In bacteria, the pentaheme cytochrome *c* NrfA requires CCMF/CCMH orthologs solely dedicated to attach heme to the atypical CXXCK (CWSCK) heme binding motif, an observation that reinforces the notion that CcmFH carries the heme ligation activity in cytochrome *c* assembly (Eaves *et al.*, 1998).

CcmH is a membrane-bound thiol-disulfide oxidoreductase, with a soluble domain facing the *p*-side and containing a redox active CXXC motif. The C-terminal of CcmH displays features of a TPR (tetratricopeptide repeat) domain. In some bacteria, this domain occurs as a distinct component (CcmI) whose proposed function is to chaperone apocytochrome

c prior to the heme ligation reaction (Verissimo *et al.*, 2015). The crystal structure of the soluble domain of bacterial CcmH revealed a three-helix bundle fold that is unlike any other thiol-oxido reductase (Di Matteo *et al.*, 2007). Exposure of the C-terminal cysteine to solvent indicates that this residue is the reactive one when forming the mixed disulfide with the apocytochrome *c* substrate. *In vitro*, a recombinant form of CcmH soluble domain can form a crosslink between the second cysteine of its redox motif and the first cysteine

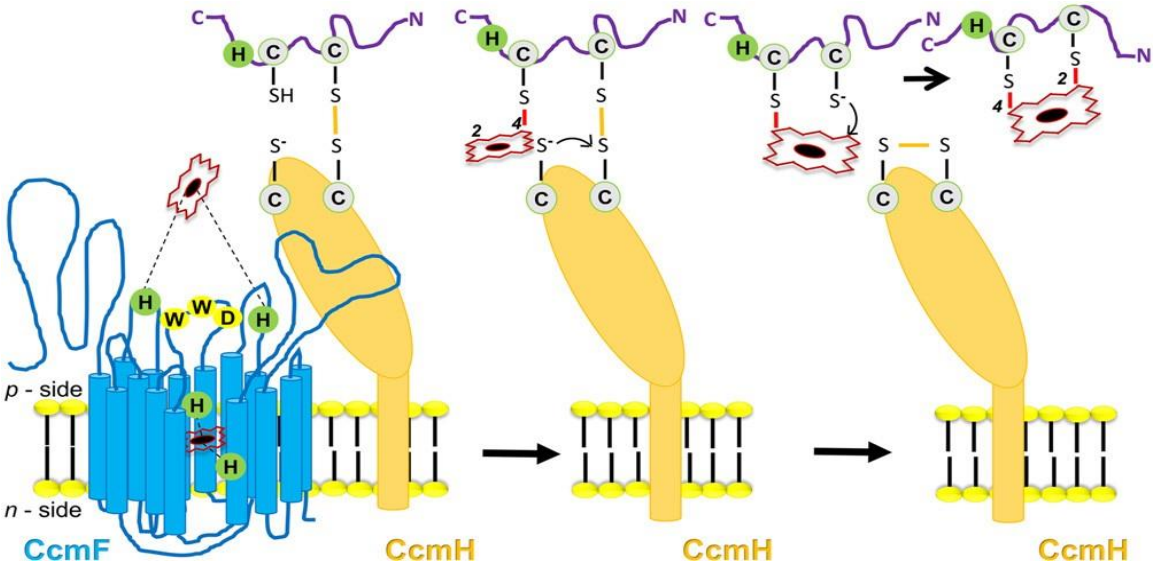

Figure 1.9. CcmF-dependent heme ligation

CcmF presents heme to apocytochrome *c* via the "WWD" domain, and the conserved histidine of the C*XX*CH motif of apocytochrome *c* could function as the axial ligand to coordinate heme. CcmH forms a disulfide link (yellow bond) with the first cysteine of apocytochrome *c*, followed by formation of thioether linkage between the second cysteine of apocytochrome *c* with 4-vinyl group of heme (red bond). The last step of heme ligation involves formation of the second thioether bond between the first cysteine of apocytchrome *c* and 2-vinyl of heme, and reoxidation of CcmH. CcmH is re-oxidized via resolution of the CcmH-apocytochrome *c* disulfide via CcmG (not shown) or via the second cysteine of CcmH as shown on the figure. The image is extracted from (Das *et al.*, 2021).

of C*XX*CH motif of apocytochrome *c* (Di Matteo *et al.*, 2007; Verissimo *et al.*, 2014; Verissimo *et al.*, 2017). This finding led to the hypothesis that formation of this disulfide bond between CcmH and apocytochrome *c* provides redox control and enable the formation of the first thioether bond between the second cysteine of apocytochrome *c* and the 4-vinyl group of heme, which is presented to apocytochrome *c* via 'WWD' domain of CcmF (Fig. 1.9). Formation of the first thioether bond is followed by the second thioether bond formation between the first cysteine of CcmH and 2-vinyl of heme, and reoxidation of CcmH by CcmG or, by the second cysteine of CcmH (Das *et al.*, 2021; Verissimo *et al.*, 2017) (Fig. 1.9). The crystal structure of the soluble domain of bacterial CcmH revealed a three-helix bundle fold that is unlike any other thiol-oxido reductase (Di Matteo *et al.*, 2007). Recently, the solved structure of recombinant CcmF from *Thermus thermophilus* provided a possible mechanistic view of heme transfer from CcmE to CcmF (Brausemann *et al.*, 2021).

The crystal structure of CcmF uncovered that this integral membrane protein harbors two vestibules that are separated by a narrow, hydrophobic constriction. Both vestibules form heme binding cavities, one on the cytoplasmic side and one on the periplasmic side. However, the structural heme B is found only on the cytoplasmic binding cavity while the periplasmic cavity opens up towards the periplasm (Brausemann *et al.*, 2021). The NMR structure of free CcmE revealed a compact β-barrel fold indicating that the heme cofactor, when bound, must be largely exposed to the milieu (Arnesano *et al.*, 2002; Brausemann *et al.*, 2021; Enggist *et al.*, 2002). One attractive model is that the periplasmic cavity in CcmF provides a lipid environment to receive the heme substrate when attached to CcmE.

While a role of the ABC transporter CcmAB in heme transport across the membrane (Page *et al.*, 1999; Schulz *et al.*, 1999) has been ruled out, Bauman et al. have formulated alternative model in which CcmAB could function as a heme flippase to enrich heme on the periplasmic side for delivery to CcmE or control the rotation of the heme substrate to facilitate presentation to CcmE (Brausemann *et al.*, 2021). Regardless of the mechanism by which heme is relayed across the membrane, the following model is favored in which once heme is loaded onto CcmE via CcmC, it is presented to the periplasmic vestibule of CcmF. At this step, CcmE functions as a chaperone and ensures heme is inserted in CcmF in the correct orientation to facilitate stereospecific attachment of heme to apocytochrome *c* in the subsequent step (Brausemann *et al.*, 2021).

III.B.4. Substrate specificity of system I

Although System I was initially thought to recognize substrates that minimally contains two cysteine thiols in the heme-binding motif (C_1XXC_2H) (Allen *et al.*, 2009; Allen *et al.*, 2002), later studies on single-cysteine variants evidence that System I also supports formation of holocytochrome with A*XX*CH motif (but not C*XX*AH) (Goddard *et al.*, 2010). This system also recognizes substrates that are as short as 10-12 residues in length (Braun *et al.*, 2005) and substrates that contain multiple hemes (demonstrated by the characterization of decaheme cytochrome *MtrA* in *Shewanella oneidensis*) (Pitts *et al.*, 2003).

III. C. SYSTEM II or CCS PATHWAY

The CCS pathway (**c**ytochrome ***c*** **s**ynthesis) or System II first emerged during analysis of cytochrome *c* assembly in the green alga *Chlamydomonas reinhardtii* (Das *et al.*, 2021; Gabilly *et al.*, 2017; Simon *et al.*, 2011; Xie *et al.*, 1998; Xie *et al.*, 1998), and later in the bacteria *Bordetella pertussis* (Beckett *et al.*, 2000; Feissner *et al.*, 2005; Kranz *et al.*, 2002) and *Bacillus subtilis* (Le Brun *et al.*, 2000; Schiött *et al.*, 1997; Schiött *et al.*, 1997). The first System II components to be described are two integral membrane proteins, CCS1 and CcsA identified during a genetic screen of 'cytochrome *c* synthesis' or ***ccs*** mutants in *C. reinhardtii* (Xie *et al.*, 1998; Xie *et al.*, 1996, 1998). In *B. subtilis*, CCS1 and CcsA are known as ResB and ResC, because the genes encoding these proteins are part of the *resABCDE* cluster on the chromosome (Sun *et al.*, 1996). The CCS pathway was also recognized as a cytochrome *c* maturation pathway in cyanobacteria, the ancestor of the chloroplast by the identification of CcsB/ResB, the signature assembly factor of System II (Kranz *et al.*, 2009; Simon *et al.*, 2011). In System II, CCS1/CcsB/ResB and CcsA/ResC combine the activity of heme transfer from *n*-side to the *p*-side and the covalent attachment to apocytochrome *c*. On the other hand, cysteinyl thiols of the C*XX*CH motif in apocytochrome *c* are maintained in a reduced state by ResA/CcsX (in System II bacteria such as *B. pertussis* and *B. subtilis*). Also known as CCS5/HCF164 in chloroplasts, ResA/CcsX/CCS5 are reduced by the provision of reductants by a transmembrane thiol disulfide oxidoreductase (TDOR), DsbD in most bacterial Systems II. In other System II bacteria and in plastids, CcdA is the TDOR involved in the transfer of electrons (Das *et al.*, 2021; Gabilly *et al.*, 2017; Hamel *et al.*, 2009; Simon *et al.*, 2011). The details of the

cytochrome *c* maturation by System II pathway are described below. For simplicity, I will use CcsB/ CCS1 and CcsA when referring to the proteins.

III.C. 1. Heme delivery from *n*-side to the *p*-side and ligation to apocytochrome *c*

Conserved features of CcsB/CCS1 and CcsA proteins include histidine residues, one in the transmembrane domain of CcsB, one in the transmembrane domain of CcsA, two in the periplasmic domain of CcsA, and a 'WWD' motif in CcsA (Dreyfuss *et al.*, 2003; Sutherland *et al.*, 2018). A subset of System II bacteria, such as in *Helicobacter, Bacteroides, Wolinella* and *Campylobacteria* encode CcsB and CcsA as a single, fused open reading frame, an indication that CcsBA interact functionally (Frawley *et al.*, 2009; Kranz *et al.*, 2009; Richard-Fogal *et al.*, 2009). This view is reinforced by the finding that CCS1/CcsB and CcsA can be detected as a protein complex in plastids and bacteria (Feissner *et al.*, 2005; Hamel *et al.*, 2003).

The presence of a tryptophan – rich "WWD" motif (WGXΦWXWD, where Φ is an aromatic residue) histidinyl residues that are known heme ligands in both CcsA and Ccs1/CcsB, and the occurrence of CcsA and Ccs1/CcsB in a complex, led to the speculation the two proteins work together to deliver heme from *n*-side to *p*-side of the membrane (Das *et al.*, 2021; Dreyfuss *et al.*, 2003; Gabilly *et al.*, 2017) (Fig. 1.10). Biochemical purification of recombinant *H. hepaticus* CcsBA identifies *n*- and *p*-side heme binding domains and supports the view that CcsBA work as a heme channel (Frawley *et al.*, 2009)which exploits the natural tendency of a cysteinyl thiol and heme vinyl group to spontaneously form a thioether bond when in close proximity, have shown that CcsBA

binds heme via its ‘WWD’ domain in the absence of the acceptor apocytochrome *c*, unlike CcmC, where heme crosslinking to the ‘WWD’ domain is dependent on the presence of the acceptor CcmE (Sutherland *et al.*, 2018; Sutherland *et al.*, 2018). Heme co-purifies with recombinant CcsBA but is no longer detected when both *p*-side histidines in CcsA are altered by site-directed mutagenesis (Frawley *et al.*, 2009). This led to the definition of an external heme binding domain provided by the WWD domain and the *p*-side histidines, which might serve a platform for heme presentation to apocytochrome *c* (Fig. 1.10). The proposal that heme is translocated to the *p*-side via CcsBA by entering an internal heme binding domain was based on the observation that upon mutation of the histidine residues, heme was no longer bound to purified CcsBA and cytochrome *c* assembly was abolished as well (Frawley *et al.*, 2009). A defect in cytochrome *c* assembly in CcsBA due to alteration of the *n*-side histidine could be rescued by application of exogenous imidazole (side chain in histidine). This finding substantiated the notion of heme binding pocket in CcsBA whose access is provided by the *n*-side histidine residues (Das *et al.*, 2021; Kern *et al.*, 2010; Richard-Fogal *et al.*, 2009; Sutherland *et al.*, 2018) (Fig. 10). CryoEM-derived structures of CcsBA revealed the occurrence of two states for the heme translocator (Mendez *et al.*, 2022). In one state, heme is trapped at the internal heme binding site on the *n*-side and the periplasmic domain locks the CcsBA channel in a closed conformation (Mendez *et al.*, 2022). In the other state, heme is found in both internal and external binding sites of the channel. The occurrence of heme in the external binding site on the *p*-side produces an open conformation of the CcsBA channel, creating a periplasmic reaction

chamber where heme is accessible and ideally positioned to react with the thiols of the C*XX*CH motif (Mendez *et al.*, 2022).

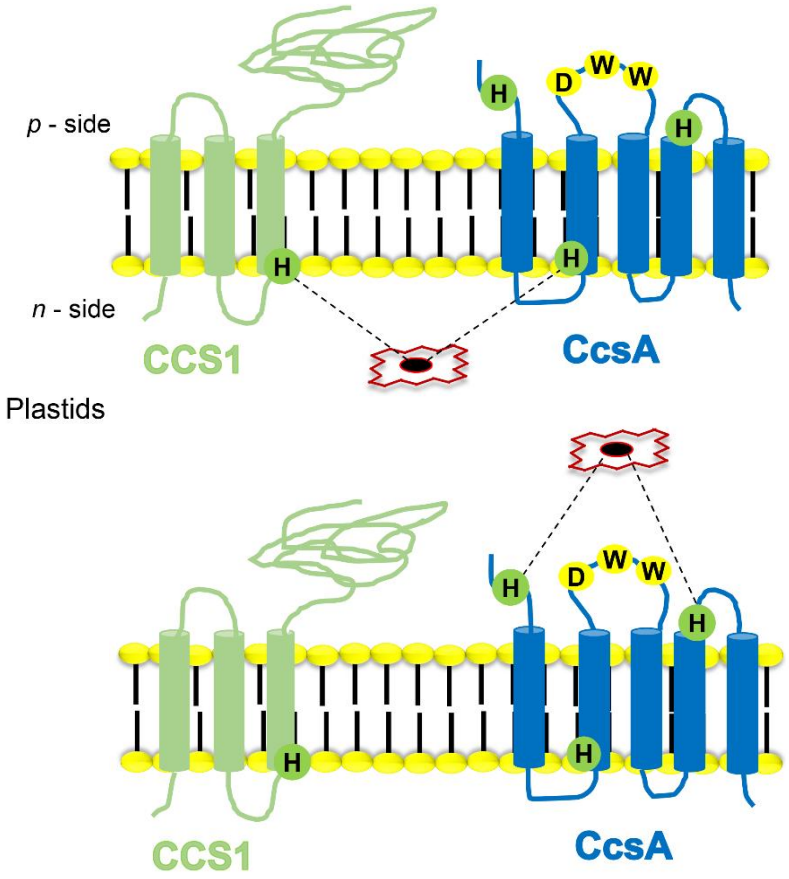

Figure 1.10. CCS-dependent heme translocation from *n*-side to *p*-side

CCS1 and CcsA function as a complex to deliver heme across the thylakoid membrane and also a holocytochrome *c* synthase. The plastid heme trafficking pathway is inferred from the analysis of bacterial natural CcsBA fusion where CcsB corresponds to CCS1. The *n*-side histidines coordinate heme and provide an entry site into the Ccs heme exporter. Heme is translocated across the lipid bilayer and handled by the "WWD" motif and coordinated by the *p*-side histidines, that form the external heme binding site CcmC, CcmF and CcsA are heme handling proteins (HHP family) that contain conserved "WWD" motif, represented by yellow circles. Conserved histidines that participate in axial ligation of heme are represented by green circles.

The requirement of a trans-thylakoid disulfide-reducing pathway in system II was first established by forward and reverse genetics approach in bacteria and plastids and are described in more details in the 'Disulfide bond reduction in plastids' section and in Chapter 2.

III.D. System III or HCCS pathway

III.D.1. HCCS carries the heme ligation reaction

In animal and fungal mitochondria, the heme attachment reaction during holocytochrome *c* maturation is catalyzed holocytochrome *c* synthases or HCCS by System III or HCCS pathway (Allen, 2011; Hamel *et al.*, 2009). The initial definition of a holocytochrome *c* synthase, previously incorrectly known as heme lyase, came from biochemical work in yeast where the *CYC3* gene was cloned and proposed to encode CCHL (now HCCS), the enzyme catalyzing heme ligation to apocytochrome *c* (Dumont *et al.*, 1987). CC_1HL (now HCC_1S) is encoded by the *CYT2* gene and was discovered by the study of yeast mutants with a specific defect in holocytochrome c_1 accumulation (Zollner *et al.*, 1994). Although HCCS and HCC_1S were initially described to be specific for the maturation of cytochrome *c* and c_1 respectively, only HCC_1S specificity towards cytochrome c_1 appeared to be strict, while HCCS reactivity towards cytochrome c_1, although inherently weak, could be promoted by amino acid substitutions in HCCS or cytochrome c_1 (Bernard *et al.*, 2003; Das *et al.*, 2021; Hamel *et al.*, 2009). In multicellular eukaryotes, a single HCCS occurs and acts on both apocytochrome *c* and c_1. HCCS mediated cytochrome *c* assembly is proposed to follow a four step process (Fig. 1.11): 1) HCCS binds to heme (Fe^{2+}) non

covalently, while a strictly conserved Histidine residue acts as the axial ligand to the heme iron, 2) Heme-containing HCCS binds to apocytochrome *c*, with the histidine of the C_1XXC_2H motif serving as the second axial ligand for the iron in the heme substrate, bringing C_2 of the apocytochrome *c* heme binding motif next to vinyl-4 of heme and C_1 next to vinyl-2 of heme, 3) the C_1 and C_2 thiols spontaneously forms thioether linkage with vinyl carbons in heme, and 4) holocytochrome *c* is released from HCCS to undergo protein folding (Babbitt *et al.*, 2017; Babbitt *et al.*, 2015; San Francisco *et al.*, 2013).

This four step model of HCCS-mediated cytochrome *c* maturation is derived from the reconstitution of human holocytochrome *c* assembly by its cognate HCCS in the bacterial cytoplasm (Babbitt *et al.*, 2015). The *in vitro* reconstitution of holocytochrome *c* synthase activity using equine apocytochrome *c* was recently achieved (Sutherland *et al.*, 2021). In reducing conditions, heme binding by HCCS in step 1 is followed by recognition of the apocytochrome *c* peptide in step 2, provided the peptide is minimally 16-mer and contains

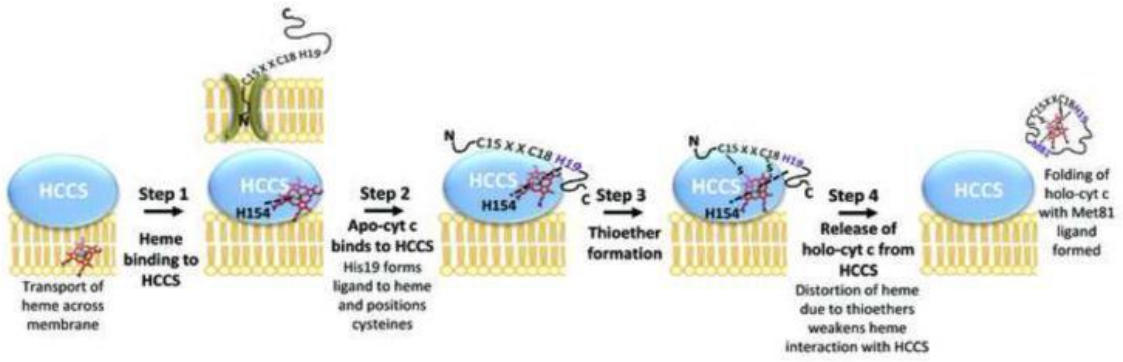

Figure 1.11. Mechanisms of cytochrome *c* biogenesis by mitochondrial HCCS

The schematic depicts the ordered step of HCCS-mediated cytochrome c assembly. HCCS is represented as a blue oval with its heme ligand (His). Heme is in red with a grey iron (Fe2+) atom. Apocytochrome c is depicted in its unfolded state with the conserved CXXCH motif and its N and C termini. The image and legend are from (Babbitt *et al.*, 2015).

the N -terminal α-helix 1 sequence that is critical for recognition could be achieved (Sutherland *et al.*, 2021). Since the mitochondrial *c*-type cytochromes in Euglenozoa contains an uncharacteristic XXXCH motif (Babbitt *et al.*, 2017), the importance of the presence of two thiols for substrate recognition by HCCS was tested by substituting each cysteine of the C*XX*CH motif in apocytochrome with serine, homocysteine and D-cysteine. All substitutions were recognized by HCCS *in vitro* and led to the formation of at least a single thioether bond, suggesting that the specificity of recognition could depend on the N-terminal α-helix and the proximal axial ligand in apocytochrome *c* (Sutherland *et al.*, 2021).

III.D.2. Cyc2p, a heme reductase in variants of system III

Cyc2p is considered an auxiliary cytochrome *c* assembly factor as it appears to be restricted to fungi where HCCS and $HCCS_1$ activities are carried by two distinct proteins (Allen, 2011). Cyc2p was first identified in the genetic analysis of mutants deficient for cytochrome *c* assembly in yeast mitochondria. Cyc2p is anchored to the inner membrane with an IMS-facing domain containing a FAD moiety (Bernard *et al.*, 2005). The ability of recombinant Cyc2p to carry the NADPH-dependent reduction of ferricyanide, led to the postulation that Cyc2p is a redox component assisting the cytochrome *c* assembly process (Bernard *et al.*, 2003; Bernard *et al.*, 2005; Corvest *et al.*, 2012). Detailed phenotypic analyses of *cyc2* mutants in yeast revealed that Cyc2p is not strictly necessary for the maturation of mitochondrial cytochrome *c*, because a *cyc2* null mutant can still accumulate residual levels of holocytochrome *c* (Bernard *et al.*, 2005). Application of exogenous reductants such as TCEP and DTT can compensate for the loss of Cyc2p, a finding that

supports the view that the protein functions in providing reducing equivalents in the heme attachment reaction (Corvest *et al.*, 2012). Based on the similarity between Cyc2p and cytochrome b_5 reductase-like proteins that reduce heme in cytochrome b_5, it was postulated that Cyc2p acts a heme reductase (Bernard *et al.*, 2005), and a recombinant form of Cyc2p is able to catalyze NADP(H)-dependent reduction of hemin *in vitro*, but is not active as a apocytochrome c/c_1 C*XX*CH disulfide reductase (Corvest *et al.*, 2012). Y2H experiments show that Cyc2p interacts with HCCS (but not HCCS1) as well as with apocytochrome *c* and c_1, suggesting Cyc2p is a dedicated heme reductase for HCCS-dependent cytochrome maturation.

Pioneer experiments in yeast evidenced that heme reduction requires NADPH and FAD for *in organello* reconstitution of soluble holocytochrome *c* assembly but NADH and FMN for the conversion of membrane apocytochrome c_1 to its corresponding holoform (Bonnard *et al.*, 2010; Hamel *et al.*, 2009). This suggests the operation of a distinct heme reductase for $HCCS_1$ dependent maturation of holocytochrome c_1. In organisms where one HCCS assembles both cytochrome *c* and c_1, the identity of the heme reductase remains elusive as no Cyc2p-like proteins can be identified.

IV. THIOREDOXINS

Considering the focus of my Ph.D. work on thiol-disulfide chemistry in the context of cytochrome *c* assembly, I describe in this section thioredoxins and thioredoxin-like proteins which are enzymes mediating thiol-disulfide exchanges in several biological systems.

Thioredoxins (Trxs) are one of the major molecules that function in pathways that catalyze disulfide bond reduction (Collet *et al.*, 2010). First discovered in *E. coli* in 1964, Trxs are small 12-kDa enzymes (Laurent *et al.*, 1964; Moore *et al.*, 1964) present in nearly all organisms from bacteria to animals, including photosynthetic organisms such as *Chlamydomonas reinhardtii*, which has served as model organism to study Trx function for many years (Lemaire *et al.*, 2003). Trxs are classified as a general protein disulfide reductant because their target is a structural or regulatory disulfide in protein substrates. Because Trxs play a key role in redox regulation and oxidative stress response, they are viewed as antioxidant enzymes (Michelet *et al.*, 2009).

IV.A. Thioredoxin conserved residues, mechanism, and structure

All Trx proteins contain a highly conserved fold, referred to as the Trx fold that consists of a conserved WCGPC redox active motif. While there are several conserved residues in Trxs proteins, the invariable residues that participate directly in the thiol-disulfide reactions are the essential cysteine residues in the CGPC motif in the catalytic site. The N-terminal active cysteine in the CGPC motif is highly reactive due to low pKa (pKa~7) (Dillet *et al.*, 1998; Dyson *et al.*, 1991), and can perform a nucleophilic attack on the disulfide bond of a target protein, resulting in the release of a free thiol and formation of a mixed disulfide between Trx and the substrate. This disulfide is then immediately resolved by the second active cysteine in the CGPC motif, which has a higher pKa (pKa~9) and is present as a thiol (Bulaj *et al.*, 1998; Lutolf *et al.*, 2001), resulting in the release of a reduced substrate and oxidized Trx (Collet *et al.*, 2010; Roos *et al.*, 2009). Trx is then converted back into

the reduced state by reduction by thioredoxin reductase (TrxR) at the expense of NADPH (Collet *et al.*, 2010; Jacquot *et al.*, 1994; Lennon *et al.*, 2000). Trxs also contain three conserved proline residues, with one of them located between the cysteines of the catalytic motif. This proline residue is key and maintains the reducing power of Trxs, and substituting this residue with serine or threonine vastly affects the proteins redox state and stability (Krause *et al.*, 1991; Lewin *et al.*, 2008; Mössner *et al.*, 1998; Roos *et al.*, 2007). The second conserved proline residue, located five residues away from the catalytic motif, is not essential for the redox properties of the protein but mutating this residue destabilizes the structure of Trx (Chakrabarti *et al.*, 1999; de Lamotte-Guéry *et al.*, 1997). The third conserved proline residue is located in a cis-conformation across the CGPC catalytic motif and is essential for maintaining the conformation of the active site as well as the redox potential of the protein (Gleason, 1992).

During the assembly of cytochromes *c*, a major component required for the direct reduction of apocytochrome *c* is a Trx-like protein *viz*., CcmG/HelX in System I and ResA/CcsX/CCS5/HCF164/ in System II, (Cline *et al.*, 2006; Colbert *et al.*, 2006; Gabilly *et al.*, 2010; Hodson *et al.*, 2008; Lennartz *et al.*, 2001; Motohashi *et al.*, 2006) . Trx-like proteins are typically larger molecules and hence not classified as Trx. They do contain a conserved Trx-like fold. The difference between Trxs and a protein containing a Trx-like fold is illustrated in Fig. 1.12, which is derived from the first crystal structure of a Trx determined by Holmgren *et al.* in 1975 (Holmgren *et al.*, 1975). Fig. 1.12 shows that the fold of Trx proteins contains five β-strands surrounded by four α-helices. The β-sheets and α-helices can be divided into N-terminal $\beta_1\alpha_1\beta_2\alpha_2\beta_3$ and C-terminal $\beta_4\beta_5\alpha_4$ connected by

the α_3-helix. The β sheets at the N-terminal run parallel to each other while the β sheets at the C-terminal run anti-parallel. Helices α_1 of the N terminal and α_3 of the C-terminal line

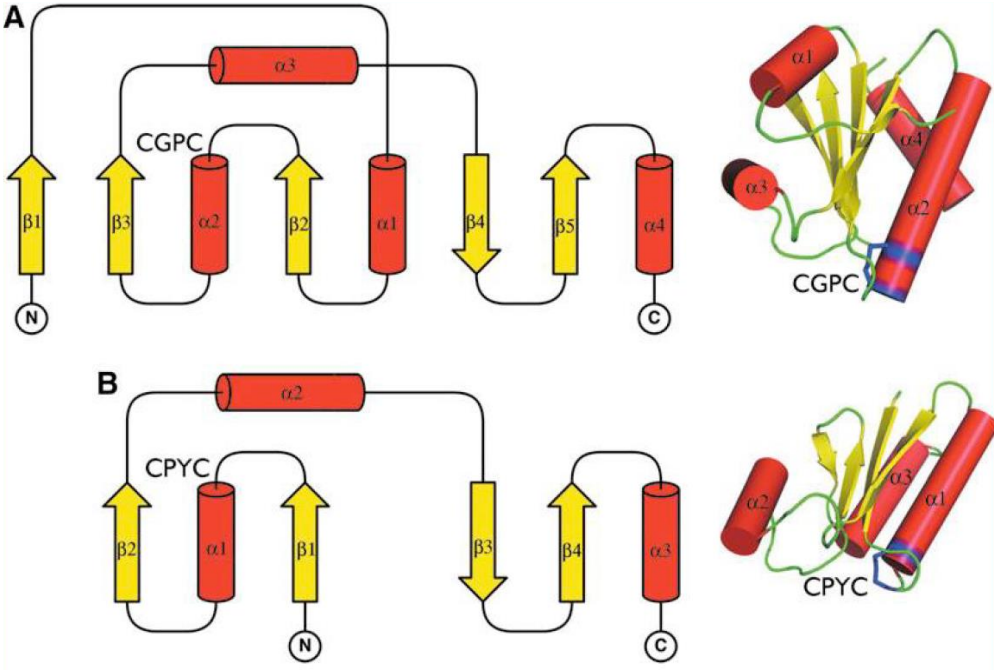

Figure 1.12. Structure of fold of thioredoxins vs a thioredoxin fold

(A) Fold of a thioredoxin contains five β-strands surrounded by four α-helices. All these together are characteristic of the conserved fold of Thioredoxins, where the CGPC motif is in a short segment at the amino end of the α_2 helix. (B) The 'thioredoxin-like' fold is a minimal version of this structure without the β_1 strand and the α_1 helix (Collet *et al.*, 2010; Martin, 1995).

up in a parallel fashion on one side of the sheet, while α_2 helix is located opposite to the β-sheet and is oriented perpendicular to α_1 and α_3 helices (Collet *et al.*, 2010; Holmgren *et al.*, 1975). All these together are characteristic of the conserved fold of Thioredoxins, where the CGPC motif is in a short segment at the amino end of the α_2 helix.

The 'thioredoxin-like' fold is a minimal version of this structure without the β_1 strand and the α_1 helix (Collet *et al.*, 2010; Martin, 1995), and has been identified in proteins from different classes including thioredoxins, glutaredoxins (GRX) (Xia *et al.*, 2001),

glutathione transferases (Reinemer *et al.*, 1991), glutathione peroxidases (Ren *et al.*, 1997) and thiol-disulfide oxido-reductases such as the disulfide bond forming protein DsbA (Martin *et al.*, 1993), the inner membrane disulfide reductase DsbD (Haebel *et al.*, 2002; Katzen *et al.*, 2000), and protein disulfide isomerases such as DsbG (Depuydt *et al.*, 2009; Holmgren, 1989; McCarthy *et al.*, 2000; Tian *et al.*, 2006).

IV.B. Thioredoxins of the chloroplast

In photosynthetic organisms, Trxs have been known for many years to play a major role in light signaling through regulation of several carbon metabolism enzymes in the stroma, including the Calvin Benson cycle (Michelet *et al.*, 2009). The first Trx in chloroplasts was identified in plants in the late 1970s (Schürmann *et al.*, 1976). In chloroplasts, light signal triggers a photosynthetic electron transfer reaction which reduces ferredoxin and produces NADPH and ATP. Reduced ferredoxin transfers electrons to Trx via ferredoxin-dependent Trx reductase (FTR), allowing Trx to function as a general disulfide reducing proteins in the stroma (Michelet *et al.*, 2009). In *Arabidopsis,* there are 20 Trx-encoding genes that specify proteins that can be classified into six types: 9 Trx-*h* (cytosolic and mitochondrial), 2 Trx-*o* (mitochondrial), 9 plastidial thioredoxins: 4 Trx-*m*, 2 Trx-*f*, 1 Trx-*x* and 2 Trx-*y*. The *Chlamydomonas* genome also encodes the same six classes of thioredoxins but with fewer isoforms: 2 Trx-*h* (cytosolic), 1 Trx-*o* (mitochondrial), 1 Trx-*m*, 2 Trx-*f*, 1 Trx-*x*, and 1 Trx-*y* (plastidial) (Michelet *et al.*, 2009; Schurmann *et al.*, 2000).

V. THIOL-DISULFIDE CHEMISTRY ON THE *p*-SIDE OF THE ENERGY TRANSDUCING MEMBRANE

Disulfides are important building blocks in the secondary and tertiary structure of proteins (Trivedi *et al.*, 2009). While the native disulfide bonds were initially thought to contribute to the conformational and structural stability of proteins, it is now well established that disulfide bond formation and breakage are responsible and required for the assembly and diverse dynamic properties of several enzymes (Nagy, 2013; Trivedi *et al.*, 2009). The main chemical reaction by which disulfide bonds are formed and cleaved *in vivo* is termed thiol-disulfide exchange or thiol-disulfide chemistry. Disulfide bond formation involves the oxidation of two cysteine thiols and the release of reducing equivalents while the scission of a disulfide requires reducing equivalents to convert the disulfide into free thiols (Nagy, 2013; Poole, 2015). During a thiol-disulfide exchange reaction, a dithiol in protein A reacts with a disulfide in protein B, yielding the formation of a disulfide bonded protein A and a dithiol protein B. *In vivo,* there are dedicated enzymes that catalyze thiol-disulfide exchange reactions on the *p*-side or positive side of energy transducing membranes. The *p*-side of the such membranes correspond to the bacterial or archaeal periplasm, the chloroplast lumen and the mitochondrial intermembrane space, and are evolutionarily related (Gabilly *et al.*, 2017). In this section, we discuss and review the several factors dedicated to the catalysis of disulfide bond formation and reduction in these specialized compartments. This information is pertinent to the question of cytochrome *c* assembly since heme attachment occurs on cysteines that need to be maintained reduced in compartments where cysteines containing substrates are also the target of the disulfide bond machinery (Al-Habib *et al.*, 2021; Karamoko *et al.*, 2013; Landeta *et al.*, 2018).

V.A. Disulfide Bond Formation in Bacteria

The formation of disulfide-bond has been best described in Gram-negative bacteria where extensive genetic and physiological studies in *Escherichia coli* led to the description of the Dsb pathway or Disulfide bond forming pathway (involving DsbA and DsbB) (Bardwell *et al.*, 1993; Bardwell *et al.*, 1991; Dailey *et al.*, 1993; Missiakas *et al.*, 1993). Bioinformatic genome analyses suggest that most Gram-negative bacteria and archaea contain Dsb pathways except for some obligate anaerobes (Dutton *et al.*, 2008; Landeta *et al.*, 2018; Mallick *et al.*, 2002). Proteins that require disulfide bonds in their final folded state are translocated from the cytoplasm, which is typically considered as a reducing environment due to the presence of numerous reductants and reducing agents such as glutathione (Berkmen, 2012), to the more oxidizing periplasmic space, where DsB enzymes necessary for disulfide bond formation reside (Berkmen, 2012; Manta *et al.*, 2019). In *E. coli*, almost ~300 cysteine-containing proteins are translocated to the periplasm (Dutton *et al.*, 2008; Hiniker *et al.*, 2004) and oxidized by DsbA and DsbB via disulfide bond formation. DsbA (**d**isulfide **b**ond protein **A**) is the first catalyst that introduces a disulfide bond into a substrate and is recycled to its oxidized form by DsbB (**d**isulfide **b**ond protein **B**). In Gram-positive bacteria disulfide bond formation takes place in the periplasm, and BdbAB-dependent disulfide bond forming pathway is best studied in *Bacillus subtilis*. The BdbAB (**B**acillus **d**isulfide **b**ond) proteins share ~20% amino acid conservation with *E. coli* DsbAB proteins (Bolhuis *et al.*, 1999; Depuydt *et al.*, 2011; Ishihara *et al.*, 1995; Landeta *et al.*, 2018). Studies in other Gram-positive Actinobacteria

such as *Mycobacterium* have revealed the activity of a membrane-associated DsbA-like protein, MdbA (**m**onoderm **d**isulfide **b**ond forming protein **A**) (Landeta *et al.*, 2018) and VKOR, a homologue of human Vitamin K epoxide reductase instead of DsbB (Dutton *et al.*, 2008; Singh *et al.*, 2008). In this section, we will focus on the disulfide bond formation pathway in Gram-negative bacteria.

V.A.1. Disulfide bond formation by DsbA

In *E. coli*, almost ~40% of the envelope proteome is known or predicted to be oxidized by DsbA (Denoncin *et al.*, 2013; Dutton *et al.*, 2008). Thus, *dsbA* null mutants show a pleiotropic phenotype including loss of motility, reduced alkaline phosphatase activity, and hypersensitivity to DTT, metals and benzylpenicilline due to a defect in disulfide bond formation (Missiakas *et al.*, 1993; Stafford *et al.*, 1999). For example, loss of motility is caused by a defect in FlgI, a disulfide bonded protein critical for flagellar movement (Bardwell *et al.*, 1991; Dailey *et al.*, 1993). Loss of DsbA function yields a decreased abundance of disulfide bonded proteins such as OmpA (**O**uter **m**embrane **p**rotein **A**) and alkaline phosphatase, and misfolding of proteins such as β-lactamase (Bardwell *et al.*, 1991). DsbA is a 21-kDa monomeric protein and belongs to the thioredoxin superfamily (Atkinson *et al.*, 2009). Members included in this family harbor a highly conserved thioredoxin-like fold with a canonical C*XX*C active site (Denoncin *et al.*, 2013; Martin *et al.*, 1993). The highly conserved Trx-like fold is characterized by an N-terminal βαβ motif and a C-terminal ββα motif, which, unlike thioredoxins, are separated by an extended α helical domain (Atkinson *et al.*, 2009; Collet *et al.*, 2010; Martin *et al.*, 1993). This α helical

insertion contains several hydrophobic residues that contribute to the protein-binding properties of DsbA (Couprie *et al.*, 2000), a feature also found in glutathione transferases (Atkinson *et al.*, 2009). The catalytic C*XX*C (CPHC) sequence is present in the N-terminal and is maintained in an oxidized state (Joly *et al.*, 1997), which enables DsbA to catalyze disulfide bond formation in substrates entering the periplasm (Atkinson *et al.*, 2009; Collet *et al.*, 2010; Denoncin *et al.*, 2013; Martin *et al.*, 1993). First, a mixed disulfide complex is formed between DsbA and the substrate following a nucleophilic attack by an active Cys residue of the substrate on the first Cys of the oxidized CXXC motif of DsbA. The mixed disulfide intermediate is then resolved by another Cys of the substrate when it is nearing completion of folding, which results in oxidation of the substrate and subsequent release of the intermediate and reduction of DsbA (Bardwell *et al.*, 1991; Darby *et al.*, 1995; Kadokura *et al.*, 2004). Much of DsbA oxidizing ability can be attributed to a pK_a value = 3.5 of the N-terminal Cys_{30} of the CXXC active site in the thioredoxin-fold, as compared to the pK_a of a normal cysteine which is 8.7 (Nelson *et al.*, 1994). This unusually low pK_a value maintains the strong redox potential of DsbA by ensuring that thiols of DsbA remain ionized and thus, capable of carrying thiol disulfide exchange reactions (Nelson *et al.*, 1994). Note that the pK_a value refers to the pH at which 50% of a species is in an ionized form, and thus disulfide exchange between DsbA and a target protein is favorable even in acidic conditions (pK_a = 4), whereas, in contrast, disulfide exchange between a target protein and oxidized glutathione is almost negligible at this pH (Darby *et al.*, 1995; Nelson *et al.*, 1994). Reactions involving DsbA have been shown to be $10^2 – 10^6$ times more rapid than spontaneous thiol-disulfide exchange reactions (Darby *et al.*, 1995). Kinetic studies

have also shown that the reduced form of DsbA is more stable than the oxidized form due to formation of multiple hydrogen bonds that stabilizes the Cys_{30} thiolate anion ($-S^-$) in the reduced form (Guddat *et al.*, 1997). Structural analyses have revealed hydrogen bonds between His_{32}, which lies between Cys_{30} and Cys_{33} in the CPHC motif, and Cys_{30} in the reduced form, between thiolate anion of Cys_{30} and thiol of Cys_{33}, and between thiolate anion of Cys_{30} and the backbone amide of His_{32} and Cys_{33} (Guddat *et al.*, 1997). Presence of such stabilizing hydrogen bonds in the reduced form, but not in the oxidized form of DsbA, thermodynamically drives it to donate electrons to substrates, making it one of the strongest oxidizing proteins in nature (Guddat *et al.*, 1997; Zapun *et al.*, 1993).

V.A.2. Recycling of DsbA by DsbB

DsbA is released in the reduced form after transferring disulfides to target proteins, and is reoxidized by DsbB, a 20 kDa transmembrane protein that was simultaneously reported by two groups (Bardwell *et al.*, 1993; Missiakas *et al.*, 1993). That DsbA and DsbB function in the same oxidizing pathway was evidenced by the fact that *dsbB* null mutants exhibit similar pleiotropic defects in disulfide bond formation as *dsbA* null mutants and accumulate DsbA in the reduced form (Bader *et al.*, 1998; Bardwell *et al.*, 1993; Guilhot *et al.*, 1995; Kishigami *et al.*, 1995). DsbB contains two periplasmic loops each harboring two redox active cysteine residues, Cys_{41} – Cys_{44} (pair 1) and Cys_{104} – Cys_{130} (pair 2), four transmembrane α helices and one quinone binding site that is located in the proximity of the first pair of cysteines (Bader *et al.*, 2000; Depuydt *et al.*, 2011; Inaba *et al.*, 2006). A direct interaction between the two proteins was suggested after the isolation of a mixed disulfide between DsbA-DsbB (Bader *et al.*, 1998; Guilhot *et al.*, 1995; Kishigami *et al.*,

1995), which was further confirmed by demonstrating *in vitro* oxidation of DsbA by purified DsbB in the presence of oxygen (Bader *et al.*, 1998). The interaction between DsbA and DsbB starts by the attack on Cys_{30} of DsbA (in CPHC motif) by the Cys_{104} – Cys_{130} pair of DsbB (pair 2), resulting in a DsbA-DsbB mixed disulfide complex (Inaba *et al.*, 2006). The mixed disulfide is then transferred to DsbA resulting in its reoxidation, and regeneration of the disulfide bond by transfer of electrons to the disulfide between Cys_{41} – Cys_{44} pair of cysteines (Inaba *et al.*, 2006). Cys_{41} and Cys_{44} are finally recycled into their oxidized state by transferring electrons to quinone (Bader *et al.*, 1999). The fact that quinones are involved in the reoxidation of DsbA was evidenced by a decreased accumulation of DsbA and DsbB in mutants that are defective in synthesis of ubiquinone and menaquinone (menaquinone accepts electrons from DsbB in anaerobic conditions) production (Inaba *et al.*, 2006; Kobayashi *et al.*, 1997). *In vitro,* DsbB can generate a disulfide in DsbA by directly transferring electrons to quinones (Bader *et al.*, 1999; Bader *et al.*, 1998). Reduced quinones are then reoxidized by transferring electrons to cytochrome oxidases *bd* and *bo* (expressed in aerobic and anaerobic conditions, respectively), which finally transfers electrons to molecular oxygen, the terminal electron acceptor in the electron transport chain (Nakamoto *et al.*, 2004).

V.B. Disulfide bond reduction in bacteria

Oxidative folding of proteins in the bacterial periplasm relies on disulfide bond formation introduced by the oxidation system (DsbAB) and isomerization by the reduction system (DsbCG). These systems utilize the oxidizing and the reducing equivalents of quinone and

NADPH, respectively, that are transmitted across the cytoplasmic membrane through integral membrane components DsbB and DsbD. In both pathways, alternating interactions between a CXXC-containing thioredoxin domain and other regulatory domain lead to the maintenance of oxidized and reduced states of the specific terminal enzymes, DsbA that oxidizes target cysteines and DsbC/DsbG that reduce an incorrect disulfide to allow its isomerization into the physiologically relevant one. Molecular details of these remarkable biochemical cascades are being rapidly unraveled by genetic, biochemical, and structural analyses in recent years.

V.C. Disulfide bond isomerization

DsbA, is a strong oxidant (with a redox potential of -119 mV in *E. coli*) (Zapun *et al.*, 1993) and catalyzes rapid thiol-disulfide exchanges. Because DsbA oxidizes cysteines indiscriminately, non-native disulfide bonds leading to incorrect protein folding and subsequent inactivation can be introduced in protein substrates. This is mostly true for proteins with more than two cysteines where the probability of forming incorrect disulfide bonds is much higher. To catalyze the rearrangement of these non-native disulfide linkages, cells have evolved an isomerization pathway (Rietsch *et al.*, 1997). In *E. coli*, DsbC and DsbG are two most important protein disulfide isomerases that share ~30% sequence identity and some structural similarity but differ in substrate specificity (Nakamoto *et al.*, 2004; Rietsch *et al.*, 1997). Both DsbC and DsbG are homodimeric proteins (2 x ~25 kDa) and like DsbA (Bessette *et al.*, 1999; Missiakas *et al.*, 1994; Zapun *et al.*, 1995) built around a thioredoxin-like fold with a catalytic CXXC motif but unlike DsbA, lacking the extended

α-helical domain that contains hydrophobic residues. Instead, DsbC and DsbG have a dimerization domain at the N-terminus of the thioredoxin fold and form V-shaped dimers (Heras *et al.*, 2004; McCarthy *et al.*, 2000). DsbC and DsbG are present in the periplasm in the reduced form (Bessette *et al.*, 1999; Rietsch *et al.*, 1997), However, unlike DsbC, DsbG is unable to reduce insulin *in vitro* and catalyze oxidative refolding of RNase efficiently, indicating functional differences between them (Nakamoto *et al.*, 2004). An important question that needs to be answered is how can DsbC distinguish between correctly vs incorrectly disulfide bonded proteins? It is hypothesized that the hydrophobic cleft of DsbC, identified from the study of its crystal structure, preferably interacts with misfolded proteins in which the hydrophobic stretch and cysteine residues are exposed as opposed to correctly disulfide bonded proteins in which they are buried and inaccessible (Berkmen, 2012; McCarthy *et al.*, 2000).

The isomerizing property of DsbC was evidenced by studies which showed that only proteins with multiple disulfide bonds are affected in a *dsbC* null mutant, whereas proteins with single disulfide bonds such as OmpA and β – lactamase are not. Additionally, defects in a *dsbC* null mutant can be partially complemented by exogenous application of reduced DTT, which supports the view that DsbC possesses a reducing activity.

V.D. Disulfide bond formation in organelles

While catalyzed thiol-disulfide chemistry was documented in bacteria, there was little support for the operation of thiol-metabolizing pathways in on the *p*-side of the energy-transducing organellar membranes in eukaryotes until recently (Al-Habib *et al.*, 2021;

Finger *et al.*, 2020; Karamoko *et al.*, 2013; Meyer *et al.*, 2019). In eukaryotes, three compartments contain dedicated machineries for introducing disulfide bonds into proteins: the endoplasmic reticulum (ER), the chloroplast, the intermembrane space of mitochondria.

V.D.1. Disulfide bond formation in mitochondria

The IMS is topologically analogous to the bacterial periplasm and several structural and biochemical studies have revealed many disulfide – bonded proteins in the IMS (Al-Habib *et al.*, 2021; Dickson-Murray *et al.*, 2021; Edwards *et al.*, 2021). While most of the proteins targeted to the mitochondrial matrix contain a N-terminal MTS (**M**itochondrial **T**argeting **S**ignal) or internal targeting signals (Chacinska *et al.*, 2009; Fischer *et al.*, 2013), the import of the majority of soluble IMS proteins is facilitated by a disulfide relay system that is linked to oxidative folding of the proteins (Edwards *et al.*, 2021; Finger *et al.*, 2020). Only a few of the IMS proteins are not imported via the disulfide relay system and are targeted to the IMS via internal targeting sequence (such as cytochrome *c* or HCCS) or a bipartite signaling sequence that includes a MTS and hydrophobic sorting signal arresting the protein into the inner membrane (such as cytochrome c_1) (Edwards *et al.*, 2021; Fischer *et al.*, 2013; Herrmann *et al.*, 2010).

V.D.1.a. Substrates of the mitochondrial disulfide relay system

Most of the IMS-targeted substrates relying on the disulfide bond forming system for their import are usually small in size (~10 kDa) and share a common core structure with two

antiparallel α-helices arranged in a helix-loop-helix motif. Each α-helix contains two conserved cysteine residues connected by disulfide bonds, and separated by either 3 or 9 residues, which are termed twin Cx_3C or CX_9C motifs, respectively (Banci *et al.*, 2008; Fischer *et al.*, 2013; Gabriel *et al.*, 2007; Longen *et al.*, 2009). The twin cysteines are engaged in intramolecular disulfide bonds spanning the two motifs, enabling the formation of an anti-parallel helix–turn–helix structure, which is typical of the canonical substrates of the disulfide relay system in the IMS. Twin Cx_3C and CX_9C proteins carry a range of functions in oxidative phosphorylation; protein import, metabolites and metal ion transport, apoptosis, and detoxification of harmful reaction products (Edwards *et al.*, 2021; Hell, 2008; Zhou *et al.*, 2017). Examples of twin cysteine motif proteins in the IMS include Cox17, Cox19 and Cox23, all belonging to twin CX_9C family and involved in the assembly of cytochrome *c* oxidase (Arnesano *et al.*, 2005; Herrmann *et al.*, 2007); Tim8, Tim9, Tim10 and Tim13 proteins that belong to the twin CX_3C family and are involved in mitochondrial import and (Curran *et al.*, 2002). In addition to twin CX_3C and CX_9C proteins, several other proteins exist in the IMS that are disulfide bonded but do not contain the consensus twin cysteine motif. Examples of non-canonical substrates include Cox 12, a subunit of cytochrome *c* oxidase (Tsukihara *et al.*, 1995); subunits of cytochrome bc_1 complex (also known as mitochondrial Complex III) Rieske and Qcr6 (Iwata *et al.*, 1998); Cox11, a Cu-binding assembly factor and Sco1, a thioredoxin-like (Chinenov, 2000) both required for Cu incorporation into the Cu_B site of mitochondrial cytochrome *c* oxidase (also known as Complex IV) (Banci *et al.*, 2004); superoxide dismutase 1 (Sod1) and copper chaperone for superoxide dismutase 1 (Ccs1) (Gross *et al.*, 2011; Kallergi *et al.*, 2012).

The presence of such disulfide-bonded proteins in the IMS suggested the existence of a disulfide bond forming pathway in the compartment that is distinct from the bacterial oxidizing pathway since no orthologs of bacterial DsbAB proteins could be found in the IMS. In 2005, Mesecke *et al*. identified a unique pathway that catalyzes oxidation of proteins in the mitochondrial IMS and involves two major components, Mia40 (**M**itochondrial **I**mport and **A**ssembly) and Erv1 (**E**ssential for **R**espiration and **V**egetative growth) (Mesecke *et al.*, 2005).

V.D.1.b. Mia40: a redox-activated protein importer in the IMS

Mia40, also known as Tim40, is a central player in mitochondrial disulfide bond formation and is ubiquitously found in the IMS of plants, fungi, and animals. Mia40 consists of a highly conserved domain of ~60 residues containing six essential and invariant cysteine residues (Chacinska *et al.*, 2004; Herrmann *et al.*, 2007; Hofmann *et al.*, 2005; Naoé *et al.*, 2004; Terziyska *et al.*, 2005). In fungi, this domain is tethered to the mitochondrial inner membrane via an N-terminal hydrophobic membrane anchor containing a bipartite pre-sequence (Naoé *et al.*, 2004; Terziyska *et al.*, 2005), whereas in plants and animals, Mia40 orthologs lack the pre-sequence and are found in soluble form in the IMS (Hofmann *et al.*, 2005). Mia40 is essential for yeast viability and depletion of Mia40 can severely affect the import of small IMS proteins with cysteine motifs (Mesecke *et al.*, 2005). In humans Mia40 is also referred to as CHCHD4 (for **C**oiled-Coil-**H**elix-**C**oiled-Coil-**H**elix **D**omain Containing **4**) and exists as two splice variants (CHCHD4.1 and CHCHD4.2) completely identical except for the very N-terminal part of the protein (Hofmann *et al.*, 2005). Mia40

consists of a redox-active CPC motif followed by a characteristic twin CX_9C motif, also found in many Mia40 substrates. The conserved domain in Mia40 forms a hydrophobic binding groove and serves as a redox-driven protein trap to import precursor proteins from cytosol to the IMS by directly interacting with them (Fischer *et al.*, 2013; Herrmann *et al.*, 2007).

In substrate, a 9 amino-acid sequence with a propensity to form an amphipathic α-helix, acts as an IMS targeting signals or mitochondrial intermembrane space sorting signals (MISS) (Dimogkioka *et al.*, 2021). The ITS, typically located upstream or downstream of the docking cysteine, is recognized by the hydrophobic binding groove of Mia40. Following this interaction, the thiolate anion of a cysteine residue in the substrate performs a nucleophilic attack on the oxidized CPC motif of Mia40 resulting in the formation of an intermolecular disulfide bond (Fischer *et al.*, 2013; Mesecke *et al.*, 2005). This disulfide bond prevents backsliding of incompletely translocated substrates into the cytosol, thus coupling oxidative protein folding to protein import (Banci *et al.*, 2010). The intermolecular disulfide bond is resolved by another nucleophilic attack by a thiolate anion in the substrate, resulting in reduction of Mia40 and consequently, release of the oxidized substrate (Bien *et al.*, 2010). It has been demonstrated that Mia40 functions more efficiently by forming a ternary complex with its substrate and the sulfhydryl oxidase Erv1, which re-oxidizes the reduced CPC motif in Mia40 (Fischer *et al.*, 2013).

V.D.1.c. Erv1: a conserved sulfhydryl oxidase in the IMS

Erv1, also known as **A**ugmenter of **L**iver **R**egeneration or ALR in mammalian cells (Fischer *et al.*, 2013), is a soluble homodimer in the IMS belonging to the Erv1/QSOX

family of flavoproteins (Fass, 2008). Members of this family contain a FAD (**f**lavin **a**denine **d**inucleotide) – binding domain with a conserved CXXC motif in the C terminus, adjacent to the isoalloxazine ring of the FAD cofactor. In fungi and animals, Erv1 proteins contain an extended N terminus with a second redox-active CXXC motif (Bien *et al.*, 2010). The N-terminal redox motif of one subunit acts as a 'shuttle arm' and transfers electrons from Mia40 to the CXXC motif in the C terminus of the second subunit of the homodimer (Bien *et al.*, 2010; Fischer *et al.*, 2013), thereby re-oxidizing Mia40. Thereafter, the N-terminal 'shuttle arm' of Erv1 swings over to the core C terminal of the second subunit and gets oxidized by the CXXC motif which, in turn, is oxidized by the redox active FAD cofactor of Erv1 (Daithankar *et al.*, 2009; Farrell *et al.*, 2005). This oxidation reaction, which regenerates a disulfide bond within the CXXC motif, is aided by the proximity between the motif and the FAD cofactor (Bien *et al.*, 2010). In addition to their role in oxidative protein folding, Mia40 and Erv1 appear to be involved in a myriad of functions. For example, Mia40 is critical for hypoxia response and mitochondrial dynamics (Yang *et al.*, 2012), whereas Erv1 is important for processes such as organ development during embryogenesis, mitochondrial fission and fusion process (Dabir *et al.*, 2013; Fischer *et al.*, 2013; Li *et al.*, 2012; Napoli *et al.*, 2013; Todd *et al.*, 2010; Wilkerson *et al.*, 2011).

V.D.2. Disulfide reduction in the mitochondrial IMS

While the maintenance of the heme-linking cysteines in a reduced state appears to be a strict biochemical requirement to counter their oxidation into disulfides, no factors controlling this aspect of the heme ligation reaction was identified in the context of

mitochondrial cytochrome *c* assembly. System I mitochondria appear to be missing the prototypical components (DsbD/CcdA and CcmG) for the delivery of reducing power. There is also no evidence for the operation of such factors in System III mitochondria. Yet, disulfide formation takes place in the mitochondrial IMS and a disulfide reduction pathway required for Cu relay to Cu-containing proteins has been described.

V.D.2.a. Disulfide reductases functioning in Cu delivery in the mitochondrial IMS

Assembly of cytochrome *c* oxidase (Cco or complex IV), the terminal enzyme in the mitochondrial respiratory chain requires the operation of disulfide reductases in the IMS. Cco is a multimeric enzyme and its biogenesis and activity depend on the formation of two copper centers, Cu_A and Cu_B, on catalytic subunits Cox2 and Cox1, respectively. The Cu

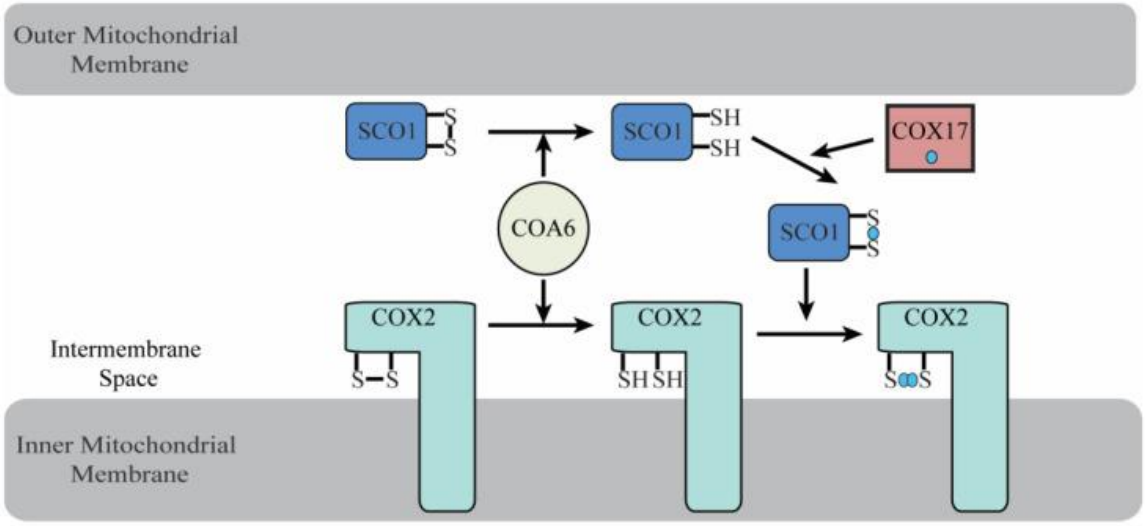

Figure 1.13. A schematic diagram of the biochemical role of COA6 in the metallation of COX2

The metallation of SCO1 and COX2 requires that their copper-binding cysteines are in the reduced form. COA6 acts as a disulfide reductase in this process, reducing the cysteines of both oxidized SCO1 and COX2, enabling their copper metallation by Cu-COX17 and Cu-SCO1, respectively (Swaminathan *et al.*, 2022).

atoms act as prosthetic groups in Cco for the transfer of electrons from cytochrome *c* to O_2. Cu is incorporated into the Cox1 and Cox2 subunits at a site where cysteine thiols provide ligands to the metal atom. Hence, Cu-binding cysteines in Cox1 and Cox2 need to be maintained reduced for the metalation reaction and it is unclear if the metal-binding cysteines are oxidized by the Mia40-Erv1 pathway.

Within the IMS, Cu is delivered to Cox2 by COX17 via SCO1, a Trx-like protein with a C*XXX*C motif acting as a metallochaperone. Cu-binding of Cox2 requires reduction of cysteinyl thiols of both SCO1 and Cox2 (Ghosh *et al.*, 2016) (Fig. 1.13). SCO2, a paralog of SCO1, also receives Cu from COX17, and acts as a Cu-dependent disulfide reductase of Cox2, a reaction necessary for its metalation by SCO1 (Morgada *et al.*, 2015; Timon-Gomez *et al.*, 2018). The reduction potentials of SCO1 and Cox2 are -280 mV and -290 mV respectively (Banci *et al.*, 2007; Morgada *et al.*, 2015), while the IMS has a reduction potential of -255 mV (Hu *et al.*, 2008), suggesting that activity of a dedicated disulfide reductase needs to exist in this otherwise oxidizing environment. In the analogous bacterial periplasm, this role is performed by TlpA, a Trx-like protein which reduces the Cu-binding cysteines in SCO1 and CoxB, the bacterial homologs of SCO1 and Cox2 (Abicht *et al.*, 2014). Recent discoveries have shown that in the mitochondrial IMS, COA6 (**c**ytochrome *c* **o**xidase **a**ssembly factor **6**), also known as C1orf31 (Szklarczyk *et al.*, 2012) functions as a disulfide reductase for copper metallochaperones SCO1 and the Cox2 subunit and is essential for biogenesis of the Cco enzyme (Pacheu-Grau *et al.*, 2020). COA6 has a characteristic $C(X)_{9\text{-}10}C$ motif with a CHCH domain, the presence of which suggests a redox function (Banci *et al.*, 2009; Swaminathan *et al.*, 2022). Although the molecular

mechanism of COA6 disulfide reductase activity is still unknown, *in vitro* and *in vivo* experiments demonstrate the ability of COA6 to reduce disulfides in SCO1, SCO2 and Cox2 in a thermodynamically favorable manner, thus allowing cysteine residues to remain reduced and interact with copper (Pacheu-Grau *et al.*, 2020; Soma *et al.*, 2019). COA6 and SCO2 have redundant functions in the reduction of the Cox2 Cu-binding cysteines. The association of COA6 and metallochaperone SCO1 to COX2 is facilitated by COX16, another assembly factor of Cco (Aich *et al.*, 2018). COX16 is single-pass mitochondrial inner membrane protein with a charged domain facing the IMS. The biochemical activity of COX16 in the Cu delivery pathway to Cox2 remains enigmatic but my work in Chapter 2 unveils a relationship to CCS4, a plastid cytochrome *c* assembly factor. The function of CCS4/COX16 in the context of thiol-disulfide chemistry is further addressed in the DISCUSSION AND PERSPECTIVES section.

V.D. Disulfide bond formation in endoplasmic reticulum

Disulfide bond formation is a favorable process in the Endoplasmic Reticulum (ER) due to a low GSH:GSSG ratio (1:1 to 1:3) and the redox potential of the ER being -150 mV to -180 mV, making the ER a highly oxidizing organelle (Bechtel *et al.*, 2017). The formation of disulfide bonds in the lumen of ER is carried out by a class of thiol-disulfide oxidoreductases, which includes PDIs (**P**rotein **D**isulfide **I**somerases). PDIs are one of the first identified thiol-disulfide oxidoreductases which, depending on the nature of the substrates and the surrounding redox environment, can catalyze disulfide bond formation, reduction, or isomerization (Goldberger *et al.*, 1963; Matsusaki *et al.*, 2020; Sevier *et al.*,

2002). Each member of the PDI family contains at least one thioredoxin-like domain with a thioredoxin fold containing a CXXC motif, and an acidic C-terminal domain that ends in a ER retention sequence (Bechtel *et al.*, 2017). The most abundant PDI protein, named PDIA1 in humans, consists of two enzymatically active (a and a') and two inactive (b and b') Trx-like domains, which are functional hallmarks of members of PDI family, and a C-terminal KDEL ER retention signal (Alanen *et al.*, 2003; Bechtel *et al.*, 2017; Feige *et al.*, 2011). In PDIA1, redox state of the catalytic CGHC motif dictates whether it will perform oxidase or isomerase function (Bechtel *et al.*, 2017). Oxidation of substrates results in the reduction of the CGHC motif, which is then re-oxidized by a protein called Ero1 (**ER o**xidoreduction **1**) (Gross *et al.*, 2004). Ero1, found in fungi, plants and animals (Meyer *et al.*, 2019), is a glycosylated luminal protein associated with the ER and containing a FAD cofactor. Reoxidation of PDIA1 is achieved by the transfer of electrons from the FAD cofactor of Ero1 to the CGHC motif of PDIA1. These electrons are then shuttled to molecular oxygen, thereby producing H_2O_2 and regenerating the FAD cofactor (Bechtel *et al.*, 2017). In contrast, Ero1 is not required for the isomerase activity of PDIA1 since there is no change in redox state of the protein. PDIA1 isomerase activity is catalyzed by the formation of a mixed disulfide formed by a nucleophilic attack of the active cysteines in the CGHC motif (with a low thiol pK_a ~ 4.5 to 5.6) on the substrate disulfide. The mixed disulfide is then resolved by another thiolate anion on the substrate generating a new disulfide bond and restoring PDIA1 to its reduced state (Bechtel *et al.*, 2017; Bulleid, 2012; Feige *et al.*, 2011; Oka *et al.*, 2013; Sevier *et al.*, 2002). In yeast ER, a second Ero1-independent disulfide bond forming pathway has been identified which involves Erv2, a

small ER oxidase with a non-covalently bound FAD cofactor. *In vivo*, oxidase activity of Erv2 is dependent on two pairs of cysteines, one in a highly conserved CXXC motif and the other in a CXC motif in the C terminal region (Sevier *et al.*, 2001; Sevier *et al.*, 2002) . Other members of PDI family that display oxidase and isomerase activity include PDIA1 (the most abundant PDI), PDIA2, PDIA3 (ERp57), PDIA4 (ERp72) and PDIA6 (ERp5) (Bechtel *et al.*, 2017; Galligan *et al.*, 2012).

V.E. Disulfide bond formation in plastids

In chloroplasts, disulfide bonded proteins are found in the envelope, stroma and thylakoid lumen, a compartment long considered to be vacant (Karamoko *et al.*, 2013; Kieselbach, 2013; Meyer *et al.*, 2019). This section will focus on the recent development of disulfide bond formation in the thylakoid lumen. Similar to other oxidizing compartments, a thiol-oxidizing pathway in the chloroplast lumen would theoretically require: a) an oxidoreductase interacting with substrates and promoting the oxidation of their cysteines into disulfides, 2) a thiol oxido-reductase to maintain the disulfide forming catalyst in the correct redox state (by recycling the reduced form to its oxidized state), and 3) an electron acceptor of the disulfide bond forming pathway (Meyer *et al.*, 2019). For the longest time, components of the thiol-oxidizing pathway in chloroplast have eluded identification since no orthologs of bacterial DsbA/DsbB – like proteins could be found in the predicted proteomes of photosynthetic eukaryotes or cyanobacteria, which are the evolutionary ancestor of the chloroplast. However, the existence of such a pathway was suspected based on the occurrence of many disulfide-bonded luminal proteins functioning in photosynthesis

(Karamoko *et al.*, 2013; Kieselbach, 2013; Simionato *et al.*, 2015). In the photosynthetic complexes, PsbO, a 26.5 kDa structural component of Photosystem II (Betts *et al.*, 1996; Burnap *et al.*, 1994; Wyman *et al.*, 2005) and Rieske, a subunit of the cytochrome b_6f complex (Carrell *et al.*, 1997) are two examples of proteins containing a single disulfide. Other examples of disulfide bonded proteins include several molecules regulating photosynthesis. The most studied example is VDE (**V**iolaxanthin **d**e **E**poxidase), a luminal enzyme involved in photoprotection which dissipates excess light energy via de-epoxidation of violaxanthin to zeaxanthin in the xanthophyll cycle (Grzyb *et al.*, 2006; Rockholm *et al.*, 1996). VDE activity is dependent upon the oxidation state of conserved cysteines forming 6 intramolecular disulfides (Bugos *et al.*, 1996; Hallin *et al.*, 2015; Simionato *et al.*, 2015).

Adaptation to light quality in photosynthesis is dependent upon Stt7/STN7, a thylakoid - bound kinase whose stroma facing catalytic domain is activated by the formation of a disulfide on the luminal domain of the protein (Depège *et al.*, 2003; Lemeille *et al.*, 2009; Wu *et al.*, 2021). Another example is $FKBP_{13}$ (**F**K506 **B**inding **P**rotein), a thylakoid lumen – localized immunophilin whose in vitro activity is dependent on a pair of cysteines oxidized into a disulfide (Buchanan *et al.*, 2005; Gopalan *et al.*, 2004; Gupta *et al.*, 2002). In addition to the presence of several disulfide bonded proteins, the existence of thiol-oxidizing pathways in this organelle was further supported by the successful production of active alkaline phosphatase (PhoA) in tobacco chloroplasts. PhoA is a homodimeric bacterial enzyme in which each subunit contains intramolecular disulfide bonds required for enzymatic activity, thus the fact that it is catalytically active when expressed in

thylakoid lumen suggests that thiol oxidizing pathways exist in this compartment (Bally *et al.*, 2008; Sone *et al.*, 1997).

A novel class of thiol-oxidizing proteins was identified in oxygenic photosynthetic organisms including cyanobacteria (Li *et al.*, 2010; Singh *et al.*, 2008), the green lineage (Grossman *et al.*, 2010) and some bacterial phyla lacking the prototypical DsbB or DsbAB proteins (Dutton *et al.*, 2008; Dutton *et al.*, 2010; Landeta *et al.*, 2018; Wang *et al.*, 2011). This class of proteins display similarities to VKORC1 (or **V**itamin **K** **E**poxide **R**eductase Complex subunit 1), an ER membrane protein. VKORC1 is well studied for its involvement in the reduction of Vitamin K and known to participate in oxidative folding of proteins in the ER lumen in partnership with TMX (**T**rans**m**embrane o**x**idoreductase) in mammals. (Karamoko *et al.*, 2013; Landeta *et al.*, 2018; Schulman *et al.*, 2010; Tie *et al.*, 2008). VKOR-like proteins (or VKORH for VKOR homologs) occur as membrane proteins with or without a soluble C-terminal extension containing a thioredoxin-like protein (Fig.14). An example of a VKORH protein containing only the membrane domain is the VKOR-like protein from *Mycobacterium tuberculosis* that can substitute for DsbB and oxidize DsbA in *E. coli* (Dutton *et al.*, 2010; Wang *et al.*, 2011). An example of a Trx-like containing VKOR is the cyanobacterial SynDsbAB which carries both the DsbA and DsbB function (Singh *et al.*, 2008).

V.E.1. LTO1, a VKOR-like protein in plastids

Since VKOR homologs in the green lineage shared structural similarity with cyanobacterial VKOR, it was hypothesized that they might act as oxidants in plastids. Indeed, a VKOR

homolog that localized to the thylakoid membrane in *Arabidopsis thaliana* was shown to be able to catalyze disulfide bond formation (Furt *et al.*, 2010; Karamoko *et al.*, 2011; Li *et al.*, 2010; Lu *et al.*, 2013; Tie *et al.*, 2008). The *Arabidopsis* VKORH, named LTO1 (**L**umen **T**hiol **O**xidoreductase **1**), is a fusion protein containing an integral membrane

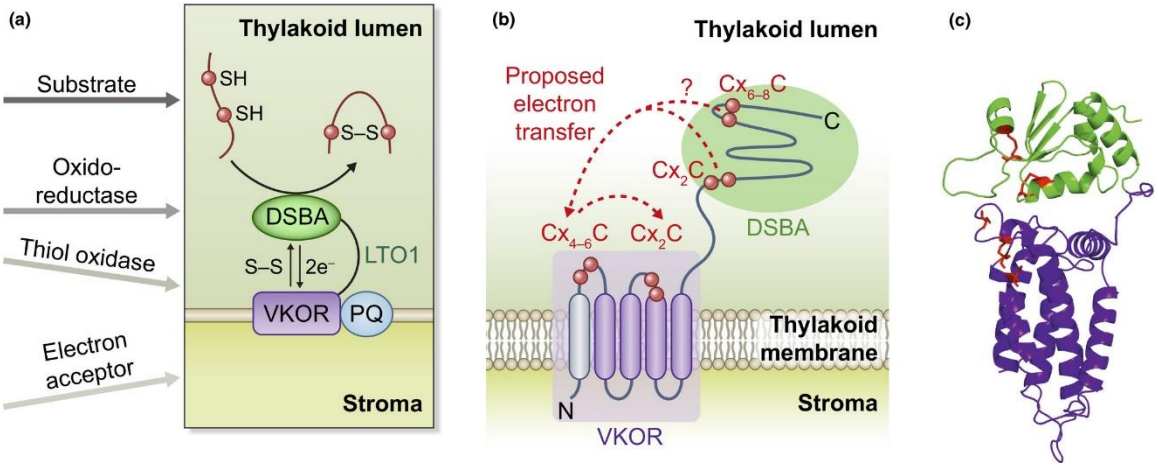

Figure 1.14. Disulfide bond formation in the thylakoid lumen

Disulfide formation in the thylakoid lumen. (a) Lumen thiol oxidoreductase 1 (LTO1) is a fusion protein that consists of a membrane-embedded vitamin-K-epoxide reductase (VKOR) domain and a soluble DsbA-like thioredoxin domain directed towards the thylakoid lumen. The DsbA domain interacts with its redox-active cysteines with substrates and then shuttles electrons towards the redox-active cysteines in the VKOR domain. These electrons are then transferred onto phylloquinone, which might then shuttle its electrons into photosystem I. It is unclear whether LTO1 can also draw on alternative electron acceptors. (b) The VKOR domain consists of four to five transmembrane helices. Alignments and transmembrane prediction of 78 isoforms revealed that the first transmembrane domain (light grey) is, in most species, relatively little hydrophobic. LTO1 contains eight highly conserved cysteines. A $Cx_{4–6}C$ motif is in the loop between transmembrane helices 1 and 2 and a Cx_2C motif is located right at the beginning of transmembrane helix 4 of VKOR. The DsbA domain contains a Cx_2C motif as well as another two cysteines. The proposed electron transfer between the conserved cysteines is indicated by the dotted arrow. (c) The modelled structure of LTO1 from *Chlamydomonas reinhardtii*. Modelling was based on the structure of cyanobacterium *Synechococcus* sp. VKOR with its thioredoxin-like domain (pdb: 4NV2) (Liu *et al.*, 2014).The figure and legends are extracted from (Meyer *et al.*, 2019).

domain that is homologous to mammalian VKORC, and a soluble DsbA-like/Trx-like

domain (Karamoko *et al.*, 2011; Karamoko *et al.*, 2013) . The VKOR domain of LTO1 consists of 4-5 transmembrane domains with the N terminus containing the targeting peptide facing the stroma (Feng *et al.*, 2011; Lu *et al.*, 2013; Meyer *et al.*, 2019). The N and C termini domains contain conserved cysteine residues facing the thylakoid lumen, which is the site of oxidation (Feng *et al.*, 2011). LTO1 contains four conserved cysteine residues in the VKOR domain, two of which are arranged in a $C(X)_{4-6}C$ motif in a loop facing the thylakoid lumen between helices 1 and 2, and two are present in helix 4 in a CXXC motif. The DsbA/Trx-like domain also contains four conserved cysteines arranged in a WCXXC and a $C(X)_{4-6}C$ motif (Meyer *et al.*, 2019). The WCXXC motif is absent in mammalian VKORC and some bacterial VKORH proteins (Goodstadt *et al.*, 2004). Using motility complementation assay, it was shown LTO1 can partially compensate for the loss of bacterial DsbAB proteins, and that all eight highly conserved cysteines are critical for promoting disulfide bond formation in a *dsbB* mutant in *E. coli* (Feng *et al.*, 2011; Karamoko *et al.*, 2011). The ability of LTO1 to functionally replace DsbAB in the bacterial periplasm was indicative of a role for LTO1 in disulfide bond formation in the thylakoid lumen, the analogous compartment in plastids. This was further evidenced by demonstration of *in vitro* oxidation of PsbO by the Trx-like soluble domain of LTO1, which is thought to harbor the sulfhydryl oxidizing activity (Karamoko *et al.*, 2011). PsbO is a structural component of Photosystem II residing in the lumen, harboring conserved cysteine residues that form a single disulfide bond that is crucial to maintain its tertiary structure and is thus, essential for PSII assembly (Tanaka *et al.*, 1989). PsbO, when reduced, is targeted for degradation, suggesting the oxidized state of the conserved

cysteines in essential for the stability of the protein (Burnap *et al.*, 1994; Hall *et al.*, 2010; Tanaka *et al.*, 1989; Wyman *et al.*, 2005). Accordingly, *lto1* knockdown or knock-out mutants in *Arabidopsis* have an impaired photosynthetic growth due to a defect in assembly of Photosystem II (Du *et al.*, 2015; Karamoko *et al.*, 2011). This defect can be attributed to a lack of oxidizing activity of LTO1 resulting in aform of PsbO with reduced cysteines, which is then targeted for degradation. Based on our understanding of the DsbAB pathway, LTO1-Trx domain promotes disulfide bond formation and is recycled to it oxidized form by interaction with the cysteines in the VKOR-like domain. The final electron acceptor of this trans-thylakoid oxidizing pathway is likely to be a phylloquinone since LTO1 is active in reducing this molecule in an *in vitro* enzymatic assay (Furt *et al.*, 2010; Yang *et al.*, 2015). Conceivably, LTO1 oxidizes cysteines in other protein substrates residing in the lumen. Eight lumen-localized and cysteine containing targets of LTO1 were identified via Y2H, out of which one, FKBP13 was shown to be disulfide-bonded by LTO1 *in vitro* (Lu *et al.*, 2014). One of the targets recovered is VDE (***V***iolaxanthine ***D***e-***E***poxidase), a protein containing six disulfides (Hallin *et al.*, 2015; Simionato *et al.*, 2015) and required to dissipate excess light energy in the form of heat (Kanervo *et al.*, 2005). The enzymatic activity of FKBP13 and VDE is dependent upon disulfide-bonded cysteines in the protein (Bugos *et al.*, 1996; Gopalan *et al.*, 2004; Hallin, 2011), further underscoring the significance of LTO1-dependent catalyzed thiol oxidation in the thylakoid lumen. Unlike the substrates of the Mia40/Erv1 pathway, the cysteines that are disulfide bonded by action of LTO1 are not found in a specific motif. Other targets of LTO1 must exist and in Chapter

3, we examine apocytochrome *f* heme-binding cysteines as a target of action of LTO1 in the context of cytochrome *c* assembly.

V.E.2. A trans-thylakoid disulfide reducing pathway in plastids.

In plastids, a trans-thylakoid disulfide reducing pathway functions to maintain the redox state of the heme-binding cysteines in apocytochrome *c*. This reduction is under the control of CCS5/HCF164, a membrane-bound *p*-side facing thioredoxin Trx -like proteinthat specifically reduces the disulfide bonded cysteines of the heme binding site into free thiols to allow for subsequent ligation with the vinyl groups of heme (Gabilly and Hamel, 2017; Simon and Hederstedt, 2011). This dedicated redox catalyst is required for the assembly of chloroplast cytochromes *c*, further underscoring the importance of thiol-based chemistry (Gabilly *et al.*, 2010). For the preparation of apocytochrome *c* as a competent substrate CCS5/HCF164 was shown to directly reduce a disul*fi*de bond formed between the heme-linking cysteines of apocytochrome *c* (Cline *et al*., 2016; Gabilly and Hamel, 2017). The Trx-like protein is maintained reduced via a member of the family of transmembrane thiol-disul*fi*de oxido-reductase (TDOR), which acts as a transducer of reducing power across the energy-transducing membranes (Bushweller, 2020; Cho and Collet, 2013). The provision of reductants occurs via sequential thiol-disul*fi*de exchanges across the membrane involving a *n*-side classical Trx, a member of the TDOR family and the *p*-side Trx-like protein dedicated to cytochrome *c* assembly (Bushweller, 2020; Cho and Collet, 2013; Davey *et al*., 2016). Members of the TDOR family involved in

cytochrome *c* biogenesis are DsbD and CcdA, which display a critical pair of cysteines located within transmembrane domains and involved in the transfer of reducing power. DsbD displays eight transmembrane segments with N-terminal and C-terminal redox domains, both exposed to the *p*-side, exhibiting an immunoglobulin- and Trx-like fold, respectively. With six transmembrane domains resembling the central hydrophobic domain of DsbD and no additional redox domains, CcdA is a "stripped-down" version of DsbD.). In chloroplasts, CCDA, an ortholog of bacterial CcdA, appears to be the only TDOR member involved in transferring the electrons to the Trx-like component involved in cytochrome *c* maturation (CCS5/HCF164). The *n*-side electron donor to the pathway is a classical Trx involved in several thiol-disul*fi*de exchange reactions, and maintained reduced by Trx reductase at the expense of NADPH (Cline *et al*., 2016, Gabilly and Hamel, 2017; Hamel *et al*., 2009).

Loss of CCS5/HCF164 can be rescued by provision of exogenous reductants, a finding consistent with the function of this component in a disulfide reducing pathway (Cline *et al*., 2016). The transmembrane delivery of reducing power also relies on CCS4/HCF153, a small protein conserved in the green lineage (Gabilly and Hamel, 2017). While CCS4/HCF153 lacks any residue or motif speaking to a function in thiol-based chemistry, the reductant-dependent rescue of *ccs4*-null mutant categorizes this component as a participant in the thiol-based chemistry required for apocytochrome *c* preparation. Although the mode of action of CCS4 still remains unknown, its involvement in the disulfide reducing pathway is

discussed in more detail in Chapter 2.

VI. Assembly of plastid *c*-type cytochromes

In plastids, three *c*- type cytochromes have been identified: membrane-bound cytochrome *f*, and soluble cytochrome c_6 and cytochrome c_{6A} (Gabilly *et al.*, 2017). All plastid *c*-type cytochromes contain a single heme attached to the conserved C*XX*CH motif in the apoprotein. Cytochrome *f* is a catalytic subunit of cytochrome b_6f complex and is essential for photosynthetic electron transport in photosynthetic eukaryotes and cyanobacteria (Cramer *et al.*, 1994; Martinez *et al.*, 1994). With a few exceptions, cytochrome *f* is encoded by the chloroplast *petA* gene and is synthesized as a precursor protein with a lumen targeting sequence which translocates the apoprotein through the thylakoid membrane (Howe *et al.*, 1994). The N-terminal soluble heme-binding domain is co-translationally translocated into the lumen and C-terminal hydrophobic domain anchors the protein to the thylakoid membrane (Gray, 1992; Howe *et al.*, 1994). Cytochrome c_6 acts as a substitute for plastocyanin in Cu-deficient conditions in green algae and cyanobacteria and is involved in the transport of electrons from cytochrome *f* of the cytochrome b_6f complex to Photosystem I (Merchant *et al.*, 1987, 1987; Merchant *et al.*, 1998). The mature cytochrome c_6 polypeptide consists of 83-90 amino acids and has a mid-point redox potential of 335-390 mV (Howe *et al.*, 2006). Cytochrome c_6 is also widely distributed in red and brown algal lineages (Kerfeld *et al.*, 1998; Sandmann *et al.*, 1983). In oxygenic photosynthetic bacteria, cytochrome c_6 also serves as an electron donor to cytochrome oxidase (Howe *et al.*, 2006; Obinger *et al.*, 1990). In land plants, plastocyanin is the major

electron transporter from cytochrome *f* to photosystem I, and cytochrome c_6 seemed to be absent until the discovery of a cytochrome c_6 -like protein named cytochrome c_{6A}. Cytochrome c_{6A} is a unique *c*-type cytochrome which was first discovered in *Arabidopsis* in a yeast two-hybrid screen as a protein interacting with the lumen-localized immunophilin FKBP13 (Buchanan *et al.*, 2005; Gupta *et al.*, 2002). Although cytochrome c_{6A} has a core structure similar to that of bacterial and algal cytochrome c_6, it is, however, unable to transfer electrons from cytochrome *f* to photosystem I even though the purified protein displayed spectroscopic characteristics of a correctly folded hemoprotein (Howe *et al.*, 2006; Molina-Heredia *et al.*, 2003; Worrall *et al.*, 2008). The redox midpoint potential of cytochrome c_{6A} is 200 mV lower than cytochrome c_6 (358 mV) or plastocyanin (365 mV), which also makes it unlikely that it will function in electron transfer from cytochrome *f* to PSI. An *Arabidopsis* plastocyanin-deficient mutant is unable to grow photosynthetically even when cytochrome c_{6A} is overproduced, demonstrating cytochrome c_{6A} cannot substitute for the loss of plastocyanin (Molina-Heredia *et al.*, 2003). Interestingly, cytochrome c_{6A} contains an additional CXXC motif (which is oxidized in the 3D structure of the molecule) that is absent in algal and cyanobacterial cytochrome c_6 (Howe *et al.*, 2006). The diversity of cytochrome c_6-like proteins increased with the discovery of cyt c_{6B} and cyt c_{6C} in cyanobacteria (Bialek *et al.*, 2008). These cyt c_6-like proteins are not involved in direct electron transport but have been speculated to act as a safety valve under light stress and during over-reduction of electron carriers to alleviate ROS (Kleiner *et al.*, 2021; Marcaida *et al.*, 2006).

The function of plastid cytochrome c_{6A} remains obscure and a loss-of-function mutant line in *Arabidopsis* shows no obvious phenotype (Gupta *et al.*, 2002). But based on the fact cytochrome c_{6A} abundance is extremely low, this cytochrome is unlikely to function in the known electron transfer reactions in photophosphorylation (Howe *et al.*, 2006; Molina-Heredia *et al.*, 2003).

VI.A. Plastid cytochrome *c* assembly

Plastid *c*-type cytochromes are assembled via System II or the CCS pathway, as described earlier. System II was first discovered by the isolation of *ccs* mutants (**c**ytochrome ***c*** **s**ynthesis) that are photosynthetically impaired (Bonnard *et al.*, 2010; Gabilly *et al.*, 2017; Hamel *et al.*, 2009; Simon *et al.*, 2011). In the following section, I describe the identification of *CCS* factors that are involved in the assembly of plastid *c*-type cytochromes.

VI.B. *ccs* mutants

While the biosynthesis of *c*-type cytochromes *c* was extensively studied in fungal systems, there was little known on the assembly of cytochromes *c* in the plastid until the 1990s. The first genetic defect in the heme attachment reaction to the apoforms of plastid cytochromes *c* was documented with the identification of the *Chlamydomonas F2D8* mutant, which was isolated from metronidazole resistant cells following UV-mutagenesis (Howe *et al.*, 1992). In photosynthetic proficient cells, metronidazole accepts electrons from reduced ferredoxin and generates toxic reactive oxygen species, such as hydrogen peroxide by interaction with

O_2. The toxicity of metronidazole depends on a functional photosynthetic transfer, thus, cells that survive the treatment are likely to have a genetic defect in one or more components of the photosynthetic machinery. Metronidazole treatment provides an enrichment in photosynthetic mutants that display an acetate-requiring phenotype (Howe *et al.*, 1992; Schmidt *et al.*, 1977). The *F2D8* mutant accumulated reduced level of holocytochrome c_6 (~5%) as compared to the wild type and exhibited a photosynthesis-minus phenotype. In *Chlamydomonas*, cytochrome c_6 is expressed in Cu-deficient conditions to substitute for plastocyanin but *F2D8* was photosynthetic deficient even in the presence of Cu. Holoplastocyanin accumulated normally in Cu-replete conditions and could not functionally complement the loss of cytochrome c_6 in *F2D8*. This result was an indication that the acetate-requiring phenotype of *F2D8* mutant was due to the loss of one or more components of the photosynthetic machinery. In addition to cytochrome c_6, the genetic lesion in *F2D8* elicited a defect in cytochrome *f* whose holoform was diminished along with a decrease in the abundance of several subunits of the cytochrome b_6f complex. Pulse-chase analysis revealed that translation of nuclear-encoded pre-apocytochrome c_6 was unaffected. Apocytochrome c_6, the processed form could be detected, an indication that the synthesized protein was translocated into the lumen but did not accumulate due to rapid degradation (Howe *et al.*, 1992, 1994). This led to the hypothesis that the phenotype in *F2D8* was due to a defect in the attachment of heme to apocytochrome c_6 in the thylakoid lumen. This analysis was extended to plastid encoded cytochrome *f* and the conclusion was that loss of holocytochrome *f* could also be attributed to a defect in the heme attachment reaction (Howe *et al.*, 1992).

This first description of a photosynthetic mutant with a dual deficiency in the holoforms of cytochrome *f* and c_6 led to the identification of a novel class of photosynthetic deficient mutants, namely the *ccs* mutants defined by a specific defect in the heme attachment reaction (Xie *et al.*, 1998). To isolate *ccs* mutants, chemically or UV- mutagenized cells or cells mutagenized with an insertional cassette were first screened for a cytochrome b_6f deficiency phenotype by fluorescence induction and decay kinetics. Mutants with a defect in cytochrome b_6f complex shows a characteristic fluorescence due to block of electron flow beyond the plastoquinone pool (Bennoun *et al.*, 1982). Candidate *ccs* mutants were further identified based on a defect in the accumulation of holocytochrome c_6. The *ccs* mutants are also expected to show a pleiotropic defect in holocytochrome c_{6A} assembly, but this could not be tested due to the low abundance of this cytochrome (Howe *et al.*, 2006). Plastocyanin, another metalloprotein in the chloroplast lumen, is assembled correctly in the *ccs* mutants, suggesting the defect is specific to plastid *c*-type cytochromes (Howe *et al.*, 1993, 1994; Xie *et al.*, 1998). Extensive genetic and biochemical analyses established that the collection of *ccs* mutants defined several loci, plastid *ccsA* and nuclear *CCS1 to CCS6* (Gabilly *et al.*, 2017; Xie *et al.*, 1998). The *ccsA* and *CCS1* loci have been cloned and their gene products inferred to function in heme transport/delivery and ligation based on the extensive biochemical analysis of the bacterial CcsBA orthologs (Dreyfuss *et al.*, 2003; Hamel *et al.*, 2003; Xie *et al.*, 1996). The *CCS2* gene encodes an OPR (Octatrico Peptide Repeat) protein postulated to regulate the translation of the plastid-encoded *ccsA* transcript (Cline *et al.*, 2017). The *CCS3* and *CCS6* gene remain unidentified at the molecular level. The *CCS4* and *CCS5* genes encode proteins controlling the redox state of

the heme linking cysteines and are discussed in Chapter 2 (Gabilly *et al.*, 2010; Gabilly *et al.*, 2011).

2. Two disulfide reducing pathways are required for the maturation of plastid c-type cytochromes in Chlamydomonas reinhardtii.

I. Abstract

In plastids, conversion of light energy into ATP relies on cytochrome *f*, a key electron carrier with a heme covalently attached to a C*XX*CH motif. Covalent heme attachment requires reduction of the disulfide bonded C*XX*CH motif by CCS5 and CCS4, a protein of unknown function. CCS5 receives electrons from the oxido-reductase CCDA at the thylakoid membrane. In *Chlamydomonas reinhardtii*, loss of CCS4 or CCS5 function yields a partial cytochrome *f* assembly defect. Here we report that the ccs4ccs5 double mutant displays a synthetic photosynthetic defect due to a complete loss of holocytochrome *f* assembly, a phenotype that can be chemically corrected by reducing agents. In ccs4, the CCDA protein accumulation is decreased, indicating that one function of CCS4 is to stabilize CCDA. Dominant suppressor mutations mapping to the CCS4 gene were identified in photosynthetic revertants of the *ccs4ccs5* mutants. The suppressor mutations yield changes in the stroma-facing domain of CCS4 that restore holocytochrome *f* assembly above the residual levels detected in ccs5. Because disulfide reduction via CCS5 no longer takes place in *ccs5,* we hypothesize the suppressor mutations enhance the supply of reducing power independent of CCS5. CCS4-like proteins occur in the green lineage, and we show that HCF153, a distant ortholog from *Arabidopsis thaliana* can substitute for *Chlamydomonas* CCS4. We discuss the operation of a CCS5-dependent and a CCS5-independent pathway that control the redox status of the heme binding cysteines of

apocytochrome *f* and the possible function of CCS4 in the context of its relationship to mitochondrial COX16, a protein involved in a disulfide reducing pathway.

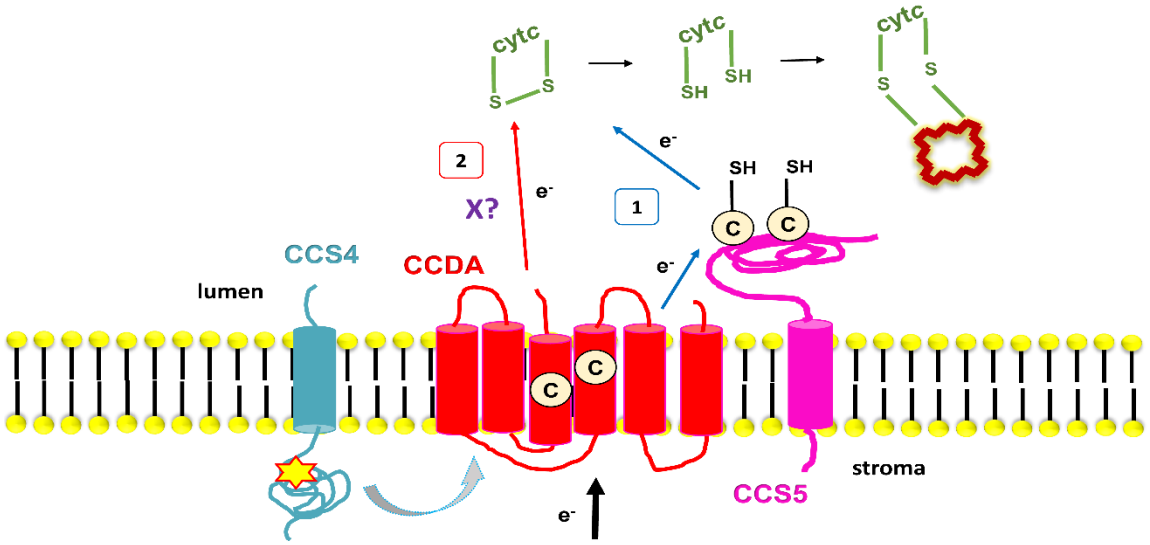

Figure 2.1. Graphical abstract.

Reduction of a disulfide formed between the heme-linking cysteines of apoforms of c-type cytochormes in the thylakoid lumen requires the provision of reducing power from stroma to apocytochrome f via thiol – disulfide exchange. Reducing power is supplied through two different pathways, pathway 1 and 2., with CCDA and CCS4 being common components to both pathways. In pathway 1, CCS5 directly reduces the disulfide bonded heme binding site. In pathway 2, one or several yet-to-be identified protein(s) (X) reduce(s) the disulfide. CCS4 functions in stabilizing CCDA. In the absence of CCS5, gain – of – function mutations in the C terminus of CCS4 (indicated by a yellow star) enhance the delivery of reducing power via CCDA to the unknown reductase(s) (X)

II. Introduction

Cytochromes *c* or *c*-type cytochromes are ubiquitous heme (ferroprotoporphyrin IX) containing proteins that function as one-electron carriers in energy-transducing membranes in bacteria, archaea, mitochondria, and plastids (Bertini *et al.*, 2006; Ma *et al.*, 2019). Cytochromes *c* located on the positive side (or *p*-side) of energy-transducing membranes (i.e., the bacterial or archaeal periplasm, the thylakoid lumen in the plastid and mitochondrial intermembrane space-IMS) carry a heme moiety covalently bound to two (or rarely one) cysteines in a typical C*XX*CH motif called the heme-binding site on the apoprotein (Alvarez-Paggi *et al.*, 2017). The histidine residue acts as an axial ligand to the iron in the heme moiety (Dickerson *et al.*, 1971). Conversion of apocytochrome *c* to its corresponding holoform requires the formation of the thioether linkage(s) between the vinyl carbons in heme and the cysteine thiol(s) in the heme-binding motif. The chemical requirements for thioether bond formation were formulated from the in vitro reconstitution of holocytochrome *c* formation and the extensive genetic and biochemical dissection of cytochrome *c* maturation in bacterial and eukaryotic model systems (Cline *et al.*, 2016; Das *et al.*, 2021). In energy-transducing membranes, apo- to holocytochrome *c* conversion occurs on the *p*-side of the membrane and requires minimally: 1) the independent transport of apocytochrome *c* and heme substrates, 2) the chemical reduction of a) ferriheme to ferroheme and b) disulfide bonded heme - linking cysteines to free thiols, and 3) the stereospecific ligation of heme to the free thiols of the C*XX*CH motif via formation of thioether bond linkages. In vivo, heme ligation to C*XX*CH cysteine thiols is a catalyzed process requiring at least four different maturation systems (Systems I, II, III and IV) which

are defined by signature assembly factors (Babbitt *et al.,* 2015; Belbelazi *et al., 2021*; Gabilly *et al.,* 2017; Mavridou *et al.,* 2013; Travaglini-Allocatelli, 2013). The diversity in cytochrome *c* assembly routes challenges our understanding of the process considering we view the stereospecific attachment of cysteine thiols to the vinyl carbons of heme as a simple chemical reaction (Bowman *et al.,* 2008).

In plastids and several bacteria, cytochrome *c* maturation is assisted by the CCS (CCS for cytochrome *c* synthesis) factors, which were first identified through the isolation of the *ccs* mutants in the green alga *Chlamydomonas reinhardtii* (Das *et al*., 2021; Gabilly *et al.,* 2017). The *ccs* mutants are specifically blocked in the attachment of heme to the apoforms of plastid cytochromes *c*, namely membrane-bound cytochrome *f* and soluble cytochrome c_6 (Das *et al.*, 2021; Gabilly *et al.*, 2017; Karamoko *et al.*, 2013). Cytochrome *f*, one of the plastid *c*-type cytochromes, is a structural subunit of the cytochrome b_6f complex and an essential electron carrier in photosynthesis, (Kuras *et al.,* 1994; Zhou *et al.,* 1996). Consequently, the *ccs* mutants are deficient for cytochrome b_6f assembly and photosynthesis (Cline *et al.*, 2016; Gabilly *et al.*, 2017).

In the thylakoid lumen, the redox state of the apocytochrome *f* C*XX*CH motif is under the control of a) CCS5, a thylakoid-bound disulfide reductase catalyzing the reduction of the disulfide bond formed between the cysteines of the heme-binding site into thiols and b) CCDA, a thylakoid membrane protein delivering reducing power from stroma to lumen (Gabilly *et al.*, 2010; Lennartz *et al.*, 2001; Motohashi *et al.*, 2006; Motohashi *et al.*, 2010; Page *et al.*, 2004). CCS5 is classified as a member of the thioredoxin-like family, a diverse group of proteins including molecules able to mediate thiol-disulfide exchange reactions

via a redox-active WC*XX*C motif (Atkinson *et al.*, 2009). CCS5 displays high similarity to membrane-anchored lumen-facing HCF164, previously identified as being required for the assembly of cytochrome b_6f in *Arabidopsis* (Gabilly *et al.*, 2010; Lennartz *et al.*, 2001). *In vitro*, a recombinant form of CCS5/HCF164 containing the WC*XX*C motif is redox-active and able to reduce a disulfide bond formed between the heme-linking cysteines of a soluble form of apocytochrome *f* (Gabilly *et al.*, 2010; Lennartz *et al.*, 2001). The cytochrome *c* assembly defect in the *ccs5*-null mutant can be chemically corrected by exogenously applied reducing agents, an observation demonstrating the physiological relevance of the disulfide reductase activity documented from the in vitro redox assays (Gabilly *et al.*, 2010; Lennartz *et al.*, 2001). Conversion of the disulfide-linked heme binding cysteines to thiols is also dependent upon CCDA whose activity is required to maintain the catalytic WC*XX*C motif in CCS5 in the reduced form (Bushweller, 2020; Page *et al.*, 2004). The proposed model is that the thiol-disulfide oxidoreductase CCDA and the thioredoxin-like protein CCS5/HCF164 define a trans-thylakoid pathway that sequentially transfers reducing power via a cascade of thiol-disulfide exchanges from stroma to the oxidized C*XX*CH motif of apocytochrome *f* (Gabilly *et al.*, 2010; Gabilly *et al.*, 2011; Lennartz *et al.*, 2001; Motohashi *et al.*, 2006; Motohashi *et al.*, 2010; Page *et al.*, 2004). Maintenance of the C*XX*CH motif in the reduced form also relies on CCS4, a small protein predicted to be membrane-bound with a soluble domain facing the stroma (Gabilly *et al.*, 2011). However, CCS4 contains no motif or residue suggestive of a redox biochemical activity, and orthologs can only be detected in a subset of green algae (Gabilly *et al.*, 2011). The placement of CCS4 in the disulfide reduction pathway for plastid cytochrome c assembly

was inferred from the finding that provision of reductants or the expression of an additional ectopic copy of CCDA suppresses the photosynthetic deficiency of the ccs4-null mutant (Gabilly *et al.*, 2011). In this manuscript, we provide genetic and biochemical evidence for the involvement of CCS4 in a CCS5-dependent and a CCS5-independent pathway for reducing the disulfide-bonded heme-binding cysteines of apocytochrome *f* and discuss the possible functions of this assembly factor.

III. Materials and Methods

III.A. Strains, media, and growth conditions: All algal strains used in this study are listed in Table S1 in supplemental material. Strains CC-124 and CC-4533 were used as wild-type; strains CC-4129, CC-5922 and CC-5936 were used as *ccs5* mutants. The CC-5936 strain is an insertional mutant (LMJRY0402.042908) from the CLiP library (Li *et al.*, 2019) and carries the APHVIII cassette inserted in exon 3 of the CCS5 gene (Cre12.g493150). The CC-4527 strain is the *ccs5* mutant (CC-4129) complemented with the wild type CCS5 gene. This strain is referred to as *ccs5(CCS5)* and was described in GABILLY et al., 2010. Strains CC-4519, *ccs4(pCB412)* and CC-4525 were used as *ccs4* mutants. The *ccs4Δccs5(9)* and *ccs4Δccs5(11)* strains that displayed a tight photosynthetic deficiency had reverted at the end of the study. The suppressed strains were renamed SU9 and SU11 and deposited in the Chlamydomonas collection center as CC-5928 and CC-5929, respectively.

Wild-type and mutant Chlamydomonas reinhardtii strains were maintained on Tris-Acetate-Phosphate (Yang *et al.*), with Hutner's trace elements, 20 mM Tris-base and 17 mM acetic acid, or Tris-Acetate-Phosphate (Yang *et al.*) supplemented with arginine (1.9 mM) (TARG) (Harris, 1989). For some strains, TAP/TARG supplemented with 25 µg.ml^{-1} hygromycin B (TAP/TARG + Hyg) or 25 µg.ml^{-1} paromomycin (TAP/TARG + Pm) were used. All algal strains were grown on solid medium at 25°C in continuous light at 0.3 µmol/m^2/s (Harris, 1989). Solid medium contains 1.5% (w/v) agar (Select Agar™, Invitrogen, 30391049).

Growth was tested on solid TAP/TARG, minimal medium, or minimal medium supplemented with 1.7 mM acetic acid under three different light conditions. For protein immunodetection, cells were grown in liquid TAP/TARG in an environmental incubator with continuous light at 0.3 µmol/m^2/s and shaking at 180-190 rpm at 25°C.

Chemo-competent Escherichia coli DH5α strains were used as hosts for molecular cloning. The bacterial strains were grown at 37ºC in Luria-Bertani (LB) broth and LB medium solidified with bacteriological agar (Silhavy *et al.*, 1984). When antibiotic selection was required, 100 µg. ml^{-1} ampicillin or 50 µg. ml^{-1} kanamycin was added.

III.B. Genetic crosses: The experimental details for sexual crosses are described in former work (Subrahmanian *et al.,* 2020; Subrahmanian *et al.,* 2020). For molecular verification of the ccs5 allele in the haploid progeny, the presence of the molecular tag (Phi "Φ" flag) inserted in the ARG7 intron used for insertional mutagenesis was detected via diagnostic PCR using the Phi-1 (5'-GTCAGATATGGACCTTGCT-3') and Phi-2 (5'-CTTCTGCGTCATGGAAGCG-3') primers (Gabilly *et al.,* 2010). The presence of the

wild-type CCS4 allele, the *ccs4-1* mutation or suppressor mutations, *CCS4-2* and *CCS4-3*, of SU9 and SU11 respectively, was tested molecularly by diagnostic digestion of a PCR product. The alleles can be distinguished by virtue of a nucleotide polymorphism that abolishes the BanII restriction site in the nonsense (*ccs4-1*) and missense and deletion mutations (*CCS4-2* and *CCS4-3*). The cell wall deficient strains CC-5925, CC-5922 and CC-5927 were generated by crossing the CC-4525 and CC-4517 strains and examining the resulting progeny for the cell wall deficient trait, by resuspending cells in 0.1% Triton X-100. Untreated cells served as a control. Cells without a cell wall lyse in the presence of Triton X-100 (Hoffmann *et al.,* 2005). The *ccs4Δccs5* mutants were generated by crossing the *ccs5* mutant (CC-4129) with the *ccs4* mutant (CC-4520) and selecting the progeny based on arginine prototrophy and paromomycin-resistance. For generating the vegetative diploids, the *ccs5::APHVIII* mutant from the CLiP collection was used. The CC-5923 and CC-5924 are haploid *ccs5::APHVIII arg7-8* progeny originating from the cross of the CC-5936 strain by a wild type *arg7-8* strain (WT-PH2). WT-PH2 was obtained after four back-crosses of the CC-5611 (Subrahmanian *et al.,* 2020) by CC-4533 or CC-5155. The *Δccs5/Δccs5* diploids were constructed by crossing the CC-4129 strain by the CC-5924 strain and selection on TAP+Pm. The *Δccs5 /Δccs5 CCS4-2* diploids were generated by crossing the CC-5931 strain by CC-4129 and selection on TAP+Pm. The CC-5931 strain is a haploid *ccs5::APHVIII CCS4-2 arg7-8* progeny issued from the cross of CC-5928 by CC-5923. The [*Δccs5/Δccs5; CCS4-3*] diploids were generated by crossing CC-5930 by CC-5924 and selection on TAP+Pm. The CC-5930 strain is a haploid [*ccs5::ARG7Φ*; *CCS4-3* progeny] from the cross of CC-5929 by CC-5590. The wild-type diploids (+/+)

were constructed by crossing CC-425 by CC-5590 and selection of the mitotic zygotes on TAP and already used in a former study (Barbieri *et al.*, 2011).

III.C. Growth assay and thiol-dependent rescue: Cells were grown on solid acetate-containing medium (TAP or TARG) for 5-7 days at 25°C under 0.3 µmol/m^2/s illumination. Two loops of cells were resuspended in 500 µl water and optical density was measured spectrophotometrically at 750 nm and normalized to OD_{750} = 2. This normalized suspension was used as the starting material (1) to make five serial ten-fold dilutions (10^{-1}, 10^{-2}, 10^{3}, 10^{-4}, and 10^{-5}). A volume of 5 µl from each dilution was plated on solid minimal medium (CO_2) for photoautotrophic growth or TAP/TARG (acetate + CO_2) for mixotrophic growth and incubated for 7 - 14 days under 30-50 µmol/m^2/s illumination for growth assay. For thiol-dependent rescue, similar ten-fold serial dilutions were performed and equal volume from each dilution was plated on solid minimal medium (CO_2) containing 1) either no MESNA (2-MercaptoEthane Sulfonate Na, Sigma, M1511-25G), or 2) 0.75 mM or 1.5 mM MESNA. Ten-fold serial dilutions were also plated on TAP/TARG (acetate + CO_2) and incubated for 14 - 21 days under 30-50 µmol/m^2/s for thiol-dependent rescue assay and under 0.3 µmol/m^2/s with no exogenously added thiols as control.

III.D. Fluorescence rise-and-decay kinetics: Fluorescence transients (also known as Kautsky effect) were measured using Handy FluorCam from Photon System Instruments that provides actinic illumination and saturating flash of light. Cells were grown mixotrophically on solid TAP/TARG under 0.3 µmol/m^2/s illumination for 5-7 days at

25°C. To measure the fluorescence, cells are dark-adapted for 15 mins followed by a saturating flash of light. The fluorescence is recorded in arbitrary units (A.U.) over an illumination period of 5 seconds.

III.E. Protein sample preparation: For heme staining and immunoblotting, two loops of cells grown on solid acetate-containing medium (TAP or TARG) for 5-7 days at 25°C under 0.3 µmol/m^2/s illumination were collected and washed with 1-2 ml of 10 mM sodium phosphate buffer (NaH_2PO_4, pH 7.0), centrifuged at top speed and resuspended in 300 µl of the same buffer. Chlorophyll was extracted by mixing 10 µl of resuspended cells with 1 ml of acetone: methanol in a ratio of 80:20. The mixture was vortexed followed by centrifugation at 16,873 x g for 5 mins. Chlorophyll concentrations were then determined by measuring the optical density of the suspension at 652 nm. Concentrations for different strains were normalized to 1 mg/ml of chlorophyll, followed by cell lysis by two freeze-thaw cycles (samples were frozen -80°C for 1 hour and thawed on ice for ~1 hour). Cells were then separated into membrane and soluble fractions by centrifugation for 5 mins at 16,873 x g (Howe *et al.*, 1992). Membrane fractions corresponding to 10 µg of chlorophyll were separated electrophoretically by SDS-PAGE (12.5% acrylamide gel) for immunoblotting. For ECL-based heme staining, an amount of 10-20 µg of chlorophyll for each sample was used whereas for in-gel heme staining by TMBZ (3,3',5,5'-tetramethylbenzidine, Sigma, 860336-1G), a quantity corresponding to 30-40 µg of chlorophyll per sample was loaded.

III.F. Heme staining and immunoblotting: The presence of covalently bound heme in c-type cytochromes was detected by two methods, a) by enhanced chemiluminescence (ECL, Thermo Scientific, 34094) and b) in-gel TMBZ staining (3,3',5,5'-Tetramethylbenzidine, Sigma, 860336-1G), both relying on the pseudo-peroxidase activity of heme (Wilks, 2002). Detection of covalently bound heme in cytochrome c by ECL was done by separating proteins corresponding to 10-20 µg of chlorophyll on 12.5% acrylamide gel, followed by transfer to a PVDF membrane (Immobilon-P, IPVH00010) at 100 V (at 4°C) for 90 mins and treatment of the membrane with ECL reagent. In-gel heme staining was performed by soaking the gel in a solution of 6.3 mM TMBZ dissolved in methanol in the dark, mixed with 1 M sodium acetate for 1-1.5 hours in the dark with periodic shaking every 15-20 minutes. Bands revealing the heme peroxidase activity appeared immediately as a blue precipitate after addition of H_2O_2 (50% w/v) to a final concentration of 30 mM. For Immunoblotting, membrane fractions corresponding to 10 µg of chlorophyll were separated by SDS-PAGE and transferred as described above. Immunodetection was done by incubating the membrane with Chlamydomonas α-CF_1 (1:10,000), α-PsbO (1:5000, Agrisera), α-cytochrome f (1:10,000), α-CCDA (1:1000), α-CCS5 (1:3,000). The CCDA and CCS5 antibodies were described in MOTOHASHI AND HISABORI, 2010 and GABILLY et al. 2010, respectively. The anti-cytochrome f antibody is produced against a recombinant form of an apocytochrome f-GST fusion. The α -rabbit (1:10,000) was used as secondary antibody. Immunoblots were quantified by ImageJ by converting scanned images to grayscale and 8-bit (Stael *et al.,* 2022). Each band was individually selected with the rectangular ROI selection and area percentage was calculated using "Analyze > Gels >

Label peaks". Relative and adjusted density of each band was calculated for anti-CCDA immunodetection and the quantification of the mean adjusted density of three independent blots are displayed as histograms. Statistical analysis was performed using the two sample t-test and statistical significance was defined for p-value < 0.05.

III.G. Construction of the suppressor strains: The ccs4 strain expressing an additional copy of the CCDA gene was generated by introducing the construct pSL18-CCDA (Gabilly *et al.,* 2011) in the CC-4525 strain via the glass-bead method (Kindle, 1990) and selecting the transformants on TARG+Pm plates. The suppressor strains were reconstructed by introducing constructs containing the CCS4 gene from SU9 and SU11 into a *ccs4Δccs5* recipient strain. For comparison a *ccs5* strain was also reconstructed by introducing the wild-type CCS4 gene in a *ccs4Δccs5* mutant. The CCS4 gene (from ATG to stop including 165 bp of 3' UTR) was cloned in front of the promoter of the beta-tubulin encoding gene (TUB2) in the pHyg3 plasmid (Berthold *et al.,* 2002). The CCS4 sequence from wild-type (CC-124), SU9 (CC-5928) and SU11 (CC-5929) was amplified with pHyg3-CCS4-F1 (5'-GTCACAACCCGCAAACGGGCCCATGTCGACCGGCATTGAG-3') and pHyg3-CCS4-R1 (3'-ATTGTACTGAGAGTGCACCATATGCCAGCTACCTACAGTC-5'), which are ApaI- and NdeI- engineered primers using purified genomic DNA as a template. The digested PCR products were cloned at ApaI and NdeI sites in pHyg3 to yield the constructs pHyg3-CCS4(WT), pHyg3-CCS4(SU9) and pHyg3-CCS4(SU11), which were introduced into the CC-4518 strain by the glass bead transformation method (Kindle, 1990). Transformants were selected on TAP+Hyg based on the Hygromycin B resistance conferred by the iHyg3 cassette (containing the APHVII gene).

III.H. Construction of the HCF153 complemented strains: A chimeric CCS4-HCF153 gene in which the sequence corresponding to the first 32 residues of the CCS4 protein (including the predicted transmembrane domain followed by three resides) is fused to a sequence encoding the soluble domain of the A. thaliana HCF153 protein (55 amino acids) was constructed. A 381 bp fragment containing part of intron 1 (42 bp), exon 2 (68 bp), intron 2 (102 bp), exon 3 (152 bp) and a short sequence following the stop codon with an XbaI site (19 bp) was synthesized (Genewiz). Part of the coding sequence in exon 2 and all codons in exon 3, which correspond to residues in the Arabidopsis protein, were optimized to reflect the codon usage of a Chlamydomonas nuclear gene. The sequence was provided as a cloned fragment in pUC57-Kan and the resulting plasmid was named pCCS4-HCF153. The 381 bp fragment was excised from pCCS4-HCF153 using the restriction enzymes NruI and XbaI and cloned at the corresponding sites in pSL18-ORF2L. In the resulting plasmid, named pSL18-HCF153, the chimeric CCS4-HCF153 gene is expressed under the PSAD promotor. The CC-4519 strain was transformed with pSL18-HCF153 using the glass bead transformation method (Kindle, 1990) and transformants were selected on TARG+Pm under 0.3 µmol/m^2/s Transformants carrying the CCS4-HCF153 chimera were identified via diagnostic PCR using primers pSAD_Pr2 (5'-TTGGAGGTACGACCGAGATG-3') and pSADT_R1 (5'-AGCTCTTCTCCATGGTACAG-3') The amplicon was sequenced to verify the presence of the chimeric gene.

III.I. Glass bead transformation: Recipient strains were cultured in liquid TAP or TARG and grown until exponential phase. At a cell density of 2-5 x 10^6 cells/ml (measured by

hemocytometer), cells were collected by centrifugation at 1,500 x g for 5 mins at 25°C, followed by resuspension and incubation in autolysin to a density of ~1 x 10^8 cells/ml for 45 – 90 mins (depending on the strain). The efficiency of enzymatic digestion of the cell wall was tested with 0.1% Triton X-100 as described above in the section detailing genetic crosses. Autolysin was removed by centrifugation of the treated cells at 1,500 x g for 5 mins at 25°C, and cells were resuspended in medium (TARG + 40 mM sucrose) to a final concentration of 1-2 x 10^8 cells/ml. After autolysin treatment, 300 µl of cells, 100 µl of 20% PEG 8,000, 300 mg of glass beads and 1-2 µg of transforming DNA (linear or uncut) were mixed in a microfuge tube and vortexed for 30 – 45 secs at maximum speed. After glass beads settle, 300 – 350 µl of the mixture was transferred to 30 ml of TARG + 40 mM Sucrose, and incubated for 16-24 hrs at 25°C under 0.3 µmol/m^2/s. After overnight recovery, cells are collected by centrifugation at 1,500 x g for 5 mins at 25°C, resuspended in 0.5 – 1 ml of TAP and plated on selective medium. Successful transformation yields colonies in 5-7 days.

III.J. Bioinformatics: BLASTp, RPS-BLAST and PSI-BLAST searches (Altschul *et al.*, 1997) against the non-redundant database at NCBI and BLASTp search against 1KP database (Matasci *et al.*, 2014) were carried out with default parameters (1 February 2020). Protein domains were identified using Pfam (El-Gebali *et al.*, 2019) and Conserved Domain (Marchler-Bauer *et al.*, 2015) databases. Profile-profile searches for domain identification were carried out using CDvist (Adebali *et al.*, 2015) and HHpred (Söding *et al.*, 2005) servers. Multiple sequence alignments were constructed using L-INS-I method in MAFFT program (Katoh *et al.*, 2019). Sequence alignments were edited in Jalview

(Waterhouse *et al.*, 2009). Transmembrane regions and signal peptides prediction from amino acid sequences were carried out using Phobius (Käll *et al.*, 2004). Sequence logos were generated using Skylign (Wheeler *et al.*, 2014).

IV. RESULTS

IV.A. CCS4 and CCS5 are functionally redundant: Previously, we showed that CCS4 and CCS5 are specifically required to maintain the heme-binding cysteines in the reduced form, a critical step for plastid cytochrome *c* assembly (Gabilly *et al.*, 2010; Gabilly *et al.*, 2011; Xie *et al.*, 1998). To define the contribution of each component in the assembly pathway, the *ccs4 (ccs4)*, *ccs5 (Δccs5)*, and *ccs4 ccs5* double mutants (*ccs4Δccs5*) were first phenotypically assessed for photosynthetic growth, which requires a correctly assembled and functional cytochrome *f*, the membrane-bound plastid cytochrome *c* (Kuras *et al.*, 1995; Zhou *et al.*, 1996). Both *ccs4* and *ccs5* mutations correspond to complete loss of function. The *ccs5* mutation is a 3-kb deletion encompassing the entire CCS5 coding sequence (Gabilly *et al.*, 2010). The *ccs4* mutation creates a stop codon at residue 50 and results in a gene product which lacks the entire C-terminal soluble domain predicted to face the stroma. Moreover the *ccs4* mutation yields a drastic decrease in CCS4 transcript accumulation and we assume that there is probably no functional protein produced in the ccs4 mutant (Gabilly *et al.*, 2011). To assess phototrophic growth, cells were grown under a light intensity of 30-50 µmol/m^2/s, where they utilize atmospheric CO_2 to perform photosynthesis. Compared to the *ccs4* and *Δccs5* single mutants that show residual photosynthetic growth, the *ccs4Δccs5* double mutants are completely deficient for growth under phototrophic conditions (Figure 2.2A). Under low light (0.3 µmol/m^2/s), all mutant strains can grow in the presence of acetate and atmospheric CO_2 due to the dominant contribution of respiration vs. photosynthesis. Next, we performed chlorophyll fluorescence rise and decay kinetics, a non-invasive measurement of photosystem II (PSII)

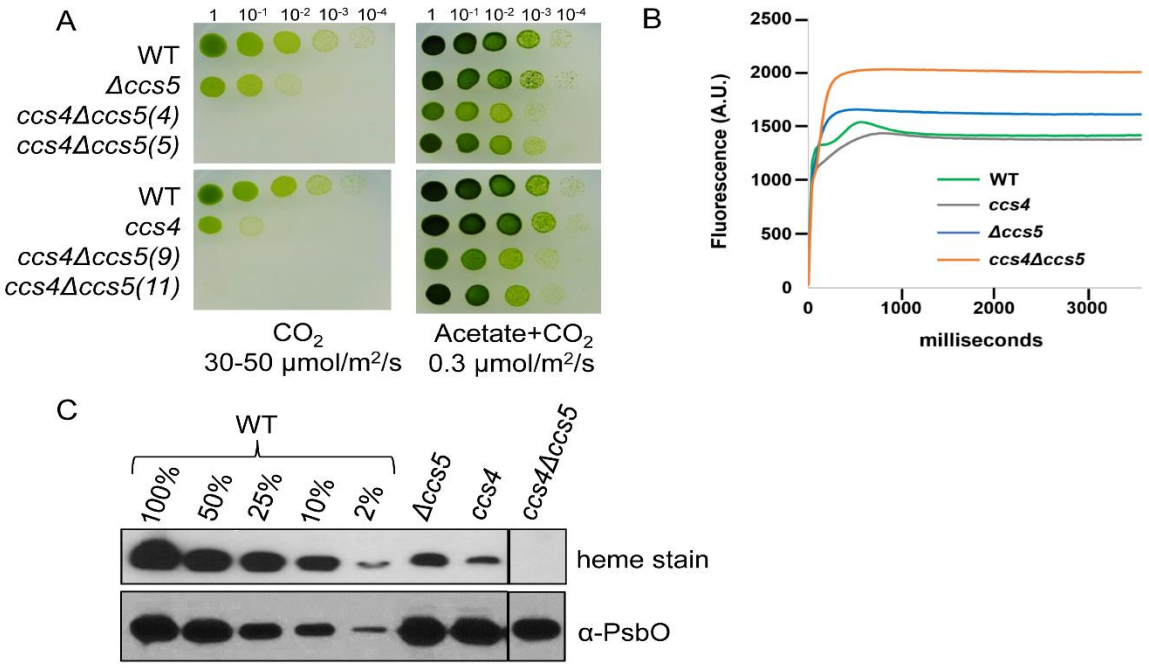

Figure 2.2. The *ccs4Δccs5* mutant exhibits a photosynthetic growth defect due to a complete loss of cytochrome *c* assembly.

(A). Ten-fold dilution series of wild type (WT, CC-124), *Δccs5* (CC-4129), *ccs4* (*ccs4(pCB412)*) and *ccs4Δccs5* (CC-4517, CC-4518 and *ccs4 ccs5 (9)*, and *(11)*) strains were plated on acetate containing (right panel) and minimal (left panel) medium. Cells grown phototrophically (CO_2) were incubated at 25°C for 7 days with 30-50 µmol/m^2/s of light. Cells grown mixotrophically (acetate + CO_2) were incubated at 25°C for 7 days with 0.3 µmol/m^2/sec of light. **(B)** The fluorescence induction and decay kinetics of *ccs4Δccs5* is shown in comparison to that of *Δccs5*, *ccs4*, and wild type. **(C)** Heme staining and α-PsbO immunodetection were performed on total protein extracts. Strains are as in 1A except for the ccs4 (CC-4519) and *ccs4Δccs5* (CC-4518). Cells were grown mixotrophically on acetate with 0.3 µmol/m^2/s of light at 25°C for 5 -7 days. Samples correspond to 30 µg of chlorophyll. Immunodetection of PsbO was used as a loading control. The vertical line indicates cropping from the same gel.

activity (Murchie *et al.*, 2013). In wild type, the initial rise indicates electron movement through PSII, which is followed by a decay that indicates electron transfer through the

cytochrome b_6f (Figure 2.2B). When the energy absorbed by the chlorophyll in PSII cannot be utilized in the photosynthetic electron transport chain because of a complete block at cytochrome b_6f, a saturating rise in fluorescence is observed with no decay phase thereafter. In *ccs4Δccs5*, the rise and plateau are a signature of a block at the level of cytochrome b_6f complex due to the absence of holocytochrome *f* (Figure 2.2B). In ccs4 and Δccs5, the decay phase is less pronounced than in wild type, an indication that the strains retained cytochrome b_6f functionality because some level of holocytochrome *f* is still assembled (Figure 2.2B), which agrees with the residual photosynthetic growth (Figure 2.2A). The level of holocytochrome *f* assembly in the different mutant strains was assessed biochemically via heme staining (Figure 2.2C). Holocytochrome *f* assembly is completely blocked in *ccs4Δccs5*, whereas the single null mutants accumulate partial levels of holocytochrome *f*, ~10% in *Δccs5* and ~>2% in *ccs4*, respectively. These results show that the synthetic photosynthetic growth defect of *ccs4Δcss5* is indeed due to a complete block in holocytochrome *f* assembly. The photosynthetic growth of the different mutant strains (Figure 2.2A) correlates with level of assembled holocytochrome *f* (Figure 2.2C). Loss of CCS4 function yields a more pronounced cytochrome *f* deficiency than loss of CCS5 function, whereas loss of both results in no cytochrome *f* assembly. Therefore, we conclude that CCS4 and CCS5 are redundant for the provision of reductants for holocytochrome *f* assembly.

IV.B. Loss of CCS4 and CCS5 can be chemically corrected by exogenous thiols: We previously showed that the partial deficiency in photosynthetic growth and holocytochrome *f* assembly in *ccs4* and *Δccs5* mutants could be rescued by the application of exogenous thiols (Gabilly *et al.*, 2010; Gabilly *et al.*, 2011). Application of reducing agents such as MESNA (2-mercaptoethane sulfonate) or DTT (Dithiothreitol, not shown)

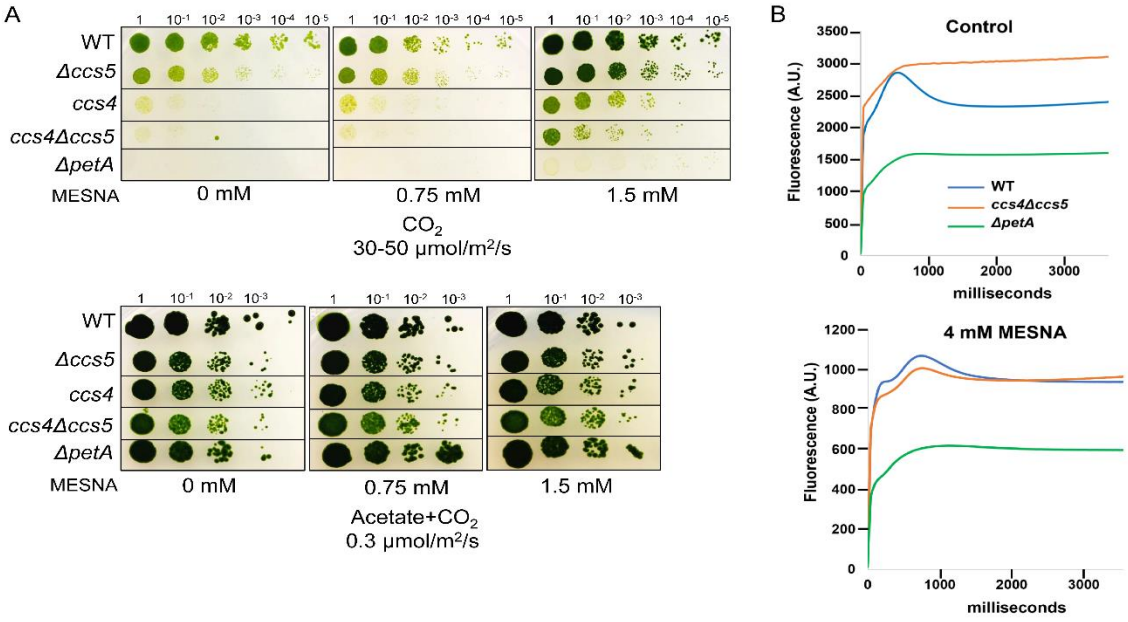

Figure 2.3. The photosynthetic defect in *ccs4Δccs5* is partially rescued by exogenous thiols.

(A) Ten-fold dilution series of wild type (WT, CC-4533), *Δccs5* (CC-5922), *ccs4* (CC-5925), *ccs4Δccs5* (CC-5927) and *ΔpetA* (CC-5935) were plated on acetate and minimal medium with or without MESNA (2-mercaptoethane sulfonate sodium). Cells grown phototrophically (CO_2) were incubated at 25°C for 20 days with 30-50 µmol/m^2/s of light. Cells grown mixotrophically (acetate + CO_2) were incubated at 25°C for 14 days with 0.3 µmol/m^2/s of light. The horizontal lines indicate cropping from the same plate of serial dilution. **(B)** Fluorescence transients were measured on cells grown on solid acetate containing media for 5 days (with 0.3 µmol/m^2/s of light) with or without MESNA. Strains are as in a except that the ccs4Δccs5 strain is CC-4518.

can also partially rescue the *ccs4Δccs5* double mutant for phototrophic growth (Figure 2.3A). Using fluorescence rise-and-decay kinetics, we documented that the chemical correction of the growth defect is due to a recovery of cytochrome b_6f function, which indicates restoration of holocytochrome *f* assembly (Figure 2.3B). Note that a higher concentration of MESNA (4 mM vs.1.5 mM) was necessary to evoke a rescue of the *ccs4Δccs5* double mutant in the fluorescence transient experiments. We presumed that this difference is because cells are grown phototrophically under 30-50 µmol/m^2/s for the growth assessment (Figure 2.3A) vs. mixotrophically under 0.3 µmol/m^2/s for the measurement of fluorescence transients (Figure 2.3B). The *ΔpetA* mutant, a null mutant in the plastid gene encoding apocytochrome f (Zhou *et al.*, 1996), is completely blocked for photosynthetic growth and does not show any rescue with exogenous thiols, as expected.

IV.C. The abundance of CCDA is diminished in the *ccs4* but not in the *ccs5* mutant:

Expression of an additional ectopic copy of CCDA encoding the trans-thylakoid thiol-disulfide oxidoreductase was shown to suppress ccs4 (Gabilly *et al.,* 2011). This result led to the hypothesis that CCS4 might be involved in the stabilization of CCDA. To test this hypothesis, we monitored the abundance of CCDA by immunoblotting using an antibody against *Arabidopsis* CCDA but cross-reacting with the algal ortholog (Motohashi *et al.*, 2010). Because the original CCDA suppressed strain (Gabilly *et al.,* 2011) lost the suppression over time, the strain was reconstructed. The suppression is weak but is best seen when the strain with an extra ectopic copy of CCDA is grown in mixotrophic conditions under 30-50 mmol/m^2/s illumination (Figure 2.3A). The CCDA protein abundance decreased to ~50% of the wild-type level in ccs4 but was restored to normal

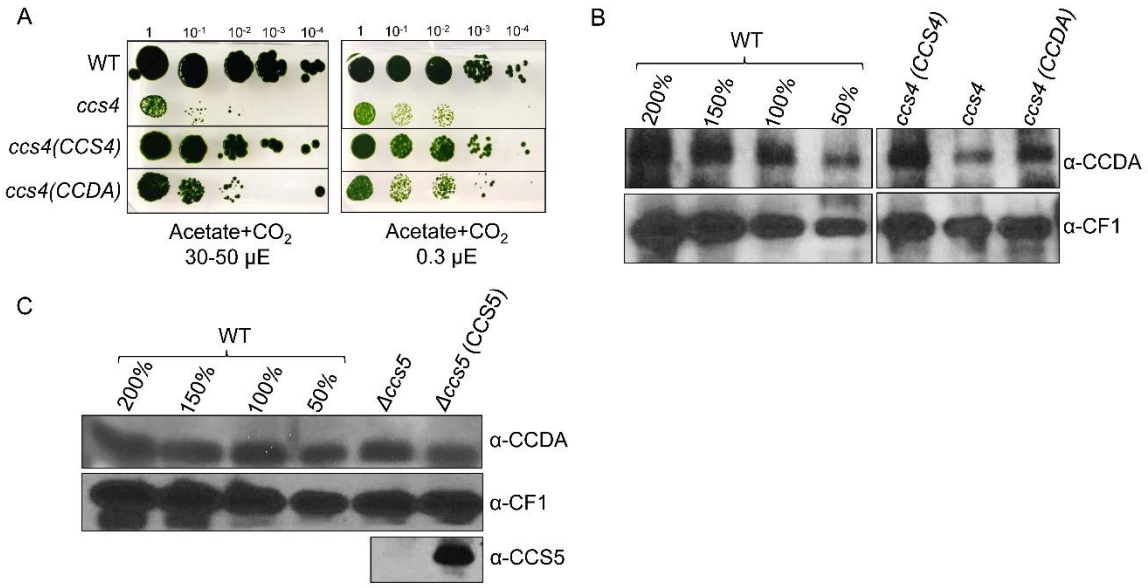

Figure 2.4. The abundance of CCDA is diminished in the *ccs4* but not in the *ccs5* mutant.

(A) Suppression of the photosynthetic growth defect in the ccs4 mutant by ectopic expression of CCDA was assessed by ten-fold dilution series. The wild type (WT, CC-124), *ccs4* (CC-4520), *ccs4* expressing (ccs4 (CCS4)), (CC-4522) and CCDA expressing (ccs4 (CCDA), CC-5926) ccs4 strains were plated on acetate medium and grown mixotrophically (with 30-50 µmol/m^2/s or 0.3 µmol/m^2/s of light) at 25°C for 14 days. The horizontal lines indicate cropping from the same plate. (B) and (C) CCDA was immunodetected on total protein extracts of strains described in (A) and the Δccs5 (CC-4129) and corresponding complemented (Δccs5(CCS5), CC-4527) strains. Cells were grown mixotrophically (on acetate with 0.3 µmol/m^2/s of light) at 25°C for 5 -7 days. The vertical line indicates cropping from the same blot. Samples (100%) correspond to 10 µg of chlorophyll. Immunodetection with antisera raised against Chlamydomonas CF_1 (Coupling Factor 1 of chloroplast ATPase) and CCS5 were used as control (Gabilly *et al.*, 2010).

levels in the CCS4 complemented strain and enhanced in the strain expressing an ectopic copy of the CCDA gene (Figure 2.4B and Figure 2.5A). Conceivably, the decrease in CCDA abundance is not specific to the loss of CCS4 but is a more general result of perturbing the function of the b_6f node. However, we showed that the loss of CCS5 has no effect on CCDA abundance (Figure 2.4C and Figure 2.5B), which suggests that the

decrease in CCDA steady-state level is specific to the loss of CCS4. From this result, we conclude that CCDA abundance is diminished when CCS4 function is compromised.

IV.D. Photosynthetic revertants of *ccs4Δccs5* double mutant are restored for cytochrome *f* assembly: Over the course of this study, we noticed that two slow-growing *ccs4Δccs5* strains (#9 and #11, Figure 2.2A) had evolved a faster growth phenotype. We suspected reversion to photosynthetic proficiency and named the strains SU9 and SU11 for suppressors of *ccs4Δccs5#9* and #11, respectively. To test for the restoration of photosynthesis, we assessed the growth on acetate under high illumination. Under such

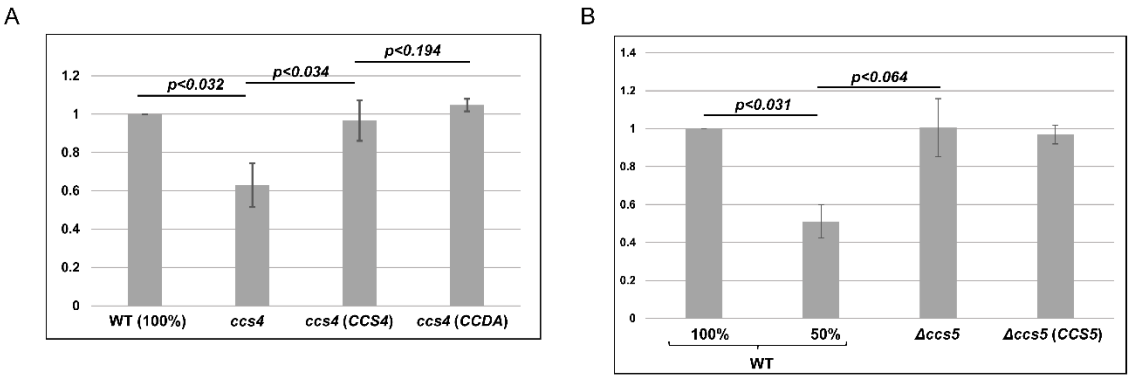

Figure 2.5. Quantification of the signal associated to CCDA immunodetection.

The adjusted relative density (relative density of CCDA/relative density of CF_1) of the imaged bands are calculated for the actual protein load (20 µg chlorophyll) and the mean relative density and the standard error of the mean are plotted against three independent blots. p-value was calculated by a two-sample t-test and statistical significance was defined for p-value < 0.05.

conditions, cytochrome b_6f deficient strains display significant photosensitivity (Malnoë *et al.*, 2014). A *ccs4Δccs5* strain that had retained a tight photosynthetic deficiency due to loss of cytochrome *f* assembly displayed a photosensitive phenotype (Figure 2.6A). Interestingly, both SU9 and SU11 were resistant to high light treatment, suggesting the

original *ccs4Δccs5#9* and *ccs4Δccs5#11* strains have recovered the b_6f function (Figure 2.6A). Fluorescence transients confirmed restoration of the b_6f function in SU9 and SU11 (Figure 2.6B). We showed that photosynthetic proficiency in SU9 and SU11 is due to recovery of holocytochrome *f* assembly, as shown by heme staining and immunodetection (Figure 2.6C). In SU9, cytochrome *f* assembly restoration is partial (~25%) but in SU11, restoration appears to be wild type like (Figure 2.6C). The level of holocytochrome *f* assembly in SU9 and SU11 (Figure 2.6C) correlates with the recovery of photosynthetic proficiency assessed by growth in mixotrophic conditions and measurement of fluorescence transients (Figures 2.6AB).

IV.E. Reversion of the *ccs4Δccs5* is due to spontaneous dominant gain-of-function mutations in *CCS4*: Next we sought to determine the molecular basis of the reversion in SU9 and SU11. We ruled out the possibility that a suppressor mutation maps to the CCS5 gene, considering a 3 kb region containing the entire coding sequence of CCS5 is missing in *Δccs5* (Gabilly *et al.*, 2010). Instead, we suspected that the point mutation (C to T) at a codon (**C**AG) encoding a glutamine (Q_{50}) in the CCS4 gene might have reverted in SU9 and SU11 (Gabilly *et al.*, 2011). Sequencing of the CCS4 gene in SU9 revealed the nonsense mutation in the original ccs4 mutant (TAG) was changed to a missense mutation (T**G**G) resulting in a tryptophan (W) residue (Figure 2.7A). Surprisingly, in SU11, the CCS4 gene carried an in-frame deletion of 3 codons removing the stop codon (GCT**TAG**ATG), resulting in a CCS4 protein shorter by 3 residues (Figure 2.7A). The intragenic mutations in the CCS4 gene alter residues in the soluble domain of CCS4, which is predicted to face the stromal side of the thylakoid membrane (Gabilly *et al.*, 2011).

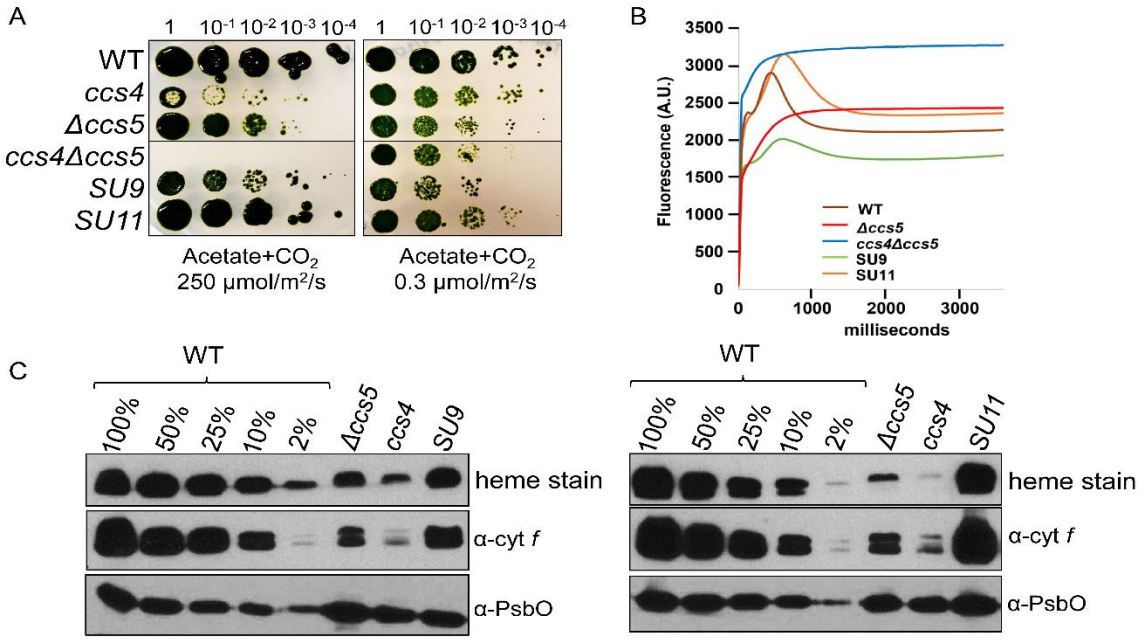

Figure 2.6. Suppressors of *ccs4Δccs5* are restored for phototrophic growth and cytochrome *f* assembly.

(A) Ten-fold dilution series of wild type (WT, CC-124), *Δccs5* (CC-4129), *ccs4* (CC-4519) and *ccs4Δccs5* (CC-4518), SU9 (CC-5928) and SU11 (CC-5934) were plated on acetate medium and grown mixotrophically (with 250 µmol/m^2/s or 0.3 µmol/m^2/s of light) at 25°C for 14-18 days. The horizontal line indicates cropping from the same plate of serial dilutions. (B) The fluorescence induction and decay kinetics observed in a dark-to-light transition of the SU9 and SU11 suppressors are shown in comparison to *ccs4Δccs5*, *Δccs5* and wild type. Strains are the same as in A. (C) Heme staining, and immunoblotting (α-cyt*f* and α-PsbO) were performed on total protein extracts prepared from cells (same strains as in A) grown mixotrophically (on acetate with 0.3 µmol/m^2/s of light) at 25°C for 5 -7 days. Samples (100%) correspond to 10 µg of chlorophyll. Immunodetection with antisera against PsbO was used as loading control.

To ascertain that the molecular changes identified in CCS4 were responsible for the suppression, we performed genetic analysis by crossing SU9 and SU11 to the original *ccs4Δccs5*, or *ccs4* or *Δccs5* mutants. However, despite several attempts, no complete

tetrads and very few viable haploid progeny were recovered from our genetic crosses. We opted to reconstruct the suppressed strains in the background of the *ccs4Δccs5* strain. The CCS4 gene from wild-type, SU9 and SU11 strains was cloned in a plasmid and the resulting constructs were introduced into a *ccs4Δccs5* mutant followed by analysis of photosynthetic growth and holocytochrome *f* assembly from representative transformants.

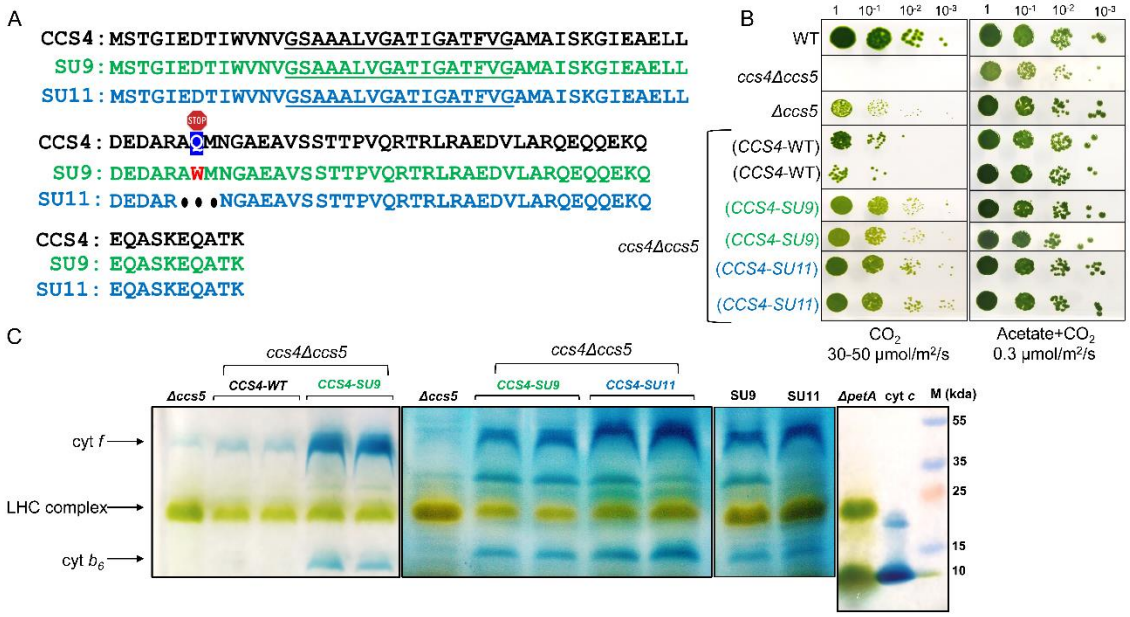

Figure 2.7. Mutations in *CCS4* suppress the cytochrome f assembly defect in the *ccs5* mutant.

(A) Amino acid sequence of CCS4 deduced from the CCS4 gene in the original ccs4-1 mutant, SU9 and SU11 are shown in black, green, and blue, respectively. The putative transmembrane domain, predicted using the TMHMM-2.0 prediction tool (Krogh *et al.*, 2001), is underlined. Sequence analysis of the *CCS4* gene shows that the original nonsense mutation in the ccs4 strain is changed to a missense mutation in SU9, resulting in the stop codon (at residue 50 of the protein) becoming a codon for tryptophan (wildtype codon is glutamine). In SU11, an in-frame deletion mutation encompassing the missense mutation resulted in a deletion of three residues $A_{49}Q_{50}M_{51}$ in the *CCS4* gene product. (B) Wild-type (WT, CC-124), *ccs5* (*Δccs5*, CC-4429), *ccs4Δccs5* (CC-4518)) and the reconstructed *ccs5* (*CCS4*-WT,CC-5932), SU9 (CCS4-SU9, CC-5933),

and SU11 (CCS4-SU11, CC-5934) strains were used for ten-fold dilution series. The Δccs5, SU9 and SU11 were reconstructed by introducing the constructs pHyg3-CCS4(WT), pHyg3-CCS4(SU9) and pHyg3-CCS4(SU11) into a *ccs4Δccs5* recipient strain. Two independent transformants for each construct are shown. Cells were plated on minimal medium and grown phototrophically (with 30-50 µmol/m^2/s of light) or mixotrophically (with 0.3 µmol/m^2/s of light) at 25°C for 14-18 days. The horizontal lines indicate cropping from the same plate of serial dilutions. (C) In-gel heme staining was performed on total protein extracts corresponding to 30 µg of chlorophyll. Samples from the Δccs5 and original SU9 (CC-5933) and SU11 (CC-5934) were loaded on the gel for comparison to the reconstructed strains. The strains are as in (B) and *ΔpetA* is CC-5935. The level of LHC complex is used as a loading control. One µg equine heart cytochrome c (~10 kDa; Sigma) is used as a control for the heme-dependent peroxidase activity.

In comparison to the recipient *ccs4Δccs5*, (that is completely blocked for photosynthetic growth), transformants expressing the wild-type CCS4 gene showed the phenotype of the *Δccs5* strain, whereas transformants expressing CCS4 with the mutations exhibit enhanced photosynthetic growth (Figure 2.7B). The phenotypes of the reconstructed suppressed strains mirrored that of the original SU9 and SU11, with the reconstructed SU11 displaying a greater suppression of the photosynthetic defect than reconstructed SU9. We further demonstrated that the restoration of photosynthetic growth in the reconstructed suppressed strains is due to restoration of cytochrome *f* assembly, as shown by heme staining (Figure 2.7C). We also noted the restoration of holocytochrome b_6 accumulation, which is dependent upon the level of holocytochrome *f*, indicating that cytochrome b_6f complex assembly is also restored (Figure 2.7C). In both the original SU9 and SU11 and the reconstructed suppressed strains, the mutations in CCS4 restore the level of holocytochrome *f* assembly above that of the ccs5-null mutant, suggesting these mutations confer a gain-of-function. The photosynthetic growth of *Δccs5* x SU9 and *Δccs5* x SU11

diploids is enhanced compared to that of *Δccs5* x *Δccs5* diploids (Figure 2.8). This demonstrates that the CCS4 mutations in SU9 and SU11 are dominant, as expected for gain-of-function mutations. We conclude that dominant suppressor mutations in CCS4 are the molecular basis for the restoration of cytochrome *f* assembly in the SU9 and SU11 strains. We named the suppressor mutations in SU9 and SU11, *CCS4-2* and *CCS4-3*, respectively.

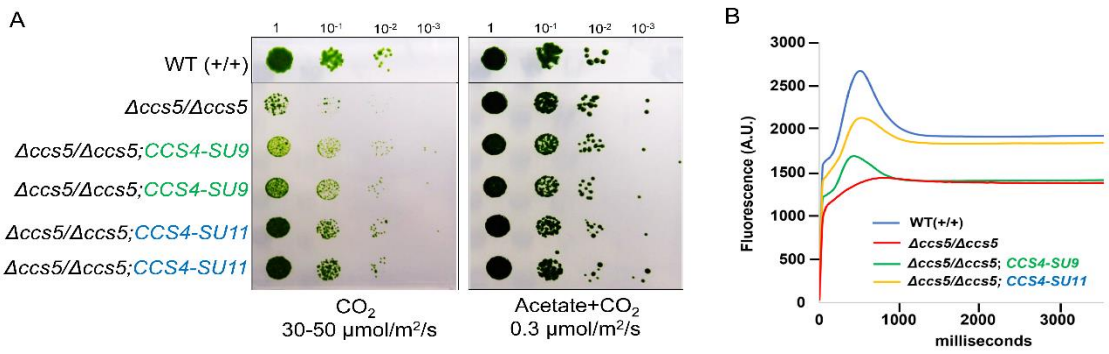

Figure 2.8. Mutations in *CCS4* in SU9 and SU11 are dominant.

(A)Ten-fold dilution series of diploid (+/+, *Δccs5* /*Δccs5*, *Δccs5*/*Δccs5*;*CCS4-SU9* and *Δccs5/Δccs5;CCS4-SU11*) strains were plated on minimal medium and grown phototrophically (with 30-50 µmol/m^2/sec of light) at 25°C for 14-18 days (left panel) and mixotrophically in 0.3 µmol/m^2/sec for 20-21 days (right panel). Two representatives of each diploid constructed with a Dccs5 strain are shown. (B) The fluorescence induction and decay kinetics of one representative diploid strain. Strains are the same as in A.

IV.F. The abundance of CCDA is unchanged in the suppressor strains: Because loss of CCS4 function yields a decrease in the abundance of CCDA (Figure 2.4B), we wondered if the steady-state level of CCDA in the suppressor strains was restored with the regain of CCS4 activity. As shown in Figure 2.9, the CCDA level in SU9 and SU11 is restored compared to a *ccs4* mutant. Immunodetection of CCDA indicated that the abundance of

the protein in the suppressor strains is comparable to that of wild-type or *Δccs5*. We conclude that alteration of the residues caused by the *CCS4-2* and *CCS4-3* mutations does not modify the accumulation of the CCDA protein.

IV.G. CCS4 – like proteins occur in the green lineage: With the exception of orthologs detected in close relatives of *Chlamydomonas*, we previously reported that CCS4 does not appear to be evolutionarily conserved (Gabilly *et al.*, 2011). CCS4-like proteins in algal species related to *Chlamydomonas* are small proteins (<100 residues) with a putative

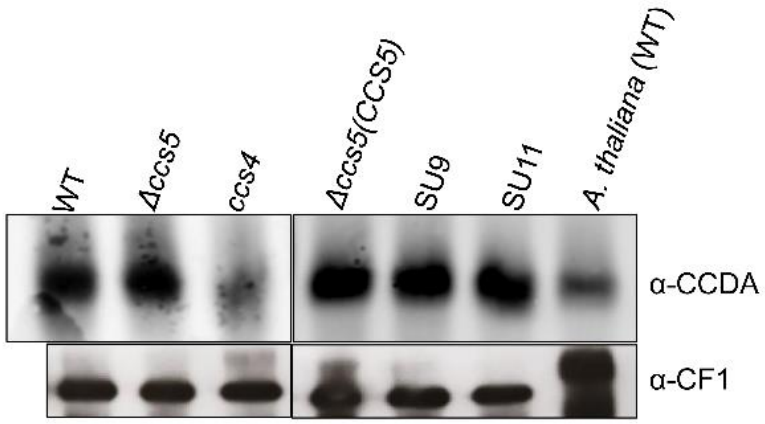

Figure 2.9. Accumulation of CCDA in the suppressor strains SU9 and SU11

CCDA was immunodetected on total protein extracts of wild – type (WT, CC-124), ccs4 (CC-4519), Δccs5 (CC-4129), Δccs5 complemented with CCS5 (CC-4527), SU9 (CC-5928) and SU11 (CC-5929) strains. Cells were grown mixotrophically (on acetate with 0.3 µmol/m^2/s of light) at 25°C for 5 -7 days. The vertical line indicates cropping from the same blot. Samples (100%) correspond to 10 µg of chlorophyll. Immunodetection with antisera raised against Chlamydomonas CF_1 (Coupling Factor 1 of chloroplast ATPase) was used as control (Gabilly *et al.*, 2010).

transmembrane domain suggesting anchoring to the membrane (Figure 2.10). Remarkably, the C-terminal domain of algal CCS4 orthologs is predicted to face the stroma and is characterized by an abundance of charged residues (Figure 2.10). To identify CCS4-like

proteins that might have considerably diverged, we performed an exhaustive search using PSI-BLAST. CCS4-like proteins were identified in several species of green algae and land plants, which constitute the Viridiplantae or the entire green lineage (Figure 2.10).

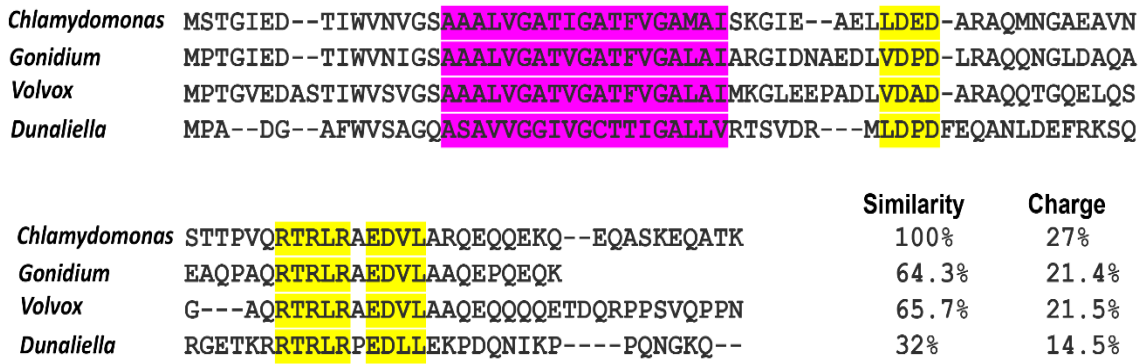

Figure 2.10. Conservation of CCS4 in chlorophytes

Alignment of CCS4 from Chlamydomonas reinhardtii (accession no. ADL27744.1), Gonium pectoral (accession no. KXZ48069.1), Volvox carteri (accession no. FD920844.1), Dunaliella salina (accession no. BM447122.1) was performed using Clustal omega (Sievers *et al.*, 2014). The putative transmembrane domain is highlighted in purple (using TMHMM-2.0 prediction tool) (Krogh *et al.*, 2001). Strictly conserved or similar amino acids are highlighted in yellow. The percentage of similarity to the Chlamydomonas ortholog is indicated. The percentage of charged residues (lysine, arginine, aspartate, and glutamate) in the stroma facing domain is provided.

IV.H. HCF153, a CCS4-like protein functions in plastid cytochrome *c* assembly: To test if the function of the CCS4-like proteins retrieved from our analysis (Figure 2.11) is conserved in the green lineage, we chose to perform a heterologous functional complementation experiment. Because the CCS4 and HCF153 proteins are most divergent in their N-termini (Gabilly *et al.*, 2011; Lennartz *et al.*, 2006), we designed a CCS4-HCF153 construct encoding a chimeric protein in which the N-terminal domain including

the putative transmembrane of CCS4 is fused to the soluble domain of HCF153 (Figure 2.12).

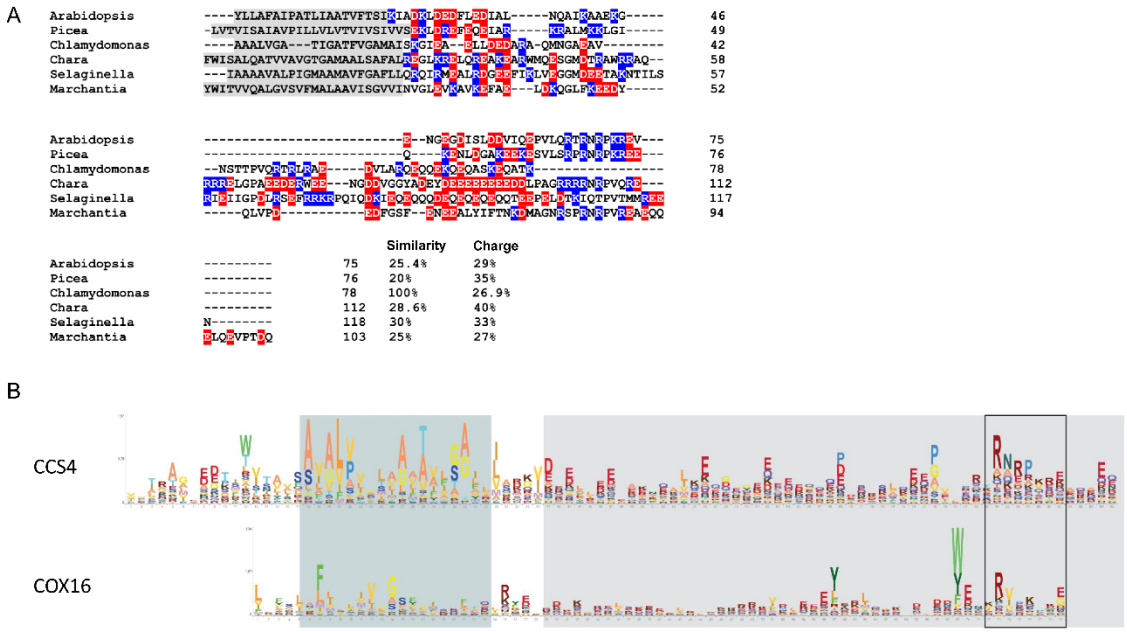

Figure 2.11. CCS4-like proteins are present throughout the green lineage.

Sequences of *Arabidopsis thaliana* (accession no. NP_194884.1), *Picea sitchensis* (Sitka spruce, accession no. ABK22505.1), *Chlamydomonas reinhardtii* (accession no. ADL27744.1), *Chara braunii* (Braun's stonewort, accession no. GBG73810.1), *Selaginella moellendorffii* (Spikemoss, accession no. XP_024543966.1) were aligned using Clustal omega (Sievers *et al.*, 2014) and manually edited in Word. The transmembrane domains are highlighted in grey, residues with positive and negative charges are highlighted in blue and red, respectively.

As shown in Figure 2.13, expression of the CCS4-HCF153 construct complements the defect due to loss of CCS4. The transformants complemented by the CCS4-HCF153 gene could not be distinguished from those expressing the CCS4 gene based on the assessment of photosynthetic growth (Figure 2.13A) and restoration of cytochrome *f* assembly and cytochrome b_6f function (Figure 2.13BC). We conclude that HCF153 functions in plastid

cytochrome *c* assembly, a finding that supports the conservation of CCS4 function from green algae to land plants.

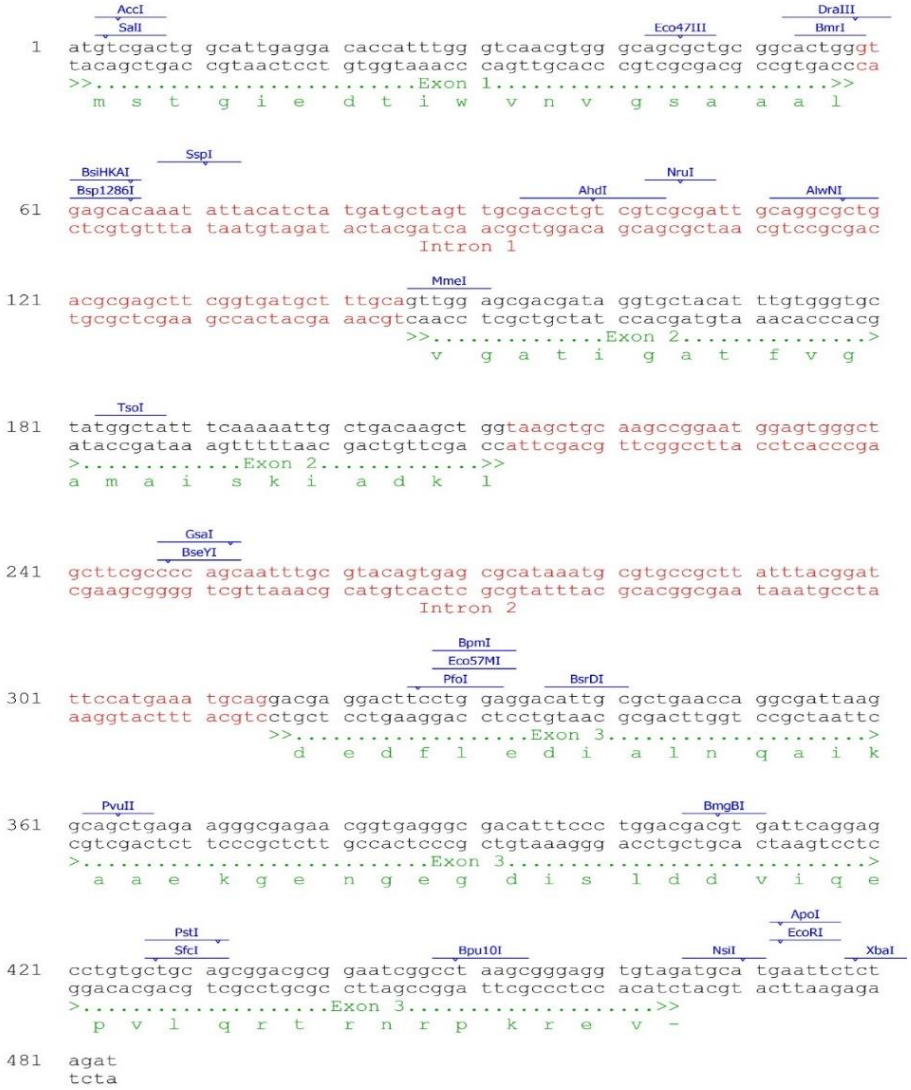

Figure 2.12. Sequence of the CCS4-HCF153 chimeric gene used for the heterologous complementation experiments.

The sequence of the constructed CCS4-HCF153 chimeric gene with three exons (in green) and two introns (in red) was annotated in Clone Manager.

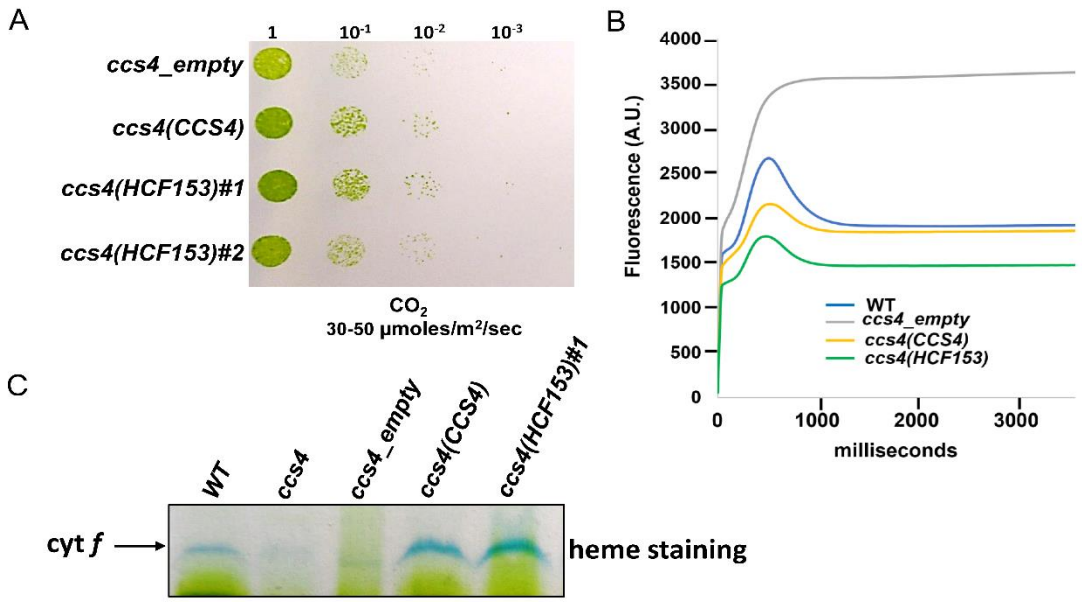

Figure 2.13. Arabidopsis HCF153 complements the *ccs4* mutant.

(A) Ten-fold dilution series of ccs4 (*ccs4_empty*, CC-4520, *ccs4* transformed by the CCS4 gene (CC-4522) and two independent ccs4 transformants carrying the CCS4-HCF153 gene (CC-5592 and CC-5593) were plated on minimal medium and grown phototrophically (with 30-50 µmol/m^2/sec of light) at 25°C for 14 days. (B) The fluorescence induction and decay kinetics of the one representative CCS4-HCF153 transformant (CC-5592) is shown in comparison to that of a wild-type (CC-124) and ccs4 strains (CC-4520). (C) In-gel heme staining was performed on total protein extracts corresponding to 30 µg of chlorophyll. The strains are as in (A) and (B) and the ccs4 strain is CC-4519.

IV.I. CCS4 – like proteins are related to mitochondrial Cox16: Interestingly, our analysis also revealed that CCS4 orthologs are related to COX16, a protein involved in the assembly of cytochrome *c* oxidase, a respiratory enzyme required for energy-transduction in mitochondria (Carlson *et al.*, 2003) (Figure 2.11B). First identified in yeast, COX16 is a mitochondrial inner membrane bound protein with a C-terminal domain facing the intermembrane space (Carlson *et al.*, 2003). The biochemical activity of COX16 still

remains enigmatic but its placement in a disulfide reducing pathway required for Cu incorporation into the Cox2 subunit of cytochrome *c* oxidase suggests COX16 and CCS4 might share some commonalities in their biochemical activity (Aich *et al.*, 2018; Cerqua *et al.*, 2018; Su *et al.*, 2017).

V. DISCUSSION

CCS4 and CCS5 are functionally redundant in the delivery of reductants: In all bacteria and plastids, cytochrome *c* maturation relies on the transfer of reducing power from the n-side to the p-side via sequential thiol-disulfide exchanges involving a membrane thiol-disulfide oxidoreductase of the DsbD family and a thioredoxin-like protein (Bushweller, 2020; Das *et al.*, 2021; Gabilly *et al.*, 2017). Operation of this transmembrane pathway is critical to counter the oxidation of the heme-linking cysteines in the C*XX*CH motif of apocytochrome *c* into a disulfide (Das *et al.*, 2021; Gabilly *et al.*, 2017). The disulfide bonded heme binding site is directly reduced by a membrane-anchored *p*-side facing thioredoxin-like named CcmG/ResA/CcsX in bacteria (Beckett *et al.*, 2000; Beckman *et al.*, 1993; Erlendsson *et al.*, 2003) and CCS5/HCF164 in plastids (Gabilly *et al.*, 2010; Lennartz *et al.*, 2001). The *Chlamydomonas ccs5*-null and the *Arabidopsis hcf164*-null mutants are still able to grow photosynthetically because they are partially deficient in plastid holocytochrome *f* (Gabilly *et al.*, 2010; Gabilly *et al.*, 2011). In bacteria, loss of the thioredoxin-like CcmG/CcsX/ResA protein results in a complete block in cytochrome *c* maturation, suggesting that redundancy in the provision of reductants is specific to the assembly of *c*-type cytochromes in the plastid (Beckett *et al.*, 2000; Beckman *et al.*, 1993; Deshmukh *et al.*, 2000; Fabianek *et al.*, 1998; Schiött *et al.*, 1997). In *Chlamydomonas*, the *ccs4*-null is still able to grow photosynthetically because it is partially deficient in plastid holocytochrome *f* (Gabilly *et al.*, 2010; Gabilly *et al.*, 2011). However, the *ccs4*-null *ccs5*-null double mutant displays a synthetic photosynthesis-minus phenotype characterized by a complete loss of holocytochrome *f* accumulation, an indication that CCS4 and CCS5 are

redundant (Figure 2.2). Evidence that *ccs4Δccs5* can be rescued by application of exogenous thiols similarly to each single *ccs4* and *Δccs5* mutants (Gabilly *et al.*, 2010; Gabilly *et al.*, 2011 and Figure 2) solidifies the view that the complete block in plastid cytochrome c maturation is attributed to a defect in the provision of reductants.

CCS4 is required to stabilize CCDA: The finding that ectopic expression of CCDA partially suppresses the photosynthetic deficiency of the *ccs4* mutant led to the proposal that CCS4 might function in the reducing pathway by stabilizing CCDA (Gabilly *et al.*, 2011). CCDA levels are significantly decreased due to loss of CCS4 function and restored upon complementation with the CCS4 gene or suppression by CCDA (Figure 2.4). Because the CCDA gene is not downregulated in the *ccs4* mutant (Gabilly *et al.*, 2011), a plausible scenario is that CCDA is still synthesized, imported into the plastid but destabilized in the absence of CCS4 and presumably partially turned over (Figure 2.4). One possibility is that the transmembrane domain of CCS4 is the structural element required for stabilizing the CCDA protein. However, a single function for CCS4 as a stabilizer of CCDA is probably an oversimplification.

The soluble domain of CCS4 controls the delivery of reducing power by CCDA?: The fact that CCS4 function is not restricted to the stabilization of CCDA was evidenced with the isolation of dominant *CCS4-2* and *CCS4-3* mutations in photosynthetic revertants of the *ccs4Δccs5* mutants (Figures 2.5 and 2.6). In the CCS4-2 mutation, the original stop codon was changed to a codon encoding a tryptophan (instead of a glutamine in the wild-type

CCS4) while in the *CCS4-3* mutation, an in-frame deletion produces a CCS4 protein which is shorter by three amino-acids (Figure 2.7A). Suppressor mutations in the CCS4 gene restore cytochrome *f* accumulation above the residual levels in the *Δccs5* mutant, suggesting that these are gain-of-function mutations (Figures 2.5 and 2.6). The mechanism of suppression is unclear but one possible interpretation is that alteration of the stroma-facing domain of CCS4, where the changes occur, enhance the transduction of reducing power across the thylakoid membrane when CCS5 no longer operates. Indeed, the CCS5 gene is deleted in SU9 and SU11 and hence the CCS5-dependent reduction of the disulfide-bonded C*XX*CH motif no longer takes place. In instance where CCS5 function is lost, the provision of reducing equivalents to the lumen is probably still dependent upon CCDA. The abundance of CCDA in the suppressor strains is like that of a *Δccs5* mutant (Figure 2.9) and we established previously that CCDA overexpression does not compensate for loss of CCS5 (Gabilly *et al.,* 2011). It is conceivable that alteration of the residues in the C-terminal domain of CCS4, predicted to face the stroma, modifies the redox activity of CCDA such that delivery of reducing power to the lumen is increased in the suppressor strains.

Conservation in the green lineage and evolutionary relationship to COX16: In this study, we also provide evidence for the occurrence of highly divergent CCS4-like proteins in Viridiplantae. Interestingly, HCF153, the CCS4-like protein in Arabidopsis (Figure 2.12) localizes to the plastid and is tightly bound to the thylakoid membrane (Lennartz *et al.,* 2006). A possible function in holocytochrome *f* maturation is supported by the fact that

loss of HCF153 elicits a cytochrome b_6f assembly defect (Lennartz *et al.,* 2006). That HCF153 is the functional equivalent to CCS4 is now established from our heterologous complementation experiments (Figure 2.13). Our result suggests that despite little sequence conservation, the function of CCS4 in plastid cytochrome *c* maturation is maintained in the green lineage. CCS4-like proteins in the plastid are related to COX16-like proteins in mitochondria, which exhibit a transmembrane domain and a charged C-terminal moiety facing the IMS (Figure 2.11B). Studies in yeast and humans have placed Cox16 in a disulfide reducing pathway for insertion of Cu in cytochrome *c* oxidase but its biochemical activity remains undeciphered (Aich *et al.,* 2018; Cerqua *et al.,* 2018; Su *et al.,* 2017). Considering there are no residues or motifs suggesting a reducing activity, CCS4 and COX16 might function in a disulfide reducing pathway to recruit the source of reducing power or to create a chemical microenvironment for efficient use of the reductant by dedicated disulfide reductases. In plastids, stromal thioredoxin-*m* is the proposed source of electrons for CCDA based on *in organello* experiments (Motohashi *et al.,* 2010). In the mitochondrial IMS, the source of electrons in the disulfide reducing pathway for Cox16-dependent metalation of Cox2 is currently unknown (Swaminathan *et al.*, 2022).

Two routes for distribution of reducing power in cytochrome c assembly: We propose that maintenance of the heme-binding cysteines in the reduced state in the lumen depends on the delivery of reducing power via two routes (1 and 2) with CCDA and CCS4/HCF153 as shared components to both routes (see graphical abstract). In a simple model, CCDA transduces the source of reducing power from stroma to lumen across the thylakoid

membrane via thiol-disulfide exchanges and is stabilized by CCS4/HCF153. CCS4/HCF153 is also likely to be directly required for the CCDA-dependent transfer of reducing power, possibly by recruiting a stromal reductant to CCDA or controlling the thiol-disulfide chemistry involving the redox active cysteines in CCDA. The CCS5-dependent pathway (route 1) is conserved in bacteria and relies on CCS5/HCF164 for the provision of reductants in the lumen. The other pathway is CCS5-independent (route 2) and must rely on one or several lumen resident enzyme(s) (X) whose identity remains unknown. If the operation of the trans-thylakoid disulfide reduction pathways is critical to counter the oxidation of the heme-linking cysteines in the CXXCH motif into a disulfide, the nature of the oxidant is unknown (Das *et al.*, 2021; Gabilly *et al.*, 2017). In bacteria, there is genetic evidence that the heme-linking cysteines are first targets of the disulfide bond forming machinery and subsequently reduced via the transmembrane disulfide reducing pathway prior to the heme ligation reaction (Erlendsson *et al.*, 2003; Erlendsson *et al.*, 2002; Small *et al.*, 2013; Turkarslan *et al.*, 2008). We envision that a similar mechanism exists in the thylakoid lumen. In Arabidopsis, a disulfide bond forming enzyme named LTO1 (Lumen Thiol Oxidoreductase1) has been described (Feng *et al.*, 2011; Karamoko *et al.*, 2011). That the CXXCH of apocytochrome *f* is a relevant target of action of LTO1 still awaits experimental testing.

3. LTO1, a VKOR-homolog is the luminal oxidant of the heme linking cysteines in apocytochrome *f*.

I. INTRODUCTION

The *c*-type cytochromes are heme-containing metalloproteins that function as one-electron carriers or as enzyme subunits (Hamel *et al.*, 2009; Kranz *et al.*, 2009; Thöny-Meyer, 1997) in ATP-producing processes such as oxidative phosphorylation and photorespiration (Bertini *et al.*, 2006; Das *et al.*, 2021; Hamel *et al.*, 2009; Ma *et al.*, 2019). Assembly or maturation of holocytochromes *c* occurs on the *p*-side of energy transducing membranes such as the bacterial periplasm, mitochondrial intermembrane space and chloroplast thylakoid lumen (Park *et al.*, 2023) via covalent attachment of a heme prosthetic group to cysteines on the apocytochrome *c* (Alvarez-Paggi *et al.*, 2017; Das *et al.*, 2021; Harvat *et al.*, 2009; Kranz *et al.*, 2009). The stereospecific covalent thioether linkage between the thiols of a conserved C*XX*CH motif in apocytochromes *c* and vinyl carbons of heme cofactor is a chemical reaction under redox control. Both apocytochrome *c* and heme need to be maintained in a reduced state via catalyzed redox reactions (Barker *et al.*, 1999; Das *et al.*, 2021; Ferguson *et al.*, 2008; Hamel *et al.*, 2009; Kranz *et al.*, 2009; Mavridou *et al.*, 2013; Nakamoto *et al.*, 2000; Thöny-Meyer, 1997). Extensive genetic and biochemical studies in different systems have shown that unique disulfide reducing systems exists to maintain the cysteinyl thiols of the C*XX*CH heme-binding motif in apocytochrome *c* and

the heme prosthetic group in a reduced state. In bacteria, apocytochrome *c* heme-binding cysteines are reduced by transfer of electrons from cytoplasm to the periplasmic space via DsbD/CcdA, a transmembrane thiol-disulfide oxidoreductase (TDOR)c, and ResA/CcsX/CcmG, a thioredoxin-like protein facing the periplasm (Bushweller, 2020; Colbert *et al.*, 2006; Hodson *et al.*, 2008; Krupp *et al.*, 2001; Mavridou *et al.*, 2009; Simon *et al.*, 2011). The current model is that apocytochrome *c* is first oxidized by the disulfide bond machinery DsbA/DsbB after entry into the periplasm, followed by subsequent thiol reduction by the thioredoxin-like protein ResA/CcsX/CcmG (Bonnard *et al.*, 2010; Hamel *et al.*, 2009; Sanders *et al.*, 2010). In chloroplasts, cytochrome *c* maturation occurs in the thylakoid lumen (*p*-side) and requires biochemical reduction of C*XX*CH heme-binding motif in apocytochrome *c*. As described in Chapter 2, apocytochrome *c* CXXCH reduction in the lumen occurs via provision of electrons from the stroma (*n*-side) to the lumen (*p*-side) via a stroma-facing protein CCS4/HCF153 (Gabilly *et al.*, 2011; Lennartz *et al.*, 2006), a trans-thylakoid thiol-disulfide oxidoreductase of the CcdA/DsbD family (Motohashi *et al.*, 2010; Page *et al.*, 2004), and a lumen-facing Trx-like protein CCS5/HCF164 (Gabilly *et al.*, 2010; Lennartz *et al.*, 2001; Motohashi *et al.*, 2006). While the operation of the disulfide reducing pathway is well established, the thylakoid lumen was long-considered empty and there was little appreciation for the need of catalyzed thiol oxidation. However, a thiol-oxidizing pathway must exist since the thylakoid lumen harbors multiple substrates that are active when disulfide bonded, such as: PsbO, a structural subunit of the oxygen evolving complex in photosystem II (Burnap *et al.*, 1994; Wyman *et al.*, 2005); Rieske, a subunit of the cytochrome b_6f complex (Carrell *et al.*, 1997);

Violaxanthin de Epoxidase (VDE), a luminal enzyme involved in photoprotection (Hallin *et al.*, 2015; Simionato *et al.*, 2015)); Stt/STN7, a kinase involved in state transitions during photosynthesis, *etc* (Wu *et al.*, 2021). Evidence of a trans-thylakoid disulfide bond forming pathway in chloroplasts came from the identification of LTO1, a VKOR-like protein in *Arabidopsis thaliana* (**V**itamin **K** epoxide **R**eductase) (Karamoko *et al.*, 2011; Lu *et al.*, 2013). LTO1 consists of an integral VKOR domain that is homologous to mammalian VKORC, and a soluble DsbA-like/Trx-like domain (Karamoko *et al.*, 2011; Karamoko *et al.*, 2013), and contains eight highly conserved redox-active cysteine residues critical for promoting disulfide bond formation (Feng *et al.*, 2011; Karamoko *et al.*, 2011). The ability of LTO1 to functionally replace DsbAB in the bacterial periplasm was indicative of a role for LTO1 in disulfide bond formation in the thylakoid lumen, the analogous compartment in plastids (Karamoko *et al.*, 2011). Analysis of *lto1* knockdown or knock-out mutants in *Arabidopsis* shows that redox-inactive mutations of conserved cysteine residues result in a pleiotropic photosynthetic deficiency that can be attributed to a defect in Photosystem II assembly (Du *et al.*, 2015; Karamoko *et al.*, 2011). Furthermore, the ability of the Trx-like soluble domain of LTO1 to oxidize PsbO *in vitro* narrowed down the PSII assembly defect in a *lto1* mutant to specific defect in the oxidation of a pair of thiols in PsbO, suggesting that a disulfide bond forming pathway is required for the biogenesis of PSII (Karamoko *et al.*, 2011). In this chapter, we investigate whether plastid apocytochrome *c* (specifically cytochrome *f*, a *c*-type cytochrome in the cytochrome b_6f complex) is a target of LTO1 oxidation in the context of holocytochrome *c* assembly. We hypothesize that, analogous to the bacterial system, heme-linking cysteine thiols in apocytochrome *f* are first oxidized by

LTO1 after translocation into the lumen and thus, requires a trans-thylakoid disulfide reducing pathway to prepare a competent substrate for subsequent stereospecific attachment of heme.

II. Materials and Methods

II.A. Strains, media, and growth conditions: All algal strains used in this study are listed in Table S1 in supplemental material. Strains CC-124 and CC-4533 were used as wild-type; strains CC-5936 were used as *ccs5* mutants. The CC-5936 strain is an insertional mutant (LMJRY0402.042908) from the CLiP library (Li *et al.*, 2019) and carries the *APHVIII* cassette inserted in exon 3 of the *CCS5* gene The CC-5995 is an insertional mutant that carries the *APHVIII* cassette in intron 5 of the *LTO1* gene (*Cre12.g493150*).

Wild-type and mutant *Chlamydomonas reinhardtii* strains were maintained on Tris-Acetate-Phosphate, with Hutner's trace elements, 20 mM Tris-base and 17 mM acetic acid, or Tris-Acetate-Phosphate supplemented with arginine (1.9 mM) (TARG) (Harris, 1989). For some strains, TAP/TARG supplemented with 25 µg.ml^{-1} hygromycin B (TAP/TARG + Hyg) or 25 µg.ml^{-1} paromomycin (TAP/TARG + Pm) were used. All algal strains were grown on solid medium at 25°C in continuous light at 0.3 µmol/m^2/s (Harris, 1989). Solid medium contains 1.5% (w/v) agar (Select Agar™, Invitrogen, 30391049).

Growth was tested on solid TAP/TARG, minimal medium, or minimal medium supplemented with 1.7 mM acetic acid under three different light conditions. For protein immunodetection, cells were grown in liquid TAP/TARG in an environmental incubator with continuous light at 0.3 µmol/m^2/s and shaking at 180-190 rpm at 25°C.

Chemo-competent Escherichia coli DH5α strains were used as hosts for molecular cloning. The bacterial strains were grown at 37ºC in Luria-Bertani (LB) broth and LB medium solidified with bacteriological agar (Silhavy *et al.*, 1984). When antibiotic selection was required, 100 µg. ml^{-1} ampicillin or 50 µg. ml^{-1} kanamycin was added.

II.B. Genetic crosses: The experimental details for sexual crosses are described in former work *(Subrahmanian et al., 2020; Subrahmanian et al., 2020)*. First, a *lto1* mutant with a compatible mating type was generated by crossing CC-5595 with a wild-type (CC-5155) and phototrophic growth assay was performed to determine that spores of the *lto1* mutant retain the photosynthetic growth defect under high light. A *lto1* mutant (*mt+*; *lto1::APHVIII*) was crossed with a *ccs4ccs5* double mutant (*mt-*; *CCS5::ARG7Φ*; *ccs4-F2D8; arg7-8*) to generate *lto1ccs5* (*mt+; lto1::APHVIII; ccs5::ARG7Φ*) and *lto1ccs4* (*mt-; lto1::APHVIII*; *ccs4-F2D8*) mutants. The *lto1ccs5* and *lto1ccs4* double mutants were crossed to generate triple mutants (*lto1::APHVIII*; *ccs5::APHVIII*; *ccs4-F2D8*). ~100 haploid progenies were tested to confirm the generation of triple mutants. For molecular verification of the *ccs5* allele in the haploid progeny, the presence of the molecular tag (Phi "Φ" flag) inserted in the *ARG7* intron used for insertional mutagenesis was detected via diagnostic PCR using the Phi-1 (5'-GTCAGATATGGACCTTGCT-3') and Phi-2 (5'-CTTCTGCGTCATGGAAGCG-3') primers (Gabilly *et al.*, 2010). The presence of the wild-type CCS4 allele vs the *ccs4-1* mutation was tested molecularly by diagnostic digestion of a PCR product. The alleles can be distinguished by virtue of a point mutation that abolishes the *Ban*II restriction site in the nonsense (*ccs4*-1). For molecular verification of the *lto1* insertional mutant, diagnostic PCR was done with primers LTO1_E5F2 (5'-GAACGCGCCTGCGGCTGTG-3') and LTO1_I5R1 (5'-. GACCGAACCGTACCGTA CAC-3').

II.C. Growth assay and thiol-dependent rescue: Cells were grown on solid acetate-containing medium (TAP or TARG) for 5-7 days at 25°C under 0.3 µmol/m^2/s

illumination. Two loops of cells were resuspended in 500 µl water and optical density was measured spectrophotometrically at 750 nm and normalized to OD_{750} = 2. This normalized suspension was used as the starting material (1) to make five serial ten-fold dilutions (10^{-1}, 10^{-2}, 10^{3}, 10^{-4}, and 10^{-5}). A volume of 5 µl from each dilution was plated on solid minimal medium (CO_2) for photoautotrophic growth or TAP/TARG (acetate + CO_2) for mixotrophic growth and incubated for 7 - 14 days under 30-50 µmol/m^2/s illumination for growth assay.

II.D. Fluorescence rise-and-decay kinetics: Fluorescence transients (also known as Kautsky effect) were measured using Handy FluorCam from Photon System Instruments that provides actinic illumination and saturating flash of light. Cells were grown mixotrophically on solid TAP/TARG under 0.3 µmol/m^2/s illumination for 5-7 days at 25°C. To measure the fluorescence, cells are dark-adapted for 15 mins followed by a saturating flash of light. The fluorescence is recorded in arbitrary units (A.U.) over an illumination period of 5 seconds.

II.E. Protein sample preparation: For heme staining and immunoblotting, two loops of cells grown on solid acetate-containing medium (TAP or TARG) for 5-7 days at 25°C under 0.3 µmol/m^2/s illumination were collected and washed with 1-2 ml of 10 mM sodium phosphate buffer (NaH_2PO_4, pH 7.0), centrifuged at top speed and resuspended in 300 µl of the same buffer. Chlorophyll was extracted by mixing 10 µl of resuspended cells with 1 ml of acetone: methanol in a ratio of 80:20. The mixture was vortexed followed by centrifugation at 16,873 x g for 5 mins. Chlorophyll concentrations were then determined

by measuring the optical density of the suspension at 652 nm. Concentrations for different strains were normalized to 1 mg/ml of chlorophyll, followed by cell lysis by two freeze-thaw cycles (samples were frozen -80°C for 1 hour and thawed on ice for ~1 hour). Cells were then separated into membrane and soluble fractions by centrifugation for 5 mins at 16,873 x g (Howe *et al.*, 1992). Membrane fractions corresponding to 10 µg of chlorophyll were separated electrophoretically by SDS-PAGE (12.5% acrylamide gel) for immunoblotting. For ECL-based heme staining, an amount of 10-20 µg of chlorophyll for each sample was used whereas for in-gel heme staining by TMBZ (3,3',5,5'-tetramethylbenzidine, Sigma, 860336-1G), a quantity corresponding to 30-40 µg of chlorophyll per sample was loaded.

II.F. Heme staining and immunoblotting: The presence of covalently bound heme in c-type cytochromes was detected by two methods, a) by enhanced chemiluminescence (ECL, Thermo Scientific, 34094) and b) in-gel TMBZ staining (3,3',5,5'-Tetramethylbenzidine, Sigma, 860336-1G), both relying on the pseudo-peroxidase activity of heme (Wilks, 2002). Detection of covalently bound heme in cytochrome *c* by ECL was done by separating proteins corresponding to 10-20 µg of chlorophyll on 12.5% acrylamide gel, followed by transfer to a PVDF membrane (Immobilon-P, IPVH00010) at 100 V (at 4°C) for 90 mins and treatment of the membrane with ECL reagent. In-gel heme staining was performed by soaking the gel in a solution of 6.3 mM TMBZ dissolved in methanol in the dark, mixed with 1 M sodium acetate for 1-1.5 hours in the dark with periodic shaking every 15-20 minutes. Bands revealing the heme peroxidase activity appeared immediately as a blue precipitate after addition of H_2O_2 (50% w/v) to a final concentration of 30 mM. For

Immunoblotting, membrane fractions corresponding to 10 µg of chlorophyll were separated by SDS-PAGE and transferred as described above. Immunodetection was done by incubating the membrane with Chlamydomonas α-CF_1 (1:10,000), α-PsbO (1:5000, Agrisera), α-D1 (1:10,000). The α -rabbit (1:10,000) was used as secondary antibody.

II.G. Construction of the LTO1 complemented strains: The *LTO1* cDNA (two cDNAs, *LTO1_C06* and *LTO1_E01*) was amplified by *Nde*I/*Xba*I site engineered primers pairs pSL18_CO6F (5'-CCACTGCTACTCACAACAAGCCCATATGAACACGGCTTTGCTTCGCTC-3') and pSL18_CO6R (5'-CGGTCCAGCTGCTGCCATCTAGATCACGGCGCCACCGCCACCGCCTCG-3'); and pSL18_E01F (5'-CTGCTACTCACAACAAGCCCATATGAACACGGCTTTGCTTCGCTCCAGC-3') and pSL18_E01R (5'-CGGTCCAGCTGCTGCCATCTAGATCACGGCGCCACCGCCACCGCCTCG-3'), and cloned into *NdeI/XbaI* site of a pSL18-derived vector carrying the *APHVII* cassette that confers resistance against Hygromycin B (instead of *APHVIII*). The resulting plasmids are PH01_LTO1_C06 and PH01_LTO1_E01. Chlamydomonas cells (strain CC-5995 and CC-6002) was transformed with plasmid both PH01_LTO1_C06 and PH01_LTO1_EO1 and transformants were selected on TAP+HygB under 0.3 µmol/m^2/s. Transformants carrying the *LTO1_EO1* cDNA were identified via diagnostic PCR using primers pSAD_Pr2 (5'-TTGGAGGTACGACCGAGATG-3') and pSADT_R1 (5'-AGCTCTTCTCCATGGTACAG-3'). The amplicon was sequenced to verify the presence of the transgene.

II.H. Glass bead transformation: Recipient strains were cultured in liquid TAP or TARG and grown until exponential phase. At a cell density of 2-5 x 10^6 cells/ml (measured by hemocytometer), cells were collected by centrifugation at 1,500 x g for 5 mins at 25°C, followed by resuspension and incubation in autolysin to a density of ~1 x 10^8 cells/ml for 45 – 90 mins (depending on the strain). The efficiency of enzymatic digestion of the cell wall was tested with 0.1% Triton X-100 as described above in the section detailing genetic crosses. Autolysin was removed by centrifugation of the treated cells at 1,500 x g for 5 mins at 25°C, and cells were resuspended in medium (TARG + 40 mM sucrose) to a final concentration of 1-2 x 10^8 cells/ml. After autolysin treatment, 300 µl of cells, 100 µl of 20% PEG 8,000, 300 mg of glass beads and 1-2 µg of transforming DNA (linear or uncut) were mixed in a microfuge tube and vortexed for 30 – 45 secs at maximum speed. After glass beads settle, 300 – 350 µl of the mixture was transferred to 30 ml of TARG + 40 mM Sucrose, and incubated for 16-24 hrs at 25°C under 0.3 µmol/m^2/s. After overnight recovery, cells are collected by centrifugation at 1,500 x g for 5 mins at 25°C, resuspended in 0.5 – 1 ml of TAP and plated on selective medium. Successful transformation yields colonies in 5-7 days.

III. RESULTS

III.A. LTO1 is required for photosynthetic growth, but not for cytochrome *f* assembly. Loss of LTO1 function (**L**umen **t**hiol **o**xidoreductase-1), a VKOR-like protein (Vitamin K Epoxide Reductase), produces an impairment in photosynthetic growth in *Arabidopsis thaliana*, specifically due to defect in assembly and activity of PSII (Du *et al.*, 2015; Karamoko *et al.*, 2011). To test if LTO1 is the oxidant of the heme-linking cysteines, we first characterized a *Chlamydomonas* insertional mutant publicly available and generated from a high throughput library for reverse genetics studies (Li *et al.*, 2016). The presence of the *APHVIII* cassette, predicted to be in intron 5 of the *LTO1* gene in was molecularly tested by diagnostic PCR (Figure 3.1A). Using a pair of primers binding inside the cassette and in the flanking region, an amplicon at the expected size (618 bp) was detected in the mutant but not in the wild type (Fig. 3.1A, *right*). Using a pair of primers binding upstream and downstream the insertion site of the cassette, an amplicon at the expected size (527 bp) was detected in the wild type but not in the mutant (due to the large size of the *APHVIII* gene, 1.8 kb). Under phototrophic conditions and high light illumination (250 µmol/m^2/s), the *lto1* mutant showed residual growth (Fig. 3.1B, *left*), although the photosynthetic growth defect is less pronounced than that of the *Δccs5* mutant, (partially deficient in cytochrome *f* assembly) (Gabilly *et al.*, 2010). Under low light illumination (0.3 µmol/m^2/s), all mutant strains can grow in the presence of acetate and atmospheric CO_2 due to the dominant contribution of respiration *vs*. photosynthesis (Figure 3.1B). Because *Arabidopsis lto1* mutants exhibit a defect in PSII assembly and activity (Du

et al., 2015; Karamoko *et al.*, 2011), we hypothesized that the photosynthetic growth defect was also due to a PSII deficiency in the *Chlamydomonas lto1* mutant.

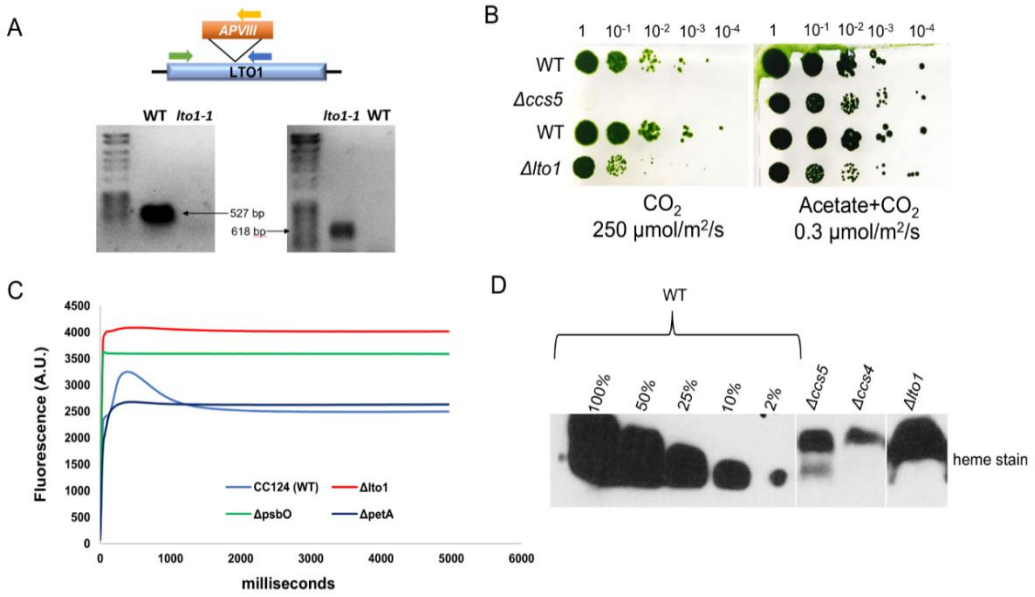

Figure 3.1. Insertional mutation in LTO1 results in a defect in PSII activity but no has no effect on holocytochrome *f* assembly.

(A) A schematic representation of LTO1 gene and location of the APHVIII antibiotic cassette. Diagnostic PCR analysis with primers across the cassette (left) and primers binding outside the cassette show. (B) Ten-fold dilution series of wild type (WT, CC-124), Δccs5 (CC-4129), wild type (WT, CC-4533) and lto1-1 (CC-5995) strains were plated on acetate containing (right panel) and minimal (left panel) medium. Cells grown phototrophically (CO_2) were incubated at 25°C for 7 days with 250 µmol/m^2/s of light. Cells grown mixotrophically (acetate + CO_2) were incubated at 25°C for 7 days with 0.3 µmol/m^2/sec of light. (C) The fluorescence induction and decay kinetics of lto1-1 is shown in comparison to that of ΔpsbO, ΔpetA, and wild type. (C) Heme staining on total protein extracts of wild type (WT, CC-4533), ccs4 (CC-4519), Δccs5 (CC-4518) and lto1-1 (CC-5995). Cells were grown mixotrophically on acetate with 0.3 µmol/m^2/s of light at 25°C for 5 -7 days. Samples correspond to 30 µg of chlorophyll. The vertical line indicates cropping from the same gel.

To test for PSII functionality, fluorescence rise and decay kinetics were performed on the *lto1* mutant. Briefly, fluorescence emission of chlorophyll from the initial dark-adapted state to the maximal level, provoked by a saturating pulse of actinic light is measured. This is a non-invasive measurement of photosystem II (PSII) activity, and the nature of the rise and decay in fluorescence is a signature of a specific defect in electron transfer either at the level of PSII or cytochrome b_6f (Murchie *et al.*, 2013). In wild type, the initial rise indicates electron movement through PSII, which is followed by a decay that indicates electron transfer through the cytochrome b_6f (Figure 3.1C). When the energy absorbed by the chlorophyll in PSII cannot be utilized in the photosynthetic electron transport chain, it displays a flat line indicative of PSII deficiency. As a preliminary assessment of PSII because of a complete block at cytochrome b_6f, a saturating rise in fluorescence is observed with no decay phase thereafter, as observed in *ΔpetA*, a null mutant in the plastid gene encoding apocytochrome *f* (Zhou *et al.*, 1996) (Figure 3.1C). In *lto1*, no gradual rise in fluorescence is observed. Instead, there is immediate sharp rise and saturation of fluorescence indicating a specific defect in electron transfer at PSII level (Figure 3.1C). A similar sharp rise in fluorescence and plateau is observed in the *Δpsbo* mutant. PsbO is a disulfide containing luminal subunit of the Oxygen Evolving Complex (OEC) in PSII and loss of PsbO elicits a PSII deficiency (Mayfield *et al.*, 1987; Pigolev *et al.*, 2015) (Figure 3.1C). Next, the accumulation of holocytochrome *f* level was assessed biochemically via heme staining (Figure 3.1D). Compared to *ccs4* and *Δccs5* single mutants which accumulate partial levels (~10% in *Δccs5* and ~>2% in *ccs4*, respectively), the *lto1* mutant appears to accumulate wildtype level of holocytochrome *f* suggesting that loss of LTO1

does not elicit a defect in cytochrome b_6f. This result agrees with the analysis of the *lto1* mutant in *Arabidopsis* where the level of cytochrome *f* was found to be unaffected (Karamoko *et al.*, 2011).

III.B. PsbO abundance is unaffected in the *Chlamydomonas lto1* mutant: Since the *lto1* mutant displays a PSII-minus phenotype based on the fluorescence transients, we tested

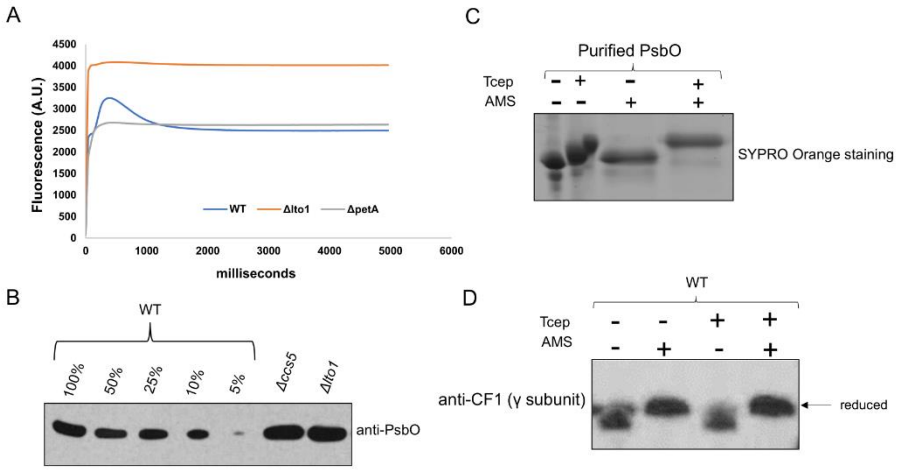

Figure 3.2. Loss of LTO1 does not affect the redox state of PsbO

(A) PsbO and D1 are immunodetected on total protein extracts of wild type, Δccs5 (CC-4129) and lto1-1 (CC-5995). Cells were grown mixotrophically (on acetate with 0.3 µmol/m^2/s of light) at 25°C for 5 -7 days. Samples (100%) correspond to 10 µg of chlorophyll. **(B)** Recombinant protein (PsbO) and was reduced with TCEP, treated with AMS, separated by nonreducing SDS-PAGE (15-16%), and visualized by SYPRO Orange staining. The positions of reduced (*PsbO$_{red}$*) and oxidized (*PsbO$_{Ox}$*) forms of PsbO are indicated by arrows. AMS is an alkylating reagent, and AMS treatment of exposed thiols in PsbO2 and LTO1 results in an increased molecular mass of the alkylated molecules. Only reduced proteins react with AMS. **(C)** CF_1 and PsbO were immunodetected after treatment of wild type cells, grown under low light on acetate for 5-7 days.

whether we could document the PSII assembly defect at the biochemical level. In *Arabidopsis*, loss of LTO1 yields a down-accumulation of PsbO, a luminal subunit of PSII and target of action of LTO1 (Karamoko *et al.*, 2011).

Because the disulfide in PsbO was shown to be determinant for the stability of this subunit and also for PSII accumulation (Burnap *et al.*, 1994; Hall *et al.*, 2010; Nikitina *et al.*, 2008), loss of disulfide bond formation in PsbO was a likely interpretation for the PSII assembly defect in the Arabidopsis *lto1* mutants (Du *et al.*, 2015; Karamoko *et al.*, 2011). Immunodetection using an antiserum against PsbO shows that the amount of protein detected in *lto1* mutant was unchanged when compared to a wild type (Figure 3.2A). This is unlike *Arabidopsis*, where a defect in PSII activity (as measured by fluorescence rise and decay kinetics) in a *lto1* mutant could be attributed to a depletion of the PsbO in PSII (Karamoko *et al.*, 2011). There was a slight decrease in the D1 (subunits of PSII) and no change in the abundance of PsaC (subunit of PSI) (not shown). One possible interpretation is that in *Chlamydomonas*, the redox state of PsbO is still affected by loss of LTO1, even though the PsbO protein level is not depleted in *lto1* mutant due to the possibility that a reduced form of PsbO is not targeted for degradation (Burnap *et al.*, 1994; Tanaka *et al.*, 1989). If this is true, we hypothesize that *in vivo*, PsbO will be detected in an oxidized form in wild type and in a reduced state in *lto1* mutant. To determine the redox state of the PsbO thiols, we first determined that air oxidized purified PsbO protein can be chemically reduced by DTT or TCEP and that the resulting free thiols are accessible to alkylation by AMS and yields a shift in electrophoretic mobility (Figure 3.2B). Unfortunately, a molecular shift expected of a successful thiol-alkylation could not be detected for PsbO in cell extracts even after artificial reduction of protein samples with high concentrations of TCEP (not shown). We were able to detect the stroma-localized γ-subunit of the CF_1 (Coupling factor 1 of chloroplast ATP*ase*) in its expected reduced form upon AMS-

labelling, an indication that stromal proteins in the reduced form are accessible to thiol modification in our assay (Kohzuma *et al.*, 2012). We reasoned that the inability to detect the redox state of PsbO might be due to incomplete reduction of protein samples, or the presence of other factors during the protein sample preparation that might be inhibiting the ability of AMS (alkylating agent) to access the free thiols of PsbO. A more sophisticated approach of protein preparation such as fractionation of thylakoid membrane vs lumen might result in a cleaner sample that is more suitable for alkylation of thiols in PsbO. Based on our results, whether PsbO is a target of LTO1 oxidation or not is still unclear and needs further examination. However, from the photosynthetic growth defect and the fluorescence transients, we concluded that the *lto1* mutant in *Chlamydomonas* elicits a PSII defect. Hence, we proceeded to test the hypothesis that apocytochrome *f* heme-linking cysteines might be a substrate of LTO1 oxidation. This is a reasonable hypothesis considering LTO1 has multiple other targets that are disulfide bonded and reside in the lumen, such as FKBP13 (Lu *et al.*, 2014) and VDE (Hallin *et al.*, 2015).

III.C. Inactivation of LTO1 restores cytochrome *f* biogenesis defect in a mutant lacking disulfide reducing pathway*:* To test if loss of the reducing pathway can be compensated by inactivation of the LTO1-dependent disulfide forming pathway, *ccs4 ccs5 lto1* triple mutant strains were constructed by genetic crosses (Fig 3.3). Out of ~>100 spores tested, only 15 were verified to harbor mutation of all three genes.

The photosynthetic growth phenotype of the triple mutants was assessed by phototrophic growth under high light where the cells utilize atmospheric CO_2 to perform photosynthesis.

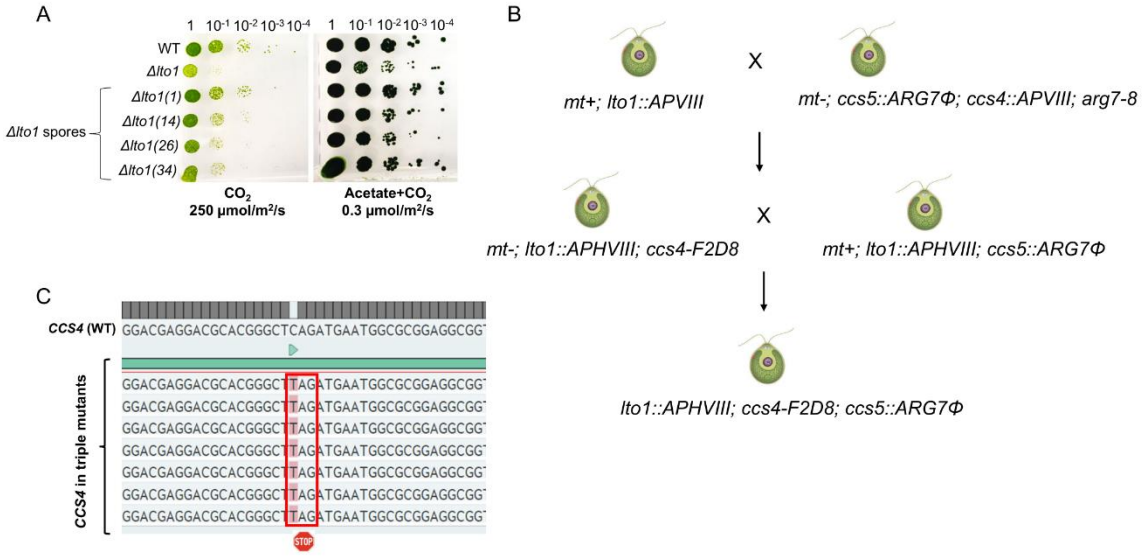

Figure 3.3. Genetic crosses to generate *ccs4ccs5lto1* triple mutants

(A). Ten-fold dilution series of wild type (WT, CC-5155), lto1-1 (CC-5995) and lto1-1 spores generated by cross between WT, CC-5155 and lto1-1 strains were plated on acetate containing (right panel) and minimal (left panel) medium. Cells grown phototrophically (CO_2) were incubated at 25°C for 7 days with 250 µmol/m^2/s of light. Cells grown mixotrophically (acetate + CO_2) were incubated at 25°C for 7 days with 0.3 µmol/m^2/sec of light. **(B)** A schematic representation of genetic crosses. A cross between lto1-1 (CC-5995) and ccs4ccs5 double mutant (CC-4518) generated ltoccs4 (CC-5998) and lto1ccs5 (CC-5999) double mutants, which were then crossed to generate ccs4ccs5lto1 triple mutants (CC-6000, CC-6001, CC-6003). **(C)** Sequence analysis shows several spores of triple mutants harbor the **C**AG to **T**AG point mutation in CCS4 gene.

Compared to the *lto1*, *ccs5* and *ccs4* single mutants that show residual photosynthetic growth, the *ccs4 ccs5 lto1* triple mutants are completely deficient for growth, like *ccs4 ccs5* double mutants (Figure 3.4A). Under low light (0.3 µmol/m^2/s), all mutant strains can grow in the presence of acetate and atmospheric CO_2 (Figure 3.4A).. Using fluorescence rise-and-decay kinetics, we document that the triple mutants display a *lto1* mutant-like PSII-phenotype, as depicted by a characteristic sharp rise and saturation of fluorescence

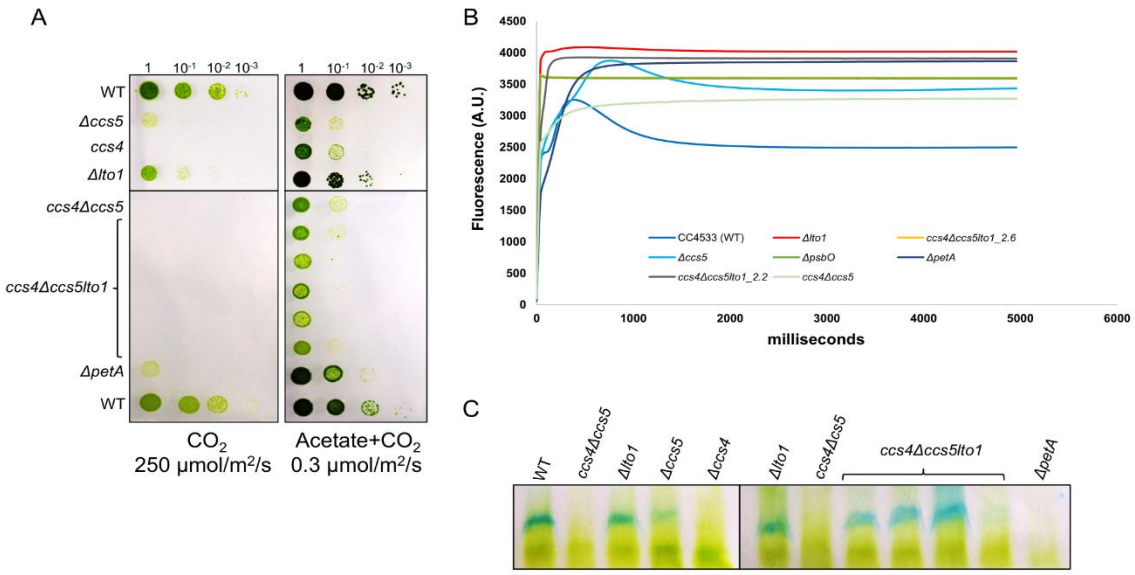

Figure 3.4. Inactivation of LTO1 restores cytochrome *f* assembly in a *ccs4Δccs5* mutant.

(A). Ten-fold dilution series of wild type (WT, CC-5155), *lto1-1* (CC-5995), *Δccs5*, *ccs4*, *ccs4Δccs5* double and *ccs4ccs5lto1* triple mutants were plated on minimal (left panel) and acetate containing (right panel) medium. Cells grown phototrophically (CO_2) were incubated at 25°C for 7 days with 250 µmol/m^2/s of light. Cells grown mixotrophically (acetate + CO_2) were incubated at 25°C for 7 days with 0.3 µmol/m^2/sec of light. (B) The fluorescence induction and decay kinetics observed in a dark-to-light transition of the *ccs4ccs5lto1* triple mutants are shown in comparison to *ccs4ccs5*, *psbO* and wild type. (C) Heme staining was performed on total protein extracts prepared from cells (same strains as in A) grown mixotrophically (on acetate with 0.3 µmol/m^2/s of light) at 25°C for 5 -7 days. Samples (100%) correspond to 20 µg of chlorophyll.

emission (Figure 3.4B). A *lto1* mutation is expected to be epistatic to any mutation causing a b_6f deficiency because during photosynthesis, electrons are transferred from PSII to cytochrome b_6f. Thus, a PSII- fluorescence transient signature is expected in the triple mutants. However, by heme staining, we show that there is a significant restoration of holocytochrome *f* assembly in the triple mutants, as compared to a *ccs4ccs5* double mutant where assembly of cytochrome *f* is completely blocked (Fig 3.4C). This is an interesting

observation which suggests that apocytochrome *f* in the triple mutants must be reduced to allow for stereospecific attachment of the heme moiety even in the absence of the CCS4/CCS5-dependent disulfide reducing pathway. From this result, we conclude that loss of LTO1 must be inactivating the oxidizing pathway, keeping apocytochrome *f* in a reduced state which consequently does not require the activity of a disulfide reducing pathway. This is supported by a preliminary result by our collaborators who show that LTO1 can partially oxidize apocytochrome *f in vitro*.

IV.D. Complementation of *lto1* and *ccs4ccs5lto1* mutants: To test if loss of LTO1 is responsible for the restoration of holocytochrome *f* assembly when the disulfide reducing pathway no longer operates a *LTO1* expressing construct was introduced in a *lto1* single and *ccs4 ccs5 lto1* triple mutant. Transformants were selected based on the presence of the antibiotic cassette (*APHVII*) on the construct and verified molecularly for the presence of the transforming DNA.

Preliminary results upon performing fluorescence rise and decay kinetics show that *lto1* mutants complemented by *LTO1* display a gradual rise in fluorescence followed by a decay phase, which is characteristic of a wild-type, suggesting complementation of the *lto1* PSII-minus phenotype (Figure 3.5A). Furthermore, expression of the same construct in a *ccs4 ccs5 lto1* triple mutant results in a rise in fluorescence followed by a saturating plateau which is characteristic of a cytochrome b_6f- like phenotype of the *ccs4ccs5* double mutant, suggesting phenotypic complementation of the triple mutant (Figure 3.5B). This result

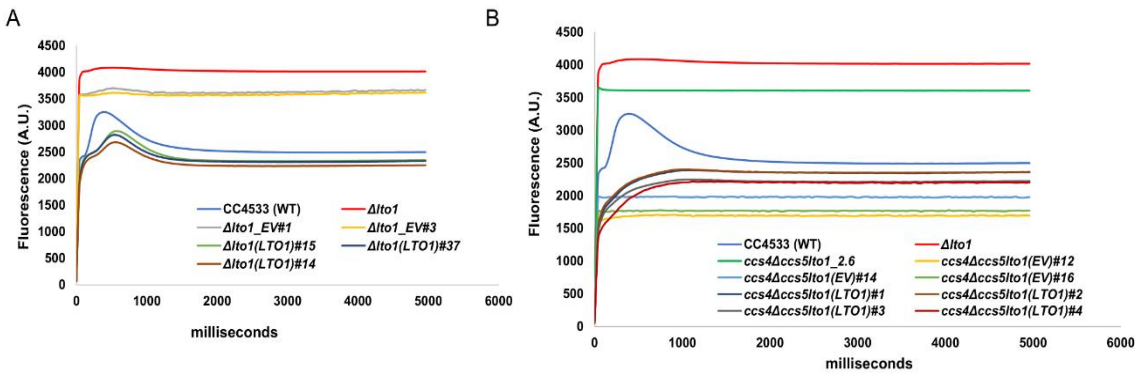

Figure 3.5. *LTO1* gene complements the *lto1* and *ccs4ccs5lto1* mutants

(A) The fluorescence induction and decay kinetics observed in *lto1-1* mutants complemented with LTO1 cDNA, *lto1(LTO1)*#14, #15 and #37 are shown in comparison to a lto1-1 mutant carrying the empty vector, lto1_EV#1 and #3. Fluorescence kinetics of WT, CC-4533 and lto1 mutant are shown as control. **(B)** The fluorescence induction and decay kinetics observed in *ccs4ccs5lto1* triple mutants complemented with LTO1 cDNA in strains *ccs4ccs5lto1(LTO1)*#1, #2, #3 and #4 show reversion to cytochrome b6f minus-like phenotype, as compared to a triple mutants carrying the empty vector in *ccs4ccs5lto1(EV)*#12, #14 and #16. Fluorescence of the recipient triple mutant *ccs4ccs5lto1_2.6*, WT CC-4533 and lto1 are shown as controls.

confirms that the molecular lesion in the *LTO1* gene is responsible for the PSII-minus and photosynthetic deficient phenotype in the *lto1* mutant we analyzed. To further confirm that LTO1 is oxidant of apocytochrome *f*, biochemical analyses by heme staining need to be conducted to assess the level of holocytochrome *f* accumulation upon complementation of the triple mutants by *LTO1*. We expect that the complemented triple mutants should no longer exhibit the restoration in cytochrome *f* assembly.

IV. DISCUSSION

In this chapter, we have explored the thiol oxidizing pathway in the context of plastid *c*-type cytochrome assembly in the thylakoid lumen. Maturation of *c*-type cytochromes involves the stereospecific covalent attachment of the α-carbons at the 2- and 4- vinyl carbons in the heme group to the heme-linking thiols in a C*XX*CH motif in apocytochrome *c* via thioether linkage (Barker *et al.*, 1999; Das *et al.*, 2021). While this covalent ligation appears chemically simple, there are several biochemical prerequisites to this reaction. A critical step is the transport of both apocytochrome *c* and heme cofactor from the stromal of the thylakoid membranes (Kim *et al.*) to the site of cytochrome *c* maturation in the thylakoid lumen, followed by maintenance of heme and heme-linking cysteines in apocytochrome *c* in a reduced state (Cline *et al.*, 2016; Das *et al.*, 2021; Kranz *et al.*, 2009; Mavridou *et al.*, 2013; Verissimo *et al.*, 2014). While the chemical reduction of the disulfide bonded heme binding cysteines post translocation across the membrane is documented, the redox state in which apocytochrome *c* is transported into the thylakoid lumen is not known. Our studies specifically focus on cytochrome *f* (subunit of the cytochrome b_6f complex), one of the three *c*-type cytochromes found in chloroplasts (Ballabani *et al.*, 2023; Gabilly *et al.*, 2017).

Is apocytochrome f a substrate of a thiol-oxidizing pathway?

Plastid-encoded apocytochrome *f* is translocated across the thylakoid lumen via Sec machinery by virtue of a N-terminal translocation signal (New *et al.*, 2018; Nohara *et al.*, 1996; Pei *et al.*, 2022) followed by peptide processing by a lumen-residing protease

(Nakamoto *et al.*, 2000). Apocytochrome *f* contains redox-active cysteines in a C*XX*CH heme-binding motif that are reduced by a disulfide reducing pathway post import (Gabilly *et al.*, 2010; Gabilly *et al.*, 2017; Gabilly *et al.*, 2011; Motohashi *et al.*, 2006, 2010). However, whether apocytochrome *f* heme binding site is oxidized before translocation or imported in the reduced form and subsequently oxidized is not known. The operation of a dedicated disulfide reducing pathway to reduce heme-binding cysteines in apocytochrome *c* is rationalized because maturation occurs on the *p*-side of energy transducing membranes that is an oxidizing compartment. The thylakoid lumen is the site of oxygen production by the oxygen evolving complex (OEC) in PSII, which suggests that sufficient levels of free oxygen must be available to induce spontaneous disulfide bond formation in the lumen. Almost 40% of luminal proteins are disulfide bonded and it is conceivable that disulfide formation in the luminal proteins is enzymatically assisted. Apocytochrome *f* is a potential substrate for a sulfhydryl-oxidizing pathway in the lumen based on its ability to form disulfide bond and from what we know about thiol-oxidation during cytochrome *c* assembly in bacteria (Deshmukh *et al.*, 2000; Erlendsson *et al.*, 2002). Furthermore, the chloroplast stroma is a highly reducing environment harboring large numbers of general reductants such as thioredoxins and glutaredoxins (Michelet *et al.*, 2009; Schurmann *et al.*, 2000), which makes it unlikely that apocytochrome *f* would be loaded onto the Sec machinery in an oxidized form.

Disulfide bond forming pathway in bacteria:

In bacteria, proteins that require disulfide bonds for their activity are translocated from the cytoplasm, which is typically considered as a reducing environment (analogous to stroma in chloroplast) due to the presence of numerous reductants and reducing agents such as glutathione (Berkmen, 2012), to the more oxidizing periplasmic space (analogous to thylakoid lumen). Enzymes involved in disulfide bond formation of numerous substrates reside in the periplasm and consists of DsbA and DsbB (Berkmen, 2012; Manta *et al.*, 2019). DsbA (**d**isulfide **b**ond protein **A**) is the first catalyst that introduces a disulfide bond into a substrate and is recycled to its oxidized form by DsbB (**d**isulfide **b**ond protein **B**) (Bushweller, 2020; Hiniker *et al.*, 2004; Landeta *et al.*, 2018). In the gram-negative bacteria *Rhodobacter capsulatus*, *dsbA* and *dsbB* null mutants are not affected for cytochrome *c* biogenesis, however, loss of DSbA and DsbB can restore the inability of a *ccdA*-null mutant to form holocytochromes *c* (Deshmukh *et al.*, 2000). CcdA is a thiol disulfide oxidoreductase belonging to the DsbD family which reduces heme-linking cysteines of apocytochromes *c* via a thioredoxin-like protein on the periplasmic side (Bushweller, 2020).

LTO1, a VKOR-like protein in the thylakoid lumen partially oxidizes apocytochrome f:

Identification of LTO1 (Lumen Thiol Oxidoreductase 1) in *Arabidopsis* as a trans-thylakoid thiol-oxidizing protein paved the way for description of a previously uncharacterized sulfhydryl-oxidizing pathway (Karamoko *et al.*, 2011). This VKOR homolog (Vitamin K Epoxide Reductase homolog is a fusion protein containing an integral membrane domain that is homologous to mammalian VKORC, and a soluble DsbA-

like/Trx-like domain (Karamoko *et al.*, 2011; Karamoko *et al.*, 2013) . LTO1 contains four conserved cysteine residues in the VKOR domain, and four conserved cysteines in the DsbA/Trx-like domain (Meyer *et al.*, 2019). The thiol-oxidizing activity of LTO1 was established via *in vitro* oxidation of the PSII subunit PsbO bond by the soluble domain of LTO1 (Karamoko *et al.*, 2011). Rouhier *et* al., show that purified soluble domain of LTO1 can oxidize purified apocytochrome *f* containing the conserved cysteine residues (not shown). Although oxidation of apocytochrome by LTO1 is partial, as compared to complete oxidation by chemical oxidizing agents such as hydrogen peroxide (H_2O_2), glutathione (GSSG) and S-Nitrosoglutathione (GSNO), it is significant when compared to the reduced form of apocytochrome *f* (not shown). This result supports our hypothesis that plastid apocytochrome *f* is a substrate of oxidizing pathway and LTO1 is the possible player in a trans-thylakoid thiol-oxidizing pathway.

A disulfide reducing pathway in plastids functions to "counter" a trans-thylakoid thiol-oxidizing pathway:

Studies in bacteria have shown that a disulfide reducing pathway consisting of a trans-thylakoid oxidoreductase DsbD/CcdA and a thioredoxin-like CcmG/ResA/CcsX exists because apocytochrome *c* is first oxidized by a thiol-oxidizing pathway composed of DsbA/DsbB and BdbB/BdbC thus requiring a targeted disulfide reducing pathway to maintain cysteinyl thiols in apocytochrome *f* in a reduced state in an otherwise oxidizing compartment to allow stereospecific ligation of heme. In this work, we show that inactivation of the potential oxidant of apocytochrome *f*, LTO1, restores the ability of a

ccs4ccs5 double mutant to assemble holocytochrome *f* (Figure 3.4C). This result is highly significant, suggesting there is a similar biochemical requirement thiol-oxidation during cytochrome *c* assembly.

Our results show that in *ccs4ccs5* double mutant, holocytochrome *f* assembly is completely blocked suggesting that apocytochrome *f* is oxidized and is targeted for degradation (Figure 3.4C). Accordingly, a *ccs4ccs5* displays a fluorescence characteristic of cytochrome b_6f minus (b_6f-) phenotype (Figure 3.4B). A *lto1* single mutant has been described to have a PSII assembly defect in *Arabidopsis* due to depletion of PSII subunits (Karamoko *et al.*, 2011). Accordingly, *lto1* mutant in *Chlamydomonas* display a fluorescence characteristic of PSII minus (PSII-) phenotype (Figure 3.1B and 3.4B). However, holocytochrome *f* assembly is not affected in *lto1* mutant (Figure 3.4C), suggesting apocytochrome *f* is reduced and heme is successfully ligated. However, this does not answer whether apocytochrome *f* is translocated in an oxidized or reduced form since the disulfide reducing pathway is functional. Thus, irrespective of what redox state apocytochrome *f* is being transported, holocytochrome *f* will be assembled in mutant lacking LTO1 as the thiol-oxidizing pathway is dispensable. In a *ccs4ccs5lto1* mutant, a fluorescence rise-and-decay kinetics corresponding to a PSII defect is observed, which can be attributed to the loss of LTO1. However, heme staining shows that high amounts of holocytochrome *f* are assembled in independent triple mutants. This contrasts with what we would expect of a mutant lacking the disulfide reducing pathway, since apocytochrome *f* would be expected to be oxidized and targeted for degradation in such a mutant. This scenario is possible only when the pathway oxidizing apocytochrome *f* is abolished, suggesting translocation of

apocytochrome *f* in a reduced form across the membrane. However, it is surprising that despite restoration of cytochrome *f* assembly, the triple *ccs4 ccs5 lto1* mutant displays a tight photosynthetic deficiency. One possible interpretation is that the inactivation of both the oxidizing and reducing pathways results in cumulative defects abolishing photosynthetic electron transfer. Another possibility is that CCS4 and CCS5 control some additional processes than the reduction of the disulfide bonded heme binding cysteines in apocytochrome *f*. We conclude that the disulfide reducing pathway composed of CCS4 and CCS5 functions to counter the trans-thylakoid oxidizing pathway of LTO1 such that when both pathways are abolished, apocytochrome *f* stays reduced and apo to holocytochrome *f* conversion takes place. Whether apocyctochrome *f* undergoes complete or partial oxidation by LTO1 cannot be ascertained from our results and needs further investigation. If it is a partial oxidation, a scenario can be imagined where apocytochrome *f* is a target of more than one oxidant. A potential source of thiol oxidation is oxygen, which is produced in the lumen by the activity of PSII as discussed earlier. This could be tested by taking a similar approach to generate a *ccs4ccs5psbO* triple mutant, PsbO being one of the structural subunits of the OEC. That loss of LTO1 is responsible for the oxidation of apocytochrome *f* is confirmed when introduction of *LTO1* in a triple mutant results in a reversion of a PSII minus phenotype to a cytochrome b_6f minus phenotype. However, this result needs further verification by phenotypic and biochemical assays.

4. Conclusions & Perspectives

In this work, we explore the unknown mechanisms of redox pathways that are required for thiol-disulfide chemistry during assembly of *c*-type cytochromes in chloroplast. Thiol-disulfide chemistry is central to the maturation of *c*-type cytochromes and requires the activity of several factors that can catalyze thiol oxidation and reduction reactions. Maturation of *c*-type cytochromes critically requires the stereospecific covalent attachment of the α-carbons at the 2- and 4- vinyl carbons in heme prosthetic group to the heme-linking thiols in a C*XX*CH motif in apocytochrome *c* to form thioether linkage (Barker *et al.*, 1999; Das *et al.*, 2021). This chemical reaction relies on the maintenance of the heme iron and heme-linking cysteines in apocytochrome *c* in a reduced state (Cline *et al.*, 2016; Das *et al.*, 2021; Kranz *et al.*, 2009; Mavridou *et al.*, 2013; Verissimo *et al.*, 2014). Previous work showed that there are at least three components functioning in a disulfide reducing pathway to maintain cysteines of C*XX*CH motif in a reduced state. These three components namely CCS4, CCDA and CCS5 are involved in the direct provision of reducing equivalents from the stroma (Lennartz *et al.*; Motohashi *et al.*) to the lumen across the thylakoid membrane (Cline *et al.*, 2016; Gabilly *et al.*, 2010; Gabilly *et al.*, 2017; Gabilly *et al.*, 2011; Motohashi *et al.*, 2010). Loss of either CCS4 or CCS5 results in a partial deficiency in phototrophic growth, that can be attributed to a partial defect in holocytochrome *f* assembly (Gabilly *et al.*, 2010; Gabilly *et al.*, 2011), whereas loss of both CCS4 and CCS5 proteins elicits a complete block in holocytochrome *f* assembly and correspondingly, a complete deficiency in phototrophic growth (this work), indicating a redundant role for CCS4 and CCS5. Application of exogenous thiols could rescue the partial phototrophic growth defect in *ccs4*

and *ccs5* null mutants and a complete block in phototrophic growth in a *ccs4ccs5* double mutant, suggesting that CCS4 and CCS5 have a similar reducing function during maturation of plastid holocytochrome *f* (Gabilly *et al.*, 2010; Gabilly *et al.*, 2011). However, unlike CCS5, CCS4 does not contain any residues or motifs that are indicative of any redox function (Gabilly *et al.*, 2010; Gabilly *et al.*, 2011). CCS5 is trx-like protein with conserved WC*XX*C motif in the lumen-facing domain of the protein, and has been shown to interact with and directly reduce apocytochrome *f* by yeast two-hybrid and *in vitro* redox assays, respectively (Gabilly *et al.*, 2010). In contrast, CCS4 has a soluble domain which is facing the stroma. This work explores a disulfide reducing pathway for apocytochrome *c* heme-linking cysteines that is CCS5 independent. CCS4 is a small 93 amino acid, stroma-facing protein with a C-terminal soluble domain unusually charged that appeared to be conserved only in green algae based on sequence similarity (Gabilly *et al.*, 2011). Although CCS4 does not contain any redox-active cysteines, it harbors, its function in a disulfide reducing pathway was inferred with the finding that a *ccs4ccs5* double mutant could be chemically rescued by application of exogenous thiols.. However, due to the absence of any redox-indicative motifs, the mechanism of CCS4 function was unclear.

Stabilization of CCDA via CCS4 and functional importance of the CCS4 soluble domain:

The finding that loss of CCS4 results in a decrease of CCDA protein level, a trans-thylakoid thiol disulfide oxidoreductase which transfers electrons to CCS5, indicates that CCS4 might be involved in a disulfide reducing pathway via stabilization of CCDA. Indeed, ectopic expression of *CCDA* in a *ccs4* mutant can partially suppress the phenotype of a

ccs4 mutant. Moreover, spontaneous mutations in the C terminal soluble domain of CCS4 in a *ccs4ccs5* double mutant background yielded a partial or complete suppression of a *ccs4ccs5* mutant, resulting in restoration of holocytochrome *f* assembly. This result suggests that spontaneous suppressor mutations in CCS4 can bypass the need of CCS5 to reduce apocytochrome *f*, highlighting the functional importance of the C-terminal domain of CCS4 for its function. t

CCS4 is found throughout the green lineage:

CCS4 is a unique protein and based on sequence similarity, it is found to be strictly conserved in green lineage. However, upon searching for CCS4-like proteins based on the presence of a highly charged soluble domain, CCS4-like proteins were found to exist throughout the green lineage. One such CCS4-like protein called HCF153 in *Arabidopsis*, had been shown to function in cytochrome b_6f assembly (Lennartz *et al.*, 2006). Although CCS4 and HCF153 do not share sequence similarity, heterologous expression of *Arabidopsis* HCF153 is able to rescue a *ccs4* mutant in *Chlamydomonas*, suggesting a similar function for the two proteins. In addition to HCF153, CCS4 has been shown to have similarity to COX16, a protein involved in the delivery of copper into cytochrome *c* oxidase (or Complex IV) in the mitochondrial IMS in the context of a disulfide reduction pathway (Aich *et al.*, 2018). Although the mechanism of Cu delivery by COX16 is not clear, the presence of a highly charged C terminal domain in COX16 and its potential role in the delivery of Cu from the *p*-side of the mitochondrial inner membrane suggests that such

CCS4-like proteins with no obvious redox activity might be present in other organelles that require catalysis of thiol-disulfide chemistry for their function.

Does CCS4 function in the reducing pathway in a CCDA-independent manner?

In *Arabidopsis,* operation of a trans-thylakoid disulfide reducing pathway to assemble cytochrome b_6f enzyme complex occurs by the function of two components, CCDA and HCF164 (CCS5-like protein in *Arabidopsis*). Complete loss of CCDA and HCF164 results in a similar defect where only ~20% of cytochrome b_6f complex is accumulated, indicating that CCDA and CCS5 function in the same pathway (Lennartz *et al.*, 2001; Motohashi *et al.*, 2006, 2010; Page *et al.*, 2004). In *Chlamydomonas,* CCDA and CCS5 function in a similar manner where CCS5 transfers electrons to apocytochrome *f* via CCDA acting in the same pathway. While CCS4 functions in a CCS5-independent manner, dependency of CCS4 activity upon CCDA is still a debate. We propose two possible scenarios: 1) CCS4 function is CCDA-dependent: In this scenario, we postulate that reducing agents are delivered from stroma to lumen via CCS4 to CCDA, which can then transfer electrons by thiol-disulfide exchange to multiple targets in the lumen, CCS5 being one of them. If this is true, we expect that loss of CCDA in *Chlamydomonas* will result in a complete loss of holocytochrome *f* assembly (unlike in Arabidopsis) since CCDA is the common distributor of electrons to luminal targets. 2) CCS4 activity is CCDA-independent: In this case, we imagine a scenario where CCS4 delivers reducing equivalents across the membrane in a CCDA-independent manner, which calls for the existence of another unidentified mechanism of translocation of reductants across the thylakoid membrane and one or

several disulfide reductases in the lumen which can receive electrons from CCS4 and transfer them to apocytochome *f* for reduction of the disulfide bonded heme-binding cysteines. If this is true, we expect a *ccs5*-like phenotype when there is loss of CCDA. However, due to the unavailability of a *ccdA* mutant, this could not be tested. We attempted to generate a CRISPR/Cas9 mediated *ccdA* mutant, as discussed in Appendix.1.

What is the function of CCS4?

CCS4 is a small protein of 93 amino acids with an unusually charged C-terminal soluble domain, and in this work, we show that CCS4 functions in a disulfide reducing pathway via stabilization of CCDA. However, since it lacks cysteine residues or any other motif indicating redox activity, it is unlikely that CCS4 performs a reducing function as a stand-alone player. Some studies have shown that the presence of highly charged residues and disordered domains contribute to the promiscuous binding ability of proteins with multiple partners (Patil *et al.*, 2006, 2007) via electrostatic interactions and complex stabilization (Patil *et al.*, 2007). Given that CCS4 has highly charged soluble domain which is intrinsically disordered (predicted by Phyre2 protein fold recognition server), we speculate that CCS4 interaction with one or more partners potentially via the stroma-facing soluble domain to deliver reducing equivalents across the thylakoid membrane. This is supported by the fact that expression of a truncated form of the protein lacking the hydrophobic transmembrane domain retained some activity in the assembly of holocytochrome *f* (Gabilly *et al.*, 2011). Note that the stroma (*n*-side) is known to be a reducing compartment and in *Chlamydomonas*, it houses five different isoforms of thioredoxins, which are one of

the major molecules that catalyze disulfide bond reduction (Collet *et al.*, 2010; Schurmann *et al.*, 2000). Studies in *Arabidopsis* have shown that only one of the thioredoxins, Trx-*m*, is responsible for delivery of electrons from the stroma to the lumen via CCDA and HCF164, the equivalent of CCS5 (Motohashi *et al.*, 2006, 2010). Based on these results, we hypothesize that CCS4 is involved in recruiting Trx-*m* to CCDA, followed by sequential reduction of CCDA and CCS5 by Trx-*m* by thiol-disulfide exchange to reduce apocytochrome *f* in the lumen (*p*-side). Keeping the promiscuous nature of binding of a highly charged protein surface in mind, we speculate that Trx-*m* and CCDA are potential interactors of CCS4. It is also likely that CCDA stabilization is dependent on recruitment of Trx-*m* by CCS4. However, we cannot rule out the possibility that CCS4 might interact with other unidentified players of the pathway. To explore this, we generated tagged CCS4 constructs and attempted to produce an anti-CCS4 antibody for subsequent immunoprecipitation experiments, as discussed in Appendix.2 and Appendix.3.

Operation of a trans-thylakoid thiol-oxidizing pathway:

It is now well established that apocytochrome *f* contains redox-active cysteines in a C*XX*CH heme-binding motif that are reduced by a disulfide reducing pathway post import (Gabilly *et al.*, 2010; Gabilly *et al.*, 2017; Gabilly *et al.*, 2011; Motohashi *et al.*, 2006, 2010). However, the activity of a thiol-oxidizing pathway in the lumen in the context cytochrome *c* assembly has not yet been investigated. Our results show that loss of LTO1, a VKOR-like protein in *Chlamydomonas*, results in restoration of the phenotype in *ccs4ccs5* double mutant, where holocytochrome *f* assembly is completely blocked

suggesting that a disulfide reducing pathway for apocytochrome *f* is required to counteract a thiol-oxidizing pathway. In the absence of LTO1, apocytochrome *f* remains reduced after import into the lumen and does not require the activity of CCS4 and CCS5, components of a trans-thylakoid disulfide reducing pathway. The identification of distinct trans-thylakoid disulfide-reducing and thiol-oxidizing pathways highlights that catalyzed thiol-disulfide chemistry is not restricted to the bacterial periplasm but also operates in the thylakoid lumen. Further genetic and biochemical studies are required to establish how these processes control the biogenesis of the thylakoid compartment and regulate photosynthesis.

APPENDIX

MATERIALS AND METHODS

In vitro cleavage of CCDA using RNP complex:

The sgRNAs for targeted editing of the *CCDA* gene were designed in the Cloud-based platform for biotech R&D, Benchling. The sgRNAs with the highest on-target and off-target score were selected, and two sgRNAs: gRNA1 and gRNA2 were synthesized (Synthego). The gRNA1 is predicted to bind to beginning of exon 1, whereas gRNA2 is predicted to bind at the end of exon 1. As a preliminary assessment of the sgRNA efficiency, *in vitro* CRISPR/Cas9 dependent digestion of a PCR template was performed. sgRNAs were mixed with Cas9 protein (Invitrogen) at 1:1 ratio and incubated at room temperature for 20 minutes to form the RNP complex. An amplicon corresponding to a portion of the *CCDA* gene carrying the site to be cleaved by Cas9 was amplified using primers CCDA-Fwd1 (5'- CACACAGCAGCCAAAATGCAGC-3'), CCDA-Rev1 (5'-TGCAAGTGAAGGGCCAGTCATTG-3') and CCDA-RV1 (5'-CCAGGCCGAACGAGAACGACAC-3'), *Taq* polymerase and a plasmid carrying *CCDA* as template. The amplicon was gel purified after electrophoresis in 1% agarose gel. The purified product was added as the template to the RNP mixture and incubated for 15 minutes or overnight at 37 °C for digestion. Fifty ng of each component (sgRNA, Cas9 and template) was used in the reaction. RNAse (20 mg/mL) was added to get rid of excess sgRNA and the product of the CRISPR/Cas9 reaction was analyzed on an 0.8 % agarose gel.

Delivery of RNP complex in cells to generate *ccdA* knock-in mutant:

CC-124 or CC-4533 WT cells were grown in TAP liquid medium under 0.3 µmol/m^2/s of light at 25°C. RNP complex was formed in vitro as described above by mixing gRNA and Cas9 at room temperature for 20 mins. As a donor DNA, the *APHVII* gene encoding the gene for Hygromycin B resistance (HygB) was amplified by PCR including the promoter and terminator using pHyg3 as template. The amplicons generated shared 25-50 bp homology to *CCDA* on either side of gRNA1 and gRNA2 cleavage site and the primers for the two guide RNAs used were: and gRNA1-HDR-F1(5'-CTGGATTTGTTTATACAGCTCAGCATTTCAATCTCACTGCAAACATTATGGAATTCGATATCAAGCTTCTTTCTTGC-3')/gRNA1-HDR-R1(CTTGAACAGTGCCAGCTGACGACTAGGCAGCGCGTACAAGTTGGTGTGGAAGCTTCCATGGGATGACGG) and gRNA2-HDR-F2(AGTCGTCAGCTGGCACTGTTCAAGCCATGTCCTGTACGCGTCGCTAGCTCGAATTCGATATCAAGCTTCTTTCTTGC)/gRNA2-HDR-R2 (CATCAGAATCTCTTTGTGTATTCCGGCCTCGACTGCTGCTTACCTGGCCGAAGCTTCCATGGGATGACGGGCCCG) as primers. Amplified insertional cassette was co-transformed with the RNP complex into wild type cells by glass bead transformation technique and transformants were selected based on resistance to hygromycin.

Generation of CCS4-HA constructs:

The plasmid pSL18 containing the Pm-resistance marker gene (*APHVIII*) for selection was used to generate *CCS4-2HA* and *CCS4- 3HA* genes are under the control of the *PSAD* promotor and terminator to generate plasmids pSL18_CCS4-2HA and pSL18_CCS4-3HA.

The sequence encoding the HA tag was engineered at the 3' end of the last coding exon of the *CCS4* gene. Transformants were generated by introducing the pSL18-based constructs into a *ccs4* mutant and selected on acetate-containing medium (containing Paromomycin).

Expression and purification of the soluble form of CCS4 for anti-CCS4 antibody production:

The plasmid pBS-SK-solCCS4 (generated by Dr. M. Karamoko) was used as a template in PCR to amplify the codon optimized cDNA sequence encoding the soluble domain (a truncated protein missing the first 31 residues) of CCS4 with *Nde*I and *Xho*I engineered oligonucleotide primers (SolCCS4_NdeI, 5'-GAAGGAGATATACATATGGCTAT CTCAAAAGGTATTG-3'/SolCCS4_XhoI, 5'- TGGTGGTGGTGGTGGTGCTCGAGT TTTGTTGCTTGTTC-3'). The amplified product was cloned into *NdeI*/*Xho*I sites of the hexahistidinyl tag vector pet24b using the In-fusion^{TM} cloning kit (Takara Bio), resulting in the pet24b_solCCS4$_{opt}$ plasmid. For expression of the recombinant His$_6$-tagged protein, 2 liters of LB broth (with 30µg/ml Kanamycin and 30µg/ml Chloramphenicol) of *E. Coli* strain BL21 (DE3) containing pet24b_solCCS4$_{opt}$ wwere grown from a 3 ml overnight primary culture. To induce overexpression of the recombinant protein, isopropyl 1-thio-β-D-galactopyranoside (IPTG) was added to a final concentration of 1 mM at A_{600} = 0.5-0.6, and the culture was further grown at 37 °C and samples were collected at 4 hrs, 6 hrs and overnight post-induction. Cells were harvested at 4,000 x *g* for 20 mins at 4°C and stored at -80°C until batch purification.

The bacterial lysate was prepared under native conditions using lysis buffer (10 mM Imidazole buffer), followed by sonication on ice for 20 secs (6X) at 5-13 watts. Batch

purification of recombinant protein from the lysate was performed following a protocol adapted from the Sotomayor laboratory at OSU using the nickel-nitrilotriacetic acid resin (Qiagen). Expression of the protein was visualized by Coomassie blue staining and immunoblotting by anti-His antibody. Recombinant solCCS4 was used as an antigen to raise antibody against the protein in rabbits (Dr. Diego González Halphen, UNAM).

APPENDIX.A.

Generation of a CRISPR/Cas9 mediated ccdA knock-in mutant:

To determine whether CCS4 functions in a CCDA-dependent or independent manner, we attempted to generate a CRISPR/Cas9 mediated knocked-in *ccdA* mutant by insertion of an antibiotic cassette harboring homologous regions with the gene at the Cas9 cut site. To verify the binding efficiency of the synthesized gRNAs, an *in vitro* cleavage assay was performed (depicted in Figure Appendix.1.A) by incubating *CCDA* DNA template with either gRNA or Cas9 or the RNP complex. No cleavage was seen when the target template was incubated with either gRNA or Cas9, whereas incubation with the premixed RNP complex clearly showed the cleaved amplicons at the expected sizes (Figure Appendix.1.B). Next, a HDR (Homology Directed Repair) approach was taken where the sgRNA/Cas9 RNP complex was co-introduced with a donor DNA (antibiotic cassette type strain (Dhokane *et al.*, 2020; Dhokane *et al.*, 2023). Upon screening of ~400 colonies for cyt b_6f deficiency by fluorescence rise and decay kinetics, only 5 clones showed a flanked with 25-50 bp homology region on each side of gRNA cleavage site) into a wild fluorescence emission characteristic of a partial or complete cytochrome b_6f defect. We tested ~60 clones selected randomly for the presence of the cassette by PCR. Upon amplification with primers that bind within the cassette, all of them were positive for the

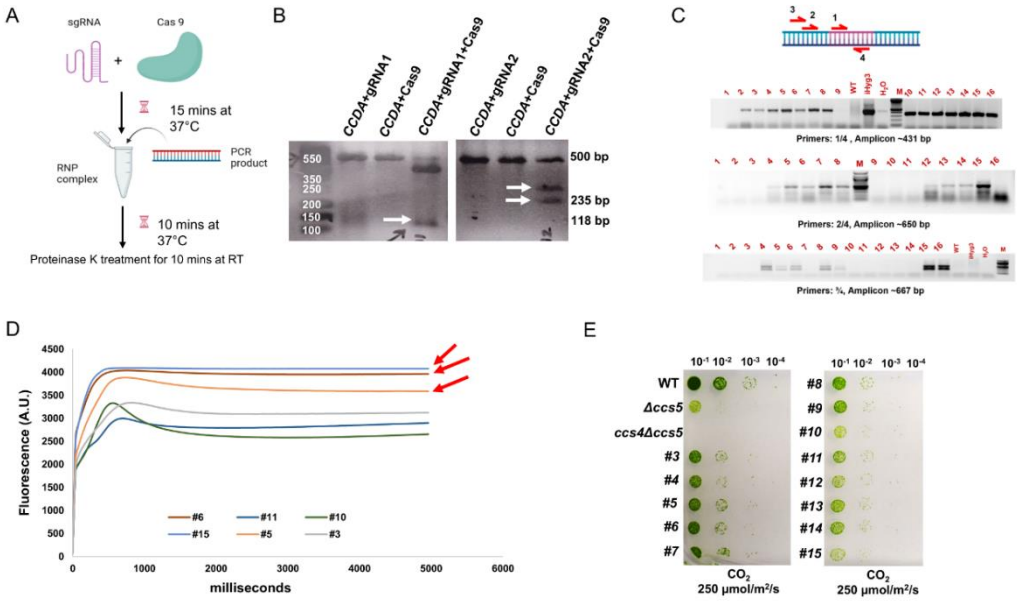

Figure Appendix.1. Screening of putative *ccdA* mutants

(A) Schematic of *in vitro* CRISPR/Cas9 mediated cleavage assay. (B) Agarose gel electrophoresis of the incubated reaction mix containing amplified partial *CCDA* gene (550 bp) with only gRNA1/gRNA2, only Cas9, or with RNP. Cleavage of *CCDA* was seen only when incubated with RNP complex and the expected amplicons after cleavage by two gRNAs are shown by white arrows. (C) Agarose gel electrophoresis showing PCR reactions with different sets of primers. Insertional cassette (in purple on the diagram) is present in all transformants (amplified by primers 1 and 4 binding within the cassette). A subset of the transformants is amplified with primer sets 2/4 and 3/4, showing insertion of the cassette as the correct site. Primers 2 and 3 bind upstream of the cut site in the *CCDA* gene. (D) Fluorescence rise and decay kinetics of 5 clones, clone names are the same as in C. (E) Ten-fold serial dilution assay) wild type (WT, CC-124), *Δccs5*, *ccs4Δccs5* and putative *ccdA* mutants were plated on acetate medium and grown mixotrophically (with 250 µmol/m^2/s) for 7-14-18 days.

presence of the cassette (only 16 shown here) (Figure Appendix.1.C). PCR with two sets of primers that amplify across the junction of the cassette showed only 5 out of the 16 were positive for both reactions, suggesting these clones have the insertional cassette at the expected site (Figure Appendix.1.C). These 5 clones (#3, #5, #6, #11 and #15) displayed a partial or complete cytochrome b_6f deficiency by fluorescence upon

preliminary testing. We tested the fluorescence rise and decay kinetics of these clones again and observed that clones #5, #6 and #15 show a clear cyt b_6f deficiency (Figure Appendix.1.D). However, upon growing these clones under phototrophic growth conditions, no significant photosynthetic growth defect was observed for any of the strains, when compared to a *ccs5* or a *ccs4ccs5* double mutant (Figure Appendix1.E). This result suggests that maybe the function of CCDA is redundant, although unlikely. However, this is a preliminary result and further tests are required to verify that there is indeed loss of CCDA protein function due to the Cas9 mediated insertion of the cassette and confirm that the tested clones are indeed *ccdA*-null mutants.

APPENDIX.B.

Characterization of CCS4_HA constructs

To identify potential interactors of CCS4, constructs were generated containing the *CCS4* gene tagged with HA tag at the C - terminus for immunoprecipitation of CCS4 (Figure Appendix.2.A). A CCS4-2HA and CCS4-3HA construct was introduced into a *ccs4* mutant and transformants were selected based on the presence of *APHVIII* gene that confers resistance to paromomycin. Upon phototrophic growth assay, it was observed that presence of the constructs rescued a *ccs4* phenotype, demonstrating that the HA tag does not interfere with the function of the protein (Figure Appendix.2.B). Immunoblotting with anti-cyt *f* antibody also shows restoration of holocytochrome *f* assembly (Fig Appendix.2.C),

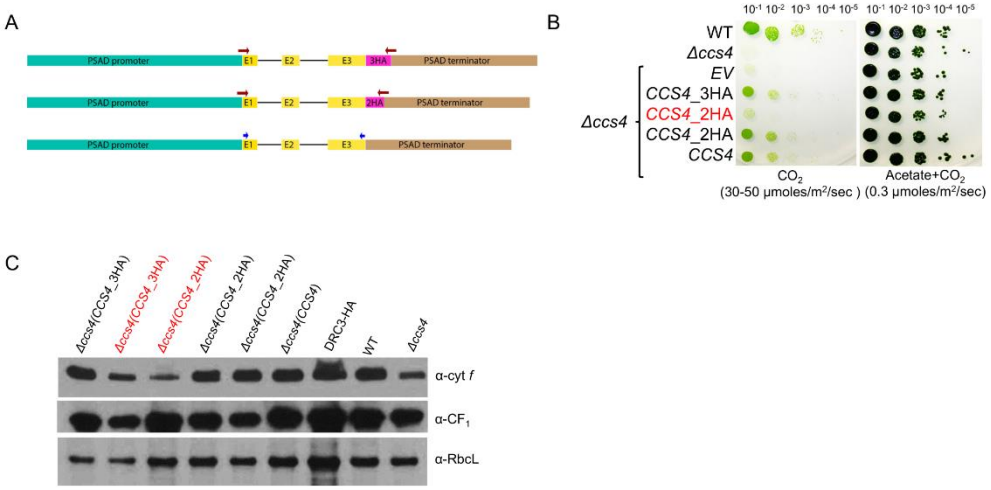

Figure Appendix.2. CCS4 protein tagged with HA is functional.

(A) Schematic representation of the CCS4 gene with and without HA tag. The CCS4 gene is represented with exons (yellow boxes) and introns (line). The positions of the diagnostic primers used for diagnostic PCR is indicated by colored arrows. (B) Ten-fold dilution series of wild type (WT, CC-124), *Δccs4*, *Δccs4_ EV (ccs4(pSL18)*, *Δccs4 (pSL18_CCS4_2HA)* and *Δccs4 (pSL18_CCS4_3HA)*. Cells were grown phototrophically (CO_2) and mixotrophically (acetate + CO_2) and incubated at 25°C for 7-14 days with 30-50 µmol/m^2/s of light. The strain in red is an example of a transformant that does not contain the construct (tested by PCR) and correspondingly does not show rescue of photosynthetic growth. (C) α-cyt *f* immunodetection were performed on total protein extracts. Strains are as in B with additional transformants restored for photosynthetic growth and carrying *CCS4-2HA* and *CCS4-3HA* constructs. WT (CC-124) and the flagellar protein DRC3-HA are positive controls, and *Δccs4* is the negative control. Strains in red correspond to transformants that are not rescued for photosynthetic growth and correspondingly are not rescued for holocytochrome *f* assembly. All cells were grown mixotrophically on acetate with 0.3 µmol/m^2/s of light at 25°C for 5 -7 days. Samples correspond to 10-15 µg of chlorophyll. Strains in red is an example of transformants that do not contain the construct Immunodetection of RbCL and CF_1 was used as a loading control.

which further validates the tag does not interfere with function. However, the protein could not be detected upon immunoblotting with anti-HA antibody (not shown).

APPENDIX.C.

Expression and purification of soluble domain of CCS4

We purified recombinant soluble domain of CCS4 which was used as the antigen to generate anti-CCS4 antibody in rabbits (raised by our collaborator Dr. González-Halphen, UNAM, Mexico).. A codon optimized recombinant $CCS4_{sol}$ with 6x-His tag (C-terminal) was produced in *E.coli* and purified by Ni-NTA protein purification method after overnight induction by IPTG. Expression of the protein was visualized by Coomassie blue staining (Figure Appendix.3.A) and the presence of the 6X-His tag was verified by immunoblotting with anti-His antibody (Figure Appendix.3.B). The expected size of the protein was 7.5 kDa, however, Coomassie blue staining suggested that size of the protein is ~13 kDa. The identity of the protein was verified by mass spectrometry, performed by Campus Chemical Instrument Center at OSU. Upon generation of the anti-CCS4 antibody, different dilutions

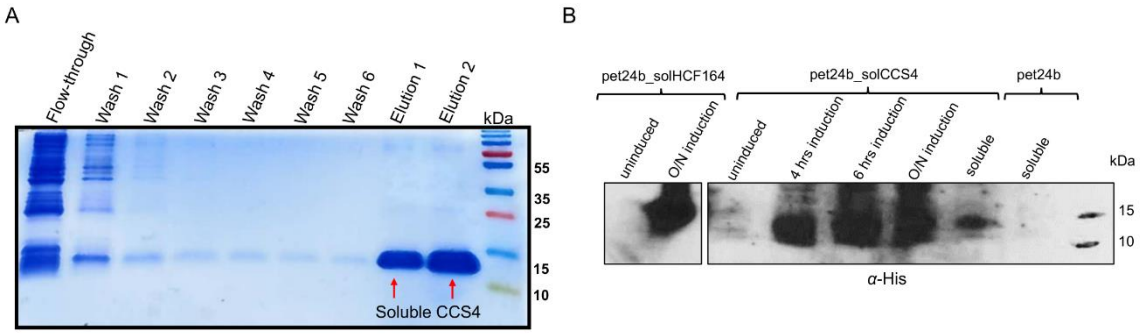

Figure Appendix.3. Expression and purification of soluble domain of CCS4

(A) Batch purification of codon optimized soluble domain of CCS4. Coomassie blue staining shows the first 'Flow-through' after mixing Ni-NTA beads with recombinant protein, followed by 'Wash' samples after washing of beads with 20 mM Imidazole buffer. Soluble CCS4 is detected at a higher molecular mass than expected (10 kDa) after elution with 250 mM Imidazole buffer. (B) Immunoblotting with anti-His antibody shows presence of 6X-His tag in samples induced for expression of pet24b_solCCS4. Detection of 6X- His tag in pet24b_solHCF164 is shown as positive control. Empty vector pet24b is shown as negative control.

of the antibody were used to test whether CCS4 protein could be detected. Unfortunately, we could not detect the recombinant protein (not shown).

Table 1. List of Chlamydomonas strains used in this work.

Strains (aliases)	Genotype	Collection center	Reference
137C	*mt⁻; nit1; nit2*	CC-124	(Pröschold *et al.*, 2005)
4C⁻	*mt⁻; arg7-8*	CC-5590	*(Subrahmanian et al., 2020)*
CMJ030	*mt⁻; cw₁₅*	CC-4533	*(Li et al., 2019)*
T78.15b-	*mt⁻; ccs5::ARG7Φ*	CC-4129	*(Gabilly et al., 2010)*
ccs5(13)	*mt⁺; ccs5::ARG7Φ; cw₁₅*	CC-5922	This work
ccs5-2	*mt⁻; cw₁₅; ccs5::APHVIII*	CC-5936	This work
PH39-35	*mt⁻; ccs5::APHVII; arg7*	CC-5923	This work
PH39-41	*mt⁺; ccs5::APHVIII; arg7*	CC-5924	This work
ccs5(CCS5)	*mt⁻; ccs5::ARG7Φ; APHVII; CCS5*	CC-4527	*(Gabilly et al., 2010)*
ccs4.1	*mt⁻; ccs4-F2D8; arg7-8*	CC-4519	*(Gabilly et al., 2011)*
ccs4(pCB412)	*mt⁻; ccs4-F2D8; ARG7*	-	*(Gabilly et al., 2011)*
ccs4cw₁₅	*mt⁻; ccs4-F2D8; cw₁₅; arg7-8*	CC-4525	*(Gabilly et al., 2011)*
ccs4(28)	*mt⁺; ccs4-F2D8; cw₁₅*	CC-5925	This work
ccs4(pSL18)	*mt⁻; ccs4-F2D8; arg7-8; APHVIII*	CC-4520	*(Gabilly et al., 2011)*
ccs4(CCS4)	*mt⁻; ccs4-F2D8; arg7-8; APHVIII; CCS4*	CC-4522	*(Gabilly et al., 2011)*
ccs4(Bushweller)	*mt⁻; ccs4-F2D8; cw₁₅; arg7-8; APHVIII; CCDA*	CC-5926	This work
ccs4ccs5(4)	*mt⁻; ccs5::ARG7Φ; ccs4-F2D8; APHVIII*	CC-4517	This work
ccs4ccs5(5)	*mt⁻; ccs5::ARG7Φ; ccs4-F2D8; APHVIII*	CC-4518	This work
ccs4ccs5(35)	*mt⁻; ccs5::ARG7Φ; ccs4-F2D8; cw₁₅*	CC-5927	This work
ccs4ccs5(9)	*mt⁺; ccs5::ARG7Φ; ccs4-F2D8; APHVIII*	see M&M	This work
ccs4ccs5(11)	*mt⁺; ccs5::ARG7Φ; ccs4-F2D8; APHVIII*	see M&M	This work
SU9	*mt⁺; ccs5::ARG7Φ; CCS4-2*	CC-5928	This work

Continued

Table 1. Continued.

SU11	*mt⁺; ccs5::ARG7Φ; CCS4-3*	CC-5929	This work
PH24-18	*mt⁻; ccs5::ARG7Φ; CCS4-3*	CC-5930	This work
PH46-1M	*mt⁺; ccs5::APHVIII; CCS4-2 arg7-8*	CC-5931	This work
CCS4-WT	*mt⁺; ccs5::ARG7Φ; ccs4-F2D8; APHVII; CCS4*	CC-5932	This work
CCS4-SU9	*mt⁺; ccs5::ARG7Φ; ccs4-F2D8;APHVII;CCS4-2*	CC-5933	This work
CCS4-SU11	*mt⁺; ccs5::ARG7Φ; ccs4-F2D8;APHVII;CCS4-3*	CC-5934	This work
ΔpetA	*mt⁺; petA::aadA*	CC-5935	*(Zhou et al., 1996)*
ccs5 / ccs5	*mt⁻; cw_{15} ; ccs5::ARG7Φ / mt⁺; ccs5::APHVIII; arg7-8*	-	This work
ccs5 / ccs5 CCS4-2	*mt⁻; ccs5::ARG7Φ / mt⁺; ccs5::APHVIII; CCS4-2; arg7-8*	-	This work
ccs5 / ccs5 CCS4-2	*mt⁺; ccs5::APHVIII; arg7-8 / mt⁻; ccs5::ARG7Φ; CCS4-3*	-	This work
ccs4(HCF153)#1	*mt⁻; ccs4-F2D8; arg7-8; CCS4-HCF153*	CC-5592	This work
ccs4(HCF153)#2	*mt⁻; ccs4-F2D8; arg7-8; CCS4-HCF153*	CC-5593	This work
ccs4(HCF153)#3	*mt⁻; ccs4-F2D8; arg7-8; CCS4-HCF153*	CC-5594	This work
lto1-1	*mt⁻; lto1::APHVIII*	CC-5995	This work
lto1ccs4ccs5#1	*mt⁺;lto1::APHVIII; ccs5::ARG7Φ; ccs4-F2D8*	CC-6000	This work
lto1ccs4ccs5#2	*mt⁻;lto1::APHVIII; ccs5::ARG7Φ; ccs4-F2D8*	CC-6001	This work
lto1ccs4ccs5#3	*mt⁺;lto1::APHVIII; ccs5::ARG7Φ; ccs4-F2D8*	CC-6003	This work

Bibliography

Abicht, H. K., Scharer, M. A., Quade, N., Ledermann, R., Mohorko, E., Capitani, G., . . . Glockshuber, R. (2014). How periplasmic thioredoxin TlpA reduces bacterial copper chaperone ScoI and cytochrome oxidase subunit II (CoxB) prior to metallation. *J Biol Chem, 289*(47), 32431-32444. doi:10.1074/jbc.M114.607127

Adebali, O., Ortega, D. R., & Zhulin, I. B. (2015). CDvist: a webserver for identification and visualization of conserved domains in protein sequences. *Bioinformatics, 31*(9), 1475-1477. doi:10.1093/bioinformatics/btu836

Ahuja, U., & Thöny-Meyer, L. (2005). CcmD is involved in complex formation between CcmC and the heme chaperone CcmE during cytochrome c maturation. *J Biol Chem, 280*(1), 236-243. doi:10.1074/jbc.M410912200

Aich, A., Wang, C., Chowdhury, A., Ronsor, C., Pacheu-Grau, D., Richter-Dennerlein, R., . . . Rehling, P. (2018). COX16 promotes COX2 metallation and assembly during respiratory complex IV biogenesis. *Elife, 7*. doi:10.7554/eLife.32572

Al-Habib, H., & Ashcroft, M. (2021). CHCHD4 (MIA40) and the mitochondrial disulfide relay system. *Biochem Soc Trans, 49*(1), 17-27. doi:10.1042/bst20190232

Alanen, H. I., Salo, K. E., Pekkala, M., Siekkinen, H. M., Pirneskoski, A., & Ruddock, L. W. (2003). Defining the domain boundaries of the human protein disulfide isomerases. *Antioxid Redox Signal, 5*(4), 367-374. doi:10.1089/152308603768295096

Allen, J. W. (2011). Cytochrome c biogenesis in mitochondria--Systems III and V. *FEBS J, 278*(22), 4198-4216. doi:10.1111/j.1742-4658.2011.08231.x

Allen, J. W., Sawyer, E. B., Ginger, M. L., Barker, P. D., & Ferguson, S. J. (2009). Variant c-type cytochromes as probes of the substrate specificity of the E. coli cytochrome c maturation (Ccm) apparatus. *Biochem J, 419*(1), 177-184, 172 p following 184. doi:10.1042/BJ20081999

Allen, J. W., Tomlinson, E. J., Hong, L., & Ferguson, S. J. (2002). The Escherichia coli cytochrome c maturation (Ccm) system does not detectably attach heme to single cysteine variants of an apocytochrome c. *J Biol Chem, 277*(37), 33559-33563. doi:10.1074/jbc.M204963200

Altschul, S. F., Madden, T. L., Schaffer, A. A., Zhang, J., Zhang, Z., Miller, W., & Lipman, D. J. (1997). Gapped BLAST and PSI-BLAST: a new generation of protein database search programs. *Nucleic Acids Res, 25*(17), 3389-3402.

Alvarez-Paggi, D., Hannibal, L., Castro, M. A., Oviedo-Rouco, S., Demicheli, V., Tórtora, V., . . . Murgida, D. H. (2017). Multifunctional Cytochrome *c*: Learning New Tricks from an Old Dog. *Chemical Reviews, 117*(21), 13382-13460. doi:10.1021/acs.chemrev.7b00257

Ambler, R. P. (1991). Sequence variability in bacterial cytochromes c. *Biochim Biophys Acta, 1058*(1), 42-47. doi:10.1016/s0005-2728(05)80266-x

Arnesano, F., Balatri, E., Banci, L., Bertini, I., & Winge, D. R. (2005). Folding studies of Cox17 reveal an important interplay of cysteine oxidation and copper binding. *Structure, 13*(5), 713-722. doi:10.1016/j.str.2005.02.015

Arnesano, F., Banci, L., Barker, P. D., Bertini, I., Rosato, A., Su, X. C., & Viezzoli, M. S. (2002). Solution structure and characterization of the heme chaperone CcmE. *Biochemistry, 41*(46), 13587-13594. doi:10.1021/bi026362w

Arnesano, F., Banci, L., Bertini, I., Faraone-Mennella, J., Rosato, A., Barker, P. D., & Fersht, A. R. (1999). The solution structure of oxidized *Escherichia coli* cytochrome b_{562}. *Biochemistry, 38*(27), 8657-8670. doi:10.1021/bi982785f

Arnold, I., Fölsch, H., Neupert, W., & Stuart, R. A. (1998). Two distinct and independent mitochondrial targeting signals function in the sorting of an inner membrane protein, cytochrome c1. *J Biol Chem, 273*(3), 1469-1476. doi:10.1074/jbc.273.3.1469

Atkinson, H. J., & Babbitt, P. C. (2009). An atlas of the thioredoxin fold class reveals the complexity of function-enabling adaptations. *PLoS Comput Biol, 5*(10), e1000541-e1000541. doi:10.1371/journal.pcbi.1000541

Babbitt, S. E., Hsu, J., Mendez, D. L., & Kranz, R. G. (2017). Biosynthesis of Single Thioether c-Type Cytochromes Provides Insight into Mechanisms Intrinsic to Holocytochrome c Synthase (HCCS). *Biochemistry, 56*(26), 3337-3346. doi:10.1021/acs.biochem.7b00286

Babbitt, S. E., Sutherland, M. C., Francisco, B. S., Mendez, D. L., & Kranz, R. G. (2015). Mitochondrial cytochrome *c* biogenesis: no longer an enigma. *Trends Biochem Sci, 40*(8), 446-455. doi:10.1016/j.tibs.2015.05.006

Bader, M., Muse, W., Ballou, D. P., Gassner, C., & Bardwell, J. C. (1999). Oxidative protein folding is driven by the electron transport system. *Cell, 98*(2), 217-227. doi:10.1016/s0092-8674(00)81016-8

Bader, M., Muse, W., Zander, T., & Bardwell, J. (1998). Reconstitution of a protein disulfide catalytic system. *J Biol Chem, 273*(17), 10302-10307. doi:10.1074/jbc.273.17.10302

Bader, M. W., Xie, T., Yu, C. A., & Bardwell, J. C. (2000). Disulfide bonds are generated by quinone reduction. *J Biol Chem, 275*(34), 26082-26088. doi:10.1074/jbc.M003850200

Ballabani, G., Forough, M., Kessler, F., & Shanmugabalaji, V. (2023). The journey of preproteins across the chloroplast membrane systems. *Frontiers in Physiology, 14*. doi:10.3389/fphys.2023.1213866

Bally, J., Paget, E., Droux, M., Job, C., Job, D., & Dubald, M. (2008). Both the stroma and thylakoid lumen of tobacco chloroplasts are competent for the formation of disulphide bonds in recombinant proteins. *Plant Biotechnol J, 6*(1), 46-61. doi:10.1111/j.1467-7652.2007.00298.x

Banci, L., Bertini, I., Cantini, F., Ciofi-Baffoni, S., Gonnelli, L., & Mangani, S. (2004). Solution structure of Cox11, a novel type of beta-immunoglobulin-like fold involved in CuB site formation of cytochrome c oxidase. *J Biol Chem, 279*(33), 34833-34839. doi:10.1074/jbc.M403655200

Banci, L., Bertini, I., Cefaro, C., Cenacchi, L., Ciofi-Baffoni, S., Felli, I. C., . . . Tokatlidis, K. (2010). Molecular chaperone function of Mia40 triggers consecutive induced folding steps of the substrate in mitochondrial protein import. *Proc Natl Acad Sci U S A, 107*(47), 20190-20195. doi:10.1073/pnas.1010095107

Banci, L., Bertini, I., Ciofi-Baffoni, S., Janicka, A., Martinelli, M., Kozlowski, H., & Palumaa, P. (2008). A structural-dynamical characterization of human Cox17. *J Biol Chem, 283*(12), 7912-7920. doi:10.1074/jbc.M708016200

Banci, L., Bertini, I., Ciofi-Baffoni, S., Leontari, I., Martinelli, M., Palumaa, P., . . . Wang, S. (2007). Human Sco1 functional studies and pathological implications of the P174L mutant. *Proc Natl Acad Sci U S A, 104*(1), 15-20. doi:10.1073/pnas.0606189103

Banci, L., Bertini, I., Ciofi-Baffoni, S., & Tokatlidis, K. (2009). The coiled coil-helix-coiled coil-helix proteins may be redox proteins. *FEBS Lett, 583*(11), 1699-1702. doi:10.1016/j.febslet.2009.03.061

Banerjee, R., & Ragsdale, S. W. (2003). The many faces of vitamin B12: catalysis by cobalamin-dependent enzymes. *Annu Rev Biochem, 72*, 209-247. doi:10.1146/annurev.biochem.72.121801.161828

Barbieri, M. R., Larosa, V., Nouet, C., Subrahmanian, N., Remacle, C., & Hamel, P. P. (2011). A forward genetic screen identifies mutants deficient for mitochondrial complex I assembly in *Chlamydomonas reinhardtii*. *Genetics, 188*(2), 349-358.

Bardwell, J. C., Lee, J. O., Jander, G., Martin, N., Belin, D., & Beckwith, J. (1993). A pathway for disulfide bond formation in vivo. *Proc Natl Acad Sci U S A, 90*(3), 1038-1042. doi:10.1073/pnas.90.3.1038

Bardwell, J. C., McGovern, K., & Beckwith, J. (1991). Identification of a protein required for disulfide bond formation in vivo. *Cell, 67*(3), 581-589. doi:10.1016/0092-8674(91)90532-4

Barker, P. D., & Ferguson, S. J. (1999). Still a puzzle: why is haem covalently attached in c-type cytochromes? *Structure, 7*(12), R281-290. doi:10.1016/s0969-2126(00)88334-3

Bechtel, T. J., & Weerapana, E. (2017). From structure to redox: The diverse functional roles of disulfides and implications in disease. *Proteomics, 17*(6). doi:10.1002/pmic.201600391

Beckett, C. S., Loughman, J. A., Karberg, K. A., Donato, G. M., Goldman, W. E., & Kranz, R. G. (2000). Four genes are required for the system II cytochrome c biogenesis pathway in Bordetella pertussis, a unique bacterial model. *Mol Microbiol, 38*(3), 465-481. doi:10.1046/j.1365-2958.2000.02174.x

Beckman, D. L., & Kranz, R. G. (1993). Cytochromes *c* biogenesis in a photosynthetic bacterium requires a periplasmic thioredoxin-like protein. *Proc. Natl. Acad. Sci. USA, 90*, 2179-2183.

Beckman, D. L., Trawick, D. R., & Kranz, R. G. (1992). Bacterial cytochromes c biogenesis. *Genes Dev, 6*(2), 268-283. doi:10.1101/gad.6.2.268

Belbelazi, A., Neish, R., Carr, M., Mottram, J. C., & Ginger, M. L. (2021). Divergent Cytochrome *c* Maturation System in Kinetoplastid Protists. *mBio, 12*(3). doi:10.1128/mBio.00166-21

Belevich, I. (2007). *Proton translocation coupled to electron transfer reactions in terminal oxidases.* University of Helsinki.

Bendall, D. S. (2016). Keilin, Cytochrome and Its Nomenclature. In W. A. Cramer & T. Kallas (Eds.), *Cytochrome Complexes: Evolution, Structures, Energy Transduction, and Signaling* (pp. 3-11). Dordrecht: Springer Netherlands.

Bennoun, P., & Delepelaire, P. (1982). Isolation of photosynthesis mutants in Chlamydomonas (pp. 25-38). Methods in Chloroplast Molecular Biology: Elsevier Biomedical Press.

Berkmen, M. (2012). Production of disulfide-bonded proteins in Escherichia coli. *Protein Expr Purif, 82*(1), 240-251. doi:10.1016/j.pep.2011.10.009

Bernard, D. G., Gabilly, S. T., Dujardin, G., Merchant, S., & Hamel, P. P. (2003). Overlapping specificities of the mitochondrial cytochrome c and c1 heme lyases. *J Biol Chem, 278*(50), 49732-49742. doi:10.1074/jbc.M308881200

Bernard, D. G., Quevillon-Cheruel, S., Merchant, S., Guiard, B., & Hamel, P. P. (2005). Cyc2p, a membrane-bound flavoprotein involved in the maturation of mitochondrial c-type cytochromes. *J Biol Chem, 280*(48), 39852-39859. doi:10.1074/jbc.M508574200

Berthold, P., Schmitt, R., & Mages, W. (2002). An engineered *Streptomyces hygroscopicus aph 7*" gene mediates dominant resistance against hygromycin B in *Chlamydomonas reinhardtii*. *Protist, 153*(4), 401-412.

Bertini, I., Cavallaro, G., & Rosato, A. (2006). Cytochrome c: occurrence and functions. *Chem Rev, 106*(1), 90-115. doi:10.1021/cr050241v

Bessette, P. H., Cotto, J. J., Gilbert, H. F., & Georgiou, G. (1999). In vivo and in vitro function of the Escherichia coli periplasmic cysteine oxidoreductase DsbG. *J Biol Chem, 274*(12), 7784-7792. doi:10.1074/jbc.274.12.7784

Betts, S. D., Ross, J. R., Hall, K. U., Pichersky, E., & Yocum, C. F. (1996). Functional reconstitution of photosystem II with recombinant manganese-stabilizing proteins containing mutations that remove the disulfide bridge. *Biochim Biophys Acta, 1274*(3), 135-142. doi:10.1016/0005-2728(96)00023-0

Bialek, W., Nelson, M., Tamiola, K., Kallas, T., & Szczepaniak, A. (2008). Deeply branching c6-like cytochromes of cyanobacteria. *Biochemistry, 47*(20), 5515-5522. doi:10.1021/bi701973g

Bien, M., Longen, S., Wagener, N., Chwalla, I., Herrmann, J. M., & Riemer, J. (2010). Mitochondrial disulfide bond formation is driven by intersubunit electron transfer in Erv1 and proofread by glutathione. *Mol Cell, 37*(4), 516-528. doi:10.1016/j.molcel.2010.01.017

Bolhuis, A., Venema, G., Quax, W. J., Bron, S., & van Dijl, J. M. (1999). Functional analysis of paralogous thiol-disulfide oxidoreductases in Bacillus subtilis. *J Biol Chem, 274*(35), 24531-24538. doi:10.1074/jbc.274.35.24531

Bonnard, G., Corvest, V., Meyer, E. H., & Hamel, P. P. (2010). Redox processes controlling the biogenesis of c-type cytochromes. *Antioxid Redox Signal, 13*(9), 1385-1401. doi:10.1089/ars.2010.3161

Bowman, S. E., & Bren, K. L. (2008). The chemistry and biochemistry of heme c: functional bases for covalent attachment. *Nat Prod Rep, 25*(6), 1118-1130. doi:10.1039/b717196j

Brandner, J. P., & Donohue, T. J. (1994). The Rhodobacter sphaeroides cytochrome c2 signal peptide is not necessary for export and heme attachment. *J Bacteriol, 176*(3), 602-609. doi:10.1128/jb.176.3.602-609.1994

Braun, M., Rubio, I. G., & Thöny-Meyer, L. (2005). A heme tag for in vivo synthesis of artificial cytochromes. *Appl Microbiol Biotechnol, 67*(2), 234-239. doi:10.1007/s00253-004-1804-2

Brausemann, A., Zhang, L., Ilcu, L., & Einsle, O. (2021). Architecture of the membrane-bound cytochrome c heme lyase CcmF. *Nature Chemical Biology, 17*(7), 800-805. doi:10.1038/s41589-021-00793-8

Brown, B. L., & Iverson, T. M. (2021). Handling heme with care. *Nature Chemical Biology, 17*(7), 751-752. doi:10.1038/s41589-021-00821-7

Bryant, D. A., Hunter, C. N., & Warren, M. J. (2020). Biosynthesis of the modified tetrapyrroles-the pigments of life. *J Biol Chem, 295*(20), 6888-6925. doi:10.1074/jbc.REV120.006194

Buchanan, B. B., & Luan, S. (2005). Redox regulation in the chloroplast thylakoid lumen: a new frontier in photosynthesis research. *J Exp Bot, 56*(416), 1439-1447. doi:10.1093/jxb/eri158

Bugos, R. C., & Yamamoto, H. Y. (1996). Molecular cloning of violaxanthin de-epoxidase from romaine lettuce and expression in *Escherichia coli*. *Proc. Natl. Acad. Sci. USA, 93*(13), 6320-6325.

Bulaj, G., Kortemme, T., & Goldenberg, D. P. (1998). Ionization-reactivity relationships for cysteine thiols in polypeptides. *Biochemistry, 37*(25), 8965-8972. doi:10.1021/bi973101r

Bulleid, N. J. (2012). Disulfide bond formation in the mammalian endoplasmic reticulum. *Cold Spring Harb Perspect Biol, 4*(11). doi:10.1101/cshperspect.a013219

Burnap, R. L., Qian, M., Shen, J. R., Inoue, Y., & Sherman, L. A. (1994). Role of disulfide linkage and putative intermolecular binding residues in the stability and binding of the extrinsic manganese-stabilizing protein to the photosystem II reaction center. *Biochemistry, 33*(46), 13712-13718. doi:10.1021/bi00250a023

Bushweller, J. H. (2020). Protein Disulfide Exchange by the Intramembrane Enzymes DsbB, DsbD, and CcdA. *J. Mol. Biol., 432*(18), 5091-5103. doi:https://doi.org/10.1016/j.jmb.2020.04.008

Camadro, J. M., Chambon, H., Jolles, J., & Labbe, P. (1986). Purification and properties of coproporphyrinogen oxidase from the yeast Saccharomyces cerevisiae. *Eur J Biochem, 156*(3), 579-587. doi:10.1111/j.1432-1033.1986.tb09617.x

Carlson, C. G., Barrientos, A., Tzagoloff, A., & Glerum, D. M. (2003). COX16 encodes a novel protein required for the assembly of cytochrome oxidase in *Saccharomyces cerevisiae*. *J. Biol. Chem., 278*(6), 3770-3775. doi:10.1074/jbc.M209893200

Carrell, C. J., Zhang, H., Cramer, W. A., & Smith, J. L. (1997). Biological identity and diversity in photosynthesis and respiration: structure of the lumen-side domain of the chloroplast Rieske protein. *Structure, 5*(12), 1613-1625. doi:10.1016/s0969-2126(97)00309-2

Cerqua, C., Morbidoni, V., Desbats, M. A., Doimo, M., Frasson, C., Sacconi, S., . . . Trevisson, E. (2018). COX16 is required for assembly of cytochrome *c* oxidase in human cells and is involved in copper delivery to COX2. *Biochim. Biophys .Acta Bioenerg., 1859*(4), 244-252. doi:10.1016/j.bbabio.2018.01.004

Chacinska, A., Koehler, C. M., Milenkovic, D., Lithgow, T., & Pfanner, N. (2009). Importing mitochondrial proteins: machineries and mechanisms. *Cell, 138*(4), 628-644. doi:10.1016/j.cell.2009.08.005

Chacinska, A., Pfannschmidt, S., Wiedemann, N., Kozjak, V., Sanjuán Szklarz, L. K., Schulze-Specking, A., . . . Pfanner, N. (2004). Essential role of Mia40 in import and assembly of mitochondrial intermembrane space proteins. *EMBO J, 23*(19), 3735-3746. doi:10.1038/sj.emboj.7600389

Chakrabarti, A., Srivastava, S., Swaminathan, C. P., Surolia, A., & Varadarajan, R. (1999). Thermodynamics of replacing an alpha-helical Pro residue in the P40S mutant of Escherichia coli thioredoxin. *Protein Sci, 8*(11), 2455-2459. doi:10.1110/ps.8.11.2455

Chambers, I. G., Willoughby, M. M., Hamza, I., & Reddi, A. R. (2021). One ring to bring them all and in the darkness bind them: The trafficking of heme without deliverers. *Biochimica et Biophysica Acta (BBA) - Molecular Cell Research, 1868*(1), 118881. doi:https://doi.org/10.1016/j.bbamcr.2020.118881

Chinenov, Y. V. (2000). Cytochrome c oxidase assembly factors with a thioredoxin fold are conserved among prokaryotes and eukaryotes. *J Mol Med (Berl), 78*(5), 239-242. doi:10.1007/s001090000110

Christensen, O., Harvat, E. M., Thöny-Meyer, L., Ferguson, S. J., & Stevens, J. M. (2007). Loss of ATP hydrolysis activity by CcmAB results in loss of c-type cytochrome synthesis and incomplete processing of CcmE. *FEBS J, 274*(9), 2322-2332. doi:10.1111/j.1742-4658.2007.05769.x

Cianciotto, N. P., Cornelis, P., & Baysse, C. (2005). Impact of the bacterial type I cytochrome c maturation system on different biological processes. *Mol Microbiol, 56*(6), 1408-1415. doi:10.1111/j.1365-2958.2005.04650.x

Cline, S., Gabilly, S., Subhramanian, N., & Hamel, P. P. (2006). Cofactor Assembly of Cytochrome bc1 - b6f Complexes. In W. A. Cramer & T. Kallas (Eds.), *Cytochrome Complexes: Evolution, Structures, Energy Transduction, and Signaling* (pp. 201-525).

Cline, S. G., Gabilly, S. T., Subrahmanian, N., & Hamel, P. P. (2016). Cofactor Assembly of Cytochrome *bc*$_1$-*b*$_6$*f* Complexes. In W. A. Cramer & T. Kallas (Eds.), *Cytochrome Complexes: Evolution, Structures, Energy Transduction, and Signaling* (pp. 501-525). Dordrecht: Springer Netherlands.

Cline, S. G., Laughbaum, I. A., & Hamel, P. P. (2017). CCS2, an Octatricopeptide-Repeat Protein, Is Required for Plastid Cytochrome c Assembly in the Green Alga Chlamydomonas reinhardtii. *Front. Plant Sci., 8*, 1306. doi:10.3389/fpls.2017.01306

Colbert, C. L., Wu, Q., Erbel, P. J., Gardner, K. H., & Deisenhofer, J. (2006). Mechanism of substrate specificity in Bacillus subtilis ResA, a thioredoxin-like protein involved in cytochrome c maturation. *Proc Natl Acad Sci U S A, 103*(12), 4410-4415. doi:10.1073/pnas.0600552103

Collet, J. F., & Messens, J. (2010). Structure, function, and mechanism of thioredoxin proteins. *Antioxid Redox Signal, 13*(8), 1205-1216. doi:10.1089/ars.2010.3114

Corvest, V., Murrey, D. A., Hirasawa, M., Knaff, D. B., Guiard, B., & Hamel, P. P. (2012). The flavoprotein Cyc2p, a mitochondrial cytochrome c assembly factor, is

a NAD(P)H-dependent haem reductase. *Mol Microbiol, 83*(5), 968-980. doi:10.1111/j.1365-2958.2012.07981.x

Couprie, J., Vinci, F., Dugave, C., Quéméneur, E., & Moutiez, M. (2000). Investigation of the DsbA mechanism through the synthesis and analysis of an irreversible enzyme-ligand complex. *Biochemistry, 39*(22), 6732-6742. doi:10.1021/bi992873f

Cramer, W. A., Martinez, S. E., Huang, D., Tae, G. S., Everly, R. M., Heymann, J. B., . . . Smith, J. L. (1994). Structural aspects of the cytochrome b6f complex; structure of the lumen-side domain of cytochrome f. *J Bioenerg Biomembr, 26*(1), 31-47. doi:10.1007/BF00763218

Crane, B. R., Arvai, A. S., Ghosh, D. K., Wu, C., Getzoff, E. D., Stuehr, D. J., & Tainer, J. A. (1998). Structure of nitric oxide synthase oxygenase dimer with pterin and substrate. *Science, 279*(5359), 2121-2126. doi:10.1126/science.279.5359.2121

Curran, S. P., Leuenberger, D., Schmidt, E., & Koehler, C. M. (2002). The role of the Tim8p-Tim13p complex in a conserved import pathway for mitochondrial polytopic inner membrane proteins. *J Cell Biol, 158*(6), 1017-1027. doi:10.1083/jcb.200205124

Dabir, D. V., Hasson, S. A., Setoguchi, K., Johnson, M. E., Wongkongkathep, P., Douglas, C. J., . . . Koehler, C. M. (2013). A small molecule inhibitor of redox-regulated protein translocation into mitochondria. *Dev Cell, 25*(1), 81-92. doi:10.1016/j.devcel.2013.03.006

Dailey, F. E., & Berg, H. C. (1993). Mutants in disulfide bond formation that disrupt flagellar assembly in Escherichia coli. *Proc Natl Acad Sci U S A, 90*(3), 1043-1047. doi:10.1073/pnas.90.3.1043

Daithankar, V. N., Farrell, S. R., & Thorpe, C. (2009). Augmenter of liver regeneration: substrate specificity of a flavin-dependent oxidoreductase from the mitochondrial intermembrane space. *Biochemistry, 48*(22), 4828-4837. doi:10.1021/bi900347v

Darby, N. J., & Creighton, T. E. (1995). Catalytic mechanism of DsbA and its comparison with that of protein disulfide isomerase. *Biochemistry, 34*(11), 3576-3587. doi:10.1021/bi00011a012

Das, A., & Hamel, P., P. (2021). Bioenergetics Theory and Components | Cytochrome *c* Assembly. In J. Jez (Ed.), *Encyclopedia of Biological Chemistry III (Third Edition)* (Vol. 2, pp. 94-107). Oxford: Elsevier.

de Lamotte-Guéry, F., Pruvost, C., Minard, P., Delsuc, M. A., Miginiac-Maslow, M., Schmitter, J. M., . . . Decottignies, P. (1997). Structural and functional roles of a conserved proline residue in the alpha2 helix of Escherichia coli thioredoxin. *Protein Eng, 10*(12), 1425-1432. doi:10.1093/protein/10.12.1425

de Vitry, C. (2011). Cytochrome c maturation system on the negative side of bioenergetic membranes: CCB or System IV. *FEBS J, 278*(22), 4189-4197. doi:10.1111/j.1742-4658.2011.08373.x

de Vitry, C., Desbois, A., Redeker, V., Zito, F., & Wollman, F. A. (2004). Biochemical and spectroscopic characterization of the covalent binding of heme to cytochrome b6. *Biochemistry, 43*(13), 3956-3968. doi:10.1021/bi036093p

De Vrij, W., Azzi, A., & Konings, W. N. (1983). Structural and functional properties of cytochrome c oxidase from Bacillus subtilis W23. *Eur J Biochem, 131*(1), 97-103. doi:10.1111/j.1432-1033.1983.tb07235.x

Denoncin, K., & Collet, J. F. (2013). Disulfide bond formation in the bacterial periplasm: major achievements and challenges ahead. *Antioxid Redox Signal, 19*(1), 63-71. doi:10.1089/ars.2012.4864

Depège, N., Bellafiore, S., & Rochaix, J. D. (2003). Role of chloroplast protein kinase Stt7 in LHCII phosphorylation and state transition in Chlamydomonas. *Science, 299*(5612), 1572-1575. doi:10.1126/science.1081397

Depuydt, M., Leonard, S. E., Vertommen, D., Denoncin, K., Morsomme, P., Wahni, K., . . . Collet, J. F. (2009). A periplasmic reducing system protects single cysteine residues from oxidation. *Science, 326*(5956), 1109-1111. doi:10.1126/science.1179557

Depuydt, M., Messens, J., & Collet, J. F. (2011). How proteins form disulfide bonds. *Antioxid Redox Signal, 15*(1), 49-66. doi:10.1089/ars.2010.3575

Deshmukh, M., Brasseur, G., & Daldal, F. (2000). Novel Rhodobacter capsulatus genes required for the biogenesis of various c-type cytochromes. *Mol Microbiol, 35*(1), 123-138. doi:10.1046/j.1365-2958.2000.01683.x

Deshmukh, M., Brasseur, G., & Daldal, F. (2000). Novel *Rhodobacter capsulatus* genes required for the biogenesis of various *c*-type cytochromes. *Mol. Microbiol., 35*(1), 123-138.

Dhokane, D., Bhadra, B., & Dasgupta, S. (2020). CRISPR based targeted genome editing of Chlamydomonas reinhardtii using programmed Cas9-gRNA ribonucleoprotein. *Mol Biol Rep, 47*(11), 8747-8755. doi:10.1007/s11033-020-05922-5

Dhokane, D., Kancharla, N., Savarimuthu, A., Bhadra, B., Bandyopadhyay, A., & Dasgupta, S. (2023). Genome Editing in Chlamydomonas reinhardtii Using Cas9-gRNA Ribonucleoprotein Complex: A Step-by-Step Guide. *Methods Mol Biol, 2653*, 207-217. doi:10.1007/978-1-0716-3131-7_14

Di Matteo, A., Gianni, S., Schininà, M. E., Giorgi, A., Altieri, F., Calosci, N., . . . Travaglini-Allocatelli, C. (2007). A strategic protein in cytochrome c maturation: three-dimensional structure of CcmH and binding to apocytochrome c. *J Biol Chem, 282*(37), 27012-27019. doi:10.1074/jbc.M702702200

Dickerson, R. E., Takano, T., Eisenberg, D., Kallai, O. B., Samson, L., Cooper, A., & Margoliash, E. (1971). Ferricytochrome c. I. General features of the horse and bonito proteins at 2.8 A resolution. *J Biol Chem, 246*(5), 1511-1535.

Dickson-Murray, E., Nedara, K., Modjtahedi, N., & Tokatlidis, K. (2021). The Mia40/CHCHD4 Oxidative Folding System: Redox Regulation and Signaling in the Mitochondrial Intermembrane Space. *Antioxidants (Basel), 10*(4). doi:10.3390/antiox10040592

Diekert, K., de Kroon, A. I., Ahting, U., Niggemeyer, B., Neupert, W., de Kruijff, B., & Lill, R. (2001). Apocytochrome c requires the TOM complex for translocation across the mitochondrial outer membrane. *EMBO J, 20*(20), 5626-5635. doi:10.1093/emboj/20.20.5626

Dillet, V., Dyson, H. J., & Bashford, D. (1998). Calculations of electrostatic interactions and pKas in the active site of Escherichia coli thioredoxin. *Biochemistry, 37*(28), 10298-10306. doi:10.1021/bi980333x

Dimogkioka, A.-R., Lees, J., Lacko, E., & Tokatlidis, K. (2021). Protein import in mitochondria biogenesis: guided by targeting signals and sustained by dedicated chaperones. *RSC Advances, 11*(51), 32476-32493. doi:10.1039/D1RA04497D

Dreyfuss, B. W., Hamel, P. P., Nakamoto, S. S., & Merchant, S. (2003). Functional analysis of a divergent system II protein, Ccs1, involved in c-type cytochrome biogenesis. *J Biol Chem, 278*(4), 2604-2613. doi:10.1074/jbc.M208652200

Driessen, A. J., Manting, E. H., & van der Does, C. (2001). The structural basis of protein targeting and translocation in bacteria. *Nat Struct Biol, 8*(6), 492-498. doi:10.1038/88549

Du, J. J., Zhan, C. Y., Lu, Y., Cui, H. R., & Wang, X. Y. (2015). The conservative cysteines in transmembrane domain of AtVKOR/LTO1 are critical for

photosynthetic growth and photosystem II activity in Arabidopsis. *Front Plant Sci, 6*, 238. doi:10.3389/fpls.2015.00238

Dumont, M. E., Cardillo, T. S., Hayes, M. K., & Sherman, F. (1991). Role of cytochrome c heme lyase in mitochondrial import and accumulation of cytochrome c in Saccharomyces cerevisiae. *Mol Cell Biol, 11*(11), 5487-5496. doi:10.1128/mcb.11.11.5487-5496.1991

Dumont, M. E., Ernst, J. F., Hampsey, D. M., & Sherman, F. (1987). Identification and sequence of the gene encoding cytochrome c heme lyase in the yeast Saccharomyces cerevisiae. *EMBO J, 6*(1), 235-241. doi:10.1002/j.1460-2075.1987.tb04744.x

Dutton, R. J., Boyd, D., Berkmen, M., & Beckwith, J. (2008). Bacterial species exhibit diversity in their mechanisms and capacity for protein disulfide bond formation. *Proc Natl Acad Sci U S A, 105*(33), 11933-11938. doi:10.1073/pnas.0804621105

Dutton, R. J., Wayman, A., Wei, J. R., Rubin, E. J., Beckwith, J., & Boyd, D. (2010). Inhibition of bacterial disulfide bond formation by the anticoagulant warfarin. *Proc Natl Acad Sci U S A, 107*(1), 297-301. doi:10.1073/pnas.0912952107

Dyson, H. J., Tennant, L. L., & Holmgren, A. (1991). Proton-transfer effects in the active-site region of Escherichia coli thioredoxin using two-dimensional 1H NMR. *Biochemistry, 30*(17), 4262-4268. doi:10.1021/bi00231a023

Eaves, D. J., Grove, J., Staudenmann, W., James, P., Poole, R. K., White, S. A., . . . Cole, J. A. (1998). Involvement of products of the nrfEFG genes in the covalent attachment of haem c to a novel cysteine-lysine motif in the cytochrome c552 nitrite reductase from Escherichia coli. *Mol Microbiol, 28*(1), 205-216. doi:10.1046/j.1365-2958.1998.00792.x

Economou, A., & Wickner, W. (1994). SecA promotes preprotein translocation by undergoing ATP-driven cycles of membrane insertion and deinsertion. *Cell, 78*(5), 835-843. doi:10.1016/s0092-8674(94)90582-7

Edwards, R., Eaglesfield, R., & Tokatlidis, K. (2021). The mitochondrial intermembrane space: the most constricted mitochondrial sub-compartment with the largest variety of protein import pathways. *Open Biol, 11*(3), 210002. doi:10.1098/rsob.210002

Einsle, O., Messerschmidt, A., Stach, P., Bourenkov, G. P., Bartunik, H. D., Huber, R., & Kroneck, P. M. (1999). Structure of cytochrome c nitrite reductase. *Nature, 400*(6743), 476-480. doi:10.1038/22802

El-Gebali, S., Mistry, J., Bateman, A., Eddy, S. R., Luciani, A., Potter, S. C., . . . Finn, R. D. (2019). The Pfam protein families database in 2019. *Nucleic Acids Res., 47*(D1), D427-d432. doi:10.1093/nar/gky995

Elder, G. H., & Evans, J. O. (1978). Evidence that the coproporphyrinogen oxidase activity of rat liver is situated in the intermembrane space of mitochondria. *Biochem J, 172*(2), 345-347. doi:10.1042/bj1720345

Enggist, E., Thöny-Meyer, L., Güntert, P., & Pervushin, K. (2002). NMR structure of the heme chaperone CcmE reveals a novel functional motif. *Structure, 10*(11), 1551-1557. doi:10.1016/s0969-2126(02)00885-7

Erlandson, K. J., Or, E., Osborne, A. R., & Rapoport, T. A. (2008). Analysis of polypeptide movement in the SecY channel during SecA-mediated protein translocation. *J Biol Chem, 283*(23), 15709-15715. doi:10.1074/jbc.M710356200

Erlendsson, L. S., Acheson, R. M., Hederstedt, L., & Le Brun, N. E. (2003). Bacillus subtilis ResA is a thiol-disulfide oxidoreductase involved in cytochrome c synthesis. *J Biol Chem, 278*(20), 17852-17858.

Erlendsson, L. S., & Hederstedt, L. (2002). Mutations in the thiol-disulfide oxidoreductases BdbC and BdbD can suppress cytochrome c deficiency of CcdA-defective Bacillus subtilis cells. *J Bacteriol, 184*(5), 1423-1429. doi:10.1128/JB.184.5.1423-1429.2002

Fabianek, R. A., Hennecke, H., & Thöny-Meyer, L. (1998). The active-site cysteines of the periplasmic thioredoxin-like protein CcmG of *Escherichia coli* are important but not essential for cytochrome *c* maturation in vivo. *J. Bacteriol., 180*(7), 1947-1950.

Farrell, S. R., & Thorpe, C. (2005). Augmenter of liver regeneration: a flavin-dependent sulfhydryl oxidase with cytochrome c reductase activity. *Biochemistry, 44*(5), 1532-1541. doi:10.1021/bi0479555

Fass, D. (2008). The Erv family of sulfhydryl oxidases. *Biochim Biophys Acta, 1783*(4), 557-566. doi:10.1016/j.bbamcr.2007.11.009

Feige, M. J., & Hendershot, L. M. (2011). Disulfide bonds in ER protein folding and homeostasis. *Curr Opin Cell Biol, 23*(2), 167-175. doi:10.1016/j.ceb.2010.10.012

Feissner, R. E., Beckett, C. S., Loughman, J. A., & Kranz, R. G. (2005). Mutations in cytochrome assembly and periplasmic redox pathways in Bordetella pertussis. *J Bacteriol, 187*(12), 3941-3949. doi:10.1128/JB.187.12.3941-3949.2005

Fekkes, P., de Wit, J. G., van der Wolk, J. P., Kimsey, H. H., Kumamoto, C. A., & Driessen, A. J. (1998). Preprotein transfer to the Escherichia coli translocase requires the co-operative binding of SecB and the signal sequence to SecA. *Mol Microbiol, 29*(5), 1179-1190. doi:10.1046/j.1365-2958.1998.00997.x

Feng, W. K., Wang, L., Lu, Y., & Wang, X. Y. (2011). A protein oxidase catalysing disulfide bond formation is localized to the chloroplast thylakoids. *FEBS J, 278*(18), 3419-3430. doi:10.1111/j.1742-4658.2011.08265.x

Ferguson, S. J., & Fulop, V. (2000). Cytochrome cd1 nitrite reductase structure raises interesting mechanistic questions. *Subcell Biochem, 35*, 519-540. doi:10.1007/0-306-46828-x_15

Ferguson, S. J., Stevens, J. M., Allen, J. W., & Robertson, I. B. (2008). Cytochrome c assembly: a tale of ever increasing variation and mystery? *Biochim Biophys Acta, 1777*(7-8), 980-984. doi:10.1016/j.bbabio.2008.03.020

Ferousi, C., Lindhoud, S., Baymann, F., Hester, E. R., Reimann, J., & Kartal, B. (2019). Discovery of a functional, contracted heme-binding motif within a multiheme cytochrome. *J. Biol. Chem., 294*(45), 16953-16965. doi:10.1074/jbc.RA119.010568

Finger, Y., & Riemer, J. (2020). Protein import by the mitochondrial disulfide relay in higher eukaryotes. *Biol Chem, 401*(6-7), 749-763. doi:10.1515/hsz-2020-0108

Fischer, M., & Riemer, J. (2013). The mitochondrial disulfide relay system: roles in oxidative protein folding and beyond. *Int J Cell Biol, 2013*, 742923. doi:10.1155/2013/742923

Frawley, E. R., & Kranz, R. G. (2009). CcsBA is a cytochrome c synthetase that also functions in heme transport. *Proc Natl Acad Sci U S A, 106*(25), 10201-10206. doi:10.1073/pnas.0903132106

Friedmann, H. C., Klein, A., & Thauer, R. K. (1990). Structure and function of the nickel porphinoid, coenzyme F430 and of its enzyme, methyl coenzyme M reductase. *FEMS Microbiol Rev, 7*(3-4), 339-348. doi:10.1111/j.1574-6968.1990.tb04934.x

Friedrich, T., Wohlwend, D., & Borisov, V. B. (2022). Recent Advances in Structural Studies of Cytochrome bd and Its Potential Application as a Drug Target. *Int J Mol Sci, 23*(6). doi:10.3390/ijms23063166

Furt, F., Oostende, C., Widhalm, J. R., Dale, M. A., Wertz, J., & Basset, G. J. (2010). A bimodular oxidoreductase mediates the specific reduction of phylloquinone (vitamin K) in chloroplasts. *Plant J., 64*(1), 38-46.

Gabilly, S. T., Dreyfuss, B. W., Karamoko, M., Corvest, V., Kropat, J., Page, M. D., . . . Hamel, P. P. (2010). CCS5, a thioredoxin-like protein involved in the assembly of plastid *c*-type cytochromes. *J. Biol. Chem., 285*(39), 29738-29749.

Gabilly, S. T., & Hamel, P. P. (2017). Maturation of Plastid. *Front Plant Sci, 8*, 1313. doi:10.3389/fpls.2017.01313

Gabilly, S. T., Kropat, J., Karamoko, M., Page, M. D., Nakamoto, S. S., Merchant, S. S., & Hamel, P. P. (2011). A novel component of the disulfide-reducing pathway required for cytochrome *c* assembly in plastids. *Genetics, 187*(3), 793-802.

Gabriel, K., Milenkovic, D., Chacinska, A., Müller, J., Guiard, B., Pfanner, N., & Meisinger, C. (2007). Novel mitochondrial intermembrane space proteins as substrates of the MIA import pathway. *J Mol Biol, 365*(3), 612-620. doi:10.1016/j.jmb.2006.10.038

Galligan, J. J., & Petersen, D. R. (2012). The human protein disulfide isomerase gene family. *Hum Genomics, 6*(1), 6. doi:10.1186/1479-7364-6-6

Ghosh, A., Pratt, A. T., Soma, S., Theriault, S. G., Griffin, A. T., Trivedi, P. P., & Gohil, V. M. (2016). Mitochondrial disease genes COA6, COX6B and SCO2 have overlapping roles in COX2 biogenesis. *Hum Mol Genet, 25*(4), 660-671. doi:10.1093/hmg/ddv503

Giegé, P., Grienenberger, J. M., & Bonnard, G. (2008). Cytochrome c biogenesis in mitochondria. *Mitochondrion, 8*(1), 61-73. doi:10.1016/j.mito.2007.10.001

Gleason, F. K. (1992). Mutation of conserved residues in Escherichia coli thioredoxin: effects on stability and function. *Protein Sci, 1*(5), 609-616. doi:10.1002/pro.5560010507

Goddard, A. D., Stevens, J. M., Rondelet, A., Nomerotskaia, E., Allen, J. W., & Ferguson, S. J. (2010). Comparing the substrate specificities of cytochrome c biogenesis Systems I and II: bioenergetics. *FEBS J, 277*(3), 726-737. doi:10.1111/j.1742-4658.2009.07517.x

Goldberger, R. F., Epstein, C. J., & Anfinsen, C. B. (1963). Acceleration of reactivation of reduced bovine pancreatic ribonuclease by a microsomal system from rat liver. *J Biol Chem, 238*, 628-635.

Goldman, B. S., & Kranz, R. G. (1998). Evolution and horizontal transfer of an entire biosynthetic pathway for cytochrome c biogenesis: Helicobacter, Deinococcus,

Archae and more. *Mol Microbiol, 27*(4), 871-873. doi:10.1046/j.1365-2958.1998.00708.x

Goodstadt, L., & Ponting, C. P. (2004). Vitamin K epoxide reductase: homology, active site and catalytic mechanism. *Trends Biochem Sci, 29*(6), 289-292. doi:10.1016/j.tibs.2004.04.004

Gopalan, G., He, Z., Balmer, Y., Romano, P., Gupta, R., Héroux, A., . . . Luan, S. (2004). Structural analysis uncovers a role for redox in regulating FKBP13, an immunophilin of the chloroplast thylakoid lumen. *Proc Natl Acad Sci U S A, 101*(38), 13945-13950. doi:10.1073/pnas.0405240101

Grandchamp, B., Phung, N., & Nordmann, Y. (1978). The mitochondrial localization of coproporphyrinogen III oxidase. *Biochem J, 176*(1), 97-102. doi:10.1042/bj1760097

Gray, J. C. (1992). Cytochrome f: Structure, function and biosynthesis. *Photosynth Res, 34*(3), 359-374. doi:10.1007/BF00029811

Gross, D. P., Burgard, C. A., Reddehase, S., Leitch, J. M., Culotta, V. C., & Hell, K. (2011). Mitochondrial Ccs1 contains a structural disulfide bond crucial for the import of this unconventional substrate by the disulfide relay system. *Mol Biol Cell, 22*(20), 3758-3767. doi:10.1091/mbc.E11-04-0296

Gross, E., Kastner, D. B., Kaiser, C. A., & Fass, D. (2004). Structure of Ero1p, source of disulfide bonds for oxidative protein folding in the cell. *Cell, 117*(5), 601-610. doi:10.1016/s0092-8674(04)00418-0

Grossman, A. R., Karpowicz, S. J., Heinnickel, M., Dewez, D., Hamel, B., Dent, R., . . . Merchant, S. S. (2010). Phylogenomic analysis of the Chlamydomonas genome unmasks proteins potentially involved in photosynthetic function and regulation. *Photosynth Res, 106*(1-2), 3-17. doi:10.1007/s11120-010-9555-7

Grzyb, J., Latowski, D., & Strzałka, K. (2006). Lipocalins - a family portrait. *J Plant Physiol, 163*(9), 895-915. doi:10.1016/j.jplph.2005.12.007

Guddat, L. W., Bardwell, J. C., Glockshuber, R., Huber-Wunderlich, M., Zander, T., & Martin, J. L. (1997). Structural analysis of three His32 mutants of DsbA: support for an electrostatic role of His32 in DsbA stability. *Protein Sci, 6*(9), 1893-1900. doi:10.1002/pro.5560060910

Guilhot, C., Jander, G., Martin, N. L., & Beckwith, J. (1995). Evidence that the pathway of disulfide bond formation in Escherichia coli involves interactions between the

cysteines of DsbB and DsbA. *Proc Natl Acad Sci U S A, 92*(21), 9895-9899. doi:10.1073/pnas.92.21.9895

Gupta, R., He, Z., & Luan, S. (2002). Functional relationship of cytochrome c(6) and plastocyanin in Arabidopsis. *Nature, 417*(6888), 567-571. doi:10.1038/417567a

Haebel, P. W., Goldstone, D., Katzen, F., Beckwith, J., & Metcalf, P. (2002). The disulfide bond isomerase DsbC is activated by an immunoglobulin-fold thiol oxidoreductase: crystal structure of the DsbC-DsbDalpha complex. *EMBO J, 21*(18), 4774-4784. doi:10.1093/emboj/cdf489

Hall, M., Mata-Cabana, A., Akerlund, H. E., Florencio, F. J., Schröder, W. P., Lindahl, M., & Kieselbach, T. (2010). Thioredoxin targets of the plant chloroplast lumen and their implications for plastid function. *Proteomics, 10*(5), 987-1001. doi:10.1002/pmic.200900654

Hall, R., Yuan, S., Wood, K., Katona, M., & Straub, A. C. (2022). Cytochrome b5 reductases: Redox regulators of cell homeostasis. *J Biol Chem, 298*(12), 102654. doi:10.1016/j.jbc.2022.102654

Hallin, E. (2011). *Expression, purification and characterization of violaxanthin de-epoxidase from spinach*
(Master Master), University of Lund, Sweden, Lund (Master thesis).

Hallin, E. I., Guo, K., & Åkerlund, H.-E. (2015). Violaxanthin de-epoxidase disulphides and their role in activity and thermal stability. *Photosyn. Res., 124*(2), 191-198. doi:10.1007/s11120-015-0118-9

Hamel, P., Corvest, V., Giegé, P., & Bonnard, G. (2009). Biochemical requirements for the maturation of mitochondrial c-type cytochromes. *Biochim Biophys Acta, 1793*(1), 125-138. doi:10.1016/j.bbamcr.2008.06.017

Hamel, P., Dreyfuss, B. W., Xie, Z., Gabilly, S. T., & Merchant, S. (2003). Essential histidine and tryptophan residues in CcsA, a system II polytopic cytochrome c biogenesis protein. *J Biol Chem, 278*(4), 2593-2603. doi:10.1074/jbc.M208651200

Harris, E. H. (1989). *The Chlamydomonas Sourcebook: A comprehensive guide to biology and laboratory use*. San Diego, CA: Academic Press.

Harvat, E. M., Redfield, C., Stevens, J. M., & Ferguson, S. J. (2009). Probing the heme-binding site of the cytochrome c maturation protein CcmE. *Biochemistry, 48*(8), 1820-1828. doi:10.1021/bi801609a

Heinemann, I. U., Jahn, M., & Jahn, D. (2008). The biochemistry of heme biosynthesis. *Arch Biochem Biophys, 474*(2), 238-251. doi:10.1016/j.abb.2008.02.015

Hell, K. (2008). The Erv1-Mia40 disulfide relay system in the intermembrane space of mitochondria. *Biochim Biophys Acta, 1783*(4), 601-609. doi:10.1016/j.bbamcr.2007.12.005

Heras, B., Edeling, M. A., Schirra, H. J., Raina, S., & Martin, J. L. (2004). Crystal structures of the DsbG disulfide isomerase reveal an unstable disulfide. *Proc Natl Acad Sci U S A, 101*(24), 8876-8881. doi:10.1073/pnas.0402769101

Herrmann, J. M., & Köhl, R. (2007). Catch me if you can! Oxidative protein trapping in the intermembrane space of mitochondria. *J Cell Biol, 176*(5), 559-563. doi:10.1083/jcb.200611060

Herrmann, J. M., & Riemer, J. (2010). The intermembrane space of mitochondria. *Antioxid Redox Signal, 13*(9), 1341-1358. doi:10.1089/ars.2009.3063

Hey, D., Ortega-Rodes, P., Fan, T., Schnurrer, F., Brings, L., Hedtke, B., & Grimm, B. (2016). Transgenic Tobacco Lines Expressing Sense or Antisense FERROCHELATASE 1 RNA Show Modified Ferrochelatase Activity in Roots and Provide Experimental Evidence for Dual Localization of Ferrochelatase 1. *Plant and Cell Physiology, 57*(12), 2576-2585. doi:10.1093/pcp/pcw171

Hiniker, A., & Bardwell, J. C. (2004). In vivo substrate specificity of periplasmic disulfide oxidoreductases. *J Biol Chem, 279*(13), 12967-12973. doi:10.1074/jbc.M311391200

Hodson, C. T., Lewin, A., Hederstedt, L., & Le Brun, N. E. (2008). The active-site cysteinyls and hydrophobic cavity residues of ResA are important for cytochrome c maturation in Bacillus subtilis. *J Bacteriol, 190*(13), 4697-4705. doi:10.1128/JB.00145-08

Hoffmann, X.-K., & Beck, C. F. (2005). Mating-Induced Shedding of Cell Walls, Removal of Walls from Vegetative Cells, and Osmotic Stress Induce Presumed Cell Wall Genes in *Chlamydomonas*. *Plant Physiol., 139*(2), 999-1014. doi:10.1104/pp.105.065037

Hofmann, S., Rothbauer, U., Mühlenbein, N., Baiker, K., Hell, K., & Bauer, M. F. (2005). Functional and mutational characterization of human MIA40 acting during import into the mitochondrial intermembrane space. *J Mol Biol, 353*(3), 517-528. doi:10.1016/j.jmb.2005.08.064

Holmgren, A. (1989). Thioredoxin and glutaredoxin systems. *J Biol Chem, 264*(24), 13963-13966.

Holmgren, A., Söderberg, B. O., Eklund, H., & Brändén, C. I. (1975). Three-dimensional structure of Escherichia coli thioredoxin-S2 to 2.8 A resolution. *Proc Natl Acad Sci U S A, 72*(6), 2305-2309. doi:10.1073/pnas.72.6.2305

Howe, C. J., Schlarb-Ridley, B. G., Wastl, J., Purton, S., & Bendall, D. S. (2006). The novel cytochrome c6 of chloroplasts: a case of evolutionary bricolage? *J Exp Bot, 57*(1), 13-22. doi:10.1093/jxb/erj023

Howe, G., & Merchant, S. (1992). The biosynthesis of membrane and soluble plastidic c-type cytochromes of Chlamydomonas reinhardtii is dependent on multiple common gene products. *EMBO J, 11*(8), 2789-2801.

Howe, G., & Merchant, S. (1992). The biosynthesis of membrane and soluble plastidic *c*-type cytochromes of *Chlamydomonas reinhardtii* is dependent on multiple common gene products. *EMBO J., 11*, 2789-2801.

Howe, G., & Merchant, S. (1993). Maturation of thylakoid lumen proteins proceeds post-translationally through an intermediate in vivo. *Proc Natl Acad Sci U S A, 90*(5), 1862-1866. doi:10.1073/pnas.90.5.1862

Howe, G., & Merchant, S. (1994). The biosynthesis of bacterial and plastidic c-type cytochromes. *Photosynth Res, 40*(2), 147-165. doi:10.1007/BF00019332

Hu, J., Dong, L., & Outten, C. E. (2008). The redox environment in the mitochondrial intermembrane space is maintained separately from the cytosol and matrix. *J Biol Chem, 283*(43), 29126-29134. doi:10.1074/jbc.M803028200

Ikegami, I., Katoh, S., & Takamiya, A. (1968). Nature of heme moiety and oxidation-reduction potential of cytochrome 558 in Euglena chloroplasts. *Biochim Biophys Acta, 162*(4), 604-606. doi:10.1016/0005-2728(68)90066-2

Inaba, K., Murakami, S., Suzuki, M., Nakagawa, A., Yamashita, E., Okada, K., & Ito, K. (2006). Crystal structure of the DsbB-DsbA complex reveals a mechanism of disulfide bond generation. *Cell, 127*(4), 789-801. doi:10.1016/j.cell.2006.10.034

Inaba, K., Takahashi, Y. H., Ito, K., & Hayashi, S. (2006). Critical role of a thiolate-quinone charge transfer complex and its adduct form in de novo disulfide bond generation by DsbB. *Proc Natl Acad Sci U S A, 103*(2), 287-292. doi:10.1073/pnas.0507570103

Ishihara, T., Tomita, H., Hasegawa, Y., Tsukagoshi, N., Yamagata, H., & Udaka, S. (1995). Cloning and characterization of the gene for a protein thiol-disulfide oxidoreductase in Bacillus brevis. *J Bacteriol, 177*(3), 745-749. doi:10.1128/jb.177.3.745-749.1995

Iwata, S., Lee, J. W., Okada, K., Lee, J. K., Iwata, M., Rasmussen, B., . . . Jap, B. K. (1998). Complete structure of the 11-subunit bovine mitochondrial cytochrome bc1 complex. *Science, 281*(5373), 64-71. doi:10.1126/science.281.5373.64

Jacquot, J. P., Rivera-Madrid, R., Marinho, P., Kollarova, M., Le Maréchal, P., Miginiac-Maslow, M., & Meyer, Y. (1994). Arabidopsis thaliana NAPHP thioredoxin reductase. cDNA characterization and expression of the recombinant protein in Escherichia coli. *J Mol Biol, 235*(4), 1357-1363. doi:10.1006/jmbi.1994.1091

Joly, J. C., & Swartz, J. R. (1997). In vitro and in vivo redox states of the Escherichia coli periplasmic oxidoreductases DsbA and DsbC. *Biochemistry, 36*(33), 10067-10072. doi:10.1021/bi9707739

Jordi, W., Hergersberg, C., & de Kruijff, B. (1992). Bilayer-penetrating properties enable apocytochrome c to follow a special import pathway into mitochondria. *Eur J Biochem, 204*(2), 841-846. doi:10.1111/j.1432-1033.1992.tb16703.x

Kadokura, H., Tian, H., Zander, T., Bardwell, J. C., & Beckwith, J. (2004). Snapshots of DsbA in action: detection of proteins in the process of oxidative folding. *Science, 303*(5657), 534-537. doi:10.1126/science.1091724

Käll, L., Krogh, A., & Sonnhammer, E. L. (2004). A combined transmembrane topology and signal peptide prediction method. *J. Mol. Biol., 338*(5), 1027-1036. doi:10.1016/j.jmb.2004.03.016

Kallergi, E., Andreadaki, M., Kritsiligkou, P., Katrakili, N., Pozidis, C., Tokatlidis, K., . . . Peruzzini, R. (2012). Targeting and maturation of Erv1/ALR in the mitochondrial intermembrane space. *ACS Chem Biol, 7*(4), 707-714. doi:10.1021/cb200485b

Kanervo, E., Suorsa, M., & Aro, E.-M. (2005). Functional flexibility and acclimation of the thylakoid membrane. *Photochem Photobiol. Sci., 4*(12), 1072-1080.

Karamanou, S., Bariami, V., Papanikou, E., Kalodimos, C. G., & Economou, A. (2008). Assembly of the translocase motor onto the preprotein-conducting channel. *Mol Microbiol, 70*(2), 311-322. doi:10.1111/j.1365-2958.2008.06402.x

Karamoko, M., Cline, S., Redding, K., Ruiz, N., & Hamel, P. P. (2011). Lumen Thiol Oxidoreductase1, a disulfide bond-forming catalyst, is required for the assembly

of photosystem II in Arabidopsis. *Plant Cell, 23*(12), 4462-4475. doi:10.1105/tpc.111.089680

Karamoko, M., Gabilly, S. T., & Hamel, P. P. (2013). Operation of trans-thylakoid thiol-metabolizing pathways in photosynthesis. *Front. Plant Sci., 4*, 476. doi:10.3389/fpls.2013.00476

Katoh, K., Rozewicki, J., & Yamada, K. D. (2019). MAFFT online service: multiple sequence alignment, interactive sequence choice and visualization. *Brief Bioinform, 20*(4), 1160-1166. doi:10.1093/bib/bbx108

Katzen, F., & Beckwith, J. (2000). Transmembrane electron transfer by the membrane protein DsbD occurs via a disulfide bond cascade. *Cell, 103*(5), 769-779. doi:10.1016/s0092-8674(00)00180-x

Kerfeld, C. A., & Krogmann, D. W. (1998). PHOTOSYNTHETIC CYTOCHROMES c IN CYANOBACTERIA, ALGAE, AND PLANTS. *Annu Rev Plant Physiol Plant Mol Biol, 49*, 397-425. doi:10.1146/annurev.arplant.49.1.397

Kern, M., Scheithauer, J., Kranz, R. G., & Simon, J. (2010). Essential histidine pairs indicate conserved haem binding in epsilonproteobacterial cytochrome c haem lyases. *Microbiology (Reading), 156*(Pt 12), 3773-3781. doi:10.1099/mic.0.042838-0

Kieselbach, T. (2013). Oxidative folding in chloroplasts. *Antioxid Redox Signal, 19*(1), 72-82. doi:10.1089/ars.2012.4582

Kim, D. B., Na, C., Hwang, I., & Lee, D. W. (2023). Understanding protein translocation across chloroplast membranes: Translocons and motor proteins. *J Integr Plant Biol, 65*(2), 408-416. doi:10.1111/jipb.13385

Kindle, K. L. (1990). High-frequency nuclear transformation of *Chlamydomonas reinhardtii*. *Proc. Natl. Acad. Sci. USA, 87*(3), 1228-1232.

Kishigami, S., Kanaya, E., Kikuchi, M., & Ito, K. (1995). DsbA-DsbB interaction through their active site cysteines. Evidence from an odd cysteine mutant of DsbA. *J Biol Chem, 270*(29), 17072-17074. doi:10.1074/jbc.270.29.17072

Kleiner, F. H., Vesteg, M., & Steiner, J. M. (2021). An ancient glaucophyte c6-like cytochrome related to higher plant cytochrome c6A is imported into muroplasts. *J Cell Sci, 134*(9). doi:10.1242/jcs.255901

Kobayashi, T., Kishigami, S., Sone, M., Inokuchi, H., Mogi, T., & Ito, K. (1997). Respiratory chain is required to maintain oxidized states of the DsbA-DsbB

disulfide bond formation system in aerobically growing Escherichia coli cells. *Proc Natl Acad Sci U S A, 94*(22), 11857-11862. doi:10.1073/pnas.94.22.11857

Kohzuma, K., Dal Bosco, C., Kanazawa, A., Dhingra, A., Nitschke, W., Meurer, J., & Kramer, D. M. (2012). Thioredoxin-insensitive plastid ATP synthase that performs moonlighting functions. *Proc Natl Acad Sci U S A, 109*(9), 3293-3298. doi:10.1073/pnas.1115728109

Kranz, R., Lill, R., Goldman, B., Bonnard, G., & Merchant, S. (1998). Molecular mechanisms of cytochrome c biogenesis: three distinct systems. *Mol Microbiol, 29*(2), 383-396. doi:10.1046/j.1365-2958.1998.00869.x

Kranz, R. G., Beckett, C. S., & Goldman, B. S. (2002). Genomic analyses of bacterial respiratory and cytochrome c assembly systems: Bordetella as a model for the system II cytochrome c biogenesis pathway. *Res Microbiol, 153*(1), 1-6. doi:10.1016/s0923-2508(01)01278-5

Kranz, R. G., Richard-Fogal, C., Taylor, J. S., & Frawley, E. R. (2009). Cytochrome c biogenesis: mechanisms for covalent modifications and trafficking of heme and for heme-iron redox control. *Microbiol Mol Biol Rev, 73*(3), 510-528, Table of Contents. doi:10.1128/MMBR.00001-09

Krause, G., Lundström, J., Barea, J. L., Pueyo de la Cuesta, C., & Holmgren, A. (1991). Mimicking the active site of protein disulfide-isomerase by substitution of proline 34 in Escherichia coli thioredoxin. *J Biol Chem, 266*(15), 9494-9500.

Krogh, A., Larsson, B., von Heijne, G., & Sonnhammer, E. L. (2001). Predicting transmembrane protein topology with a hidden Markov model: application to complete genomes. *J Mol Biol, 305*(3), 567-580. doi:10.1006/jmbi.2000.4315

Krupp, R., Chan, C., & Missiakas, D. (2001). DsbD-catalyzed transport of electrons across the membrane of Escherichia coli. *J Biol Chem, 276*(5), 3696-3701. doi:10.1074/jbc.M009500200

Kühlbrandt, W. (2019). Structure and Mechanisms of F-Type ATP Synthases. *Annu Rev Biochem, 88*, 515-549. doi:10.1146/annurev-biochem-013118-110903

Kuras, R., & Wollman, F.-A. (1994). The assembly of cytochrome b_6/f complexes: an approach using genetic transformation of the green alga *Chlamydomonas reinhardtii*. *EMBO J., 13*, 1019-1027.

Kuras, R., Wollman, F. A., & Joliot, P. (1995). Conversion of cytochrome *f* to a soluble form *in vivo* in *Chlamydomonas reinhardtii*. *Biochemistry, 34*(22), 7468-7475.

Kurisu, G., Zhang, H., Smith, J. L., & Cramer, W. A. (2003). Structure of the cytochrome b6f complex of oxygenic photosynthesis: tuning the cavity. *Science, 302*(5647), 1009-1014. doi:10.1126/science.1090165

Landeta, C., Boyd, D., & Beckwith, J. (2018). Disulfide bond formation in prokaryotes. *Nat Microbiol, 3*(3), 270-280. doi:10.1038/s41564-017-0106-2

Lang, S. E., Jenney, F. E., & Daldal, F. (1996). Rhodobacter capsulatus CycH: a bipartite gene product with pleiotropic effects on the biogenesis of structurally different c-type cytochromes. *J Bacteriol, 178*(17), 5279-5290. doi:10.1128/jb.178.17.5279-5290.1996

Laurent, T. C., Moore, E. C., & Reichard, P. (1964). ENZYMATIC SYNTHESIS OF DEOXYRIBONUCLEOTIDES. IV. ISOLATION AND CHARACTERIZATION OF THIOREDOXIN, THE HYDROGEN DONOR FROM ESCHERICHIA COLI B. *J Biol Chem, 239*, 3436-3444.

Layer, G. (2021). Heme biosynthesis in prokaryotes. *Biochim Biophys Acta Mol Cell Res, 1868*(1), 118861. doi:10.1016/j.bbamcr.2020.118861

Le Brun, N. E., Bengtsson, J., & Hederstedt, L. (2000). Genes required for cytochrome c synthesis in Bacillus subtilis. *Mol Microbiol, 36*(3), 638-650. doi:10.1046/j.1365-2958.2000.01883.x

Lee, J. H., Harvat, E. M., Stevens, J. M., Ferguson, S. J., & Saier, M. H. (2007). Evolutionary origins of members of a superfamily of integral membrane cytochrome c biogenesis proteins. *Biochim Biophys Acta, 1768*(9), 2164-2181. doi:10.1016/j.bbamem.2007.04.022

Lemaire, S. D., Collin, V., Keryer, E., Issakidis-Bourguet, E., Lavergne, D., & Miginiac-Maslow, M. (2003). *Chlamydomonas reinhardtii:* a model organism for the study of the thioredoxin family. *Plant Physiology and Biochemistry, 41*(6), 513-521. doi:https://doi.org/10.1016/S0981-9428(03)00079-2

Lemeille, S., Willig, A., Depège-Fargeix, N., Delessert, C., Bassi, R., & Rochaix, J. D. (2009). Analysis of the chloroplast protein kinase Stt7 during state transitions. *PLoS Biol, 7*(3), e45. doi:10.1371/journal.pbio.1000045

Lennartz, K., Bossmann, S., Westhoff, P., Bechtold, N., & Meierhoff, K. (2006). HCF153, a novel nuclear-encoded factor necessary during a post-translational step in biogenesis of the cytochrome bf complex. *Plant J, 45*(1), 101-112. doi:10.1111/j.1365-313X.2005.02605.x

Lennartz, K., Bossmann, S., Westhoff, P., Bechtold, N., & Meierhoff, K. (2006). HCF153, a novel nuclear-encoded factor necessary during a post-translational step in biogenesis of the cytochrome *bf* complex. *Plant J., 45*(1), 101-112.

Lennartz, K., Plucken, H., Seidler, A., Westhoff, P., Bechtold, N., & Meierhoff, K. (2001). HCF164 encodes a thioredoxin-like protein involved in the biogenesis of the cytochrome b(6)f complex in Arabidopsis. *Plant Cell, 13*(11), 2539-2551. doi:10.1105/tpc.010245

Lennon, B. W., Williams, C. H., & Ludwig, M. L. (2000). Twists in catalysis: alternating conformations of Escherichia coli thioredoxin reductase. *Science, 289*(5482), 1190-1194. doi:10.1126/science.289.5482.1190

Lewin, A., Crow, A., Hodson, C. T., Hederstedt, L., & Le Brun, N. E. (2008). Effects of substitutions in the CXXC active-site motif of the extracytoplasmic thioredoxin ResA. *Biochem J, 414*(1), 81-91. doi:10.1042/BJ20080356

Leys, D., Backers, K., Meyer, T. E., Hagen, W. R., Cusanovich, M. A., & Van Beeumen, J. J. (2000). Crystal structures of an oxygen-binding cytochrome c from Rhodobacter sphaeroides. *J Biol Chem, 275*(21), 16050-16056. doi:10.1074/jbc.275.21.16050

Li, J., Zheng, W., Gu, M., Han, L., Luo, Y., Yu, K., . . . Zhu, J. (2022). Structures of the CcmABCD heme release complex at multiple states. *Nat Commun, 13*(1), 6422. doi:10.1038/s41467-022-34136-5

Li, T., Bonkovsky, H. L., & Guo, J.-t. (2011). Structural analysis of heme proteins: implications for design and prediction. *BMC Structural Biology, 11*(1), 13. doi:10.1186/1472-6807-11-13

Li, W., Schulman, S., Dutton, R. J., Boyd, D., Beckwith, J., & Rapoport, T. A. (2010). Structure of a bacterial homologue of vitamin K epoxide reductase. *Nature, 463*(7280), 507-512. doi:10.1038/nature08720

Li, X., Patena, W., Fauser, F., Jinkerson, R. E., Saroussi, S., Meyer, M. T., . . . Jonikas, M. C. (2019). A genome-wide algal mutant library and functional screen identifies genes required for eukaryotic photosynthesis. *Nat Genet, 51*(4), 627-635. doi:10.1038/s41588-019-0370-6

Li, X., Zhang, R., Patena, W., Gang, S. S., Blum, S. R., Ivanova, N., . . . Jonikas, M. C. (2016). An Indexed, Mapped Mutant Library Enables Reverse Genetics Studies of Biological Processes in Chlamydomonas reinhardtii. *Plant Cell, 28*(2), 367-387. doi:10.1105/tpc.15.00465

Li, Y., Farooq, M., Sheng, D., Chandramouli, C., Lan, T., Mahajan, N. K., . . . Ge, R. (2012). Augmenter of liver regeneration (alr) promotes liver outgrowth during zebrafish hepatogenesis. *PLoS One, 7*(1), e30835. doi:10.1371/journal.pone.0030835

Liu, S., Cheng, W., Fowle Grider, R., Shen, G., & Li, W. (2014). Structures of an intramembrane vitamin K epoxide reductase homolog reveal control mechanisms for electron transfer. *Nat Commun, 5*, 3110. doi:10.1038/ncomms4110

Longen, S., Bien, M., Bihlmaier, K., Kloeppel, C., Kauff, F., Hammermeister, M., . . . Riemer, J. (2009). Systematic analysis of the twin cx(9)c protein family. *J Mol Biol, 393*(2), 356-368. doi:10.1016/j.jmb.2009.08.041

Lu, Y., Du, J. J., Yu, Z. B., Peng, J. J., Xu, J. N., & Wang, X. Y. (2014). Identification of potential targets for thylakoid oxidoreductase AtVKOR/LTO1 in chloroplasts. *Protein Pept Lett, 22*(3), 219-225. doi:10.2174/09298665216661411211531 38

Lu, Y., Wang, H. R., Li, H., Cui, H. R., Feng, Y. G., & Wang, X. Y. (2013). A chloroplast membrane protein LTO1/AtVKOR involving in redox regulation and ROS homeostasis. *Plant Cell Rep, 32*(9), 1427-1440. doi:10.1007/s00299-013-1455-9

Lutolf, M. P., Tirelli, N., Cerritelli, S., Cavalli, L., & Hubbell, J. A. (2001). Systematic modulation of Michael-type reactivity of thiols through the use of charged amino acids. *Bioconjug Chem, 12*(6), 1051-1056. doi:10.1021/bc015519e

Ma, S., & Ludwig, R. (2019). Direct Electron Transfer of Enzymes Facilitated by Cytochromes. *ChemElectroChem, 6*(4), 958-975. doi:10.1002/celc.201801256

Mallick, P., Boutz, D. R., Eisenberg, D., & Yeates, T. O. (2002). Genomic evidence that the intracellular proteins of archaeal microbes contain disulfide bonds. *Proc Natl Acad Sci U S A, 99*(15), 9679-9684. doi:10.1073/pnas.142310499

Malnoë, A. (2011). *A genetic suppressor approach to the biogenesis, quality control and function of photosynthetic complexes in Chlamydomonas reinhardtii*
Une approche génétique de recherche de suppresseur pour l'étude de la biogenèse, du contrôle qualité et de la fonction des complexes photosynthétiques chez Chlamydomonas reinhardtii. Université Paris Sud - Paris XI. Retrieved from https://theses.hal.science/tel-01057821 Upmc

Malnoë, A., Wang, F., Girard-Bascou, J., Wollman, F. A., & de Vitry, C. (2014). Thylakoid FtsH protease contributes to photosystem II and cytochrome b_6f remodeling in *Chlamydomonas reinhardtii* under stress conditions. *Plant Cell, 26*(1), 373-390.

Manta, B., Boyd, D., & Berkmen, M. (2019). Disulfide Bond Formation in the Periplasm of. *EcoSal Plus, 8*(2). doi:10.1128/ecosalplus.ESP-0012-2018

Marcaida, M. J., Schlarb-Ridley, B. G., Worrall, J. A., Wastl, J., Evans, T. J., Bendall, D. S., . . . Howe, C. J. (2006). Structure of cytochrome c6A, a novel dithio-cytochrome of Arabidopsis thaliana, and its reactivity with plastocyanin: implications for function. *J Mol Biol, 360*(5), 968-977. doi:10.1016/j.jmb.2006.05.065

Marchler-Bauer, A., Derbyshire, M. K., Gonzales, N. R., Lu, S., Chitsaz, F., Geer, L. Y., . . . Bryant, S. H. (2015). CDD: NCBI's conserved domain database. *Nucleic Acids Res, 43*(Database issue), D222-226. doi:10.1093/nar/gku1221

Martin, J. L. (1995). Thioredoxin--a fold for all reasons. *Structure, 3*(3), 245-250. doi:10.1016/s0969-2126(01)00154-x

Martin, J. L., Bardwell, J. C., & Kuriyan, J. (1993). Crystal structure of the DsbA protein required for disulphide bond formation in vivo. *Nature, 365*(6445), 464-468. doi:10.1038/365464a0

Martinez, S. E., Huang, D., Szczepaniak, A., Cramer, W. A., & Smith, J. L. (1994). Crystal structure of chloroplast cytochrome f reveals a novel cytochrome fold and unexpected heme ligation. *Structure, 2*(2), 95-105. doi:10.1016/s0969-2126(00)00012-5

Matasci, N., Hung, L. H., Yan, Z., Carpenter, E. J., Wickett, N. J., Mirarab, S., . . . Wong, G. K. (2014). Data access for the 1,000 Plants (1KP) project. *Gigascience, 3*, 17. doi:10.1186/2047-217x-3-17

Matsusaki, M., Kanemura, S., Kinoshita, M., Lee, Y. H., Inaba, K., & Okumura, M. (2020). The Protein Disulfide Isomerase Family: from proteostasis to pathogenesis. *Biochim Biophys Acta Gen Subj, 1864*(2), 129338. doi:10.1016/j.bbagen.2019.04.003

Mavridou, D. A., Clark, M. N., Choulat, C., Ferguson, S. J., & Stevens, J. M. (2013). Probing heme delivery processes in cytochrome c biogenesis System I. *Biochemistry, 52*(41), 7262-7270. doi:10.1021/bi400398t

Mavridou, D. A., Ferguson, S. J., & Stevens, J. M. (2013). Cytochrome c assembly. *IUBMB Life, 65*(3), 209-216. doi:10.1002/iub.1123

Mavridou, D. A. I., Stevens, J. M., Goddard, A. D., Willis, A. C., Ferguson, S. J., & Redfield, C. (2009). Control of periplasmic interdomain thiol:disulfide exchange

in the transmembrane oxidoreductase DsbD. *J Biol Chem, 284*(5), 3219-3226. doi:10.1074/jbc.M805963200

Mayfield, S. P., Bennoun, P., & Rochaix, J. D. (1987). Expression of the nuclear encoded OEE1 protein is required for oxygen evolution and stability of photosystem II particles in Chlamydomonas reinhardtii. *EMBO J, 6*(2), 313-318. doi:10.1002/j.1460-2075.1987.tb04756.x

McCarthy, A. A., Haebel, P. W., Törrönen, A., Rybin, V., Baker, E. N., & Metcalf, P. (2000). Crystal structure of the protein disulfide bond isomerase, DsbC, from Escherichia coli. *Nat Struct Biol, 7*(3), 196-199. doi:10.1038/73295

Mendez, D. L., Lowder, E. P., Tillman, D. E., Sutherland, M. C., Collier, A. L., Rau, M. J., . . . Kranz, R. G. (2022). Cryo-EM of CcsBA reveals the basis for cytochrome c biogenesis and heme transport. *Nature Chemical Biology, 18*(1), 101-108. doi:10.1038/s41589-021-00935-y

Meng, S., Ji, Y., Zhu, L., Dhoke, G. V., Davari, M. D., & Schwaneberg, U. (2022). The molecular basis and enzyme engineering strategies for improvement of coupling efficiency in cytochrome P450s. *Biotechnology Advances, 61*, 108051. doi:https://doi.org/10.1016/j.biotechadv.2022.108051

Merchant, S., & Bogorad, L. (1987). The Cu(II)-repressible plastidic cytochrome c. Cloning and sequence of a complementary DNA for the pre-apoprotein. *J Biol Chem, 262*(19), 9062-9067.

Merchant, S., & Bogorad, L. (1987). Metal ion regulated gene expression: use of a plastocyanin-less mutant of Chlamydomonas reinhardtii to study the Cu(II)-dependent expression of cytochrome c-552. *EMBO J, 6*(9), 2531-2535. doi:10.1002/j.1460-2075.1987.tb02540.x

Merchant, S., & Dreyfuss, B. W. (1998). POSTTRANSLATIONAL ASSEMBLY OF PHOTOSYNTHETIC METALLOPROTEINS. *Annu Rev Plant Physiol Plant Mol Biol, 49*, 25-51. doi:10.1146/annurev.arplant.49.1.25

Mesecke, N., Terziyska, N., Kozany, C., Baumann, F., Neupert, W., Hell, K., & Herrmann, J. M. (2005). A disulfide relay system in the intermembrane space of mitochondria that mediates protein import. *Cell, 121*(7), 1059-1069. doi:10.1016/j.cell.2005.04.011

Meyer, A. J., Riemer, J., & Rouhier, N. (2019). Oxidative protein folding: state-of-the-art and current avenues of research in plants. *New Phytol, 221*(3), 1230-1246. doi:10.1111/nph.15436

Meyer, E. H., Giegé, P., Gelhaye, E., Rayapuram, N., Ahuja, U., Thöny-Meyer, L., . . . Bonnard, G. (2005). AtCCMH, an essential component of the c-type cytochrome maturation pathway in Arabidopsis mitochondria, interacts with apocytochrome c. *Proc Natl Acad Sci U S A, 102*(44), 16113-16118. doi:10.1073/pnas.0503473102

Michelet, L., & Zaffagnini, M. (2009). Thioredoxins and Related Proteins *The Chlamydomonas Sourcebook* (pp. 401-443).

Missiakas, D., Georgopoulos, C., & Raina, S. (1993). Identification and characterization of the Escherichia coli gene dsbB, whose product is involved in the formation of disulfide bonds in vivo. *Proc Natl Acad Sci U S A, 90*(15), 7084-7088. doi:10.1073/pnas.90.15.7084

Missiakas, D., Georgopoulos, C., & Raina, S. (1994). The Escherichia coli dsbC (xprA) gene encodes a periplasmic protein involved in disulfide bond formation. *EMBO J, 13*(8), 2013-2020. doi:10.1002/j.1460-2075.1994.tb06471.x

Molina-Heredia, F. P., Wastl, J., Navarro, J. A., Bendall, D. S., Hervás, M., Howe, C. J., & De La Rosa, M. A. (2003). Photosynthesis: a new function for an old cytochrome? *Nature, 424*(6944), 33-34. doi:10.1038/424033b

Moore, E. C., Reichard, P., & Thelander, L. (1964). ENZYMATIC SYNTHESIS OF DEOXYRIBONUCLEOTIDES.V. PURIFICATION AND PROPERTIES OF THIOREDOXIN REDUCTASE FROM ESCHERICHIA COLI B. *J Biol Chem, 239*, 3445-3452.

Moore, G. (1987). Cytochromes c: Biological Aspect: Springer-Verlag, Berlin.

Moore, G. R., & Pettigrew, G. W. (1990). *Cytochromes c. Evolutionary, Structural and Physicochemical Aspects*: Springer.

Morgada, M. N., Abriata, L. A., Cefaro, C., Gajda, K., Banci, L., & Vila, A. J. (2015). Loop recognition and copper-mediated disulfide reduction underpin metal site assembly of CuA in human cytochrome oxidase. *Proc Natl Acad Sci U S A, 112*(38), 11771-11776. doi:10.1073/pnas.1505056112

Mössner, E., Huber-Wunderlich, M., & Glockshuber, R. (1998). Characterization of Escherichia coli thioredoxin variants mimicking the active-sites of other thiol/disulfide oxidoreductases. *Protein Sci, 7*(5), 1233-1244. doi:10.1002/pro.5560070519

Motohashi, K., & Hisabori, T. (2006). HCF164 Receives Reducing Equivalents from Stromal Thioredoxin across the Thylakoid Membrane and Mediates Reduction of

Target Proteins in the Thylakoid Lumen. *J. Biol. Chem., 281*(46), 35039-35047. doi:10.1074/jbc.M605938200

Motohashi, K., & Hisabori, T. (2010). CcdA is a thylakoid membrane protein required for the transfer of reducing equivalents from stroma to thylakoid lumen in the higher plant chloroplast. *Antioxid Redox Signal, 13*(8), 1169-1176. doi:10.1089/ars.2010.3138

Murchie, E. H., & Lawson, T. (2013). Chlorophyll fluorescence analysis: a guide to good practice and understanding some new applications. *J. Exp. Bot., 64*(13), 3983-3998. doi:10.1093/jxb/ert208

Nagy, P. (2013). Kinetics and mechanisms of thiol-disulfide exchange covering direct substitution and thiol oxidation-mediated pathways. *Antioxid Redox Signal, 18*(13), 1623-1641. doi:10.1089/ars.2012.4973

Nakamoto, H., & Bardwell, J. C. (2004). Catalysis of disulfide bond formation and isomerization in the Escherichia coli periplasm. *Biochim Biophys Acta, 1694*(1-3), 111-119. doi:10.1016/j.bbamcr.2004.02.012

Nakamoto, S. S., Hamel, P., & Merchant, S. (2000). Assembly of chloroplast cytochromes b and c. *Biochimie, 82*(6-7), 603-614. doi:10.1016/s0300-9084(00)00605-2

Naoé, M., Ohwa, Y., Ishikawa, D., Ohshima, C., Nishikawa, S., Yamamoto, H., & Endo, T. (2004). Identification of Tim40 that mediates protein sorting to the mitochondrial intermembrane space. *J Biol Chem, 279*(46), 47815-47821. doi:10.1074/jbc.M410272200

Napoli, E., Wong, S., Hung, C., Ross-Inta, C., Bomdica, P., & Giulivi, C. (2013). Defective mitochondrial disulfide relay system, altered mitochondrial morphology and function in Huntington's disease. *Hum Mol Genet, 22*(5), 989-1004. doi:10.1093/hmg/dds503

Nelson, J. W., & Creighton, T. E. (1994). Reactivity and ionization of the active site cysteine residues of DsbA, a protein required for disulfide bond formation in vivo. *Biochemistry, 33*(19), 5974-5983. doi:10.1021/bi00185a039

Nelson, N., & Ben-Shem, A. (2004). The complex architecture of oxygenic photosynthesis. *Nature Reviews Molecular Cell Biology, 5*(12), 971-982. doi:10.1038/nrm1525

Neupert, W. (1997). Protein import into mitochondria. *Annu Rev Biochem, 66*, 863-917. doi:10.1146/annurev.biochem.66.1.863

New, C. P., Ma, Q., & Dabney-Smith, C. (2018). Routing of thylakoid lumen proteins by the chloroplast twin arginine transport pathway. *Photosynthesis Research, 138*(3), 289-301. doi:10.1007/s11120-018-0567-z

Nikitina, J., Shutova, T., Melnik, B., Chernyshov, S., Marchenkov, V., Semisotnov, G., . . . Samuelsson, G. (2008). Importance of a single disulfide bond for the PsbO protein of photosystem II: protein structure stability and soluble overexpression in *Escherichia coli*. *Photosynth. Res., 98*(1-3), 391-403.

Nirody, J. A., Budin, I., & Rangamani, P. (2020). ATP synthase: Evolution, energetics, and membrane interactions. *J Gen Physiol, 152*(11). doi:10.1085/jgp.201912475

Nohara, T., Asai, T., Nakai, M., Sugiura, M., & Endo, T. (1996). Cytochrome f encoded by the chloroplast genome is imported into thylakoids via the SecA-dependent pathway. *Biochem Biophys Res Commun, 224*(2), 474-478. doi:10.1006/bbrc.1996.1051

Nunnari, J., Fox, T. D., & Walter, P. (1993). A mitochondrial protease with two catalytic subunits of nonoverlapping specificities. *Science, 262*(5142), 1997-2004. doi:10.1126/science.8266095

Obinger, C., Knepper, J. C., Zimmermann, U., & Peschek, G. A. (1990). Identification of a periplasmic C-type cytochrome as electron donor to the plasma membrane-bound cytochrome oxidase of the cyanobacterium Nostoc Mac. *Biochem Biophys Res Commun, 169*(2), 492-501. doi:10.1016/0006-291x(90)90358-t

Oka, O. B., & Bulleid, N. J. (2013). Forming disulfides in the endoplasmic reticulum. *Biochim Biophys Acta, 1833*(11), 2425-2429. doi:10.1016/j.bbamcr.2013.02.007

Pacheu-Grau, D., Wasilewski, M., Oeljeklaus, S., Gibhardt, C. S., Aich, A., Chudenkova, M., . . . Rehling, P. (2020). COA6 Facilitates Cytochrome c Oxidase Biogenesis as Thiol-reductase for Copper Metallochaperones in Mitochondria. *J Mol Biol, 432*(7), 2067-2079. doi:10.1016/j.jmb.2020.01.036

Page, M. D., & Ferguson, S. J. (1999). Mutational analysis of the Paracoccus denitrificans c-type cytochrome biosynthetic genes ccmABCDG: disruption of ccmC has distinct effects suggesting a role for CcmC independent of CcmAB. *Microbiology (Reading), 145 (Pt 11)*, 3047-3057. doi:10.1099/00221287-145-11-3047

Page, M. L. D., Hamel, P. P., Gabilly, S. T., Zegzouti, H., Perea, J. V., Alonso, J. M., . . . Merchant, S. (2004). A Homolog of Prokaryotic Thiol Disulfide Transporter CcdA Is Required for the Assembly of the Cytochrome b_6f Complex in

Arabidopsis Chloroplasts. *J. Biol. Chem., 279*(31), 32474-32482. doi:10.1074/jbc.M404285200

Papanikou, E., Karamanou, S., & Economou, A. (2007). Bacterial protein secretion through the translocase nanomachine. *Nature Reviews Microbiology, 5*(11), 839-851. doi:10.1038/nrmicro1771

Park, H., Wang, W., Min, S. H., Ren, Y., Shin, K., & Han, X. (2023). Artificial organelles for sustainable chemical energy conversion and production in artificial cells: Artificial mitochondrion and chloroplasts. *Biophysics Reviews, 4*(1). doi:10.1063/5.0131071

Patil, A., & Nakamura, H. (2006). Disordered domains and high surface charge confer hubs with the ability to interact with multiple proteins in interaction networks. *FEBS Lett, 580*(8), 2041-2045. doi:10.1016/j.febslet.2006.03.003

Patil, A., & Nakamura, H. (2007). The role of charged surface residues in the binding ability of small hubs in protein-protein interaction networks. *Biophysics (Nagoya-shi), 3*, 27-35. doi:10.2142/biophysics.3.27

Pei, D., & Dalbey, R. E. (2022). Membrane translocation of folded proteins. *J Biol Chem, 298*(7), 102107. doi:10.1016/j.jbc.2022.102107

Pettigrew, G. W., Leaver, J. L., Meyer, T. E., & Ryle, A. P. (1975). Purification, properties and amino acid sequence of atypical cytochrome c from two protozoa, Euglena gracilis and Crithidia oncopelti. *Biochem J, 147*(2), 291-302. doi:10.1042/bj1470291

Pfanner, N., & Geissler, A. (2001). Versatility of the mitochondrial protein import machinery. *Nat Rev Mol Cell Biol, 2*(5), 339-349. doi:10.1038/35073006

Pigolev, A. V., & Klimov, V. V. (2015). The green alga *Chlamydomonas reinhardtii* as a tool for in vivo study of site-directed mutations in PsbO protein of photosystem II. *Biochemistry (Mosc), 80*(6), 662-673. doi:10.1134/s0006297915060036

Pitts, K. E., Dobbin, P. S., Reyes-Ramirez, F., Thomson, A. J., Richardson, D. J., & Seward, H. E. (2003). Characterization of the Shewanella oneidensis MR-1 decaheme cytochrome MtrA: expression in Escherichia coli confers the ability to reduce soluble Fe(III) chelates. *J Biol Chem, 278*(30), 27758-27765. doi:10.1074/jbc.M302582200

Poole, L. B. (2015). The basics of thiols and cysteines in redox biology and chemistry. *Free Radic. Biol. Med. , 80*, 148-157. doi:10.1016/j.freeradbiomed.2014.11.013

Pratibha, P., Singh, S. K., Srinivasan, R., Bhat, S. R., & Sreenivasulu, Y. (2017). Gametophyte Development Needs Mitochondrial Coproporphyrinogen III Oxidase Function. *Plant Physiol, 174*(1), 258-275. doi:10.1104/pp.16.01482

Priest, J. W., & Hajduk, S. L. (1992). Cytochrome *c* reductase purified from *Crithidia fasciculata* contains an atypical cytochrome c_1. *J Biol Chem, 267*(28), 20188-20195.

Pröschold, T., Harris, E. H., & Coleman, A. W. (2005). Portrait of a species: *Chlamydomonas reinhardtii*. *Genetics, 170*(4), 1601-1610. doi:10.1534/genetics.105.044503

Ramseier, T. M., Winteler, H. V., & Hennecke, H. (1991). Discovery and sequence analysis of bacterial genes involved in the biogenesis of c-type cytochromes. *J Biol Chem, 266*(12), 7793-7803.

Randall, L. L., Hardy, S. J., Topping, T. B., Smith, V. F., Bruce, J. E., & Smith, R. D. (1998). The interaction between the chaperone SecB and its ligands: evidence for multiple subsites for binding. *Protein Sci, 7*(11), 2384-2390. doi:10.1002/pro.5560071115

Rayapuram, N., Hagenmuller, J., Grienenberger, J. M., Giegé, P., & Bonnard, G. (2007). AtCCMA interacts with AtCcmB to form a novel mitochondrial ABC transporter involved in cytochrome c maturation in Arabidopsis. *J Biol Chem, 282*(29), 21015-21023. doi:10.1074/jbc.M704091200

Reinemer, P., Dirr, H. W., Ladenstein, R., Schäffer, J., Gallay, O., & Huber, R. (1991). The three-dimensional structure of class pi glutathione S-transferase in complex with glutathione sulfonate at 2.3 A resolution. *EMBO J, 10*(8), 1997-2005. doi:10.1002/j.1460-2075.1991.tb07729.x

Ren, B., Huang, W., Akesson, B., & Ladenstein, R. (1997). The crystal structure of seleno-glutathione peroxidase from human plasma at 2.9 A resolution. *J Mol Biol, 268*(5), 869-885. doi:10.1006/jmbi.1997.1005

Ren, Q., Ahuja, U., & Thony-Meyer, L. (2002). A bacterial cytochrome c heme lyase. CcmF forms a complex with the heme chaperone CcmE and CcmH but not with apocytochrome c. *J Biol Chem, 277*(10), 7657-7663.

Ren, Q., & Thony-Meyer, L. (2001). Physical interaction of CcmC with heme and the heme chaperone CcmE during cytochrome c maturation. *J Biol Chem, 276*(35), 32591-32596. doi:10.1074/jbc.M103058200

Richard-Fogal, C., & Kranz, R. G. (2010). The CcmC:heme:CcmE complex in heme trafficking and cytochrome c biosynthesis. *J Mol Biol, 401*(3), 350-362. doi:10.1016/j.jmb.2010.06.041

Richard-Fogal, C. L., Frawley, E. R., Bonner, E. R., Zhu, H., San Francisco, B., & Kranz, R. G. (2009). A conserved haem redox and trafficking pathway for cofactor attachment. *EMBO J, 28*(16), 2349-2359. doi:10.1038/emboj.2009.189

Richard-Fogal, C. L., Frawley, E. R., Feissner, R. E., & Kranz, R. G. (2007). Heme concentration dependence and metalloporphyrin inhibition of the system I and II cytochrome c assembly pathways. *J Bacteriol, 189*(2), 455-463. doi:10.1128/JB.01388-06

Richard-Fogal, C. L., Frawley, E. R., & Kranz, R. G. (2008). Topology and function of CcmD in cytochrome c maturation. *J Bacteriol, 190*(10), 3489-3493. doi:10.1128/JB.00146-08

Richardson, L. G. L., & Schnell, D. J. (2020). Origins, function, and regulation of the TOC-TIC general protein import machinery of plastids. *J Exp Bot, 71*(4), 1226-1238. doi:10.1093/jxb/erz517

Rietsch, A., Bessette, P., Georgiou, G., & Beckwith, J. (1997). Reduction of the periplasmic disulfide bond isomerase, DsbC, occurs by passage of electrons from cytoplasmic thioredoxin. *J Bacteriol, 179*(21), 6602-6608. doi:10.1128/jb.179.21.6602-6608.1997

Rockholm, D. C., & Yamamoto, H. Y. (1996). Violaxanthin de-epoxidase. *Plant Physiol, 110*(2), 697-703. doi:10.1104/pp.110.2.697

Roos, G., Foloppe, N., Van Laer, K., Wyns, L., Nilsson, L., Geerlings, P., & Messens, J. (2009). How thioredoxin dissociates its mixed disulfide. *PLoS Comput Biol, 5*(8), e1000461. doi:10.1371/journal.pcbi.1000461

Roos, G., Garcia-Pino, A., Van Belle, K., Brosens, E., Wahni, K., Vandenbussche, G., . . . Messens, J. (2007). The conserved active site proline determines the reducing power of Staphylococcus aureus thioredoxin. *J Mol Biol, 368*(3), 800-811. doi:10.1016/j.jmb.2007.02.045

Sadler, I., Suda, K., Schatz, G., Kaudewitz, F., & Haid, A. (1984). Sequencing of the nuclear gene for the yeast cytochrome c1 precursor reveals an unusually complex amino-terminal presequence. *EMBO J, 3*(9), 2137-2143. doi:10.1002/j.1460-2075.1984.tb02103.x

San Francisco, B., Bretsnyder, E. C., & Kranz, R. G. (2013). Human mitochondrial holocytochrome c synthase's heme binding, maturation determinants, and complex formation with cytochrome c. *Proc Natl Acad Sci U S A, 110*(9), E788-797. doi:10.1073/pnas.1213897109

San Francisco, B., Sutherland, M. C., & Kranz, R. G. (2014). The CcmFH complex is the system I holocytochrome *c* synthetase: engineering cytochrome *c* maturation independent of CcmABCDE. *Mol Microbiol, 91*(5), 996-1008.

Sanders, C., Turkarslan, S., Lee, D. W., & Daldal, F. (2010). Cytochrome c biogenesis: the Ccm system. *Trends Microbiol, 18*(6), 266-274. doi:10.1016/j.tim.2010.03.006

Sanders, C., Turkarslan, S., Lee, D. W., Onder, O., Kranz, R. G., & Daldal, F. (2008). The cytochrome c maturation components CcmF, CcmH, and CcmI form a membrane-integral multisubunit heme ligation complex. *J Biol Chem, 283*(44), 29715-29722. doi:10.1074/jbc.M805413200

Sandmann, G., H. Reck, H., Kessler, E., & Boger, P. (1983). Distribution of plastocyanin and soluble plastidic cytochrome c in various classes of algae. (Vol. 134, pp. 23-27). Arch. Microbiol.

Schiött, T., Throne-Holst, M., & Hederstedt, L. (1997). *Bacillus subtilis CcdA*-defective mutants are blocked in a late step of cytochrome *c* biogenesis. *J. Bacteriol., 179*(14), 4523-4529.

Schiött, T., Throne-Holst, M., & Hederstedt, L. (1997). Bacillus subtilis CcdA-defective mutants are blocked in a late step of cytochrome c biogenesis. *J Bacteriol, 179*(14), 4523-4529. doi:10.1128/jb.179.14.4523-4529.1997

Schiött, T., von Wachenfeldt, C., & Hederstedt, L. (1997). Identification and characterization of the ccdA gene, required for cytochrome c synthesis in Bacillus subtilis. *J Bacteriol, 179*(6), 1962-1973. doi:10.1128/jb.179.6.1962-1973.1997

Schmidt, G. W., Matlin, K. S., & Chua, N. H. (1977). A rapid procedure for selective enrichment of photosynthetic electron transport mutants. *Proc Natl Acad Sci U S A, 74*(2), 610-614. doi:10.1073/pnas.74.2.610

Schulman, S., Wang, B., Li, W., & Rapoport, T. A. (2010). Vitamin K epoxide reductase prefers ER membrane-anchored thioredoxin-like redox partners. *Proc Natl Acad Sci U S A, 107*(34), 15027-15032. doi:10.1073/pnas.1009972107

Schulz, H., Fabianek, R. A., Pellicioli, E. C., Hennecke, H., & Thöny-Meyer, L. (1999). Heme transfer to the heme chaperone CcmE during cytochrome c maturation

requires the CcmC protein, which may function independently of the ABC-transporter CcmAB. *Proc Natl Acad Sci U S A, 96*(11), 6462-6467. doi:10.1073/pnas.96.11.6462

Schurmann, P., & Jacquot, J. P. (2000). PLANT THIOREDOXIN SYSTEMS REVISITED. *Annu Rev Plant Physiol Plant Mol Biol, 51*, 371-400. doi:10.1146/annurev.arplant.51.1.371

Schürmann, P., Wolosiuk, R. A., Breazeale, V. D., & Buchanan, B. B. (1976). Two proteins function in the regulation of photosynthetic CO_2 assimilation in chloroplasts. *Nature, 263*(5574), 257-258. doi:10.1038/263257a0

Sevier, C. S., Cuozzo, J. W., Vala, A., Aslund, F., & Kaiser, C. A. (2001). A flavoprotein oxidase defines a new endoplasmic reticulum pathway for biosynthetic disulphide bond formation. *Nat Cell Biol, 3*(10), 874-882. doi:10.1038/ncb1001-874

Sevier, C. S., & Kaiser, C. A. (2002). Formation and transfer of disulphide bonds in living cells. *Nat Rev Mol Cell Biol, 3*(11), 836-847. doi:10.1038/nrm954

Sievers, F., & Higgins, D. G. (2014). Clustal omega. *Curr. Protoc. Bioinformatics, 48*, 3.13.11-16. doi:10.1002/0471250953.bi0313s48

Silhavy, T. J., Berman, M. L., & Enquist, L. W. (1984). *Experiments with gene fusions*. Plainview, N.Y.: Cold Spring Harbor Laboratory Press.

Simionato, D., Basso, S., Zaffagnini, M., Lana, T., Marzotto, F., Trost, P., & Morosinotto, T. (2015). Protein redox regulation in the thylakoid lumen: The importance of disulfide bonds for violaxanthin de-epoxidase. *FEBS Lett., 589*(8), 919-923. doi:doi:10.1016/j.febslet.2015.02.033

Simon, J., & Hederstedt, L. (2011). Composition and function of cytochrome c biogenesis System II. *FEBS J, 278*(22), 4179-4188. doi:10.1111/j.1742-4658.2011.08374.x

Singh, A. K., Bhattacharyya-Pakrasi, M., & Pakrasi, H. B. (2008). Identification of an atypical membrane protein involved in the formation of protein disulfide bonds in oxygenic photosynthetic organisms. *J Biol Chem, 283*(23), 15762-15770. doi:10.1074/jbc.M800982200

Small, J. L., Park, S. W., Kana, B. D., Ioerger, T. R., Sacchettini, J. C., & Ehrt, S. (2013). Perturbation of cytochrome *c* maturation reveals adaptability of the respiratory chain in *Mycobacterium tuberculosis*. *mBio, 4*(5), e00475-00413. doi:10.1128/mBio.00475-13

Smith, L. J., Kahraman, A., & Thornton, J. M. (2010). Heme proteins—Diversity in structural characteristics, function, and folding. *Proteins: Structure, Function, and Bioinformatics, 78*(10), 2349-2368. doi:https://doi.org/10.1002/prot.22747

Söding, J., Biegert, A., & Lupas, A. N. (2005). The HHpred interactive server for protein homology detection and structure prediction. *Nucleic Acids Res, 33*(Web Server issue), W244-248. doi:10.1093/nar/gki408

Soma, S., Morgada, M. N., Naik, M. T., Boulet, A., Roesler, A. A., Dziuba, N., . . . Gohil, V. M. (2019). COA6 Is Structurally Tuned to Function as a Thiol-Disulfide Oxidoreductase in Copper Delivery to Mitochondrial Cytochrome c Oxidase. *Cell Rep, 29*(12), 4114-4126 e4115. doi:10.1016/j.celrep.2019.11.054

Sone, M., Kishigami, S., Yoshihisa, T., & Ito, K. (1997). Roles of disulfide bonds in bacterial alkaline phosphatase. *J Biol Chem, 272*(10), 6174-6178. doi:10.1074/jbc.272.10.6174

Spielewoy, N., Schulz, H., Grienenberger, J. M., Thony-Meyer, L., & Bonnard, G. (2001). CCME, a nuclear-encoded heme-binding protein involved in cytochrome c maturation in plant mitochondria. *J Biol Chem, 276*(8), 5491-5497. doi:10.1074/jbc.M008853200

Stael, S., Miller, L. P., Fernandez-Fernandez, A. D., & Van Breusegem, F. (2022). Detection of Damage-Activated Metacaspase Activity by Western Blot in Plants. *Methods Mol. Biol., 2447*, 127-137. doi:10.1007/978-1-0716-2079-3_11

Stafford, S. J., Humphreys, D. P., & Lund, P. A. (1999). Mutations in dsbA and dsbB, but not dsbC, lead to an enhanced sensitivity of Escherichia coli to Hg2+ and Cd2+. *FEMS Microbiol Lett, 174*(1), 179-184. doi:10.1111/j.1574-6968.1999.tb13566.x

Stroebel, D., Choquet, Y., Popot, J. L., & Picot, D. (2003). An atypical haem in the cytochrome b(6)f complex. *Nature, 426*(6965), 413-418. doi:10.1038/nature02155

Su, C. H., & Tzagoloff, A. (2017). Cox16 protein is physically associated with Cox1p assembly intermediates and with cytochrome oxidase. *J. Biol. Chem., 292*(39), 16277-16283. doi:10.1074/jbc.M117.801811

Subrahmanian, N., Castonguay, A. D., Fatnes, T. A., & Hamel, P. P. (2020). *Chlamydomonas reinhardtii* as a plant model system to study mitochondrial complex I dysfunction. *Plant Direct, 4*(2), e00200. doi:10.1002/pld3.200

Subrahmanian, N., Castonguay, A. D., Remacle, C., & Hamel, P. P. (2020). Assembly of Mitochondrial Complex I Requires the Low-Complexity Protein AMC1 in

Chlamydomonas reinhardtii. *Genetics, 214*(4), 895-911. doi:10.1534/genetics.120.303029

Sun, G., Sharkova, E., Chesnut, R., Birkey, S., Duggan, M. F., Sorokin, A., . . . Hulett, F. M. (1996). Regulators of aerobic and anaerobic respiration in Bacillus subtilis. *J Bacteriol, 178*(5), 1374-1385. doi:10.1128/jb.178.5.1374-1385.1996

Sutherland, M. C., Jarodsky, J. M., Ovchinnikov, S., Baker, D., & Kranz, R. G. (2018). Structurally Mapping Endogenous Heme in the CcmCDE Membrane Complex for Cytochrome c Biogenesis. *J Mol Biol, 430*(8), 1065-1080. doi:10.1016/j.jmb.2018.01.022

Sutherland, M. C., Mendez, D. L., Babbitt, S. E., Tillman, D. E., Melnikov, O., Tran, N. L., . . . Kranz, R. G. (2021). In vitro reconstitution reveals major differences between human and bacterial cytochrome c synthases. *Elife, 10*. doi:10.7554/eLife.64891

Sutherland, M. C., Tran, N. L., Tillman, D. E., Jarodsky, J. M., Yuan, J., & Kranz, R. G. (2018). Structure-Function Analysis of the Bifunctional CcsBA Heme Exporter and Cytochrome. *mBio, 9*(6). doi:10.1128/mBio.02134-18

Swaminathan, A. B., & Gohil, V. M. (2022). The Role of COA6 in the Mitochondrial Copper Delivery Pathway to Cytochrome c Oxidase. *Biomolecules, 12*(1). doi:10.3390/biom12010125

Swenson, S. A., Moore, C. M., Marcero, J. R., Medlock, A. E., Reddi, A. R., & Khalimonchuk, O. (2020). From Synthesis to Utilization: The Ins and Outs of Mitochondrial Heme. *Cells, 9*(3). doi:10.3390/cells9030579

Szklarczyk, R., Wanschers, B. F., Cuypers, T. D., Esseling, J. J., Riemersma, M., van den Brand, M. A., . . . Huynen, M. A. (2012). Iterative orthology prediction uncovers new mitochondrial proteins and identifies C12orf62 as the human ortholog of COX14, a protein involved in the assembly of cytochrome c oxidase. *Genome Biol, 13*(2), R12. doi:10.1186/gb-2012-13-2-r12

Tanaka, S., Kawata, Y., Wada, K., & Hamaguchi, K. (1989). Extrinsic 33-kilodalton protein of spinach oxygen-evolving complexes: kinetic studies of folding and disulfide reduction. *Biochemistry, 28*(18), 7188-7193. doi:10.1021/bi00444a009

Terziyska, N., Lutz, T., Kozany, C., Mokranjac, D., Mesecke, N., Neupert, W., . . . Hell, K. (2005). Mia40, a novel factor for protein import into the intermembrane space of mitochondria is able to bind metal ions. *FEBS Lett, 579*(1), 179-184. doi:10.1016/j.febslet.2004.11.072

Thauer, R. K., & Bonacker, L. G. (1994). Biosynthesis of coenzyme F430, a nickel porphinoid involved in methanogenesis. *Ciba Found Symp, 180*, 210-222; discussion 222-217. doi:10.1002/9780470514535.ch12

Thöny-Meyer, L. (1997). Biogenesis of respiratory cytochromes in bacteria. *Microbiol Mol Biol Rev, 61*(3), 337-376. doi:10.1128/mmbr.61.3.337-376.1997

Thöny-Meyer, L., Fischer, F., Künzler, P., Ritz, D., & Hennecke, H. (1995). Escherichia coli genes required for cytochrome c maturation. *J Bacteriol, 177*(15), 4321-4326. doi:10.1128/jb.177.15.4321-4326.1995

Thöny-Meyer, L., & Künzler, P. (1997). Translocation to the periplasm and signal sequence cleavage of preapocytochrome c depend on sec and lep, but not on the ccm gene products. *Eur J Biochem, 246*(3), 794-799. doi:10.1111/j.1432-1033.1997.t01-1-00794.x

Tian, G., Xiang, S., Noiva, R., Lennarz, W. J., & Schindelin, H. (2006). The crystal structure of yeast protein disulfide isomerase suggests cooperativity between its active sites. *Cell, 124*(1), 61-73. doi:10.1016/j.cell.2005.10.044

Tie, J. K., & Stafford, D. W. (2008). Structure and function of vitamin K epoxide reductase. *Vitam Horm, 78*, 103-130. doi:10.1016/S0083-6729(07)00006-4

Timon-Gomez, A., Nyvltova, E., Abriata, L. A., Vila, A. J., Hosler, J., & Barrientos, A. (2018). Mitochondrial cytochrome c oxidase biogenesis: Recent developments. *Semin Cell Dev Biol, 76*, 163-178. doi:10.1016/j.semcdb.2017.08.055

Todd, L. R., Damin, M. N., Gomathinayagam, R., Horn, S. R., Means, A. R., & Sankar, U. (2010). Growth factor erv1-like modulates Drp1 to preserve mitochondrial dynamics and function in mouse embryonic stem cells. *Mol Biol Cell, 21*(7), 1225-1236. doi:10.1091/mbc.e09-11-0937

Travaglini-Allocatelli, C. (2013). Protein Machineries Involved in the Attachment of Heme to Cytochrome c: Protein Structures and Molecular Mechanisms. *Scientifica (Cairo), 2013*, 505714. doi:10.1155/2013/505714

Trivedi, M. V., Laurence, J. S., & Siahaan, T. J. (2009). The role of thiols and disulfides on protein stability. *Curr Protein Pept Sci, 10*(6), 614-625. doi:10.2174/138920309789630534

Tsirigotaki, A., De Geyter, J., Šoštaric, N., Economou, A., & Karamanou, S. (2017). Protein export through the bacterial Sec pathway. *Nat Rev Microbiol, 15*(1), 21-36. doi:10.1038/nrmicro.2016.161

Tsirigotaki, A., De Geyter, J., Šoštaric´, N., Economou, A., & Karamanou, S. (2017). Protein export through the bacterial Sec pathway. *Nature Reviews Microbiology, 15*(1), 21-36. doi:10.1038/nrmicro.2016.161

Tsukihara, T., Aoyama, H., Yamashita, E., Tomizaki, T., Yamaguchi, H., Shinzawa-Itoh, K., . . . Yoshikawa, S. (1995). Structures of metal sites of oxidized bovine heart cytochrome c oxidase at 2.8 A. *Science, 269*(5227), 1069-1074. doi:10.1126/science.7652554

Turkarslan, S., Sanders, C., Ekici, S., & Daldal, F. (2008). Compensatory thio-redox interactions between DsbA, CcdA and CcmG unveil the apocytochrome c holdase role of CcmG during cytochrome *c* maturation. *Mol. Microbiol., 70*(3), 652-666. doi:10.1111/j.1365-2958.2008.06441.x

Unseld, M., Marienfeld, J. R., Brandt, P., & Brennicke, A. (1997). The mitochondrial genome of Arabidopsis thaliana contains 57 genes in 366,924 nucleotides. *Nat Genet, 15*(1), 57-61. doi:10.1038/ng0197-57

van der Wolk, J. P., de Wit, J. G., & Driessen, A. J. (1997). The catalytic cycle of the escherichia coli SecA ATPase comprises two distinct preprotein translocation events. *EMBO J, 16*(24), 7297-7304. doi:10.1093/emboj/16.24.7297

van Lis, R., Atteia, A., Nogaj, L. A., & Beale, S. I. (2005). Subcellular Localization and Light-Regulated Expression of Protoporphyrinogen IX Oxidase and Ferrochelatase in *Chlamydomonas reinhardtii*. *Plant Physiol., 139*(4), 1946-1958. doi:10.1104/pp.105.069732

Vavilin, D. V., & Vermaas, W. F. (2002). Regulation of the tetrapyrrole biosynthetic pathway leading to heme and chlorophyll in plants and cyanobacteria. *Physiol Plant, 115*(1), 9-24. doi:10.1034/j.1399-3054.2002.1150102.x

Vercellino, I., & Sazanov, L. A. (2022). The assembly, regulation and function of the mitochondrial respiratory chain. *Nature Reviews Molecular Cell Biology, 23*(2), 141-161. doi:10.1038/s41580-021-00415-0

Verissimo, A. F., & Daldal, F. (2014). Cytochrome c biogenesis System I: an intricate process catalyzed by a maturase supercomplex? *Biochim Biophys Acta, 1837*(7), 989-998. doi:10.1016/j.bbabio.2014.03.003

Verissimo, A. F., Khalfaoui-Hassani, B., Hwang, J., Steimle, S., Selamoglu, N., Sanders, C., . . . Daldal, F. (2017). The thioreduction component CcmG confers efficiency and the heme ligation component CcmH ensures stereo-specificity during cytochrome. *J Biol Chem, 292*(32), 13154-13167. doi:10.1074/jbc.M117.794586

Verissimo, A. F., Shroff, N. P., & Daldal, F. (2015). During Cytochrome c Maturation CcmI Chaperones the Class I Apocytochromes until the Formation of Their b-Type Cytochrome Intermediates. *J Biol Chem, 290*(27), 16989-17003. doi:10.1074/jbc.M115.652818

Verissimo, A. F., Yang, H., Wu, X., Sanders, C., & Daldal, F. (2011). CcmI subunit of CcmFHI heme ligation complex functions as an apocytochrome c chaperone during c-type cytochrome maturation. *J Biol Chem, 286*(47), 40452-40463. doi:10.1074/jbc.M111.277764

Wang, X., Dutton, R. J., Beckwith, J., & Boyd, D. (2011). Membrane topology and mutational analysis of Mycobacterium tuberculosis VKOR, a protein involved in disulfide bond formation and a homologue of human vitamin K epoxide reductase. *Antioxid Redox Signal, 14*(8), 1413-1420. doi:10.1089/ars.2010.3558

Waterhouse, A. M., Procter, J. B., Martin, D. M., Clamp, M., & Barton, G. J. (2009). Jalview Version 2--a multiple sequence alignment editor and analysis workbench. *Bioinformatics, 25*(9), 1189-1191. doi:10.1093/bioinformatics/btp033

Wheeler, T. J., Clements, J., & Finn, R. D. (2014). Skylign: a tool for creating informative, interactive logos representing sequence alignments and profile hidden Markov models. *BMC Bioinformatics, 15*, 7. doi:10.1186/1471-2105-15-7

Wiedemann, N., Kozjak, V., Prinz, T., Ryan, M. T., Meisinger, C., Pfanner, N., & Truscott, K. N. (2003). Biogenesis of yeast mitochondrial cytochrome c: a unique relationship to the TOM machinery. *J Mol Biol, 327*(2), 465-474. doi:10.1016/s0022-2836(03)00118-9

Wilkerson, D. C., & Sankar, U. (2011). Mitochondria: a sulfhydryl oxidase and fission GTPase connect mitochondrial dynamics with pluripotency in embryonic stem cells. *Int J Biochem Cell Biol, 43*(9), 1252-1256. doi:10.1016/j.biocel.2011.05.005

Wilks, A. (2002). Analysis of Heme and Hemoproteins. In A. G. Smith & M. Witty (Eds.), *Heme, Chlorophyll, and Bilins: Methods and Protocols* (pp. 157-184). Totowa, NJ: Humana Press.

Willows, R. D., Lagarias, J. C., & Duanmu, D. (2023). Chapter 21 - Tetrapyrrole biosynthesis and signaling (chlorophyll, heme, and bilins). In A. R. Grossman & F.-A. Wollman (Eds.), *The Chlamydomonas Sourcebook (Third Edition)* (pp. 691-731). London: Academic Press.

Worrall, J. A., Luisi, B. F., Schlarb-Ridley, B. G., Bendall, D. S., & Howe, C. J. (2008). Cytochrome c6A: discovery, structure and properties responsible for its low haem

redox potential. *Biochem Soc Trans, 36*(Pt 6), 1175-1179. doi:10.1042/BST0361175

Wu, J., Rong, L., Lin, W., Kong, L., Wei, D., Zhang, L., . . . Xu, X. (2021). Erratum to: Functional redox links between lumen thiol oxidoreductase1 and serine/threonine-protein kinase STN7. *Plant Physiol, 187*(3), 1837. doi:10.1093/plphys/kiab267

Wu, J., Rong, L., Lin, W., Kong, L., Wei, D., Zhang, L., . . . Xu, X. (2021). Functional redox links between lumen thiol oxidoreductase1 and serine/threonine-protein kinase STN7. *Plant Physiol, 186*(2), 964-976. doi:10.1093/plphys/kiab091

Wyman, A. J., & Yocum, C. F. (2005). Structure and activity of the photosystem II manganese-stabilizing protein: role of the conserved disulfide bond. *Photosynth Res, 85*(3), 359-372. doi:10.1007/s11120-005-7385-9

Xia, B., Vlamis-Gardikas, A., Holmgren, A., Wright, P. E., & Dyson, H. J. (2001). Solution structure of Escherichia coli glutaredoxin-2 shows similarity to mammalian glutathione-S-transferases. *J Mol Biol, 310*(4), 907-918. doi:10.1006/jmbi.2001.4721

Xie, Z., Culler, D., Dreyfuss, B. W., Kuras, R., Wollman, F. A., Girard-Bascou, J., & Merchant, S. (1998). Genetic analysis of chloroplast c-type cytochrome assembly in Chlamydomonas reinhardtii: One chloroplast locus and at least four nuclear loci are required for heme attachment. *Genetics, 148*(2), 681-692. doi:10.1093/genetics/148.2.681

Xie, Z., & Merchant, S. (1996). The plastid-encoded ccsA gene is required for heme attachment to chloroplast c-type cytochromes. *J Biol Chem, 271*(9), 4632-4639. doi:10.1074/jbc.271.9.4632

Xie, Z., & Merchant, S. (1998). A novel pathway for cytochromes c biogenesis in chloroplasts. *Biochim Biophys Acta, 1365*(1-2), 309-318. doi:10.1016/s0005-2728(98)00085-1

Yahia, E. M., Carrillo-López, A., Barrera, G. M., Suzán-Azpiri, H., & Bolaños, M. Q. (2019). Chapter 3 - Photosynthesis. In E. M. Yahia (Ed.), *Postharvest Physiology and Biochemistry of Fruits and Vegetables* (pp. 47-72): Woodhead Publishing.

Yang, J., Staples, O., Thomas, L. W., Briston, T., Robson, M., Poon, E., . . . Ashcroft, M. (2012). Human CHCHD4 mitochondrial proteins regulate cellular oxygen consumption rate and metabolism and provide a critical role in hypoxia signaling and tumor progression. *J Clin Invest, 122*(2), 600-611. doi:10.1172/JCI58780

Yang, X. J., Cui, H. R., Yu, Z. B., Du, J. J., Xu, J. N., & Wang, X. Y. (2015). Key Amino Acids of Arabidopsis VKOR in the Activity of Phylloquinone Reduction and Disulfide Bond Formation. *Protein Pept Lett, 22*(1), 81-86.

Zapun, A., Bardwell, J. C., & Creighton, T. E. (1993). The reactive and destabilizing disulfide bond of DsbA, a protein required for protein disulfide bond formation in vivo. *Biochemistry, 32*(19), 5083-5092. doi:10.1021/bi00070a016

Zapun, A., Missiakas, D., Raina, S., & Creighton, T. E. (1995). Structural and functional characterization of DsbC, a protein involved in disulfide bond formation in Escherichia coli. *Biochemistry, 34*(15), 5075-5089. doi:10.1021/bi00015a019

Zhou, J., Fernandez-Velasco, J. G., & Malkin, R. (1996). N-terminal mutants of chloroplast cytochrome *f*. Effect on redox reactions and growth in *Chlamydomonas reinhardtii*. *J. Biol. Chem., 271*(11), 6225-6232.

Zhou, J., Fernandez-Velasco, J. G., & Malkin, R. (1996). N-terminal mutants of chloroplast cytochrome f. Effect on redox reactions and growth in Chlamydomonas reinhardtII. *J Biol Chem, 271*(11), 6225-6232. doi:10.1074/jbc.271.11.6225

Zhou, J., Fernandez-Velasco, J. G., & Malkin, R. (1996). N-terminal mutants of chloroplast cytochrome *f*. Effect on redox reactions and growth in *Chlamydomonas reinhardtII*. *J. Biol. Chem, 271*(11), 6225-6232.

Zhou, Z.-D., Saw, W.-T., & Tan, E.-K. (2017). Mitochondrial CHCHD-Containing Proteins: Physiologic Functions and Link with Neurodegenerative Diseases. *Molecular Neurobiology, 54*(7), 5534-5546. doi:10.1007/s12035-016-0099-5

Zollner, A., Rödel, G., & Haid, A. (1994). Expression of the Saccharomyces cerevisiae CYT2 gene, encoding cytochrome c1 heme lyase. *Curr Genet, 25*(4), 291-298. doi:10.1007/BF00351480